

BIOCHEMICAL AND STRUCTURAL CHARACTERIZATION OF
LEVANSUCRASE FROM *Bacillus licheniformis* RN-01

Miss Santhana Nakapong

A Dissertation Submitted in Partial Fulfillment of the Requirements
for the Degree of Doctor of Philosophy Program in Biochemistry

Department of Biochemistry

Faculty of Science

Chulalongkorn University

Academic Year 2011

Copyright of Chulalongkorn University

บทคัดย่อและแฟ้มข้อมูลฉบับเต็มของวิทยานิพนธ์ตั้งแต่ปีการศึกษา 2554 ที่ให้บริการในคลังปัญญาจุฬาฯ (CUIR)

เป็นแฟ้มข้อมูลของนิสิตเจ้าของวิทยานิพนธ์ที่ส่งผ่านทางบัณฑิตวิทยาลัย

The abstract and full text of theses from the academic year 2011 in Chulalongkorn University Intellectual Repository (CUIR)

are the thesis authors' files submitted through the Graduate School.

ลักษณะสมบัติทางชีวเคมีและเชิงโครงสร้างของเลแวนซูเครสจาก

Bacillus licheniformis RN-01

นางสาวสันทนา นาคะพงศ์

วิทยานิพนธ์นี้เป็นส่วนหนึ่งของการศึกษาตามหลักสูตรปริญญาวิทยาศาสตรดุษฎีบัณฑิต

สาขาวิชาชีวเคมี ภาควิชาชีวเคมี

คณะวิทยาศาสตร์ จุฬาลงกรณ์มหาวิทยาลัย

ปีการศึกษา 2554

ลิขสิทธิ์ของจุฬาลงกรณ์มหาวิทยาลัย

Thesis Title	BIOCHEMICAL AND STRUCTURAL CHARACTERIZATION OF LEVANSUCRASE FROM <i>Bacillus licheniformis</i> RN-01
By	Miss Santhana Nakapong
Field of Study	Biochemistry
Thesis Advisor	Professor Piamsook Pongsawasdi, Ph.D.
Thesis Co-advisor	Assistant Professor Rath Pichyangkura, Ph.D.
Thesis Co-advisor	Associate Professor Kazuo Ito, Ph.D.

Accepted by the Faculty of Science, Chulalongkorn University in Partial Fulfillment of the Requirements for the Doctoral Degree.

.....Dean of the Faculty of Science
(Professor Supot Hannongbua, Dr.rer.nat.)

THESIS COMMITTEE

.....Chairman
(Professor Anchalee Tassanakajon, Ph.D.)

.....Thesis Advisor
(Professor Piamsook Pongsawasdi, Ph.D.)

.....Thesis Co-advisor
(Assistant Professor Rath Pichyangkura, Ph.D.)

.....Thesis Co-advisor
(Associate Professor Kazuo Ito, Ph.D.)

.....Examiner
(Assistant Professor Kanoktip Packdibumrung, Ph.D.)

.....Examiner
(Associate Professor Teerapong Buaboocha, Ph.D.)

.....External Examiner
(Associate Professor Sunanta Ratanapo, Ph.D.)

สันทนา นาคะพงศ์ : ลักษณะสมบัติทางชีวเคมีและเชิงโครงสร้างของเลแวนซูเครส *Bacillus licheniformis* RN-01(Biochemical and structural characterization of levansucrase from *Bacillus licheniformis* RN-01) อ.ที่ปริกษาวิทยานิพนธ์ : ศ.ดร.เปี่ยมสุข พงษ์สวัสดิ์, อ.ที่ปริกษาวิทยานิพนธ์ร่วม : ผศ.ดร.รัฐ พิษญาณกูร, อ.ที่ปริกษาวิทยานิพนธ์ร่วม : รศ.ดร. Kazuo Ito, จำนวนหน้า .

เลแวนซูเครสเป็นฟรุกโทซิลทรานส์เฟอเรสในกลุ่มของไกลโคซิลทรานส์เฟอเรสแฟมิลี 68 เอนไซม์สามารถผลิตเลแวนซึ่งเป็นพอลิเมอร์ของฟรุกโทสโดยใช้ซูโครสเป็นสารตั้งต้นเพียงชนิดเดียวได้ *Bacillus licheniformis* RN-01 ซึ่งแยกจากดินในประเทศไทยผลิตเลแวนซูเครสได้ในปริมาณสูง เมื่อเลี้ยงในอาหารเลี้ยงเชื้อที่มีซูโครสเป็นส่วนประกอบ พบเลแวนซูเครสทั้งในอาหารเลี้ยงเชื้อและส่วนที่ติดกับเชื้อหุ้มเซลล์ เพื่อศึกษาลักษณะของเอนไซม์จึงได้โคลนยีนเลแวนซูเครสจาก *B. licheniformis* RN-01 จากลำดับ นิวคลีโอไทด์ขนาด 1793 คู่เบส พบว่า 1446 คู่เบสสามารถถอดรหัสได้ และพบ putative endogenous promoter ทางด้าน 5' ของยีนเลแวนซูเครส เมื่อถอดรหัสได้พอลิเปปไทด์ซึ่งประกอบด้วยกรดอะมิโน 482 ตัว โดยมี signal peptide อยู่ทางด้านปลายอะมิโนจำนวนกรดอะมิโน 29 ตัว ในงานนี้ได้ทดลองแสดงออกยีนเลแวนซูเครสด้วยระบบการแสดงออก 2 ระบบ คือ endogenous promoter และ T7 promoter พบว่าภาวะที่ผลิตเลแวนซูเครสจากสายพันธุ์ RN-01 (LsRN) ได้ดีที่สุดคือการแสดงออกภายใต้ endogenous promoter โดย *E. coli* Top-10 ในอาหารเลี้ยงเชื้อ 3xLB นาน 36 ชั่วโมง หลังจากนั้นได้ทำ LsRN ให้บริสุทธิ์โดยคอลัมน์ DEAE และ Butyl toyopearl-650M ภาวะที่เหมาะสมในการเร่งปฏิกิริยาของ LsRN คือ 50 °C ในโซเดียมซิเตรทบัฟเฟอร์ พีเอช 6.0 ค่า K_m , k_{cat} และ k_{cat} / K_m สำหรับปฏิกิริยาไฮดรอลิซิสเป็น 9.12 mM, 86.0 s⁻¹ และ 9.43 mM⁻¹s⁻¹ ส่วนสำหรับปฏิกิริยาทรานส์ฟรุกโทซิเลชันเป็น 6.94 mM, 32.3 s⁻¹ และ 4.65 mM⁻¹s⁻¹ ตามลำดับ เมื่อระบุชนิดของพอลิเมอร์ที่สังเคราะห์โดย LsRN ด้วย ¹³C-NMR พบว่าพอลิเมอร์ดังกล่าวคือ เลแวน จากการทดลองวิเคราะห์น้ำหนักโมเลกุลของเลแวนโดย HPLC พบว่าอุณหภูมิและการเติมเกลือโซเดียมคลอไรด์มีผลต่อขนาดของเลแวน เราได้สร้างเลแวนซูเครสกลายด้วยวิธีการกลายสองแบบ โดย rational mutagenesis พบว่าการแทนที่ N251 ที่ subsite +2 ทำลายความสามารถในการสังเคราะห์พอลิเมอร์ของ LsRN เมื่อทำการกลายแบบสุ่ม พบว่า Y246 ซึ่งเป็นกรดอะมิโนที่อยู่ที่ยีนผิวโมเลกุลเกี่ยวข้องกับการควบคุมขนาดของผลิตภัณฑ์ ส่งผลให้ผลิตภัณฑ์หลักเปลี่ยนจากเลแวนพอลิเมอร์เป็นอออลิโกเมอร์ ในด้านการประยุกต์ใช้เราได้สังเคราะห์อนุภาคขนาดนาโนของเลแวนซึ่งสามารถใช้เก็บกัก O-acetyl- α -tocopherol ในอนุภาคดังกล่าวได้

ภาควิชา.....ชีวเคมี.....ลายมือชื่อนิสิต.....
 สาขาวิชา.....ชีวเคมี.....ลายมือชื่ออาจารย์ที่ปริกษา.....
 ปีการศึกษา.....2554.....

5073887823: MAJOR BIOCHEMISTRY

KEY WORD: LEVAN / LEVANSUCRASE / EXPRESSION / NANOPARTICLES

SANTHANA NAKAPONG: BIOCHEMICAL AND STRUCTURAL CHARACTERIZATION OF LEVANSUCRASE FROM *Bacillus licheniformis* RN-01. THESIS ADVISOR: PIAMSOOK PONGSAWASDI, Ph.D., THESIS CO-ADVISOR: RATH PICHYANGKURA, Ph.D., THESIS CO-ADVISOR: KAZUO ITO, Ph.D., pp. ISBN

Levansucrase (Ls) is a fructosyltransferase belonging to family 68 of glycosyltransferase using sucrose as a sole substrate to synthesize levan, a fructose polymer. *Bacillus licheniformis* RN-01, isolated from soil in Thailand was found to produce high Ls activity. In sucrose containing medium, Ls was detected mainly in culture medium and membrane-bound fraction. To characterize the enzyme, *ls* of *B. licheniformis* RN-01 was cloned. The nucleotide sequence of 1793 bp revealed a single open reading frame of 1446 bp and the putative endogenous promoter at 5' of the structural gene. The encoded amino acid sequence contained 482 amino acids with N-terminal signal peptide of 29 residues. The *ls* was expressed under two expression systems, the endogenous promoter and T7 promoter. The best condition to produce Ls from the strain RN-01 (LsRN) was the expression under putative promoter by *E. coli* Top-10 in 3xLB medium for 36 h. LsRN was purified by DEAE-and Butyl Toyopearl-650M. The optimal condition for catalysis was at 50°C in sodium citrate pH 6.0. The K_m , k_{cat} , and k_{cat} / K_m values were 9.12 mM, 86.0 s⁻¹, and 9.43 mM⁻¹s⁻¹ for hydrolysis reaction, and 6.94 mM, 32.3 s⁻¹ and 4.65 mM⁻¹s⁻¹ for transfructosylation reaction. The polymer synthesized by LsRN was identified as a levan by ¹³C-NMR. The Mw of levan was determined by HPLC, the reaction temperature and the addition of NaCl affected the size of levan. By rational mutagenesis, N251 was identified at +2 subsite. Mutation at this residue abolished the synthesis of levan polymer. By error prone PCR, the surface residue Y246 was involved in control of product size distribution. Mutation at this residue shifted the main product from levan polymer to oligomer. For applicable use, levan nanoparticles (NPs) were enzymatically synthesized and their ability to encapsulate *O*-acetyl- α -tocopherol was demonstrated.

Department.....Biochemistry.... Student's signature.....

Field of Study...Biochemistry....Advisor's signature.....

Academic year.....2011.....

ACKNOWLEDGEMENT

I would like to thank Professor Dr. Piamsook Pongsawasdi, Assistance Professor Dr. Rath Pichyangkura and Associate Professor Kazuo Ito for their excellent advisor and mentor. I also thank for his patience, understanding and encouragement though the years. Without their kindness and understanding, this work could not be accomplished.

My gratitude is also to Professor Dr. Masaru Iizuka, Professor Dr. Suwabun Chirachanchai, and Assistant Professor Dr. Warinthorn Chavasiri for their supports in the product analysis. Professor Dr. Anchalee Tassanakajon, Associated Professor Dr. Sunanta Ratanapo, Assistance Professor Dr. Kanoktip Packdibumrung, and Associate Professor Dr. Teerapong Buaboocha for serving as the members of my thesis committee, for their valuable comments and also for useful suggestions.

I also wish to thank all staff members and students of the Biochemistry Department for their help in laboratory and discussion. I also thank them for their sincerity and friendships. Special thanks are also extended to all members of 709 and Starch and Cyclodextrin research unit, especially for Dr. Kamoltip Kattiyawong and Dr. Kuakarun Krusong for their helpfulness and kind suggestions.

This work was supported by the Program Strategic Scholarships for Frontier Research Networks of Commission of Higher Education, Thailand, and by a Chulalongkorn University graduate scholarship to commemorate the 72nd Anniversary of His Majesty King Bhumibol Adulyadej.

Finally, the greatest indebtedness is expressed to my family for their unlimited love, understanding and encouragement.

CONTENTS

	Page
THAI ABSTRACT.....	iv
ENGLISH ABSTRACT.....	v
ACKNOWLEDGMENT.....	vi
CONTENTS.....	vii
LIST OF FIGURES.....	x
LIST OF TABLES.....	xiii
LIST OF ABBREVIATIONS.....	ix
CHAPTER I	
INTRODUCTION.....	
Levan.....	1
Application of levan and its oligosaccharides.....	2
Levansucrase.....	7
3D-structure and mechanism.....	9
Carbohydrate-based nanoparticles.....	15
CHAPTER II.....	
MATERIALS AND METHODS.....	
Equipments.....	18
Chemicals.....	18
Restriction enzymes and DNA modifying enzyme.....	19
Plasmid vectors.....	19
Microorganisms.....	20
Computer Programs.....	20
Media preparation.....	21
Bacterial growth conditions.....	22
Storage of bacteria.....	22
DNA manipulation techniques.....	22
Bacterial identification.....	26
Protein manipulation techniques.....	30
Characterization of levansucrase.....	33

	Page
Production and identification of levan polysaccharide.....	36
Product size analysis.....	37
Preparation and characterization of levan nanoparticles.....	38
Molecular modeling techniques.....	39
Structure superimposition.....	39
Molecular docking.....	40
CHAPTER III	
RESULTS.....	
Screening for high levansucrase –producing strains.....	41
Species identification of the isolated TN-1.....	43
Cloning of levansucrase gene by PCR technique.....	44
<i>ls</i> analysis.....	52
Expression of levansucrase in <i>E. coli</i>	63
Purification of levansucrase.....	71
Characterization of levansucrase.....	76
Identification of levan.....	97
<i>In situ</i> synthesis of levan nanoparticles.....	100
Encapsulation of <i>O</i> -acetyl- α -tocopherol in levan nanoparticles.....	104
Analysis of chemical structure of encapsulated levan NPs.....	104
Identification of amino acid residues involved in product size determination and distribution.....	107
Rational mutagenesis of LsRN.....	112
Random mutation.....	122
CHAPTER IV.....	
DISCUSSION.....	
Screening for high activity levansucrase	150
Identification of the strain TN-1.....	151
Cloning and analysis of <i>ls</i>	151
Expression of <i>ls</i>	154

	Page
Purification of LsRN.....	154
Characterization of LsRN.....	155
Characterization of levan product.....	157
Enzymatic synthesis of levan nanoparticles.....	158
Encapsulation of <i>O</i> -acetyl- α -tocopherol into levan NPs.....	158
Homology modeling of LsRN.....	159
Mutation at the position N251 influenced transfructosylation reaction and polysaccharide synthesis.....	159
Random mutagenesis.....	160
Y246 controlled the size distribution of levan product.....	161
Three surface motifs play different role in levan synthesis by LsRN.....	161
CHAPTER V	
CONCLUSION.....	
REFERENCES.....	
APPENDICES.....	
BIOGRAPHY.....	

LIST OF FIGURES

Figure	Page
1.1 Chemical structure of fructan.....	4
1.2 Cartoon diagram of levansucrase from <i>B. subtilis</i> (1OYG).....	11
1.3 Details of the active site of levansucrase from <i>B. subtilis</i>	13
1.4 Possible reaction pathway of Ls.....	14
3.1 Morphological of 6 isolated strains used for levansucrase production on LB agar plate containing 5 % (w/v) sucrose	42
3.2 Levansucrase production by the selected isolated strains in medium containing 0-20% (w/v) sucrose	45
3.3 Identification of the TN-1 isolated by 16S rRNA gene comparison....	47
3.4 Comparison of 16S rRNA gene of <i>Bacillus</i> sp TN-1 to <i>B. subtilis</i> and <i>B. lentus</i>	49
3.5 <i>In vitro</i> amplification of <i>ls</i> from <i>B. licheniformis</i>	50
3.6 Cloning of <i>ls</i> from <i>B. licheniformis</i>	51
3.7 <i>In vitro</i> amplification of <i>ls</i> from <i>Bacillus</i> sp. TN-1.....	54
3.8 Cloning of <i>ls</i> from <i>Bacillus</i> sp. TN-1.....	55
3.9 Comparison of nucleotide sequences of <i>ls</i> from <i>B. licheniformis</i>	56
3.10 Comparison of deduced amino acid sequences of Ls from <i>B. licheniformis</i>	59
3.11 The nucleotide and deduced amino acid sequences of Ls from <i>Bacillus</i> sp. TN-1	61
3.12 Recombinants levansucrase of <i>B. licheniformis</i> expressed in <i>E. coli</i> Top-10 during 4 day.....	64
3.13 Optimization of LsRN production.....	65
3.14 <i>In vitro</i> amplification of <i>ls</i> from <i>B. licheniformis</i> RN-01.....	67
3.15 Sub-cloning of <i>ls</i> from <i>Bacillus</i> sp. TN-1 into pET-19b.....	68
3.16 Expression of LsRN under T7 promoter.....	69
3.17 Expression of <i>ls</i> RN under T7 promoter	70
3.18 DEAE Toyopearl-650M Chromatographic profile of LsRN.....	72

Figure	Page
3.19 Butyl Toyopearl-650M Chromatographic profile of LsRN	73
3.20 SDS-PAGE of recombinant LsRN.....	75
3.21 Sephadex G75 (SF) Chromatographic profile of LsRN	77
3.22 Optimum temperature of LsRN.....	79
3.23 Temperature stability of LsRN.....	79
3.24 Optimum pH of LsRN.....	80
3.25 pH stability of LsRN.....	80
3.26 Hydrolysis versus transfructosylation of LsRN at various sucrose concentrations.....	83
3.27 TLC analysis of reaction products formed after incubation with various sucrose concentrations.....	84
3.28 TLC analysis of reaction products at different time points.....	85
3.29 Analysis of the product pattern of LsRN by HPAEC.....	87
3.30 MALDI-TOF MS spectrum of LsRN reaction products.....	88
3.31 Analysis of synthesized levan by HPLC.....	89
3.32 Analysis of monosaccharide acceptor specificity of LsRN by TLC...	92
3.33 Analysis of disaccharide acceptor specificity of LsRN by TLC.....	93
3.34 Analysis of sugar alcohol and amino acceptor specificity of LsRN by TLC.....	94
3.35 Effect of substrate concentration on rate of Ls hydrolysis.....	95
3.36 Effect of substrate concentration on rate of Ls transfructosylation...	96
3.37 Purification of the polymer synthesized from LsRN by Biogel P-100 column.....	98
3.38 Identification of levan polymer synthesized by LsRN.....	99
3.39 Suspension of levan nanoparticle.....	101
3.40 TEM-based micrographs of the levan NPs.....	102
3.41 AFM photographs.....	103
3.42 TEM-based micrographs of the <i>O</i> -acetyl- α -tocopherol-encapsulated levan NPs.....	105

Figure	Page
3.43 Comparison of the FTIR spectra for levam NPs <i>O</i> -acetyl- α -tocopherol and the tocopherol-encapsulated levam NPs.....	106
3.44 Homology modeling structure of LsRN constructed by SWISS-MODEL.....	108
3.45 Superimposition of raffinose-bound structure of LsRN and invertase from <i>T. maritima</i>	111
3.46 Site-directed mutagenesis of asparagine at position 251.....	114
3.47 SDS-PAGE analysis of purified N251 mutated Ls enzymes.....	116
3.48 TLC-analysis of reaction products of mutated N251.....	118
3.49 Analysis of the product pattern of LsRN by HPAEC.....	119
3.50 MALDI-TOF MS spectrum of mutated enzyme reaction products.....	121
3.51 Error prone PCR.....	123
3.52 TLC analyze of reaction products of the selected mutated clones.....	124
3.53 Distribution of nucleotide substitutions with <i>lsRN</i>	125
3.54 Mapping of amino acid substitution on protein structure.....	126
3.55 Site-directed mutagenesis of Y246S and N414T Ls.....	128
3.56 SDS-PAGE analysis of purified mutated Ls.....	130
3.57 TLC analysis of reaction products of mutated Ls.....	132
3.58 Analysis of the product pattern of mutated enzymes by HPAEC.....	133
3.59 MALDI-TOF MS spectrum of the reaction products of Y246S, N414T, and Y246S/N414T.....	135
3.60 Site-directed mutagenesis of Y246.....	137
3.61 Purification of Y246 mutated series of Ls.....	141
3.62 TLC analysis of reaction products of mutated enzyme.....	143
3.63 Analysis of the product pattern of mutated enzymes by HPAEC.....	144
3.64 MALDI-TOF MS spectrum of the reaction products of Y246 series of Ls.....	148
4.1 A phylogenetic tree for amino acid sequences of levansucrases.....	153
4.2 Three different function surface motifs of LsRN.....	162

LIST OF TABLES

Table		Page
1.1	Carbohydrate-based nanoparticles.....	16
2.1	List of extra facilities.....	18
2.2	List of the enzymes used in this work.....	19
2.3	List of plasmid vectors.....	19
2.4	List of microorganisms.....	20
2.5	List of computer programs.....	20
2.6	Antibiotics.....	22
2.7	PCR primers.....	27
3.1	Comparison of amino acid sequence of LsRN, LsSK, and LsTH with other levansucrases deposited in GenBank.....	60
3.2	Comparison of amino acid sequence of LsTN with other levansucrases deposited in GenBank.....	62
3.3	Purification of LsRN by two chromatographic steps.....	74
3.4	Comparison of Mw of LsRN determined by different techniques.....	76
3.5	Effect of metal ions and chelating agent on LsRN activity.....	81
3.6	Comparison of Mw of levan synthesized in different reaction conditions.....	90
3.7	Comparison of the ¹³ C-NMR chemical shift of the levans produced from different sources.....	97
3.8	QMEAN4 global scores.....	107
3.9	RMSD values of re-docked conformations of raffinose in 1BYN.....	110
3.10	Purification of mutated N251.....	115
3.11	Kinetic parameters of N251 Ls.....	117
3.12	Nucleotide substitutions reflected type of mutations and amino acid substitutions	125
3.13	Purification of Y246S/N414T, Y246S and N414T Ls.....	129
3.14	Kinetic parameters of mutated enzymes.....	131
3.15	Purification of Y246 mutated Ls.....	139
3.16	Kinetic parameters of mutated enzymes.....	142

LIST OF ABBREVIATIONS

3D	Three Dimension
A	Absorbance
Å	Angstrom
BLAST	Basic Local Alignment Search Tool
Bp	Base pair
°C	Degree Celsius
Da	Dalton
DNA	Deoxyribonucleic acid
FOS	Fructooligosaccharide
g	Gram
GF	Glucose-Fructose
GH	Glycosyhydrolase
L	Litre
Ls	Levansucrase
M	Molar
min	Minute
mL	Millilitre
mM	Millimolar
Mw	Molecular weight
nm	Nanometre
NP	Nanoparticle
PCR	Polymerase Chain Reaction
rpm	Revolution per minute
SDS-PAGE	Sodiumdodecylsulphate Polyacrylamide Gel Electrophoresis
µg	Microgram
µL	Microlitre
µM	Micromolar

CHAPTER I

INTRODUCTION

Due to several economic and environmental advantages, biopolymers have gained the great attention worldwide. They exert a sustainable basis and could be produced from renewable starting materials. Almost biopolymers are biodegradable, and biocompatible to human system. So far, the biopolymers originated from plants and animals such as cellulose, starch and chitin are intensively studied, resulting in a numerous applications. By an increase of demand in biopolymers, the future of products is dependent on their cost competitiveness. The time consuming and large area needed for biopolymer production from plants and animals may unsatisfy consumers by the high-cost of investment and production. An alternative resource of biopolymer attracts the interest is from a variety of microorganisms. Several of microbial polysaccharides are now widely accepted industrial products [1]. Among them, levan is one of the high potential polymers, as a result of a simple synthesis method and low-cost of starting material.

1.1 Levan

Fructan, one of the most polysaccharides found in nature, is composed of D-fructosyl repeating unit linked by β -(2, 6) or β -(2, 1). There are two types of fructan; levan and inulin, distinguishing by the type of linkage (Fig 1.1). Levan predominantly joined by β -(2, 6) linkage as 6-kestose of the basic trisaccharide, with some β -(2, 1) linked at the branching points. While inulin mainly joined by β -(2, 1) linkage in the main chain with some branch point linked by β -(2, 6) linkage [2].

The extracellularly synthesized microbial levan is detected in a sucrose-containing medium, giving rise the cells to a typical mucoid-like morphology. Levan plays a role in the symbiosis, phytopathogenesis, and participation in the defense mechanism against cold and drought conditions [3]. Numerous microorganisms reported as the levan-producing organism. Due to the presence in human dental caries, oral bacteria such as *Streptococcus salivarius* [4] received much attention, together with soil microorganisms, *Bacillus subtilis* [5] and *Bacillus polymyxa* [6]. Furthermore, levan from several bacteria such as *Pseudomonas* sp. [7], [8], *Zymomonas mobilis* [9], [10] and *Lactobacillus reuteri* [11] was also reported.

Levan is highly soluble in water at room temperature and has an unusually low intrinsic viscosity for a polymer of high molecular weight at 0.14 dL/g. By way of comparison, it is noted that the intrinsic viscosity of dextrose is around 1 dL/g and for thickeners, like carboxymethylcellulose (CMC), it approaches 100 dL/g [12]. Levan is relatively acid stable. Dissolved in acid solution with the pH less than 3 and held at 70°C, over an hour is needed for complete hydrolysis [13]. Levan has good heat stability, melting with decomposition at 225°C. The glass transition temperature is 133°C. Levan absorbs UV radiation, particularly in the UV-C range [14]. Levan has a tensile strength of 991 pounds per square inch, while the CMC and inulin have a tensile strength of 193 and 124 pounds per square inch, respectively [15].

1.2 Application of levan and its oligosaccharides

Levan and its oligosaccharides have great potential as functional saccharides in food, cosmetic, and pharmaceutical uses.

1.2.1 Applicable use in foods and feeds

Levan has been reported as prebiotic in milked-based fermented products. The saccharides were delivered to the GI tract and stimulated beneficial probiotic bacterial growth. A supplementation of milk by high Mw (2000 kDa) levan from *Z. mobilis* stimulated the growth of starter ABT-5 (a dairy starter culture containing *Streptococcus thermophilus*, *Lactobacillus acidophilus* LA-5 and *Bifidobacterium lactis* BB-12), higher level of acidification 10-14 percentage over the control test [16]. When the levan type fructooligosaccharides (L-FOSs) were tested as glucose substitutes with the commercial strain *Bifidobacterium lactis* Bb-12, they also exhibited an increase in cell count and acidification power [17]. *Bifidobacterium adolescentis*, *Bifidobacterium longum*, *Bifidobacterium breve*, and *Bifidobacterium pseudocatenulatum* were also *in vitro* studied for their capability of metabolizing low Mw levan prepared by acid hydrolysis. Growth, decrease in pH, formation of short- chain fatty acids (lactate, acetate, formate) and degradation of low Mw levan were markedly different among species. In those report, *B. adolescentis* showed the best growth, produced the highest amounts of organic acids and metabolized both short- and long-chain oligosaccharides [18].

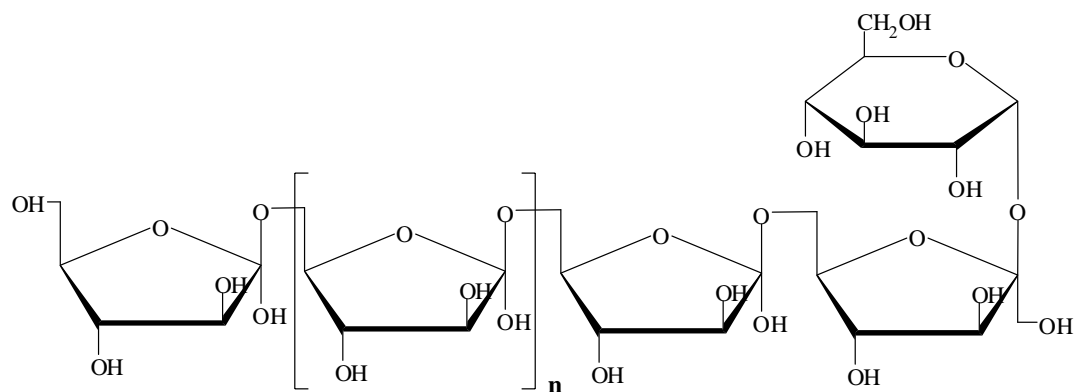
Cholesterol and triacylglycerol reducing properties of levan have also been reported. High Mw levan (2000 kDa) and its effect on the lipid metabolism in rats fed with cholesterol-free diets were studied. Although body weight gain and changes in morphology of the

digestive tract, the serum triacylglycerol and glucose concentrations were not affected by feeding levan diets for 4 weeks. Serum cholesterol level was decreased to 83% or 59% by feeding a 1% or 5% levan supplemented diet, respectively. The hypocholesterolemic effect was accompanied by a significant increase in fecal excretion of sterols and lipids [19]. Moreover, it was reported that in high-fat diet-induced obese rats, the supplementation of 1-10 percent levan could decrease adiposity and postprandial lipidamia (Transient abnormally high concentration of lipid in the blood occurring after the ingestion of foods with a large content of fat) [20]. The key enzymes in fatty acid synthesis, hepatic fatty acid synthase and acetyl CoA carboxylase were down-regulated, in contrast to the hepatic peroxisome proliferator-activated receptor mRNA expression which was up-regulated by levan dose dependent in 1-10 percent levan fed rats resulted by lipogenesis inhibition and lipolysis stimulation [21].

Boosting mineral absorption effect of levan has been claimed. High (6000 kDa) and low (700 kDa) Mw levan were administered to rats. The intakes of minerals were not different among test groups. However fecal excretion of Mg (79.62% for control, 90.09% for high Mw levan and 94.23% for low Mw levan) and Fe (46.62% for control, 82.64% for high Mw levan and 81.58% for low Mw levan) were significantly different, indicating the apparent absorption is affected by the experimental administration of levan. Unlike Mg and Fe, Zn was significantly absorbed after the administration of low Mw levan by 1.5 fold of the control [22].

Levan has been shown to have immuno-stimulating properties. The effects of dietary levan on the survival of *Cyprinus carpio* juveniles were studied. Fishes were fed with feed containing levan, at concentrations ranging from 0.1 to 1.0%. One hundred percent survival was obtained with 0.5% levan in the feed. But increasing the concentration to 1% probably increased the antigenic load, leading to immuno-suppression and thus reducing the protection efficiency [23]. Moreover, the immuno-protective effect of levan on *Labeo rohita* juveniles challenged with *Aeromonas hydrophila* was investigated. The hemoglobin content, total leukocyte and erythrocyte count were increased with a dietary supplementation of levan at 1 to 1.25 %. A gradual increase in serum lysozyme activity was also observed with the levan fed group [24].

A)



B)

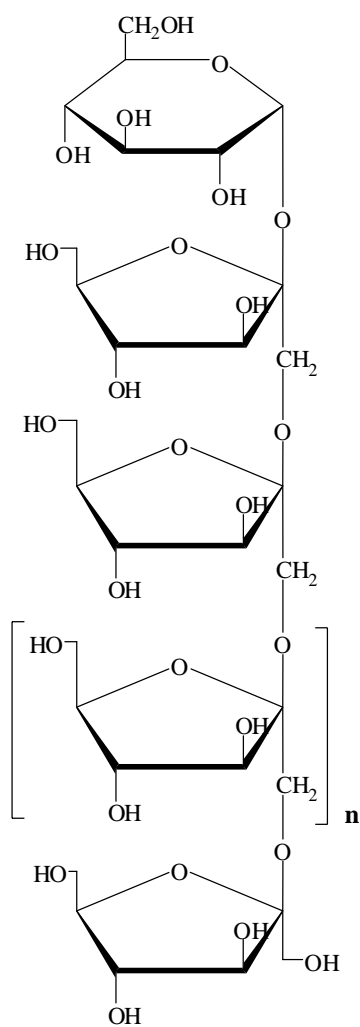


Figure 1.1 Chemical structure of fructan

A) a β -(2,6) linkage levan

B) a β -(2,1) linkage inulin

1.2.2 Applicable use in medicine

The biological activities of levan have been reported for years. The antitumor activity of levan from different microorganisms, *Microbacterium laevaniformans* (M-levan; Mw = 710 kDa), *Rahnella aquatilis* (R-levan; Mw = 380 kDa), and *Z. mobilis* (Z-levan; Mw = 570 kDa), were tested against different tumor cell lines. A relatively stronger activity was observed from the SNU-1, a stomach carcinoma cell and HepG2, hepatocellular carcinoma cell line. The M-levan and R-levan showed the significantly high activity against SNU-1, while M-levan showed the highest activity against HepG2. M-levan, R-levan and Z-levan showed strong antitumor activity on Sarcoma-180 [25]. Not only Mw of levan but degree of branching also related to its biological activities. Levan from *M. laevaniformans* (branching degree of 12.3%) was structurally modified by inulase (specifically hydrolyzed β -(2, 1) glycosidic bonds at the branching point of levan) to reduce the degree of branching. As the degree of branching decreased, the antitumour activity against the SNU-1 was linearly decreased. The antitumour activity against HepG2 was dramatically dropped when the branching decreased to 9.3%, and slightly increased as the branching degree of levan further decreased [26].

The antiviral activity of levan has been reported. Levans produced by different isolates of *B. subtilis* were antiviral activity tested on HPAI and H5N1, respiratory virus and adenovirus type 40, enteric virus. The levan with Mw of 43.5 and 71.9 kDa showed antiviral effect by decreased the infectivity of adenovirus type 40 to 50 and 60 % of the control, respectively. The levan with Mw of 40.9, 71.9 and 77.8 kDa showed the effects on HPAI and H5N1 infectivity. However, antiviral activities were detected only when pre-mixed the polymer with the virus one hour before infection of the virus into the test cells. Levan had no effect on the virus when inoculated simultaneously with the virus just after mixing or after 1h of infection [27].

The effect of levan on oxidative stress and hyperglycemia in alloxan-induced diabetic rats was evaluated. The oral administration of levan in diabetic rats resulted in increase in glycogen level and a decrease in glucose level in plasma [28]. The polysaccharide administration also caused the significant decrease in hepatic and renal indices toxicity. The study demonstrates that levan is efficient in inhibiting hyperglycemia and oxidative stress induced by diabetes and suggests that levan supplemented to diet may be helpful in preventing diabetes [29].

1.2.3 Applicable use in industry

In addition of the usage mentioned above, other applications of levan have been reported in chemical and biotechnological industry. A PEG/levan two-phase liquid system could be used to purify biological materials by selectively partitioning. The 60% PEG (w/w)/6.77% levan (w/w) two-phase system showed phase-separation phenomena with pectin, locust bean gum, and PEG likes the PEG/dextran system [30]. Levan has been utilized as an environmentally friendly adhesive. By the relatively high tensile strength and shear strength, levan is a competitor with many petrochemical based adhesives. Montana Biotech SE Inc. has developed two forms of levan-based adhesive. The water soluble levan-based adhesive is useful for temporary bonds and certain indoor applications, and the cross-linked levan-based adhesive is utilized as a water resistance adhesive for a long term purpose. The company expects that the cross-linked levan will be used in the wood adhesive industry, and in biodegradable plastic production. Levan is developed to be used as water resistant film for food preservation and for shale stabilization in the oil drilling industry. The adhesive strength, film-forming ability, and non-toxicity of levan are its selling properties, and are comparable to petrochemical derivatives in many applications [30]. Levan has been used as a cryoprotectant for freeze-preservation of animal cells, fish and the delicate texture of frozen desserts [31].

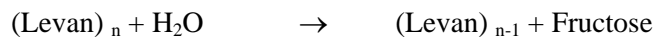
1.3 Levansucrase

Levan is synthesized by levansucrase (Ls, sucrose: α -D-glucosyl-(1 \rightarrow 2)-(2 \rightarrow 6)- β -D-fructan 6- β -D-fructosyltransferase, EC 2.4.1.10), using sucrose as a sole substrate. Ls, a member of family 68 glycosylhydrolase, catalyzes hydrolysis of sucrose into glucose and fructose, using bond energy to coupling fructosyl moiety to form both β -(2, 6) and β -(2, 1) glycosidic bond. The enzyme catalyzes a fructosyl transfer from sucrose to various acceptor molecules by the following reactions:

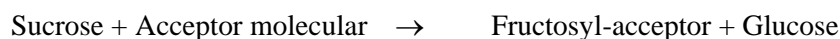
1. Polymerization reaction



2. Hydrolysis reaction



3. Acceptor reaction



4. Exchange reaction



5. Disproportionation reaction



To synthesize levan, Ls concomitantly catalyzes hydrolysis and polymerization reactions (reaction 1). The enzyme hydrolyzes sucrose, liberating glucose and transfers fructose to sucrose acceptor to form a fructose polymer. When water acts as an acceptor, a free fructose is generated from both sucrose and levan (reaction 2). This reaction occurs in all the levansucrase-catalyzed reactions mentioned above, but the rate is far slower when compared with a sugar acceptor. Reaction 3 occurs in the presence of another acceptor molecule in the reaction. The enzyme transfers the fructosyl moiety of sucrose specifically to the hydroxyl group in the acceptor. Certain compounds containing hydroxyl groups, such as alcohol and oligosaccharides, can act as fructosyl acceptors to yield a nonreducing sugar compound and a series of oligosaccharides. Reaction 4 is considered as an analogous of reactions 2 and 3, but differs in the regeneration of (¹⁴C) sucrose. The Ls also catalyzes reaction 5, a disproportionation reaction. The enzyme transfers the FOS from a donor molecule to an acceptor, i.e. levan and L-FOS.

The above five reactions compete with one another and, yielding a specific major product with some minor products but they are predominantly controlled by reaction parameters such as type and concentration of donor and acceptor, ionic strength and temperature [32]. Levan formed by Ls is hydrolyzed by the enzyme itself (reaction 2). For example, after saturation of levan formation, *R. aquatilis* Ls showed strong levan hydrolysis activity at 50 °C. The amounts of FOS and free fructose produced in the reaction mixture were consequently increased with the increase in temperature and incubation time [33]. The Ls recognizes saccharide with a α -1, 2 linkage between glucose and fructose residues. The

most preferably substrate of the Ls is sucrose, but raffinose (α -D-galactopyranosyl-(1 \rightarrow 6)- α -D-glucopyranosyl-(1 \rightarrow 2) β -D-fructofuranoside) can also serve as a substrate (reaction 3).

Levansucrases, produced by wide varieties of organisms, are mainly found in bacteria such as *Acetobacter xylinum* [34], *B. subtilis* [5], [35], *Bacillus megaterium* [36], *Gluconacetobacter diazotrophicus* [37], *L. reuteri* [11], *Leuconostoc mesenteroides* [38], *P. syringae* pv. *Phaseolicola* [8], *R. aquatilis* [33] and *Z. mobilis* [9], [10]. Based on amino acid similarity, bacterial levansucrases can be categorized into two groups, the first are levansucrases from gram positive bacteria, the relatively high similarity (>50%) in amino acid sequence when compared with those sequences of the second group, the gram negative bacteria. However, little similarity (<30%) exists among the genes from two different groups [32]. Most of the enzyme characteristics and levan products of bacterial Ls are different depending on sources of enzymes. However, some properties are found shared among Ls, e.g. the enzyme has high activity at pH 5-6, and is stable at pH 4-7. No activity was observed below pH 3 and above pH 9. High molecular weight levan is far more processively synthesized at low temperature than at room temperature or at higher temperature, although sucrose hydrolysis activity is quite small at low temperature [7], [39].

1.4 3D-structure and mechanism

As yet, only three Ls were investigated for their 3D- structure by X-ray crystallography, two from the gram-positive bacteria, *B. subtilis* (PDB ID; 1OYG) [40] as well as *B. megaterium* (PDB ID; 3OM2) [36] and one from the gram-negative bacterium *G. diazotrophicus* (PDB ID; 1W18) [41]. All three proteins revealed a five-bladed β -propeller fold with a deep funnel-like central cavity (Fig 1.2), resembling the same fold with invertase from *Thermotoga maritima* [42] (PDB ID; 1W2T). The five β -sheets modules, designated as blade I-V from N-terminal to C-terminal, arranged in consecutive order with pseudosymmetry around a central cavity. Each β -sheet modules is consisted of four antiparallel β -sheets with the classical W-topology (each β -strand displays a strong twist with an average of 90° between the first and the last strand). Ls does not show a canonical 'molecular velcro', a term designating the closure of the β -propeller structure by joining both termini in the same β -sheet. Here, the fold stabilization is provided by the packing of the N- and C- terminal of the polypeptide. The Ls N-terminus runs along the perimeter of blade IV forming a clamp-like loop (residues 34-83) that adds a fifth β -strand (residues 44-46) to blade III.

To date, two ligand-bound 3D structures are available from *B. subtilis* levansucrase: sucrose and a raffinose bound complexed with mutated Ls (E342A) (PDB IDs; 1PT2 and 3BYN). Active sites are positioned at the end of funnel-like cavity with an entrance opening towards the surface. In the sucrose bound complex, -1 (fructosyl residue) and +1 (glucosyl residue) sugar binding subsites were identified by the presence of the fructose and glucose moiety, respectively. It was clearly showed that three conserved acidic residues constituted the catalytic triad in the central pocket were function as nucleophile (D86), general acid (E342), and the transition state stabilization (D247). The carboxyl group of D247 forms hydrogen bonds to the amide backbone of R343 and two water molecules, positioned coincide with the fructosyl C3' and C4' hydroxyls in the ligand-bound state (Fig 1.3 A). The side chain of D86 forms a hydrogen bond to S164, and the E342 carboxylate forms a salt bridge with R246 and hydrogen bond to the hydroxyl group of W411. W411 also forms a hydrogen bond with N ϵ of R360, the residue required for polymerase activity. The molecular surface shows that the head group of R360 is located exactly adjacent to the central pocket, surrounding by E342 and E340 (Fig 1.3 B). However, R360 makes only weak direct interactions with the latter residues. Indeed, both R360 and E340 form tight H-bond contacts with the glucosyl moiety in the +1 subsite. The specific contacts in the -1 and +1 subsite lock the fructosyl and glucosyl moiety into a proximal orientation, allowing catalysis to occur (Fig. 1.3 C). Mutagenesis data for subset of +1 subsite amino acids in Ls of *B. megaterium* showed that alanine substituted for each amino acid at +1 subsite decreased the catalytic efficiency of hydrolysis reaction by 10%. Levan polymer was not found, only oligomers were produced [36]. While amino acid exchanged at subsite +1, especially at R360 of *B. subtilis* Ls, affected only transfructosylation but hydrolysis was still intact. From above mentioned, Seibel et al. proposed the possible reaction pathway of Ls as shown in Fig 1.4. When, sucrose coordinates in the active site of Ls. E342, as a general acid/ base catalyst, protonates the glycosidic oxygen of the substrate, making the glycosidic linkage weaker. The ionized carboxy group of D247 acts to stabilize the developing intermediate. Then release D-glucose to form an oxocarbenium ion of the fructosyl residue, and subsequently attacks by D86. The retaining mechanism further proceeds through the formation of a covalent glycosyl-enzyme intermediate with the enzyme and a nucleophilic attack of the acceptor substrate [43].

In the raffinose bound complex, the galactosyl unit protrudes out of the active site. The -1 subsite is highly specific for fructose units, while the +1 binding site shows more variability, allowing binding of either glucose or fructose. The low affinity of acceptor binding helps explain the sucrose-dependent switch between hydrolysis and polymerase activity in *B. subtilis* Ls. The fructose specific -1 site enables high affinity binding of the

donor. In this way, sucrose hydrolysis can occur even at lower sucrose concentrations (<250 mM). To promote levan polymerization, only a high concentration (>250 mM) of the acceptor substrate (initially sucrose), can lead to a productive binding at the +1 and +2 binding sites [44]. Subsite +2 is reported at position N242. Substitution of N242 (*B. subtilis* Ls numbering) to alanine or glycine in *B. megaterium* Ls completely abolished polysaccharide production without significantly changed in K_m and k_{cat} values, but causing the mutated enzyme to switch from mainly polysaccharide synthesis to hydrolysis. From this result it is suggested that +2 subsite helps allow the enzyme to stabilize the third fructosyl unit of the growing levan chain and directs it as an acceptor substrate into the optimal position for further transfructosylation [45].

Recently, amino acids outside the active site are reported as a platform for a possible stabilization of the acceptor fructan chain. Mutation of K373 in *B. megaterium* to alanine lowered the tri- and tetrasaccharide synthesis, while slightly enhanced the penta- and hexasaccharide synthesis and the oligosaccharides exceeding six units were undetectable. Not only eliminated levan synthesis, but the hydrolytic activity was also increased almost 33%. Moreover, Y247 was found to influence on the levan formation activity. The substitution of this residue to alanine led to the formation of short oligosaccharides. The formation of octa- and nanosaccharides was slightly enhanced and the transfructosylation was completely eliminated after decasaccharide [46].

Though, Ls are not known to require a metal cofactor for catalysis, *B. subtilis* Ls showed a low binding affinity to Ca^{2+} . D339 was identified as a residue, coordinating to Ca^{2+} ions. Sequence alignments within GH68 revealed that residues involved in calcium binding are conserved in most enzymes of gram-positive bacteria, but are absent in proteins of gram-negative bacteria [47, 48]. In gram negative bacteria a disulphide bridge may play a similar role, is observed in the 3D structure of *G. diazotrophicus* Ls. It is suggested that the binding of calcium ion to the enzyme may play a role in the fold stability of the protein [41].

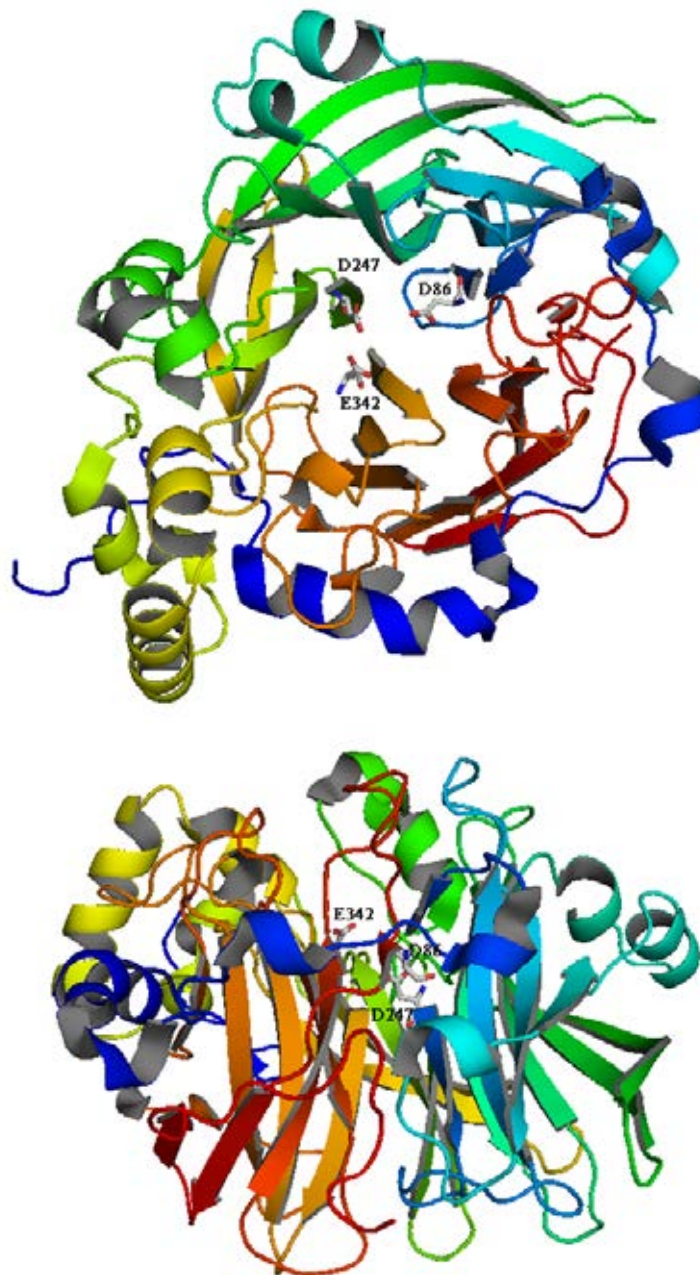


Figure 1.2 **Cartoon diagram of levansucrase from *B. subtilis* (1OYG)**

Superior (A) and lateral (B) views of the five-bladed β -propeller fold with catalytic residues shown in sticks. The protein is colored according to sequence succession (N-terminal in blue and C-terminal in red). Figure was prepared using PyMOL.

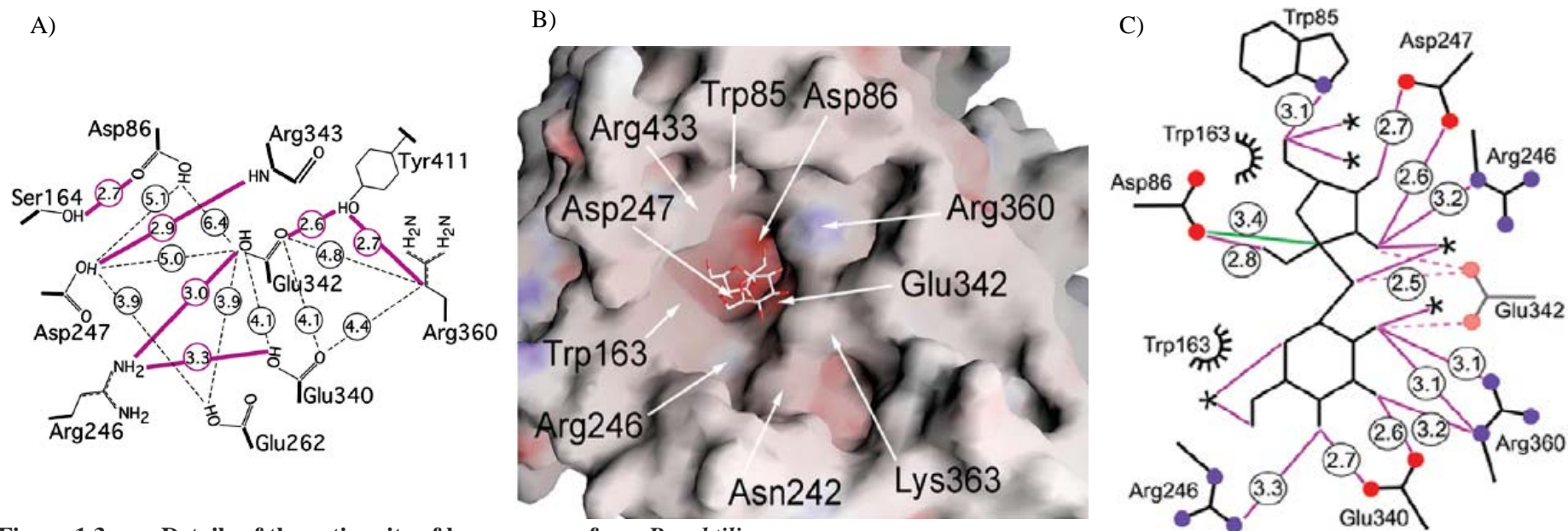


Figure 1.3 Details of the active site of levansucrase from *B. subtilis*.

A) Interatomic distances between critical residues in the active site. Non-contact distances are shown as dashed lines, hydrogen bonds by solid lines in magenta; distances are given in Å.

B) Close-up view of the central pocket of the Ls. The surface was colored according to electrostatic surface potential (negative charges in red, positive charges in blue). Sucrose molecule shown is of the complex structure.

C) Sucrose-protein contacts in the substrate-bound complex. Water molecules are asterisks. Putative interactions of Glu342 with sucrose are indicated in lighter color and with dashed lines.

* The figures are reproduced from Meng et al 2003.

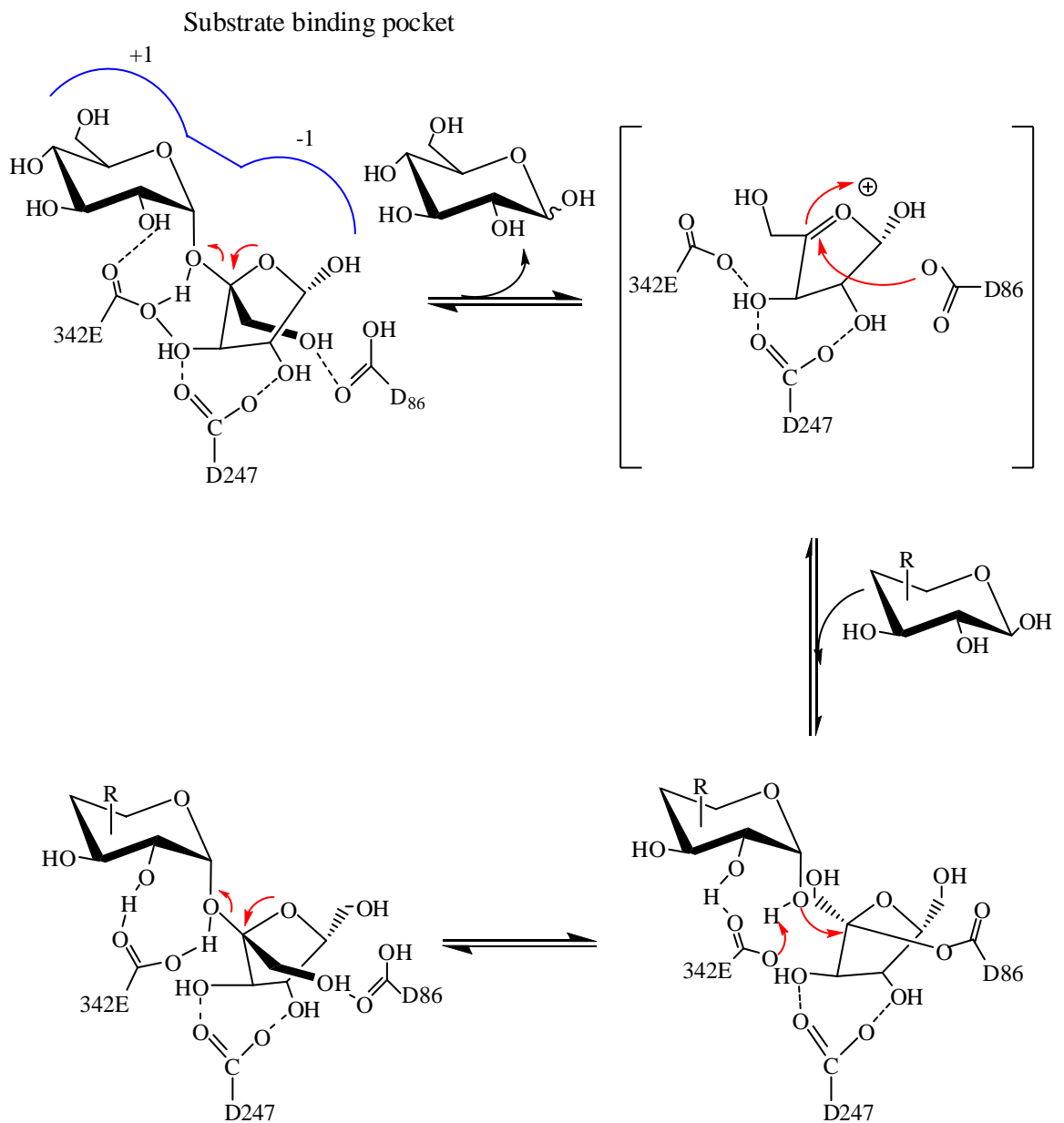


Figure 1.4 Possible reaction pathway of Ls

- A) Sucrose coordinates in the active site of the enzyme.
- B) D-Glucose is released and a reactive oxocarbenium ion of the fructosyl-residue is formed and subsequently attacked by D86 of the Ls.
- C) Covalent fructosyl enzyme complex, substituted by the acceptor to form a sucrose analogue.
- D) Coordination of the sucrose-analogue in the active site of the enzyme.

* The figures are reproduced from Seibel et al., 2006, using BioDraw Ultra 10.0.

1.5 Carbohydrate-based nanoparticles

Because of their good merits such as a large number of reactive groups, a wide range of Mw and a high diversity of chemical structure as well as their various compositions, polysaccharides have gained attention as biomaterial. Numerous applications of nanoparticles i.e., nanoreactor, nucleating reagent and drug delivery have been reported. For years, some polysaccharides shown in Table 1.1 have been reported as raw materials in preparation of nanoparticles (NPs). Levan was also reported as material for NPs preparation. The self-assemble levan NPs prepared by stirring method showed a potential to deliver the selected protein BSA [49]. And the self-assemble levan NPs synthesized by *Z. mobilis* exhibited high ethanol stability and substantial moisturizing effect, thus is useful as an active ingredient in the formulation of cosmetics [31, 50].

1.6 Aim of the study

In order to gain deep understanding on the reaction mechanism of Ls, structural and biochemical characterization of Ls from *B. licheniformis* RN-01 are our aim. This study shall provide the basic biochemical approach to alter product spectrum and/or tailor-made a specific size of levan for the further pilot scale production by biotechnological approach.

The specific objectives of this dissertation are;

- To screen for high activity levansucrases from the well characterized *Bacilli*
- To compare levansucrases from *B. subtilis* and *B. licheniformis* in terms of genes and their expression
- To characterize Ls from *B. licheniformis* RN-01
- To identify the amino acids involved in product size determination through site-directed and PCR-mediated random mutagenesis
- To synthesize levan NPs and introduce its applicable use in α -tocopherol encapsulation

Table 1.1 Carbohydrate-based nanoparticles

Carbohydrate	Examples of recently report of application
Alginate	<ul style="list-style-type: none">• Enhancement in the relative bioavailability of encapsulated antituberculosis drugs [51]• Controlled release of vaccine-like peptide to treat autoimmune encephalomyelitis [52]• Nutraceutical delivery vehicle to enhance the absorption of vitamin D3 [53]
Amylose	<ul style="list-style-type: none">• In vitro enhanced stability and improved O₂ release property of Hemoglobin [54], [55]• Increase mechanical strength, reduce water permeability and uptake, possible use as materials for eco-friendly food packaging
Carrageenan	<ul style="list-style-type: none">• Increase both solubility and dissolution rate of poorly water-soluble compounds [56]• Increase plasticizer properties, reduce water permeability and shelf-life extension of food products [57]• Drug controlled release; peptide drug model [58], Dexchlorpheniramine maleate [59], Mercaptopurine [60]
Chitosan	<ul style="list-style-type: none">• Vitamin C nanocarrier through the gastrointestinal tract [61]• PEG-crosslinked chitosan nanoparticle formulations for deep lung delivery of Hydrofluoroalkane from pressurized metered dose inhalers [62]• Entrapped together with bacterial cells onto the surface of graphite electrode to form microbial biosensors [63]• Improved NP mediated gene delivery system [64]• Enzyme immobilization; glucose oxidase for glucose electrode development [65] and neutral lipase for detergent development [66]

Table 1.1 Carbohydrate-based nanoparticles

Carbohydrates	Examples of recently reports of application
Cyclodextrin	<ul style="list-style-type: none"> • Drug controlled release; Acyclovir [67], Artemisinin [68], Camptothecin [69], Doxorubicin [70], Paclitaxel [71] and Tamoxifen citrate [72] • Safe polysaccharide nanocarriers for gene delivery to the airway epithelium [73] • Effective carrier-sensitizer system in photodynamic cancer therapy [74] • Novel adsorbent to adsorb hydroquinol and possible use in downstream separation process [75]
Dextran	<ul style="list-style-type: none"> • Use as a core-shell for an artificial oxygen nanocarrier [76] • Formation of colloidal carrier for oral insulin delivery [77] • Preparation of immunomagnetic iron-dextran NPs and application in rapid isolation of <i>E.coli</i> from foods [78]
Hyaluronic acid	<ul style="list-style-type: none"> • Use as novel non-viral gene delivery vectors capable of transferring exogenous genes into primary chondrocytes for the treatment of joint diseases [79] • Carrier of the hydrophobic photosensitizer for tumor-targeted imaging and therapy [80] • Use as muco-adhesive nanocarriers in antiasthmatic therapy [81]
Levan	<ul style="list-style-type: none"> • Nanocarrier for peptide and protein drug delivery [49] • Encapsulation of α-tocopherol [This work]
Pullulan	<ul style="list-style-type: none"> • Decrease enzymatic degradation of peptide-based drug using insulin as a drug payload [85] • Anticancer drug delivery carrier[86], epirubicin [87] • Effective intratumoral radioisotope carrier using ^{99m}Tc as a payload [88]

CHAPTER II

MATERIALS AND METHODS

2.1 Equipments

If not stated otherwise, all equipments used throughout this study are available at Department of Biochemistry, Faculty of Science, Chulalongkorn University and Laboratory of Enzyme Chemistry, Faculty of Science, Osaka City University, Japan. Only were major equipments and extra facilities therefore listed below.

Table 2.1 List of extra facilities

Equipment	Model	Manufacture
Atomic Force Microscopy	Nano Scope IV	Veeco Metrology, USA
Fourier Transform Infrared Spectroscopy	Spectrum One	Perkin Elmer, USA
MALDI-TOF Mass Spectrometer	Axima-CFRplus	Shimadzu Kratos, Japan
Nuclear Magnetic Resonance apparatus	UNITY plus 500 NMR spectrometer	Varian, USA
Transmission Electron Microscopy	TEM H-7650	Hitachi, Japan

2.2 Chemicals

If not stated otherwise, all chemicals used in this work were analytical grade and purchased from the following companies; Amersham Biosciences(U.S.A), Acumic (India), BDH (England), Biobasic (Canada), Biomark (India), Biorad (U.S.A), Carlo Erba (French), Criterion (USA), Fluka (Switzerland) , Genplus (USA), J.T. Baker (USA), Kanto-Chemica (Japan), Lab-Scan (Ireland), Labchem (Australia), Merck (Germany), Riedel de Haen (Germany), Scharlua (Spain), Sigma-Aldrich (U.S.A), Univar (Australia), and Wako (Japan).

2.3 Restriction enzymes and DNA modifying enzymes

Restriction enzymes and DNA modifying enzymes used in this work are listed in Table 2.2

Table 2.2 List of the enzymes used in this work

Enzyme	Supplier
Lysozyme	Sigma, U.S.A.
<i>Pfu</i> DNA polymerase	Promega, U.S.A
<i>Phusion</i> DNA polymerase	New England Biolabs, USA
PrimeStar HS DNA polymerase	TAKARA Bioscience, Japan
Proteinase K	GIBCOBRL, USA
Restriction endonucleases	New England Biolabs, USA Fermentas, Sweden Roche, Switzerland TAKARA Bioscience, Japan
RNase A	Sigma, USA
T ₄ DNA ligase	New England Biolabs, USA
<i>Taq</i> DNA Polymerase	Fermentas, Sweden

2.4 Plasmid vectors

The following plasmids used in this work are shown in Table 2.3

Table 2.3 List of plasmid vectors

Plasmid vector	Purpose of use	Supplier
pBlueScript/SK ⁻	Cloning vector	Stratagene, USA
pET17b	Expression vector	Invitrogen, German
pET19b	Expression vector	Invitrogen, German
pGEM T-easy	Cloning vector	Promega, USA

2.5 Microorganisms

Table 2.4 summarized the bacteria used throughout.

Table 2.4 List of microorganisms

Bacterial strain	Relevant Characteristics	Supplier or Source
<i>B. circulans</i> PP-8	Reported as a levan producing bacterium [87]	Isolated from soil in Thailand [88]
<i>B. licheniformis</i> PR-1	<i>ls</i> ⁺	Isolated from soil in Thailand [89]
<i>B. licheniformis</i> RN-01	<i>ls</i> ⁺	Isolated from soil in Thailand
<i>B. licheniformis</i> SK-1	<i>ls</i> ⁺	Isolated from soil in Thailand [90]
<i>B. licheniformis</i> TH4-2	<i>ls</i> ⁺	Isolated from soil in Thailand [91]
<i>Bacillus</i> sp. TN-1	<i>ls</i> ⁺	Isolated from fermented bean
<i>E. coli</i> BL21(DE3) plysS	F ⁻ <i>ompT hsdSB</i> (rB-mB-) <i>gal dcm</i> (DE3) pLysS (Cam ^R)	Invitrogen
<i>E. coli</i> DH5- α	F ⁻ ϕ 80 <i>lacZ</i> Δ M15 Δ (<i>lacZYA-argF</i>)U169 <i>deoR recA1 endA1 hsdR17</i> (r _k ⁻ , m _k ⁺) <i>phoA supE44 thi-1 gyrA96 relA1 λ</i> ⁻	Invitrogen
<i>E. coli</i> Rosetta (DE3) pLysS	F ⁻ <i>ompT hsdS</i> (r _{BmB}) <i>gal dcm lacY1</i> (DE3) pLysSRARE (Cm ^R)	Invitrogen
<i>E. coli</i> TOP10	F ⁻ <i>mcrA</i> , Δ (<i>mrr-hsdRMS-mcrBC</i>) ϕ 80 <i>lacZ</i> Δ M15 Δ <i>lacX74 deoR recA1 araD139 Δ(ara-leu) 7697galU galK rpsL</i> (Str ^R) <i>endA1 nupG</i>	Invitrogen
<i>E. coli</i> XL-10 Gold	Tet ^r Δ (<i>mcrA</i>)183 Δ (<i>mcrCB-hsdSMR-mrr</i>)173 <i>endA1 supE44 thi-1 recA1 gyrA96 relA1 lac Hte</i> [F ⁻ <i>proAB lacIqZ</i> Δ M15 Tn10 (Tet ^r) Amy Cam ^r]	STRATAGENE

2.6 Computer Programs

The computer programs and server links used in this study are listed in Table 2.5

Table 2.5 List of computer programs

Program/Server	Purpose of use	Provider/WEB server
Bioedit	Restriction and plasmid map drawing	Tom Hall, Ibis Biosciences, USA
Blast [92]	Similarity searching	http://blast.ncbi.nlm.nih.gov
ConSurf [93]	Identification of functional region in proteins	http://consurftest.tau.ac.il
ClustalW [94]	DNA/protein alignment	http://www.clustal.org
ExPaSy [95]	Nucleotide and amino acid sequences analysis	http://expasy.org
GenBank	DNA data bank	http://www.ncbi.nlm.nih.gov
Molecular Evolutionary Genetics Analysis version 5 (MEGA5)[96]	Software for building sequence alignments and phylogenetic trees	http://www.megasoftware.net
Molegro Virtual Docker 2008 3.0.0 (MVD 2008 3.0.0)	Predicting protein-ligand interactions	Molegro ApS, Denmark
Primer premier 5	PCR primer design	Premier Biosoft, USA
Primer X	The automate site-directed mutagenic primers design	Carlo Lapid and Yimin Gao, Philippines
Protein DATA Bank	Retrieving the 3D structure of proteins	http://www.rcsb.org
PyMOL; Molecular Graphics System	Protein 3D structure visualization	Schrödinger LLC., USA
QMEN4 [97]	3D Structure assessment	http://swissmodel.expasy.org/qmean/cgi/index.cgi

Table 2.5 List of computer programs

Program/Server	Purpose of use	Provider/WEB server
SignalP [98]	Protein localization prediction	http://www.cbs.dtu.dk/services/SignalP
SuperPose 1.0 [99]	Protein superimposition server	http://wishart.biology.ualberta.ca/SuperPose
SWEET2 [100]	Construction of saccharides 3D models	http://www.glycosciences.de
SWISS MODEL [101]	Protein 3D structure prediction	http://swissmodel.expasy.org

2.7 Media preparation

2.7.1 Luria-Bertani (LB medium)

LB broth consisted of 1% (w/v) tryptone, 0.5% (w/v) yeast extract and 0.5% (w/v) NaCl. For solid medium, 1.5% (w/v) agar was added.

2.7.2 3x Luria-Bertani (3xLB medium)

3xLB consisted of 3% (w/v) tryptone, 1.5% (w/v) yeast extract and 1.5% (w/v) NaCl.

2.7.3 Terrific broth

The medium consisted of 1.2% (w/v) tryptone, 2.4% (w/v) yeast extract and 0.004 % (v/v) glycerol, after sterilized, 10 mL phosphate mixture (0.17M KH_2PO_4 and 0.72 M K_2HPO_4) was separately added.

2.7.3 SOC-medium

The components of the SOC medium are 0.5% (w/v) yeast extract, 2% (w/v) tryptone, 10 mM NaCl, 2.5 mM KCl, 10 mM MgCl_2 , 10 mM MgSO_4 and 20 mM glucose.

If required, the antibiotic was added after media was cooled down to below 50 °C. Depending on the plasmid and bacterial strain, the following concentrations of antibiotic were used.

Table 2.6 Antibiotics

Antibiotic	Final concentration ($\mu\text{g/mL}$)
Ampicillin	100
Chloramphenicol	34
Streptomycin	25

2.8 Bacterial growth conditions

B. circulans, *B. licheniformis* and *B. subtilis* were grown at 37 and 50 °C in LB or 5-20% (w/v) sucrose containing medium, respectively. *E. coli* was grown at 37 °C in LB medium. For liquid medium, the cells were cultured in above conditions with shaking at 250 rpm.

2.9 Storage of bacteria

Freshly grown bacteria were suspended in 1 mL of 15% (v/v) glycerol and stored at -80 °C.

2.10 DNA manipulation techniques

Molecular biological methods used in this work were derived from standard methods and protocols [102], [103].

2.10.1 Chromosomal DNA extraction

Bacterial cells were cultured in LB broth or appropriate media (1.5 mL) and harvested by centrifugation at 5000 x g, 4 °C for 3 min. The packed cells were resuspended in 450 μL of SET buffet (50 mM sucrose, 25 mM Tris-HCl, pH 8.0, 10 mM Na_2EDTA , containing 5 $\mu\text{g/mL}$ lysozyme and 20 $\mu\text{g/mL}$ RNaseA), mixed well by inverting. The mixture was incubated at 37 °C for 1 h. Then 50 μL of 10% (w/v) SDS was added together with 20 $\mu\text{g/mL}$ ProteinaseK, incubating at 50 °C for overnight. A 50 μL of 5.0 M CH_3COONa was added, following by protein extraction by one volume of phenol: chloroform: isoamyl alcohol (25:24:1). After centrifugation at 10,000 x g for 10 min, aqueous phase was collected. To precipitate DNA, two volumes of absolute alcohol were added. The DNA was collected by

adhere to swirling pipette tip and then washed with 70% (v/v) ethanol and air dried for 10 min. The DNA pellet was dissolved in TE buffer or sterile water.

2.10.2 Preparation of competent cells

A single colony of *E. coli* was cultured as a starter in 2 mL of LB-broth and incubated at 37 °C with 250 rpm shaking for an overnight. The starter was diluted in 200 ml of LB-broth, and the culture was incubated at 37 °C with 250 rpm shaking until the optical density at 600 nm of the cells reached 0.5-0.6 (~3-4 h). The culture was chilled on ice for 15 min and the cells were harvested by centrifugation at 5,000 x g for 15 min at 4 °C. The supernatant was discarded. The cell pellet was washed twice with 1 volume and 0.5 volume of cold sterile ultra-pure water, respectively. The cells were resuspended and centrifuged at 5,000 x g for 15 min at 4°C. The supernatant was discarded. The pellet was washed with 10 ml of ice cold sterile 10% (v/v) glycerol, and finally resuspended in a final volume of 1-2 mL of ice cold sterile 10% glycerol. The cell suspension was divided into 40 µL aliquots and store at -80°C until used.

2.10.3 Transformation

2.10.3.1 Electro-transformation

The competent cells were thawed on ice. Forty mL of the cell suspension was mixed with 1-2 µL of the ligation mixture. Then mixed thoroughly and placed on ice for 1 min. The mixture was electroporated in a cold 0.2 cm cuvette with the apparatus setting as follows; 2.5 µF, 200 Ω of the pulse controller unit and 2.50 kV. After one pulse was applied, the cells were resuspended in 1 mL of LB broth and incubated at 37 °C for 1 h with shaking at 250 rpm. The cell culture was spread on the LB agar, containing ampicillin and/or appropriated amount of IPTG and X-gal for the blue-white colony screening.

2.10.3.2 Heat shock transformation

An *E. coli* Top-10 Ultra-competent was thawed on ice. Mutagenic PCR products were mixed with the competent and incubated on ice for 30 min. The sample was immediately heated to 42 °C for 90 s. Then 500 µL of SOC-medium were added into the cells, followed by shaking at 250 rpm 37 °C for 1 h.

2.10.4 Plasmid preparation

Plasmid harboring cells were cultured in LB broth (1.5 ml) and harvested by centrifugation at 5000 x g, 4°C for 3 min. The packed cells were resuspended in 100 µL of

Solution I (25 mM Tris-HCl, pH 8.0, 10 mM Na₂EDTA and 50 mM glucose), mixed by vortexing well and kept on ice for 15 min. A 200 µL of Solution II (1% SDS, 0.2 N NaOH) was added, mixed by inversion and kept on ice for 5 min. The mixture was neutralized by adding 150 µL of Solution III (3 M sodium acetate, pH 4.8), mixed by inversion and kept on ice for 30 min. After centrifugation at 10,000 x g for 10 min, aqueous phase was collected. The supernatant was extracted with one volume of phenol: chloroform: isoamyl alcohol (25:24:1). Two volumes of absolute alcohol were added, mixed and stored at -20 °C for 30 min. The plasmid was pelleted by centrifugation at 10,000 x g for 10 min, washed with 70% (v/v) ethanol and air dried for 10 min. The pellet was dissolved in TE buffer containing 20 µg/mL DNase-free RNaseA.

2.10.5 Agarose gel electrophoresis

To determine the size of DNA using 0.7-1.5% agarose gel in TAE buffer (40 mM Tris-HCl, 20 mM acetic acid and 2 mM EDTA, pH 8.0), DNA samples with 1x tracking dye were loaded into the wells. The gels were run at 100 volts for 1 h, or until bromophenol blue reached the bottom of the gel. After electrophoresis, the gels were stained with ethidium bromide solution (2.5 µg/mL) for 2-5 min, and the DNA bands were visualized under UV light from UV transilluminator. The gels were photographed through SynGene gel documentation. The sizes of DNA fragments were determined by comparing the relative mobility with those of the standard DNA fragments (λ /HindIII).

2.10.6 DNA fragment extraction from agarose gel

To extract the DNA fragment from agarose gels, the gel extraction kits (QIAGEN, USA and Geneoid, Taiwan) were used as recommended by the manufacturer.

2.10.7 Restriction digest

Digestions of DNA with restriction endonucleases were performed under the standard procedure. Reaction buffers, conditions and DNA concentrations were chosen according to manufacture technical references.

2.10.8 Ligation of DNA fragment

For sticky end ligation, the digested insert DNA and proportional linearized plasmid DNA were mixed with 1 unit of T4 ligase in ligation buffer, providing by the manufacturer.

The ligation mixtures were incubated in ice-bucket, using the starting temperature of 10 °C. Let the reaction proceed for overnight.

For blunt end ligation using pGEM-T easy ligation kit, the reaction was performed followed the manufacturer procedure.

2.10.9 Design and synthesis of oligonucleotide primers

To design the PCR primer for whole gene amplification, Primer premier 5 was used to design and analyze the oligonucleotide. For mutagenic PCR primer, PrimerX server was used to design the primer based on *E. coli* codon usage. The PCR primers used in this study were shown in Table 2.7. The PCR primers were made by order by First Base, Singapore and Invitrogen, Japan.

2.10.10 Amplification of DNA by Polymerase Chain Reaction (PCR)

The amplification of *ls* from chromosomal or plasmid DNA was carried out by PCR, using DNA polymerase with proof-reading activity. Standard PCR mixtures of 50 μ L contained template DNA (50 ng of chromosomal DNA/ 20 ng of plasmid DNA or under manufacturer recommend), forward and reverse primer (0.25 pmole each), Deoxyribonucleotide; dNTPs (0.2 mM each), DNA polymerase and the appropriate reaction buffer. PCR was performed by a program according to polymerase's manufacture technical references.

For an error-prone PCR[104], *Taq* polymerase was used because of its naturally high error rate, with errors biased toward AT to GC changes. To compensate the enzyme bias, 0.2 μ M each of dGTP and dATP and 1.0 μ M each of dCTP and dTTP were used. And the error rate of DNA polymerase was promoted by adding 50-250 mM $MnCl_2$. The PCR fragments were ligated to pBlueScript/SK⁻ and transformed into *E. coli* Top-10, resulting in a mutated library.

For site-directed mutagenesis, the PCR reaction and conditions were employed using Quick Change site-directed mutagenesis protocol as briefly described. The whole plasmids amplification and incorporation of mismatch nucleotides were simultaneously performed using DNA polymerase with proof-reading activity. Only are 16-18 PCR cycles performed to minimize PCR errors. To remove the parental DNA, the dam methylated DNAs were digested with *DpnI*, following by directly transformed into *E. coli* competent.

2.10.11 DNA sequencing

To check the identity of the inserted DNA, the correct construction and the successful modification of plasmid DNA, nucleotide sequencing was performed by First Base Nucleotide Sequencing Service. All oligonucleotide primers used in this work were listed in Table 2.7.

2.11 Bacterial Identification

Bacillus strain TN-01 was species identified based on its biochemical characteristics and similarity of 16s rRNA gene.

2.11.1 Biochemical characteristics

Culture of TN-01 was physiologically and biochemically characterized by The National Institute of Health, Department of Medical Sciences, Ministry of Public Health, Thailand.

2.11.2 Characterization of 16S rRNA gene [105]

The partial 16S ribosomal RNA gene of the strain TN-01 was *in vitro* amplified via the PCR technique. The amplified PCR product was purified and cloned into pGEM T-easy, then transformed to *E. coli* Top-10. The recombinant colonies were selected by blue-white colony screening. The plasmid containing 16S ribosomal RNA gene was subjected to sequence by First Base Sequencing Service. The sequence of 16S rRNA gene was aligned with others obtained from GenBank using BLAST.

Table 2.7 PCR primers

Name	Length (base)	Sequence (5' to 3')	Restriction site	Purpose of use
F-pA	20	AGAGTTTGATCCTGGCTCAG	-	Amplification of 16s rRNA gene
R-pD	18	CAGCAGCCGCGGTAATAC	-	Amplification of 16s rRNA gene
F-BILs	36	<u><i>TGCTCTAGA</i></u> CGATTCCCGCTTATACAGACTATAGAT	<i>Xba</i> I	Amplification of levansucrase gene from <i>B. licheniformis</i>
R-BILs	33	<u><i>CGGGATCC</i></u> TTATTTGTTTACCGTTAGTTCTCCC	<i>Bam</i> HI	Amplification of levansucrase gene from <i>B. licheniformis</i>
F-BsLspET	31	<u><i>CGCCATATG</i></u> AACATCAAAAARWTTGYAAAAC	<i>Nde</i> I	Amplification of levansucrase gene from <i>B. subtilis</i> and clone to pET17b
R-BsLspET	36	<u><i>CGGGATCC</i></u> TTATTGWGTTRACTGTYARYTGTTCCTTG	<i>Bam</i> HI	Amplification of levansucrase gene from <i>B. subtilis</i> and clone to pET17b
F-BILspET	35	CAT <u><i>GCCATGG</i></u> ACATCAAAAACATTGCTAAAAAAGC	<i>Nco</i> I	Amplification of levansucrase gene from <i>B. licheniformis</i> and clone to pET19b

* Restriction site and enzyme-clamp site were shown in bold italic-underlined and italic-underlined alphabets, respectively.

Table 2.7 PCR primers

Name	Length (base)	Sequence (5' to 3')	Restriction site	Purpose of use
F-Y194A	34	CCGGCACGCAAG <u>CGGG</u> CAAGCAGACGCTGACAAC	-	Substitution of Y194 with A
R-Y194A	34	GTCTGCTTGCC <u>CGCT</u> TGCGTGCCGGAAAAAGCTG	-	Substitution of Y194 with A
F-Y194W	34	TTCCGGCACGCAAT <u>GGGG</u> CAAGCAGACGCTGAC	-	Substitution of Y194 with W
R-Y194W	34	GCGTCTGCTTGCC <u>CC</u> ATTGCGTGCCGGAAAAACG	-	Substitution of Y194 with W
F-N251A	37	CTACAGCTCCGGCGAC <u>GCGC</u> ATACGATGAGAGACCCG	-	Substitution of N251 with A
R-N251A	37	CGGGTCTCTCATCGTAT <u>GCGC</u> GTCCGGAGCTGTAG	-	Substitution of N251 with A
F-N251D	30	CTACAGCTCCGGCGAC <u>GATC</u> ATACGATGAG	-	Substitution of N251 with D
R-N251D	30	GGTCTCTCATCGTAT <u>GATC</u> GTCCGGAGC	-	Substitution of N251 with D
F-N251K	28	AGCTCCGGCGACAA <u>A</u> CATACGATGAGAG	-	Substitution of N251 with K
R-N251K	28	TCTCTCATCGTATG <u>T</u> TTGTCCGGAGC	-	Substitution of N251 with K
F-N251Y	30	GCTCCGGCGACT <u>ATC</u> ATACGATGAGAGACC	-	Substitution of N251 with Y
R-N251Y	31	GTCTCTCATCGTAT <u>GATG</u> TCGCCGGAGCTG	-	Substitution of N251 with Y
F-Y246A	32	TTGACGAAGGAAAC <u>GCG</u> AGCTCCGGCGACAAC	-	Substitution of N246 with A
R-Y246A	32	TTGTCGCCGGAGCTC <u>GCG</u> TTTCCTTCGTCAAT	-	Substitution of N246 with A

* Mutagenic nucleotides were shown in underlined alphabets

Table 2.7 PCR primers

Name	Length (base)	Sequence (5' to 3')	Restriction site	Purpose of use
F-Y246D	35	CATTGACGAAGGAAAC <u>GAT</u> AGCTCCGGCGACAACC	-	Substitution of N246 with D
R-Y246D	35	GGTTGTCGCCGGAGCT <u>ATC</u> GTTTCCTTCGTCAATG	-	Substitution of N246 with D
F-Y246F	31	TGACGAAGGAAACT <u>TT</u> AGCTCCGGCGACAAC	-	Substitution of N246 with F
R-Y246F	31	TTGTCGCCGGAGCT <u>AA</u> AGTTTCCTTCGTCAA	-	Substitution of N246 with F
F-Y246I	36	TCATTGACGAAGGAAAC <u>ATT</u> AGCTCCGGCGACAACC	-	Substitution of N246 with I
R-Y246I	36	TGGTTGTCGCCGGAGCT <u>AAT</u> GTTTCCTTCGTCAATG	-	Substitution of N246 with I
F-Y246L	34	ATTGACGAAGGAAAC <u>CTG</u> AGCTCCGGCGACAACC	-	Substitution of N246 with L
R-Y246L	34	GTTGTCGCCGGAGCT <u>CAG</u> GTTTCCTTCGTCAATG	-	Substitution of N246 with L
F-Y246S	32	TTGACGAAGGAAAC <u>AGC</u> AGCTCCGGCGACAAC	-	Substitution of N246 with S
R-Y246S	31	GGTTGTCGCCGGAGCT <u>CTG</u> CTGTTTCCTTCGTTC	-	Substitution of N246 with S
F-Y246W	32	TTGACGAAGGAAACT <u>GG</u> AGCTCCGGCGACAAC	-	Substitution of N246 with W
R-Y246W	31	GGTTGTCGCCGGAGCT <u>CC</u> AGTTTCCTTCGTTC	-	Substitution of N246 with W
F-N414T	35	CATATGGACCAGGATTAC <u>CCG</u> ACATCACGTTTAC	-	Substitution of N414 with T
R-N414T	35	AATAAGTAAACGTGATG <u>TCCG</u> TGTAATCCTGGTCC	-	Substitution of N414 with T

* Mutagenic nucleotides were shown in underlined alphabet

2.12 protein manipulation techniques

2.12.1 Production of Ls by selected bacteria

To screen for high Ls producing bacterium, 6 isolated strains; *B. circulans* PP-8, *B. licheniformis* PR-1, *B. licheniformis* RN-01, *B. licheniformis* SK-1, *B. licheniformis* TH4-2 and *Bacillus sp.* TN-1 available in our research group were cultured in different media. The single colony of each strain was grown in LB medium at optimal temperature indicated in 2.8 for overnight then using as a starter culture. The starters at OD₆₀₀ around 2 units were inoculated to 1% (v/v) inoculums into LB containing 5-25% (w/v) sucrose. The Ls production time courses were investigated over 5 days-culture period. Every 24 h, 2 mL of culture medium was withdrawn. Ls activities in different subcellular fractions were explored.

2.12.2 Expression of levansucrase in *E. coli*

To maximize expression of *ls* gene, two expression systems were compared

2.12.2.1 Expression of *ls* under putative endogenous promoter

To compare the activity of recombinant levansucrases from *B. licheniformis* RN-01, SK-1 and TH4-2, recombinant plasmids carried *ls* from those bacteria were transformed into *E. coli* Top-10. The Ls activities in LB medium were monitored over 4 days-culture period. The highest Ls producing-recombinant was further optimized. The selected recombinant plasmid (*p_{ls}RN*) was re-transformed into three different *E. coli* strains: DH-5 α , Top-10 and XL-10 Gold, then grown in LB, 3xLB and terrific broth. *E. coli* starters at around 2 units of OD₆₀₀ were 1% inoculated to each medium, shaking at 250 rpm, 37 °C. The cultures were collected at 6 h interval for 48 h. Ls activity in extracellular, periplasmic and cytosolic fractions (see 2.12.3) was investigated.

2.12.2.2 Expression of *ls* under T7 promoter

To express under T7 promoter, the recombinant plasmid was re-transformed to expression host, *E. coli* BL-21(DE3)*pLysS* and *E. coli* Rosetta (DE3)*pLysS*. *E. coli* starters at around 2 units of OD₆₀₀ were 1% inoculated to LB, 3xLB and terrific broth, shaking at 250 rpm, 37 °C. Until OD₆₀₀ reached 0.4, 1 M IPTG was added to initiate the induction. The induced samples were collected over 16 h. Ls activity in culture medium and total cellular proteins were examined.

2.12.3 Protein subcellular fractionation

Protein subcellular fractionation was performed according to Coligan, 2003. The culture media were centrifuged at 5000 x g for 10 min and the collected supernatants were designated as the extracellular protein fraction. To prepare the periplasmic proteins, cell pellets obtained were then washed by phosphate buffer saline. The cell pellets were resuspended in 100 L of ice cold osmotic-shock solution (20% w/v sucrose, 10 mM Tris-HCl, 2.5 mM EDTA), leaving the mixture on ice for 10 min then centrifuge to collect the shocked cells. The periplasmic proteins were released by resuspended in 200 µL of 10 mM citrate buffer, pH 6.0 and then centrifuged to collect the supernatant periplasmic fraction. The remaining pellets were further resuspended in 50 mM citrate buffer, pH 6.0 and sonicated 4-15 sec at medium power. After centrifugation at 10,000 x g at 4 °C for 10 min, the supernatants were collected and designated as the cytosolic fractions.

2.12.4 Preparation of total cellular protein (TCP)

To prepare a total cellular protein, the freeze-thawing method was used. The cell pellets were resuspended in 50 mM citrate buffer, pH 6.0 and subsequently frozen at -80 °C for 30 min. The frozen cells were immediately thawed in 37°C water bath for 10 min. Repeated the steps for three times and followed by centrifuge at 10,000 x g at 4 °C for 10 min to collect the total cellular protein.

2.12.5 Protein purification

The culture medium was harvested by centrifugation, then diluted to 4 fold in order to decrease NaCl concentration of the crude enzyme and directly loaded onto a DEAE-Toyopearl-650M (Tosoh Bioscience) column (2.4 x 22 cm i.d.) equilibrated with 50 mM sodium acetate buffer (pH 6.0). After unbound protein wash, elution was performed by applying a linear NaCl gradient with increase in NaCl concentration from 0 to 1 M in the same buffer. The 4 mL fractions were collected and monitored for protein by the absorbance at 280 nm as well as for Ls activity. The active fractions were then pooled and loaded onto a Butyl-Toyopearl-650M (Tosoh Bioscience) column (1.5 x 6 cm i.d.) equilibrated with 25 mM sodium acetate buffer, pH 6.0 containing 1.33 M ammonium sulfate. Elution was made with a linear $(\text{NH}_4)_2\text{SO}_4$ gradient with decrease in $(\text{NH}_4)_2\text{SO}_4$ concentration from 1.33 to 0 M in the in 25 mM sodium acetate, pH 6.0. Ls enzyme active fractions were then pooled, dialyzed and stored at 4 °C.

2.12.6 Mw determination by gel filtration chromatography

To estimate the Mw of Ls, the purified enzyme was applied to a Sephadex G75 (SF) (Amersham Pharmacia Biotech, USA) column (2 x 37.5 cm i.d.). The column was previously conditioned with 25 mM sodium acetate buffer (pH 6.0), containing 0.15 M NaCl. The 2 mL fractions were collected and monitored for protein by the absorbance at 280 nm as well as for Ls activity. The fraction with highest Ls activity was used in the Mw estimation. Elution volume was compared with those of BSA (65 kDa), ovalbumin (43 kDa) and chymotrypsin (25 kDa).

2.12.7 Determination of protein concentration

Protein concentrations were determined using modified Bradford method[106]. 800 μ L of dye solution (0.5% (w/v) Coomassie Brilliant Blue G-250, 25% (v/v) absolute ethanol and 50% (v/v) of 85% phosphoric acid) were added in to 200 μ L of protein solution. The mixtures were stand for 15 min to complete binding of the dye to protein, The absorbance was measured at 595 nm. A standard curve was constructed using bovine serum albumin at various concentrations from 0-15 μ g.

2.12.8 Protein precipitation by trichloroacetic acid (TCA)

10% (w/v) TCA was added to protein solution, mixed and left on ice for 30 min. After collected the protein pellet by centrifugation at 10,000 x g for 10 min, the pellet was washed with ice-cold acetone. The air-dried pellet was redissolved in 50 mM citrate, pH 6.0.

2.12.9 Analysis of Ls by sodium-dodecyl-sulfate-polyacrylamide gel electrophoresis (SDS-PAGE)

The protein samples were analyzed by SDS-PAGE with coomassie blue staining for protein and Ls activity zymogram staining for enzyme activity.

For SDS-PAGE, proteins were loaded onto a mini protein gel apparatus (Bio-Rad). The acrylamide content in the stacking and separating gels were 5% and 10%, respectively. The electrophoresis was conducted at a constant current of 20 mA for each gel slap. The gels were then stained for 30 min with a staining solution (1% (w/v) Coomassie Brilliant Blue R250, 45% (v/v) methanol and 10% (v/v) glacial acetic acid), followed by destaining solution (10% (v/v) methanol and 10% (v/v) glacial acetic acid). The molecular weight of Ls was estimated by comparing the migration distance to those of molecular weight standard proteins.

For the in-gel Ls activity assay (Zymogram), after SDS-PAGE, the SDS in the denaturing gel was removed by soaking in 0.1% (v/v) TritonX-100 in 50 mM sodium acetate buffer (pH 6.0) for 2 h. The excess Triton-X was then removed by washing the gel in deionized water then performed enzymatic reaction by soaking overnight in 20% (w/v) sucrose in the same buffer. The position of the enzyme on the gel was observed by the accumulation of the mucous-like levan product.

2.13 Characterization of Levansucrase

2.13.1 Levansucrase activity assay

Three enzymatic activities were assayed using sucrose as substrate in a temperature-controlled water bath. The hydrolytic (A) and transfructosylation (B) activities of Ls, as shown in the following reactions:



Where Fru is fructose, Glc-Fru is sucrose, Glc is glucose, GlcFru_n and $\text{GlcFru}_{(n+1)}$ are FOSs (fructooligosaccharides) and/or levan.

From above equations, sucrose conversion by Ls yields i) fructose, which is then partly coupled to the growing levan polymer, and ii) glucose in a 1:1 molar ratio to the amount of sucrose converted. Subtracting the total amount of reducing sugar by amount of glucose indicated the amount of free fructose in the reaction.

The hydrolysis activity was indicated by amount of free fructose in the reaction. One hydrolytic unit of Ls is defined as the amount of the enzyme produced 1 μmol of the fructose per min.

The transfructosylation activity was indicated by the amount of glucose minus the amount of free fructose. One transfructosylation unit of Ls is defined as the amount of the protein released 1 μmol of glucose as a result of transferring fructose, per min.

The third Ls activity was the total Ls activity which was indicated by the amount of total reducing sugar in the reaction. One unit of total Ls activity was defined as the amount of the enzyme liberated 1 μmol of the reducing sugars (glucose and fructose) per min.

The total amount of free glucose was determined by a glucose oxidase-peroxidase kit (WAKO Chemical) under manufacturer recommendation.

The total reducing sugars (glucose plus fructose) was determined using the DNS method [107]. The release of reducing sugar was quantified by adding 500 μ L of the DNS solution (1% (w/v) 3, 5-dinitrosalicylic acid, 30% (w/v) potassium sodium tartrate and 0.2 M NaOH) into 500 μ L of sample solution. Boiled the mixture for 15 min and diluted 5 fold by distilled water. The absorbance of the reduction product was measured at 540 nm. A standard curve was constructed, plotting glucose concentration versus absorbance at 540 nm.

2.13.2 Optimum temperature and pH.

To determine the optimal reaction condition, 0.5 U of the purified enzyme was incubated with 20% (w/v) sucrose in 50 mM of broad range of pH varying from 3 to 9 using different buffer systems; sodium citrate buffer (pH 3.0-6.0), potassium phosphate buffer (pH 6.0-7.0) and Tris-HCl buffer (pH 7.0-9.0) and at various temperatures ranging from 20 to 60 $^{\circ}$ C.

2.13.3 Thermal and pH Stability

To determine thermal stability of Ls, the protein was pre-incubated either at various temperatures from 20-60 $^{\circ}$ C or with broad range of pH varying from 4 to 10. The enzyme samples were taken at 1 h interval for 2 h. The remaining activities were measured at optimal condition, comparing to those of the enzyme without pre-incubation.

2.13.4 Effect of metal ion and chelation agent on Ls activity

To investigate the effect of metal ions or the chelator EDTA on the Ls activity, the purified enzyme was dialyzed against 1 mM EDTA in 10 mM sodium acetate buffer, pH 6.0 to remove the bound ion. 0.5 U of purified Ls was then incubated at optimal conditions with or without the addition of 1 mM of the various metal ion chloride salts or EDTA. The remaining Ls activity was measured by using the control without salt or EDTA added as 100% Ls activity.

2.13.5 Acceptor specificity

To investigate the acceptor specificity of the enzyme, mono-, di-saccharide and sugar alcohol were used in this investigation. The reactions were incubated at optimal conditions with 0.5, 1.5 and 2.5 M acceptor molecules (molar ratio of sucrose and acceptor molecule was 1:1, 1:1.5 and 1:2.5, respectively). The acceptor reaction products were analyzed by thin layer chromatography.

2.13.6 Kinetic parameters

For determination of kinetic parameters, initial rate measurements were performed at the optimal condition by addition of Ls enzyme to the reaction supplemented with sucrose concentrations ranging from 3.13 to 100 mM. The measurements were plotted on a saturation curve of the initial reaction rate (V) versus sucrose substrate concentration (S) and converted to the Lineweaver-Burk plot in order to compute the apparent Michaelis-Menten constant (K_m) and the maximum velocity (V_{max}) for both transfructosylation and hydrolytic activities of the enzyme.

2.14 Production and identification of levan polysaccharide

2.14.1 Effect of temperature and NaCl concentration on polymer size

To determine the factors that affect the M_w of synthesized levan, 20 U of the purified Ls was incubated overnight in 20% (w/v) sucrose at 30 and 50 °C with or without the addition of 0.5 M NaCl. The levan products from each reaction were harvested (see 2.14.2), lyophilized and purified (see 2.14.3) prior to analysis by High Performance Liquid Chromatography.

2.14.2 Production of levan polymer

In order to produce the levan polymer, 20 U of the Ls was incubated overnight in 20% (w/v) sucrose at the optimal conditions. The levan product was then recovered by adding 2 volumes of absolute ethanol and harvested by centrifugation at 10,000 x g for 10 min. The pellet was resuspended in deionized water and consecutively dialyzed against deionized water for 24 h. The dialyzed levan was lyophilized for further purification by Bio-gel P-100.

2.14.3 Purification of levan polymer by Bio-Gel P100

The lyophilized levan was dissolved to 20 mg/mL and passed through a Bio-Gel P100 (Bio-Rad) column (4 x 40 cm i.d.), using deionized water as a running solution. The 5 mL fractions were collected and monitored for total carbohydrate by phenol-sulfuric acid method [108]. The carbohydrate fractions were pooled and lyophilized for further NMR identification.

2.14.4 Identification of levan by Nuclear magnetic resonance

The levan was dissolved in D₂O and the spectra were obtained at 40 °C on a Varian VNMRS-500 operating at 125 MHz for ¹³C and 500 MHz for ¹H. Chemical shifts were measured relative to dimethylsilapentane-5-sulphonate (DSS) as the internal standard.

2.15 Product size analysis

2.15.1 Purification of reaction product by activated charcoal

To analyze by TLC and MALDI-TOF-MS, mono- and di-saccharides were removed by activated charcoal mini-column. The activated charcoal was packed in microcentrifuge tube. The reactions were applied to the column. Washed off by deionized water and 5-10% (v/v) ethanol was the small saccharides. Elution of tri- to longer saccharides was by increasing ethanol concentration from 20-75% (v/v). The trace ethanol was removed and the eluted saccharides were concentrated simultaneously by vacuum drying.

2.15.2 Thin Layer Chromatography (TLC)

The reaction products were analyzed using TLC at room temperature by applying on silica thin-layer plates (TLC aluminium sheets 10 x 20, silica gel 60 F₂₅₄, MERCK, Germany). The saccharides were separated using three ascents in 1-butanol: acetic acid: deionized water 3: 3: 1. Saccharide spots were detected by dipping the plates into the detecting reagent (10% (v/v) concentrated sulfuric acid in ethanol), followed by heating at 110 °C for 10 min. The product size was determined by comparing the relative mobility to GlcFru_n (GF_n).

2.15.3 High Performance Liquid Chromatography (HPLC)

The molecular weight of purified levan fraction was estimated using Asahipak column (QF-510HQ) (Asahi Chemical Industry). The known molecular weight levans synthesized by *B. subtilis* were used as reference standard. Elution was by distilled water at a flow rate of 1.0 mL min⁻¹ at room temperature. The sugars were monitored with Gilson refractive index detector Model 131.

2.15.4 High Performance Anion Exchange Chromatography with Pulsed Amperometric Detection (HPAEC-PAD)

Separation of oligosaccharides was achieved by HPAEC-PAD, using CarboPac PA1, 4 mm x 250 mm (Dionex, USA). Elution was made at 35°C by a linear gradient of 0.6 M

sodium acetate (0-60 min, increasing from 0% to 100% sodium acetate; 60-65min, 100% sodium acetate) in 100mM NaOH with a flow rate of 1 mL min⁻¹. Detection was performed with an ED40 electrochemical detector with an Au working electrode, and an Ag/ AgCl reference electrode.

2.15.5 Matrix Assisted Laser Desorption Ionization-Time Of Flight Mass spectroscopy (MALDI-TOF MS)

The 0.5 μ L of saccharide sample was applied to an anchorchip target plate (Bruker Daltonics, Germany), to which was added a 0.5 μ L of matrix solution (1% (w/v) 2, 5-dihydroxybenzoic acid, 4% (v/v) acetonitrile and 0.6% (v/v) trifluoroacetic acid). MALDI-TOF MS spectra was obtained on an Axima-CFRplus (Shimadzu Kratos, Japan). In the MALDI-TOF MS reflector mode using negative ionization, ions were generated by a pulsed UV laser beam and accelerated to a kinetic energy of 20 kV.

2.16 Preparation and characterization of levan nanoparticles

2.16.1 Enzymatic synthesis of levan nanoparticles

To synthesize levan NPs, 20 U of the purified Ls was incubated in 20 % (w/v) sucrose under the optimal conditions for 16 h with shaking at 150 rpm. The levan NPs were harvested by centrifugation at 15,000 x g for 20 min. The nanoparticles packed at the bottom of the centrifuge tube were subsequently washed three times with deionized water and dialyzed for overnight.

2.16.2 Encapsulation of α -tocopherol

In order to encapsulate *O*-acetyl- α -tocopherol, the vitamin derivative was added directly into the above described sucrose-Ls enzyme reaction at a 1% (v/v) final concentration. The acetyl- α -tocopherol-encapsulated levan NPs and the excess vitamin derivative were separated by centrifugation. The encapsulated NPs packed at the bottom of the centrifuge tube were separated from the oil and aqueous phase and washed as described for the unencapsulated NPs.

2.16.3 Transmission electron microscopy (TEM) analysis of levan NPs

The NPs were diluted to a million-fold in deionized water. All diluted NP suspensions were sonicated for 5 min, dropped onto a carbon-copper grid and air dried for 24

h. TEM analysis was performed using a TEM H-7650 (Hitachi, Japan) at an accelerate voltage of 100 kV.

2.16.4 Atomic force microscopy (AFM)

To acquire AFM photographs, a glass slide was dipped into the obtained suspension to gain the smooth film of nanoparticles on surface of the glass slide, subsequently overnight air-dried. The photographs were taken, using Nano Scope IV (Veeco Metrology, USA)

2.16.5 Fourier transform infrared (FTIR) spectroscopy

FTIR spectra of levan NPs, *O*-acetyl- α -tocopherol and *O*-Acetyl- α -tocopherol-encapsulated levan NPs were compared. FTIR spectroscopy measurements employed KBr discs and thin film on a Spectrum One-FTIR spectrometer (Perkin Elmer, USA). The spectra were acquired at 650 – 4000 cm^{-1} with a 1 cm^{-1} resolution.

2.17 Molecular modeling technique

2.17.1 Prediction of 3D structure of Ls

The amino acid sequence was subjected to predict 3D-structure, using an automated mode of SWISS MODEL. The structure was specifically modeled based on x-ray structure of Ls from *B. subtilis* (1OYG).

2.17.2 Prediction of 3D structure of sugar ligands

The sugar ligand, raffinose and GF series used in molecular docking were 3D structure predicted by SWEET2. Because no evaluation algorithm combined in SWEET2, the predicted raffinose was superimposed to x-ray structure retrieved from the Protein Data blank.

2.18 Structure superimposition

Two superimposition means; PyMol and SuperPose were used to align protein structures. Only were the structures with RMSDs under 0.5 used in this work.

2.19 Molecular docking

To understand how saccharides bind to Ls, the molecular dockings were preformed using Molegro Virtual Docker 2008 3.0.0 (MVD).

2.18.1 Re-docking

To evaluate whether MVD or Hex produced good quality of docking model or not, x-ray structure of Ls from *B. subtilis* reported together with raffinose ligand (3BYN) was re-docked by those methods. The result models were superimposed and root mean square deviation (RMSD) was compared.

2.18.2 Docking of raffinose and GFs to Ls from *B. licheniformis*

The selected docking method from 2.18.1 was then used to predict the interaction of ligands to interested enzymes e.g. Ls from *B. licheniformis* and invertase from *T. maritima*.

2.18.3 Identification of amino acids involved in product size determination by structure superimposition

To explore which amino acids involved in product size determination, predicted ligand-bound structure of Ls from *B. licheniformis* and *B. subtilis* were compared to those of an invertase from *T. maritima* (1W2T), an enzyme catalyzes hydrolysis of sucrose with no transfructosylation activity.

CHAPTER III

RESULTS

3.1 Screening for high levansucrase-producing strains

By genome sequence database searching and through literature review, we found wide varieties of organisms have been reported to carry levansucrase gene either expressed or putative. Among them, *Bacilli* species that are available in our research group, *B. circulans*, *B. licheniformis* and *Bacillus* sp. were screened for levansucrase (Ls) production in this study.

Six isolated strains of 3 *Bacilli* species: *B. circulans* PP8, *B. licheniformis* PR-1, RN-01, SK-1, TH4-2 and *Bacillus* sp. TN-01 (Fig. 3.1) were cultured for 5 days in various media for Ls production. At one-day interval, subcellular fractions: extracellular, membrane-bound and cytosolic fractions were prepared as described in Materials and Methods. In LB medium, Ls activities of all 6 isolated strains were undetectable. In LB containing 5-20 % (w/v) sucrose, RN-01, SK-1, TH4-2 and TN-01 produced different level of Ls activity. The higher sucrose concentration in the media, the higher Ls activity produced. On the other hand, Ls activity from the strains PP8 and PR-1 were undetectable.

B. licheniformis RN-01 produced Ls both in extracellular and membrane-bound fractions while trace amount of activity was found in cytoplasmic fraction. The highest extracellular Ls activity of 3.7 U/mL with specific activity of 42.6 U/mg protein was observed in the medium containing 20% sucrose at day 3 of cultivation while activity decreased to 0.2 U/mL was found at day 5 (Fig 3.2 A). In the same medium, the highest membrane-bound Ls observed (5.5 U/mL with specific activity of 74.1 U/mg protein) at day 1 of cultivation, gradually decreased to negligible amount at day 5 (Fig 3.2 B). Thus, Ls activity was higher in membrane-bound than the extracellular fraction. Lower Ls activity was observed in LB medium containing 5-15% sucrose.

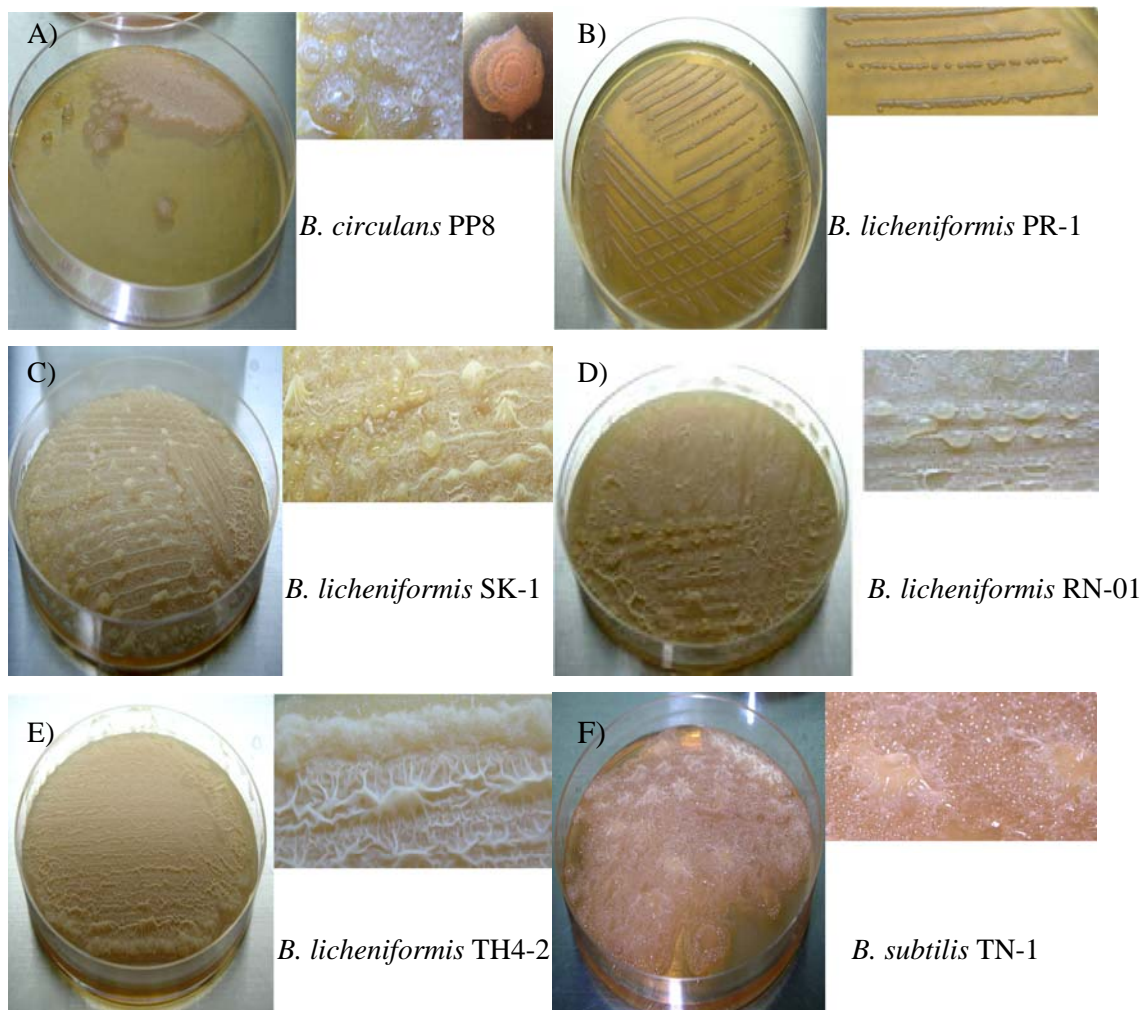


Figure 3.1 Morphology of 6 isolated strains used for levansucrase production on LB agar plate containing 5 % (w/v) sucrose

- | | | | |
|----|------------------------------|----|------------------------------|
| A) | <i>B. circulans</i> PP8 | B) | <i>B.licheniformis</i> PR-1 |
| C) | <i>B. licheniformis</i> SK-1 | D) | <i>B.licheniformis</i> RN-01 |
| E) | <i>B.licheniformis</i> TH4-2 | F) | <i>B.licheniformis</i> TN-1 |

Production pattern of Ls from three other strains: SK-1, TH4-2, and TN-1 (Fig 3.2 C–H) was more or less similar to what was observed with the strain RN-01 except productions in membrane-bound fraction of SK-1 and in extracellular fraction of TH4-2. For SK-1, highest specific activity was found in membrane-bound fraction at day 3 (Fig 3.2 D). For TH4-2, production pattern in both extracellular and membrane-bound fractions was similar, highest at day 1 (Fig 3.2 E-F). All strains showed higher Ls activity in membrane-bound fraction than in extracellular fraction. In addition, of all the four strains, RN-01 gave the highest value of enzyme specific activity (Fig 3.2 A)

3.2 Species identification of the isolate TN-1

Among six strains studied, only the TN-1 strain has not yet been species identified. Thus identification was carried out as follows.

3.2.1 Physiological and biochemical identification

Through physiological and biochemical properties, the TN-1 isolate was identified as *Bacillus lentus* (performed by The National Institute of Health, Department of Medical Sciences, Ministry of Public Health).

3.2.2 Characterization of a gene encoding for 16S ribosomal RNA

PCR amplification of partial 16S ribosomal RNA gene was performed by using chromosomal DNA of the TN-1 isolated strain as a template, giving the expected PCR product of 1.5 kb in size as shown in Fig 3.3 A. The PCR product was then ligated to pGEM T-easy and the resulted recombinant plasmid was designated as p16S TN-1 then transformed to *E. coli* Top-10. The recombinant colonies were selected by blue-white screening and verified the insertion as shown in Fig. 3.3 B. The positive recombinant plasmid which carried 1.5 kb inserted fragment was subjected to nucleotide sequence at First Base Sequencing service. The obtained sequence contained 1556 bp. Blastn based searching of the NCBI database showed the highest sequence similarity of 99% identity to the reported 16S rRNA gene of *B. subtilis* (GenBank accession number; AB110589.1). While only 93% identity was obtained when compared with the reported 16S rRNA gene of *B. lentus* (GenBank accession number; D16272.1) (Fig 3.4).

Since two identification techniques gave different result, we decided to designate this strain as *Bacillus* sp. TN-1.

3.3 Cloning of levansucrase gene by PCR technique

3.3.1 Cloning of *ls* from *B. licheniformis* by PCR technique

PCR amplification of *ls* was performed by using chromosomal DNA of the 4 isolated strains of *B. licheniformis*, as templates. The primers, BILs*Xba*I-F and BILs*Bam*HI-R, were designed based on a genome sequence of *B. licheniformis* ATCC14580. BILs*Xba*I-F was a specific primer with 25 bases, starting at 350 nucleotides upstream of the ATG start codon. BILs*Bam*HI-R was a specific primer with 27 bases, starting at 24 nucleotides upstream of a TAA codon. When used the chromosomal DNA of the strain RN-01, SK-1 and TH4-2 as the template, expected PCR products of approximately 1,800 bp in size were obtained. While no PCR product was found when used chromosomal DNA of the strain PR-1 as template (Fig 3.5). The PCR products were then harvested and digested with *Xba*I and *Bam*HI which were incorporated to the PCR products in an amplification step. The PCR products were subsequently ligated to pBlueScript(II)/SK⁻ and verified the insertion by restriction digested and agarose gel electrophoresis as shown in Fig 3.6. The positive clones which carried the 1.8 kb inserted fragment were designated as plsRN, plsSK and plsTH and subjected to nucleotide sequencing.

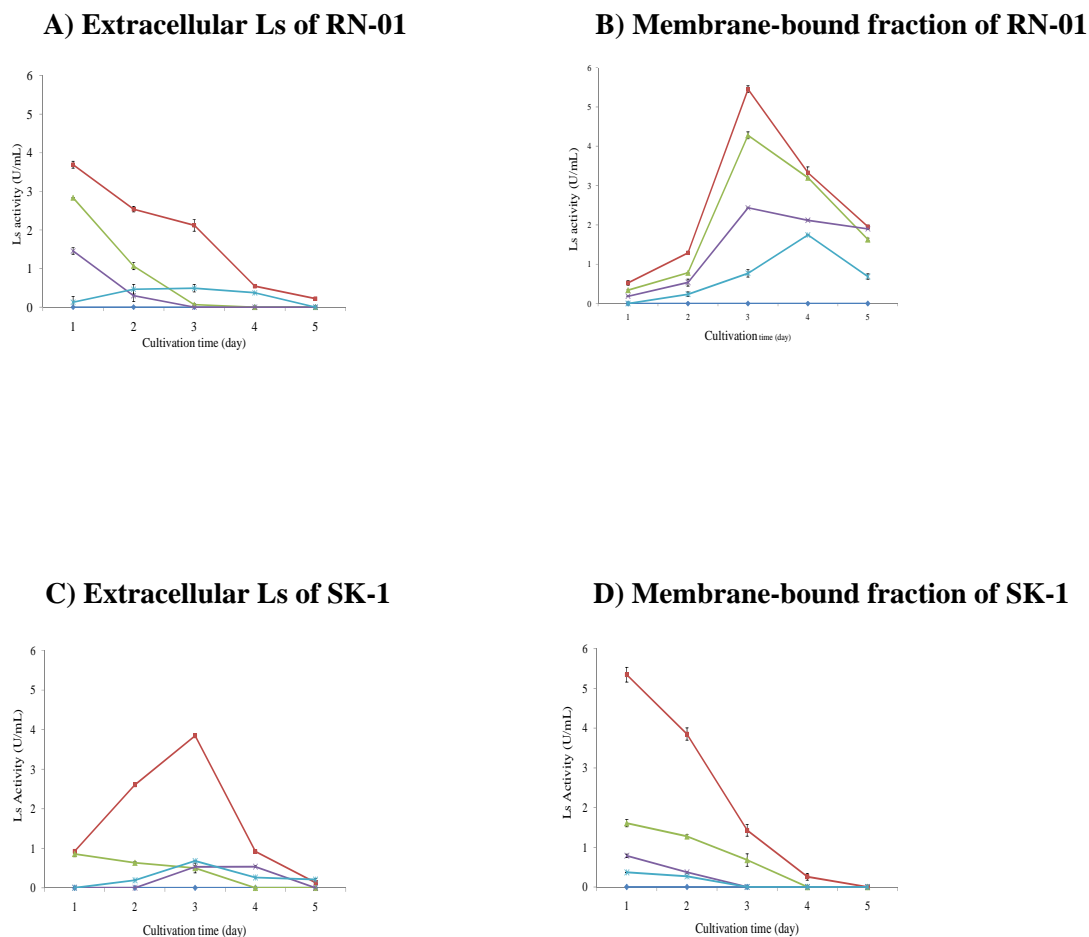


Figure 3.2 Levanucrase production by the isolated strains in LB medium containing 0-20% (w/v) sucrose

The isolated strains were grown in the LB medium containing 0% sucrose (◆), 5% sucrose (*), 10% sucrose (×), 15% sucrose (▲) and 20% sucrose (■). Ls activities of extracellular and membrane-bound fractions at each time point were measured according to methods.

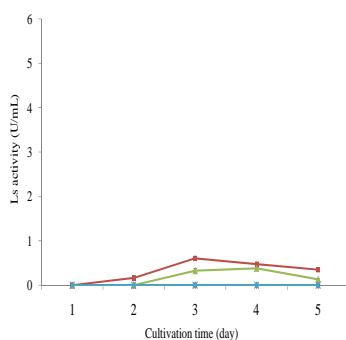
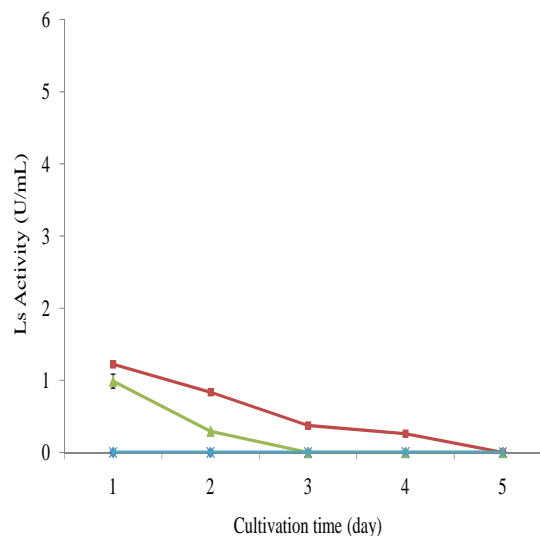
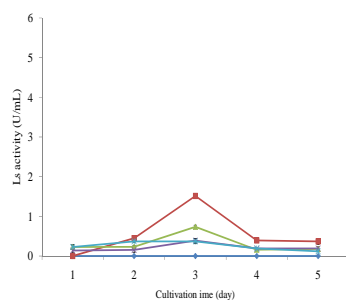
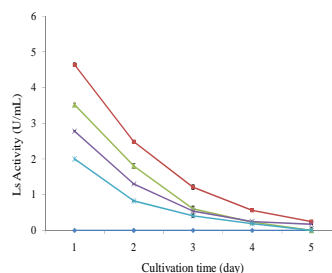
E) Extracellular Ls of TH4-2**F) Membrane-bound fraction of TH4-2****G) Extracellular Ls of TN-1****H) Membrane-bound fraction of TN-1**

Figure 3.2 Levansucrase production by the isolated strains in LB medium containing 0-20% (w/v) sucrose

The isolated strains were grown in the LB medium containing 0% sucrose (◆), 5% sucrose (*), 10% sucrose (×), 15% sucrose (▲) and 20% sucrose (■). Ls activities of extracellular and membrane-bound fractions at each time point were measured according methods.

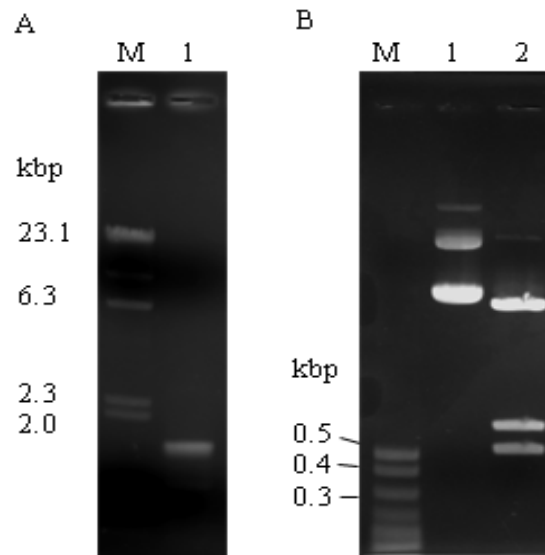


Figure 3.3 Identification of the TN-1 isolated by 16S rRNA gene comparison

A) 0.7% agarose gel electrophoresis of the amplification of 16S rRNA gene

Lane M: λ /HindIII Marker

Lane 1: the PCR product of 16S rRNA gene of the TN-1 isolated

B) 1.2 % agarose gel electrophoresis of restriction enzyme digested pattern of p16S

TN-1

Lane M: λ /MspI

Lane 1: undigested p16S TN

Lane 2: p16S TN-1/EcoRI


```

B_subtilis      GGGAGCGAACAGGATTAGATACCCTGGTAGTCCACGCCGTAAACGATGAGTGCTAAGTGT 834
TN-1            GGGAGCGAACAGGATTAGATACCCTGGTAGTCCACGCCGTAAACGATGAGTGCTAAGTGT 837
B_lentus        GGGAGCGAACAGGATTAGATACCCTGGTAGTCCACGCCGTAAACGATGAGTGCTAAGTGT 813
                *****

B_subtilis      TAGGGGTTTCCGCCCTTAGTGTGCAGCTAACGCATTAAGCACTCCGCCCTGGGGAGTA 894
TN-1            TAGGGGTTTCCGCCCTTAGTGTGCAGCTAACGCATTAAGCACTCCGCCCTGGGGAGTA 897
B_lentus        TAGAGGGTTTCCGCCCTTAGTGTGCAGCTAACGCATTAAGCACTCCGCCCTGGGGAGTA 873
                *** *****

B_subtilis      CGGTCGCAAGACTGAAACTCAAAGGAATTGACGGGGGCCCGCACAAAGCGGTGGAGCATGT 954
TN-1            CGGTCGCAAGACTGAAACTCAAAGGAATTGACGGGGGCCCGCACAAAGCGGTGGAGCATGT 957
B_lentus        CGGTCGCAAGACTGAAACTCAAAGGAATTGACGGGGGCCCGCACAAAGCGGTGGAGCATGT 933
                *** *****

B_subtilis      GGTTAATTGAAGCAACGCGAAGAACCCTTACCAGGTCTTGACATCCTCTGACAATCCTA 1014
TN-1            GGTTAATTGAAGCAACGCGAAGAACCCTTACCAGGTCTTGACATCCTCTGACAATCCTA 1017
B_lentus        GGTTAATTGAAGCAACGCGAAGAACCCTTACCAGGTCTTGACATCCTCTGACAATCCTA 993
                ***** *

B_subtilis      GAGATAGG-ACGTCCCCTTCGGGGG-CAGAGTGACAGGTGGTGCATGGTTGTCGTCAGCT 1072
TN-1            GAGATAGG-ACGTCCCCTTCGGGGG-CAGAGTGACAGGTGGTGCATGGTTGTCGTCAGCT 1075
B_lentus        GAGATAGGACTTCCCCTTCGGGGGACAGAGTGACAGGTGGTGCATGGTTGTCGTCAGCT 1053
                ***** *

B_subtilis      CGTGTGCGTGAGATGTTGGGTTAAGTCCCAGCAACGAGCGCAACCCTTGATCTTAGTTGCCA 1132
TN-1            CGTGTGCGTGAGATGTTGGGTTAAGTCCCAGCAACGAGCGCAACCCTTGATCTTAGTTGCCA 1135
B_lentus        CGTGTGCGTGAGATGTTGGGTTAAGTCCCAGCAACGAGCGCAACCCTTAACCTTAGTTGCCA 1113
                ***** *

B_subtilis      GCATTAGTTGGGCACTCTAAGGTGACTGCCGGTGACAAACCGGAGGAAGGTGGGGATGA 1192
TN-1            GCATTAGTTGGGCACTCTAAGGTGACTGCCGGTGACAAACCGGAGGAAGGTGGGGATGA 1195
B_lentus        GCATTAGTTGGGCACTCTAAGGTGACTGCCGGTGACAAACCGGAGGAAGGTGGGGATGA 1173
                *****

B_subtilis      CGTCAAATCATCATGCCCTTATGACCTGGGCTACACACGTGCTACAATGGACAGAACAA 1252
TN-1            CGTCAAATCATCATGCCCTTATGACCTGGGCTACACACGTGCTACAATGGACAGAACAA 1255
B_lentus        CGTCAAATCATCATGCCCTTATGACCTGGGCTACACACGTGCTACAATGGATGGTACAA 1233
                ***** *

B_subtilis      AGGGCAGCGAAACCGCGAGGTTAAGCCAATCCCACAAATCTGTTCTCAGTTCGGATCGCA 1312
TN-1            AGGGCAGCGAAACCGCGAGGTTAAGCCAATCCCACAAATCTGTTCTCAGTTCGGATCGCA 1315
B_lentus        AGGGTTGCAAGACCGCGAGGTTAGCTAATCCCATAAAACCATTTCTCAGTTCGGATCGCA 1293
                **** *

B_subtilis      GTCTGCAACTCGACTGCGTGAAGCTGGAATCGTAGTAATCGCGGATCAGCATGCCCGGG 1372
TN-1            GTCTGCAACTCGACTGCGTGAAGCTGGAATCGTAGTAATCGCGGATCAGCATGCCCGGG 1375
B_lentus        GCTGCAACTCGCTGCAATGAAGCGGAATCGTAGTAATCGTGGATCAGCATGCCACGG 1353
                * *****

B_subtilis      TGAATACGTTCCCGGCCTTGTACACACCGCCCGTCACACCACGAGAGTTTGTAAACCCC 1432
TN-1            TGAATACGTTCCCGGCCTTGTACACACCGCCCGTCACACCACGAGAGTTTGTAAACCCC 1435
B_lentus        TGAATACGTTCCCGGCCTTGTACACACCGCCCGTCACACCACGAGAGTTTGTAAACCCC 1413
                *****

B_subtilis      GAAGTCGGTGAGGTAACCTTTTAGGAGCCAGCCGCCGAAGGTGGGA----- 1478
TN-1            GAAGTCGGTGAGGTAACCTTTTAGGAGCCAGCCGCCGAAGGTGGGACAGATGATTGGGGT 1495
B_lentus        GAAGTCGGTGGGGTACATCTACGGGAGCCAGCCGCCGAAGGTGGGACAGATGATTGGGGT 1473
                ***** *

```

```

B_subtilis -----
TN-1      GAAGTCGTAACAAGGTAGCCGTATCGGAAGGTGCGGCTGCATCACCTCCTTAATCACTAG 1555
B_lentus  GAAGTCGTAACAA----- 1486

B_subtilis -
TN-1      T 1556
B_lentus  -

```

Figure 3.4 Comparison of 16S rRNA gene of *Bacillus* sp. TN-1 to *B. subtilis* and *B. lentus*

The sequences was derived from GenBank entries with accession number of AB110589.1; *B. subtilis* and D16272.1; *B. lentus*. The non-conserved nucleotides are labeled in yellow for the nucleotide of *B. subtilis* and the TN-1 isolated strain, gray for the nucleotide of *B. lentus*. The green alphabets indicate the non-conserved nucleotides of *B. subtilis* and the TN-1 isolated strain.

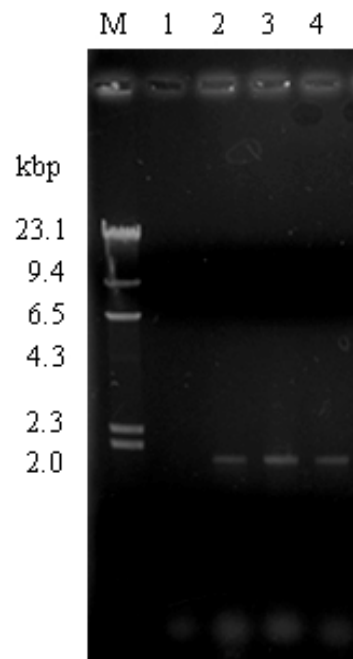


Figure 3.5 *In vitro* amplification of *ls* from *B. licheniformis*

Lane M: λ /HindIII Marker

Lane 1: the PCR product of *ls* of PR-1 isolated strain (1.8 kb)

Lane 2: the PCR product of *ls* of RN-01 isolated strain (1.8 kb)

Lane 3: the PCR product of *ls* of SK-1 isolated strain (1.8 kb)

Lane 4: the PCR product of *ls* of TH4-2 isolated strain (1.8 kb)

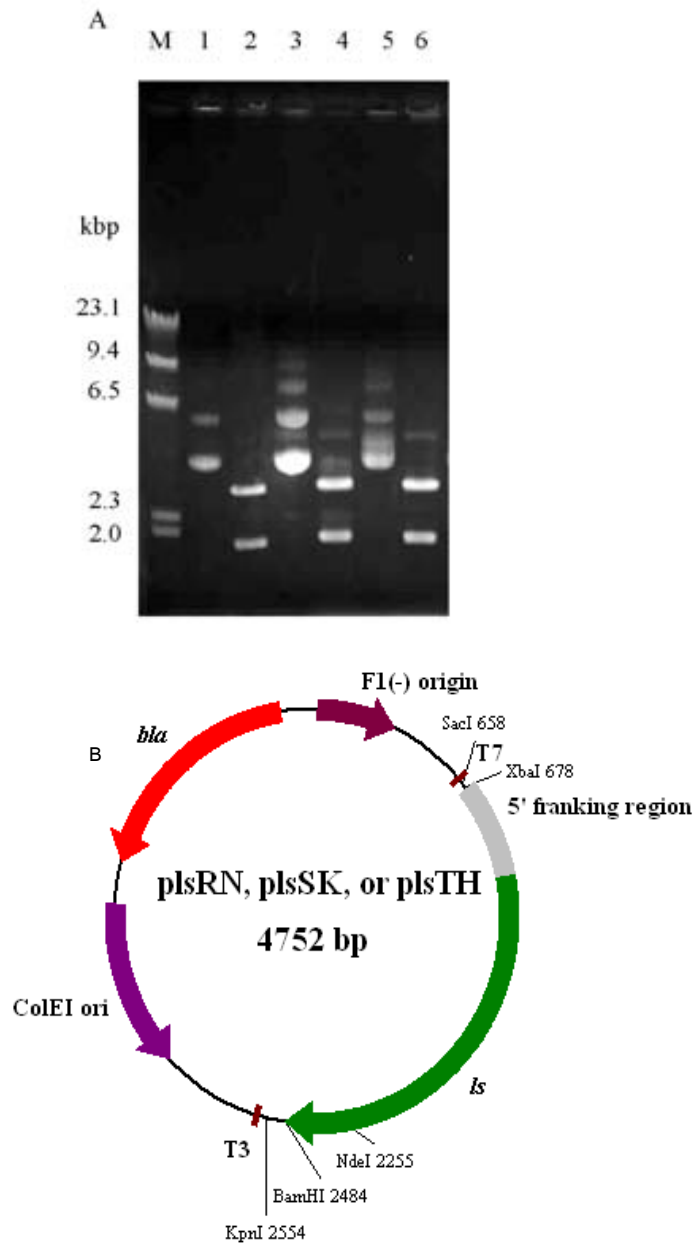


Figure 3.6 Cloning of *ls* from *B. licheniformis*

A) Agarose gel analysis of recombinant plasmids carrying *ls* from *B. licheniformis*

Lane M: λ /HindIII Marker

Lane 1: Undigested plsRN

Lane 2: plsRN digested with *Xba*I and *Bam*HI

Lane 3: Undigested plsSK

Lane 4: plsSK digested with *Xba*I and *Bam*HI

Lane 5: Undigested plsTH

Lane 6: plsTH digested with *Xba*I and *Bam*HI

B) Plasmid map of plsRN, plsSK, and plsTH

3.3.2 Cloning of *ls* from *Bacillus* sp. TN-1 by PCR technique

The PCR primers, BsLs*Nde*I-F and BsLs*Bam*HI-R, were degenerated based on Ls gene from *B. amyloliquefaciens* (GenBank accession number; X52988.1) *B. subtilis* (GenBank accession number; X02730.1), and *B. stearothermophilus* (GenBank accession number; U34874.1). PCR amplification of *ls* from the TN-1 was performed by using chromosomal DNA of the strain TN-1 as a template, giving an expected PCR product of 1.4 kb as shown in Fig. 3.6. The PCR product was then in frame ligated to pET17-b by *Nde*I and *Bam*HI digestion and verified the insertion by restriction digested and agarose gel electrophoresis (Fig 3.7). The positive clones which carried the 1.4 kb inserted fragment was designated as plsTN and subjected to nucleotide sequencing.

3.4 *ls* analysis

3.4.1 Analysis of *ls* from *B. licheniformis*

The nucleotide sequences of 1,793 bp which were obtained from positive clones of pLsSK, pLsRN, and pLsTH revealed a single open reading frame of 1,446 bp with a predicted putative promoter sequence. The putative promoter sequence were identified 34 bp upstream of a transcription start site, with -35 (TTGAGT) and -10 (TAGAAT) sequence separated by 17 nucleotides with the Neural Network Promoter Prediction Algorithm. A potential ribosome binding sites with the sequence AGGAA was located 11 bp upstream from the ATG start site. The three nucleotide sequences were compared with *ls* gene from *B. licheniformis* ATCC 14580 by ClustalW2 as shown in Fig. 3.9. The result showed 100% identity between *ls* from ATCC14580 and *ls* gene from SK-1 (GenBank accession number; JN712303) and 99% identity from RN-01 (GenBank accession number; ACI15886.1) and TH4-2 (GenBank accession number; JN712304).

The deduced amino acid sequences contained 482 amino acids residues. The predicted signal peptide sequence of 29 amino acids was found at N-terminal, followed by a high potential signal peptidase cleavage site between A29 and K30 designated by SignalP. The calculated molecular weight and pI of the full length proteins of LsRN, LsSK and LsTH were 53.7 kDa and pI of 8.2 while the values for the mature proteins were 50.9 kDa and pI of 7.0. The deduced amino acid sequences of Ls from three *B. licheniformis* strains were 99% identities with that from ATCC14580. As shown in Fig 3.10, two amino acid exchanges were found. Y80 was substituted by C in LsTH. A271 was substituted by D in LsRN. Blastp search with deduced amino acid sequences of LsRN, LsTH and LsSK showed high similarity to Ls from other *Bacilli* but low similarity to those from *L. reuteri* and Ls from gram negative

bacteria as shown in Table 3.1. Amino acid sequences from the selected strains contained four signature conserved domains usually found in GH68 e.g. WMNDPNG-motif contained D93, a predicted nucleophile, WSGSAT-motif, RDP-motif contained D156, a predicted transition state stabilization and IERAN-motif contained E351, a predicted acid/base catalyst.

3.4.2 Analysis of *ls* from *Bacillus* sp. TN-1

The nucleotide sequence of *ls* from *Bacillus* sp. TN-1 revealed a single open reading frame of 1,422 bp, encoding for 473 amino acid residues. As shown in Fig 3.11, the predicted signal peptide sequence of 29 amino acids were found at N-terminal, followed by a high potential signal peptidase cleavage site between A29 and K30 designated by SignalP. The calculated molecular weight and pI of the full length protein was 53.0 kDa and pI of 6.8 while those for the mature protein was 50.0 kDa and pI of 5.8.

The deduced amino acid sequence was compared with other Ls deposited in GenBank by Blastp. Ls of the strain TN-1 showed high similarity to those from *Bacilli* species, especially the well known levansucrase from *B. subtilis*, but low similarity to those from gram negative bacteria, as shown in Table 3.2. Deduced amino acid sequence of the TN-1 Ls also contained four signature conserved domains usually found in GH68 e.g. the three catalytic triad motif, D86 as a predicted nucleophile in WMNDPNG-motif, D247 as a transition state stabilizer in RDP-motif, and E480 as a predicted acid/base in IERAN-motif. Another domain was the WSGSAT- substrate binding motif.

Since there has been no previous report on levansucrase from *B. licheniformis*, Ls from the three isolated strains, LsRN, LsSK and LsTH were selected for further experiment.

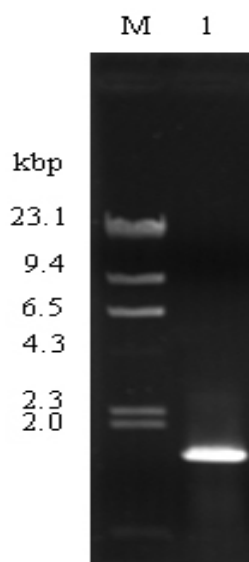


Figure 3.7 *In vitro* amplification of *ls* from *Bacillus* sp. TN-1

Lane M: λ /*Hind*III Marker

Lane 1: the PCR product of *ls* of TN-1 isolated strain (1.4 kb)

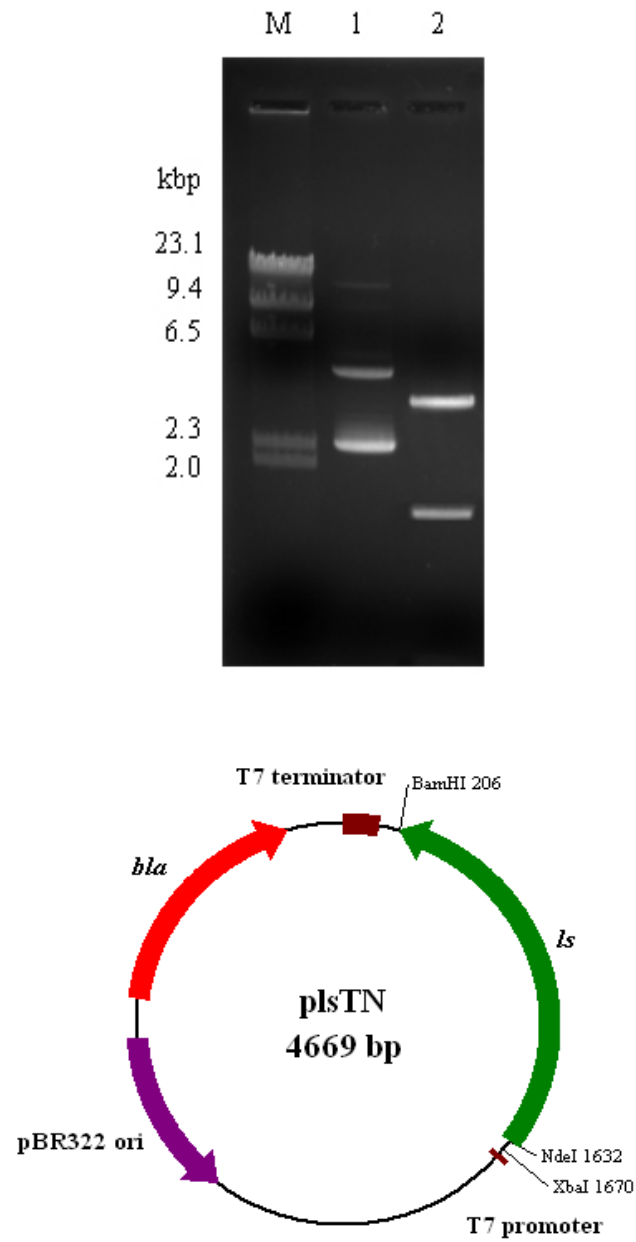


Figure 3.8 Cloning of *ls* from *Bacillus* sp. TN-1

A) Agarose gel analysis of recombinant plasmids carrying *ls* from *Bacillus* sp. TN-1

Lane M: λ HindIII Marker

Lane 1: Undigested plsTN

Lane 2: plsTN digested by *Nde*I and *Bam*HI

B) Plasmid map of plsTN

ATCC14580 CGATTCCCGCTTATACAGACTATAGATTCATATAAAAAAGGTGTCTTTCCGCTTAAAATC 60
 lsSK CGATTCCCGCTTATACAGACTATAGATTCATATAAAAAAGGTGTCTTTCCGCTTAAAATC 60
 lsTH CGATTCCCGCTTATACAGACTATAGATTCATATAAAAAAGGTGTCTTTCCGCTTAAAATC 60
 lsRN CGATTCCCGCTTATACAGACTATAGATTCATATAAAAAAGGTGTCTTTCCGCTTAAAATC 60

 -35
 ATCC14580 GGTGTCATTTGCATAAAAAATGTATAGGAAAAGAGGAACTTAGACCAGTTGAGTCCCAGAG 120
 lsSK GGTGTCATTTGCATAAAAAATGTATAGGAAAAGAGGAACTTAGACCAGTTGAGTCCCAGAG 120
 lsTH GGTGTCATTTGCATAAAAAATGTATAGGAAAAGAGGAACTTAGACCAGTTGAGTCCCAGAG 120
 lsRN GGTGTCATTTGCATAAAAAATGTATAGGAAAAGAGGAACTTAGACCAGTTGAGTCCCAGAG 120

 -10 +1
 ATCC14580 ATGAGTATATTAGAATGATGGTAATTCAATATCGTCGGGATTGTTACTGTCTAAGCAGGC 180
 lsSK ATGAGTATATTAGAATGATGGTAATTCAATATCGTCGGGATTGTTACTGTCTAAGCAGGC 180
 lsTH ATGAGTATATTAGAATGATGGTAATTCAATATCGTCGGGATTGTTACTGTCTAAGCAGGC 180
 lsRN ATGAGTATATTAGAATGATGGTAATTCAATATCGTCGGGATTGTTACTGTCTAAGCAGGC 180

 ATCC14580 AAGACCTAAAATGTGTGAAGGGCGAAATCTATCTTTTGCCTATATGAACCTGCACATTTT 240
 lsSK AAGACCTAAAATGTGTGAAGGGCGAAATCTATCTTTTGCCTATATGAACCTGCACATTTT 240
 lsTH AAGACCTAAAATGTGTGAAGGGCGAAATCTATCTTTTGCCTATATGAACCTGCACATTTT 240
 lsRN AAGACCTAAAATGTGTGAAGGGCGAAATCTATCTTTTGCCTATATGAACCTGCACATTTT 240

 ATCC14580 AGGTCTTTTTTCTGTTCTTCAGGACAATGCCGCAGTTAGGAGGGATGATTGGGAACGTTT 300
 lsSK AGGTCTTTTTTCTGTTCTTCAGGACAATGCCGCAGTTAGGAGGGATGATTGGGAACGTTT 300
 lsTH AGGTCTTTTTTCTGTTCTTCAGGACAATGCCGCAGTTAGGAGGGATGATTGGGAACGTTT 300
 lsRN AGGTCTTTTTTCTGTTCTTCAGGACAATGCCGCAGTTAGGAGGGATGATTGGGAACGTTT 300

 RBS
 ATCC14580 ATGTTGTCAGAAGCAATCTATTACATATTGAAAAGGGAGGAAATATTGATGAACATCAA 360
 lsSK ATGTTGTCAGAAGCAATCTATTACATATTGAAAAGGGAGGAAATATTGATGAACATCAA 360
 lsTH ATGTTGTCAGAAGCAATCTATTACATATTGAAAAGGGAGGAAATATTGATGAACATCAA 360
 lsRN ATGTTGTCAGAAGCAATCTATTACATATTGAAAAGGGAGGAAATATTGATGAACATCAA 360

 ATCC14580 AAACATTGCTAAAAAGCGTCAGCCTTAACCGTTGCTGCGGCACTGCTGGCCGGAGGTGC 420
 lsSK AAACATTGCTAAAAAGCGTCAGCCTTAACCGTTGCTGCGGCACTGCTGGCCGGAGGTGC 420
 lsTH AAACATTGCTAAAAAGCGTCAGCCTTAACCGTTGCTGCGGCACTGCTGGCCGGAGGTGC 420
 lsRN AAACATTGCTAAAAAGCGTCAGCCTTAACCGTTGCTGCGGCACTGCTGGCCGGAGGTGC 420

 ATCC14580 GCCGCAAACCTTTGCAAAGAAACGCAGGATTACAAGAAAAGCTACGGATTTTCTCATAT 480
 lsSK GCCGCAAACCTTTGCAAAGAAACGCAGGATTACAAGAAAAGCTACGGATTTTCTCATAT 480
 lsTH GCCGCAAACCTTTGCAAAGAAACGCAGGATTACAAGAAAAGCTACGGATTTTCTCATAT 480
 lsRN GCCGCAAACCTTTGCAAAGAAACGCAGGATTACAAGAAAAGCTACGGATTTTCTCATAT 480

 ATCC14580 CACAAGACATGACATGCTGAAAATTTCCCGAGCAGCAAAAAGAGCGAACAATTTAAAGTTCC 540
 lsSK CACAAGACATGACATGCTGAAAATTTCCCGAGCAGCAAAAAGAGCGAACAATTTAAAGTTCC 540
 lsTH CACAAGACATGACATGCTGAAAATTTCCCGAGCAGCAAAAAGAGCGAACAATTTAAAGTTCC 540
 lsRN CACAAGACATGACATGCTGAAAATTTCCCGAGCAGCAAAAAGAGCGAACAATTTAAAGTTCC 540

 ATCC14580 TCAATTCGATCCGAAAACAATCAAAAACATCCCTTCTGCAAAGGGTATAACAAAAATGG 600
 lsSK TCAATTCGATCCGAAAACAATCAAAAACATCCCTTCTGCAAAGGGTATAACAAAAATGG 600
 lsTH TCAATTCGATCCGAAAACAATCAAAAACATCCCTTCTGCAAAGGGTATAACAAAAATGG 600
 lsRN TCAATTCGATCCGAAAACAATCAAAAACATCCCTTCTGCAAAGGGTATAACAAAAATGG 600

 ATCC14580 AGAGCTGATCGATTTAGACGTATGGGACAGCTGGCCGCTGCAAAATGCCGACGGGACGGT 660
 lsSK AGAGCTGATCGATTTAGACGTATGGGACAGCTGGCCGCTGCAAAATGCCGACGGGACGGT 660
 lsTH AGAGCTGATCGATTTAGACGTATGGGACAGCTGGCCGCTGCAAAATGCCGACGGGACGGT 660
 lsRN AGAGCTGATCGATTTAGACGTATGGGACAGCTGGCCGCTGCAAAATGCCGACGGGACGGT 660

ATCC14580 TGCTACATAACCACGGCTACAATCTGTGTTTTCGCGCTGGCGGGCGATCCGAAAGACGTCTGA 720
 lsSK TGCTACATAACCACGGCTACAATCTGTGTTTTCGCGCTGGCGGGCGATCCGAAAGACGTCTGA 720
 lsTH TGCTACATAACCACGGCTACAATCTGTGTTTTCGCGCTGGCGGGCGATCCGAAAGACGTCTGA 720
 lsRN TGCTACATAACCACGGCTACAATCTGTGTTTTCGCGCTGGCGGGCGATCCGAAAGACGTCTGA 720

ATCC14580 TGACACATCCATCTATTTGTTCTATCAAAAGAAAGGCGAAACTTCTATCGACAGCTGGAA 780
 lsSK TGACACATCCATCTATTTGTTCTATCAAAAGAAAGGCGAAACTTCTATCGACAGCTGGAA 780
 lsTH TGACACATCCATCTATTTGTTCTATCAAAAGAAAGGCGAAACTTCTATCGACAGCTGGAA 780
 lsRN TGACACATCCATCTATTTGTTCTATCAAAAGAAAGGCGAAACTTCTATCGACAGCTGGAA 780

ATCC14580 AAACGCCGGCAGAGTGTGTTAAAGACAGCGACAAATTTGTTCCAGACGATCCGTACCTCAA 840
 lsSK AAACGCCGGCAGAGTGTGTTAAAGACAGCGACAAATTTGTTCCAGACGATCCGTACCTCAA 840
 lsTH AAACGCCGGCAGAGTGTGTTAAAGACAGCGACAAATTTGTTCCAGACGATCCGTACCTCAA 840
 lsRN AAACGCCGGCAGAGTGTGTTAAAGACAGCGACAAATTTGTTCCAGACGATCCGTACCTCAA 840

ATCC14580 ACATCAAACACAGGAATGGTCAGGTTCTGCCACGCTGACAAAAGACGGAAGTCCGACT 900
 lsSK ACATCAAACACAGGAATGGTCAGGTTCTGCCACGCTGACAAAAGACGGAAGTCCGACT 900
 lsTH ACATCAAACACAGGAATGGTCAGGTTCTGCCACGCTGACAAAAGACGGAAGTCCGACT 900
 lsRN ACATCAAACACAGGAATGGTCAGGTTCTGCCACGCTGACAAAAGACGGAAGTCCGACT 900

ATCC14580 GTTTTACACAGCTTTTTCCGGCAGCAATACGGCAAGCAGACGCTGACAACAGCTCAGGT 960
 lsSK GTTTTACACAGCTTTTTCCGGCAGCAATACGGCAAGCAGACGCTGACAACAGCTCAGGT 960
 lsTH GTTTTACACAGCTTTTTCCGGCAGCAATACGGCAAGCAGACGCTGACAACAGCTCAGGT 960
 lsRN GTTTTACACAGCTTTTTCCGGCAGCAATACGGCAAGCAGACGCTGACAACAGCTCAGGT 960

ATCC14580 CAATTTCTCTCAGCCGATTCCGGACACGCTCAAATTTGACGGTGTAGAAGATCATAAATC 1020
 lsSK CAATTTCTCTCAGCCGATTCCGGACACGCTCAAATTTGACGGTGTAGAAGATCATAAATC 1020
 lsTH CAATTTCTCTCAGCCGATTCCGGACACGCTCAAATTTGACGGTGTAGAAGATCATAAATC 1020
 lsRN CAATTTCTCTCAGCCGATTCCGGACACGCTCAAATTTGACGGTGTAGAAGATCATAAATC 1020

ATCC14580 GGTCTTTGACGGCGCCGACGGCAGGTATACCAAACGTTTACGCAATTCATTGACGAAGG 1080
 lsSK GGTCTTTGACGGCGCCGACGGCAGGTATACCAAACGTTTACGCAATTCATTGACGAAGG 1080
 lsTH GGTCTTTGACGGCGCCGACGGCAGGTATACCAAACGTTTACGCAATTCATTGACGAAGG 1080
 lsRN GGTCTTTGACGGCGCCGACGGCAGGTATACCAAACGTTTACGCAATTCATTGACGAAGG 1080

ATCC14580 AAATACAGCTCCGGCGACAACCATACGATGAGAGACCCGATTATGTGGAAGACCGCGG 1140
 lsSK AAATACAGCTCCGGCGACAACCATACGATGAGAGACCCGATTATGTGGAAGACCGCGG 1140
 lsTH AAATACAGCTCCGGCGACAACCATACGATGAGAGACCCGATTATGTGGAAGACCGCGG 1140
 lsRN AAATACAGCTCCGGCGACAACCATACGATGAGAGACCCGATTATGTGGAAGACCGCGG 1140

ATCC14580 CCATAAATATCTCGTATTTGAAGCCAATACGGGAACAAAAACCGCTACCAAGGAGAAGA 1200
 lsSK CCATAAATATCTCGTATTTGAAGCCAATACGGGAACAAAAACCGCTACCAAGGAGAAGA 1200
 lsTH CCATAAATATCTCGTATTTGAAGCCAATACGGGAACAAAAACCGCTACCAAGGAGAAGA 1200
 lsRN CCATAAATATCTCGTATTTGAAGCCAATACGGGAACAAAAACCGCTACCAAGGAGAAGA 1200

ATCC14580 CTCCTATTCAACAGAGCCTACTACGGGGGAGCAAGAAGTTCCTTTAAAGAAGAAAGCAG 1260
 lsSK CTCCTATTCAACAGAGCCTACTACGGGGGAGCAAGAAGTTCCTTTAAAGAAGAAAGCAG 1260
 lsTH CTCCTATTCAACAGAGCCTACTACGGGGGAGCAAGAAGTTCCTTTAAAGAAGAAAGCAG 1260
 lsRN CTCCTATTCAACAGAGCCTACTACGGGGGAGCAAGAAGTTCCTTTAAAGAAGAAAGCAG 1260

ATCC14580 CAAGCTGCTGCAAGGTGCGAACAAAAAGAACGCTTCGCTGGCTAACGGCGCTCTCGGAAT 1320
 lsSK CAAGCTGCTGCAAGGTGCGAACAAAAAGAACGCTTCGCTGGCTAACGGCGCTCTCGGAAT 1320
 lsTH CAAGCTGCTGCAAGGTGCGAACAAAAAGAACGCTTCGCTGGCTAACGGCGCTCTCGGAAT 1320
 lsRN CAAGCTGCTGCAAGGTGCGAACAAAAAGAACGCTTCGCTGGCTAACGGCGCTCTCGGAAT 1320

```

ATCC14580      CATCGAATTAATAACGATTATACACTGAAAAAAGTCATGAAGCCTTTGATCGCCTCCAA 1380
lsSK          CATCGAATTAATAACGATTATACACTGAAAAAAGTCATGAAGCCTTTGATCGCCTCCAA 1380
lsTH          CATCGAATTAATAACGATTATACACTGAAAAAAGTCATGAAGCCTTTGATCGCCTCCAA 1380
lsRN          CATCGAATTAATAACGATTATACACTGAAAAAAGTCATGAAGCCTTTGATCGCCTCCAA 1380
*****

ATCC14580      TACGGTGACAGATGAAATCGAACGGGCCAACCTCTTCAAATGAATGGAAAATGGTATCT 1440
lsSK          TACGGTGACAGATGAAATCGAACGGGCCAACCTCTTCAAATGAATGGAAAATGGTATCT 1440
lsTH          TACGGTGACAGATGAAATCGAACGGGCCAACCTCTTCAAATGAATGGAAAATGGTATCT 1440
lsRN          TACGGTGACAGATGAAATCGAACGGGCCAACCTCTTCAAATGAATGGAAAATGGTATCT 1440
*****

ATCC14580      GTTCACAGATTCAAGAGGATCAAAAATGACAATTGACGGCATCGGTTCAAAGACATTTA 1500
lsSK          GTTCACAGATTCAAGAGGATCAAAAATGACAATTGACGGCATCGGTTCAAAGACATTTA 1500
lsTH          GTTCACAGATTCAAGAGGATCAAAAATGACAATTGACGGCATCGGTTCAAAGACATTTA 1500
lsRN          GTTCACAGATTCAAGAGGATCAAAAATGACAATTGACGGCATCGGTTCAAAGACATTTA 1500
*****

ATCC14580      TATGCTCGGCTATGTATCAGGTTCAATTAACCGGACCATTCAAGCCTTTAAACAAATCCGG 1560
lsSK          TATGCTCGGCTATGTATCAGGTTCAATTAACCGGACCATTCAAGCCTTTAAACAAATCCGG 1560
lsTH          TATGCTCGGCTATGTATCAGGTTCAATTAACCGGACCATTCAAGCCTTTAAACAAATCCGG 1560
lsRN          TATGCTCGGCTATGTATCAGGTTCAATTAACCGGACCATTCAAGCCTTTAAACAAATCCGG 1560
*****

ATCC14580      ACTTGTTTTGCATATGGACCAGGATTACAATGACATCACGTTTACTTATTCACACTTTGC 1620
lsSK          ACTTGTTTTGCATATGGACCAGGATTACAATGACATCACGTTTACTTATTCACACTTTGC 1620
lsTH          ACTTGTTTTGCATATGGACCAGGATTACAATGACATCACGTTTACTTATTCACACTTTGC 1620
lsRN          ACTTGTTTTGCATATGGACCAGGATTACAATGACATCACGTTTACTTATTCACACTTTGC 1620
*****

ATCC14580      CGTACCGCAGAAAAAAGGCGACGAAGTCGTCATTACAAGCTACATCACAACAGAGGGAT 1680
lsSK          CGTACCGCAGAAAAAAGGCGACGAAGTCGTCATTACAAGCTACATCACAACAGAGGGAT 1680
lsTH          CGTACCGCAGAAAAAAGGCGACGAAGTCGTCATTACAAGCTACATCACAACAGAGGGAT 1680
lsRN          CGTACCGCAGAAAAAAGGCGACGAAGTCGTCATTACAAGCTACATCACAACAGAGGGAT 1680
*****

ATCC14580      TTCGAACGAGCATCACGCCACGTTTGACCAAGCTTTTGTGCTGAAGATCAAAGGATCAA 1740
lsSK          TTCGAACGAGCATCACGCCACGTTTGACCAAGCTTTTGTGCTGAAGATCAAAGGATCAA 1740
lsTH          TTCGAACGAGCATCACGCCACGTTTGACCAAGCTTTTGTGCTGAAGATCAAAGGATCAA 1740
lsRN          TTCGAACGAGCATCACGCCACGTTTGACCAAGCTTTTGTGCTGAAGATCAAAGGATCAA 1740
*****

ATCC14580      AACATCCGTTGTCAAAAACAGCATCCTTGAACAGGGACAACCTAACGGTAAACAAATAA 1798
lsSK          AACATCCGTTGTCAAAAACAGCATCCTTGAACAGGGACAACCTAACGGTAAACAAATAA 1798
lsTH          AACATCCGTTGTCAAAAACAGCATCCTTGAACAGGGACAACCTAACGGTAAACAAATAA 1798
lsRN          AACATCCGTTGTCAAAAACAGCATCCTTGAACAGGGACAACCTAACGGTAAACAAATAA 1798
*****

```

Figure 3.9 Comparison of nucleotide sequences of *ls* from *B. licheniformis*

Nucleotide alignment was performed by ClustalW. The nucleotide sequence of levansucrase gene from the genome sequence of *Bacillus licheniformis* ATCC14580 was retrieved from GenBank. The putative promoter region and Ribosome Binding Site (RBS) are labeled in gray. The transcription start site is shown in violet alphabet. The translation start site and stop codon are shown in green and red alphabets, respectively. The non-conserved nucleotides are labeled in yellow.


```

LsATCC      MNIKNIAKKASALTVAALLLAGGAPQTFAKETQDYKKS YGFSHITRHDMLKIPEQQKSEQFKVPQFDPKTIKNIPSAKGYNKNNGELIDLVDSWPLQNA 100
LsSK        MNIKNIAKKASALTVAALLLAGGAPQTFAKETQDYKKS YGFSHITRHDMLKIPEQQKSEQFKVPQFDPKTIKNIPSAKGYNKNNGELIDLVDSWPLQNA 100
LsTH        MNIKNIAKKASALTVAALLLAGGAPQTFAKETQDYKKS YGFSHITRHDMLKIPEQQKSEQFKVPQFDPKTIKNIPSAKGCNKNNGELIDLVDSWPLQNA 100
LsRN        MNIKNIAKKASALTVAALLLAGGAPQTFAKETQDYKKS YGFSHITRHDMLKIPEQQKSEQFKVPQFDPKTIKNIPSAKGYNKNNGELIDLVDSWPLQNA 100
*****

LsATCC      DGTVATYHGYNLVFALAGDPKDVDDTSIYLFYQKKGETSIDSWKNAGRVFKDSDFVDDPYLKHQTQEWSGSATLTkdGKvRlFYtAFSGTQYgKqTlT 200
LsSK        DGTVATYHGYNLVFALAGDPKDVDDTSIYLFYQKKGETSIDSWKNAGRVFKDSDFVDDPYLKHQTQEWSGSATLTkdGKvRlFYtAFSGTQYgKqTlT 200
LsTH        DGTVATYHGYNLVFALAGDPKDVDDTSIYLFYQKKGETSIDSWKNAGRVFKDSDFVDDPYLKHQTQEWSGSATLTkdGKvRlFYtAFSGTQYgKqTlT 200
LsRN        DGTVATYHGYNLVFALAGDPKDVDDTSIYLFYQKKGETSIDSWKNAGRVFKDSDFVDDPYLKHQTQEWSGSATLTkdGKvRlFYtAFSGTQYgKqTlT 200
*****

LsATCC      TAQVNFSQPDSDTLKIDGVEDHKSVFDGADGTVYQNVQQFIDEGNYSSGDNHTMRDPHYVEDRGHKYLVFEANTGTKTGYQGEDSLFNRAYYGGSKKFFK 300
LsSK        TAQVNFSQPDSDTLKIDGVEDHKSVFDGADGTVYQNVQQFIDEGNYSSGDNHTMRDPHYVEDRGHKYLVFEANTGTKTGYQGEDSLFNRAYYGGSKKFFK 300
LsTH        TAQVNFSQPDSDTLKIDGVEDHKSVFDGADGTVYQNVQQFIDEGNYSSGDNHTMRDPHYVEDRGHKYLVFEANTGTKTGYQGEDSLFNRAYYGGSKKFFK 300
LsRN        TAQVNFSQPDSDTLKIDGVEDHKSVFDGADGTVYQNVQQFIDEGNYSSGDNHTMRDPHYVEDRGHKYLVFEANTGTKTGYQGEDSLFNRAYYGGSKKFFK 300
*****

LsATCC      EESSKLLQGANKKNASLANGALGIIELNNDYTLKKVMKPLIASNTVDEISRANLFKMNGKWYLFTDSRGSKMTIDGIGSKDIYMLGYVSGSLTGPFKPL 400
LsSK        EESSKLLQGANKKNASLANGALGIIELNNDYTLKKVMKPLIASNTVDEISRANLFKMNGKWYLFTDSRGSKMTIDGIGSKDIYMLGYVSGSLTGPFKPL 400
LsTh        EESSKLLQGANKKNASLANGALGIIELNNDYTLKKVMKPLIASNTVDEISRANLFKMNGKWYLFTDSRGSKMTIDGIGSKDIYMLGYVSGSLTGPFKPL 400
LsRN        EESSKLLQGANKKNASLANGALGIIELNNDYTLKKVMKPLIASNTVDEISRANLFKMNGKWYLFTDSRGSKMTIDGIGSKDIYMLGYVSGSLTGPFKPL 400
*****

LsATCC      NKSGLVLHMDQDYNDITFTYSHFAVPQKKGDEVVITSYITNRGISNEHHATFAPSFLKIKGSKTSVVKNSILEQGQLTVNK 482
LsSK        NKSGLVLHMDQDYNDITFTYSHFAVPQKKGDEVVITSYITNRGISNEHHATFAPSFLKIKGSKTSVVKNSILEQGQLTVNK 482
LsTH        NKSGLVLHMDQDYNDITFTYSHFAVPQKKGDEVVITSYITNRGISNEHHATFAPSFLKIKGSKTSVVKNSILEQGQLTVNK 482
LsRN        NKSGLVLHMDQDYNDITFTYSHFAVPQKKGDEVVITSYITNRGISNEHHATFAPSFLKIKGSKTSVVKNSILEQGQLTVNK 482
*****

```

Figure 3.10 Comparison of deduced amino acid sequences of Ls from *B. licheniformis*

Amino acid sequences alignment was performed by ClustalW. The amino acid sequence of Ls from the genome sequence of *Bacillus licheniformis* ATCC14580 was retrieved from GenBank. The predicted signal peptide is labeled in gray. The non-conserved amino acids are labeled in yellow. The signature conserved domains are remarked in green box. The catalytic triad is indicated in bold red alphabets.

Table 3.1 Comparison of amino acid sequence of LsRN, LsSK and LsTH with other levansucrases deposited in GenBank.

Organism (Accession Number)	Sequence length	% Identity	% Similarity
Gram positive bacteria			
<i>B. atrophaeus</i> (YP003974884.1)	474	79	87
<i>B. megaterium</i> (YP003596776.1)	483	78	87
<i>B. subtilis</i> (BAI87054.1)	473	77	86
<i>B. amyloliquefaciens</i> (ACD39394.1)	472	76	86
<i>Paenibacillus polymyxa</i> (CAB39327.1)	499	68	80
<i>L. reuteri</i> (ZP03974578.1)	591	40	60
Gram negative bacteria			
<i>L. mesenteroides</i> (AAY19523.1)	1022	44	64
<i>R. aquatilis</i> (AAC36458.1)	415	28	45
<i>P.chlororaphis</i> (AAL09386.1)	431	27	43
<i>Z. mobilis</i> (BAA04475.1)	423	26	43
<i>E. amylowora</i> (CAA52972.1)	415	25	43
<i>G. diazotrophicus</i> (Q43998.1)	584	26	40

```

atgaacatcaaaaagattgcaaaacaagcaacagattgacctttactactgcaactgctggcaggaggc
M N I K K I A K Q A T V L T F T T A L L A G G
gcaactcaagcgtttgcaaaagaacaaacccaaaagccatataaggaaacgtacggcatttcccatatt
A T Q A F A K E T N Q K P Y K E T Y G I S H I
acacgccatgacatgctgcaaatccctgaacagcaaaaaaatgaaaaatatcaagtgctgaattcgat
T R H D M L Q I P E Q Q K N E K Y Q V P E F D
ccgtccacaattaaaaatatctcttctgcaaaaggcctggacgtttgggacagctggccattacaaaac
P S T I K N I S S A K G L D V W D S W P L Q N
gctgatggcacagctgcaaaactatcacggctaccacatcgctctttgcattagccggagatcctaaaaat
A D G T V A N Y H G Y H I V F A L A G D P K N
gcgatgacacatcgatttacatgcttctatcaaaaagtcggcgaaaacttctattgacagctggaaaaac
A D D T S I Y M F Y Q K V G E T S I D S W K N
gctggccgctctttaaagacagcgacaaaattcgatgcaaatgattctatcctaaaagaccaaacgcaa
A G R V F K D S D K F D A N D S I L K D Q T Q
gaatgggcaggttcagccacatttacatctgacggaaaaatccgtttattctatactgatttctccggt
E W S G S A T F T S D G K I R L F Y T D F S G
aaacattacggcaaaacaaactgacaactgcacaggttaacgtatcagcatcagacagctccttgaac
K H Y G K Q T L T T A Q V N V S A S D S S L N
atcaacgggtgtagaggattataaatcaatctttgacggtgacggcaaaacgtatcaaatgtacagcag
I N G V E D Y K S I F D G D G K T Y Q N V Q Q
ttcatgatgaaggcaactacagctcagggcacaaccatacagctgagagatcctcactactagaagat
F I D E G N Y S S G D N H T L R D P H Y V E D
aaaggccacaaatacttagtatttgaagcaaacactggaactgaagatggctaccaaggcgaagaatct
K G H K Y L V F E A N T G T E D G Y Q G E E S
ttatttaacaaagcatactatggcaaaagcacatcgcttctccgtcaagaaagtcaaaaacttctgcaa
L F N K A Y Y G K S T S F F R Q E S Q K L L Q
agcgataaaaaacgcacggctgagtttagcaaacggcgccctcggcatgattgagctaaacgatgactac
S D K K R T A E L A N G A L G M I E L N D D Y
aactgaaaaaagtgatgaaaccgctgattgcatctaacacagtaacagatgaaattgaacgcgcgaac
T L K K V M K P L I A S N T V T D E I E R A N
gtctttaaaatgaacggcaaatggtacctgcttactgactcccgcggatcaaaaatgacgattgacggc
V F K M N G K W Y L F T D S R G S K M T I D G
attacgtctaacgatatttacatgcttgggtatgcttctaattctttaactggccatacaagccgctg
I T S N D I Y M L G Y V S N S L T G P Y K P L
aacaaaactggccttgtgttaaaaatggatcttgatcctaacgatgtaacctttacttactcacacttc
N K T G L V L K M D L D P N D V T F T Y S H F
gctgtacctcaagcgaaaggaaacaatgtcgtgattacaagctatatgacaaaacagaggggttctacgca
A V P Q A K G N N V V I T S Y M T N R G F Y A
gacaaacaatcaacggtttgcgccaagcttctgctgaacatcaaaggcaagaaaacatctgtgtgcaaa
D K Q S T F A P S F L L N I K G K K T S V V K
gacagcatccttgaacaaggacaactgacagtcaccaataa
D S I L E Q G Q L T V N Q *

```

Figure 3.11 The nucleotide and deduced amino acid sequences of Ls from *Bacillus* sp. TN-1

The predicted signal peptide, the core signatures of GH68 and the signature conserved domains are remarked in gray and green, respectively. The catalytic triad is indicated in bold red alphabets.

Table 3.2 Comparison of amino acid sequence of LsTN with other levansucrases deposited in GenBank.

Organism (Accession Number)	Sequence length	% Identity	% Similarity
Gram positive bacteria			
<i>B. subtilis</i> (BAI87054.1)	473	99	99
<i>B. stearothermophilus</i> (AAB97111.1)	473	97	98
<i>B. atrophaeus</i> (YP003974884.1)	474	91	96
<i>B. amyloliquefaciens</i> (ACD39394.1)	472	90	96
<i>B. megaterium</i> (YP003596776.1)	483	77	86
<i>B. licheniformis</i> (ACI15886.1)	482	77	86
<i>Paenibacillus polymyxa</i> (CAB39327.1)	499	68	79
<i>L. reuteri</i> (ZP03974578.1)	591	41	60
Gram negative bacteria			
<i>L. mesenteroides</i> (AAY19523.1)	1022	44	63
<i>R. aquatilis</i> (AAC36458.1)	415	28	44
<i>Z. mobilis</i> (BAA04475.1)	423	27	44
<i>P. chlororaphis</i> (AAL09386.1)	431	26	44
<i>E. amylowora</i> (CAA52972.1)	415	26	44
<i>G. diazotrophicus</i> (Q43998.1)	584	25	40

3.5 Expression of levansucrase in *E. coli*

3.5.1 Expression of *ls* under putative endogenous promoter

Levansucrase genes from the three isolated strains of *B. licheniformis* were expressed under their own putative endogenous promoters using *E. coli* top-10 as an expression host in LB medium. Three transformant colonies of each clone were grown and extracellular Ls activity was monitored for 4 days. As shown in Fig 3.12, the recombinant LsRN, LsSK and LsTH expression patterns by *E. coli* Top-10 were similar. Ls activities were detected in the first day of cultivation and consecutively produced for three days, then decreased on day 4. The *E. coli* carried *plsRN* produced higher enzyme activity than those carried the other two. The LsRN reached its highest activity of 0.9 U/mL after cultivation for two days while the LsSK and LsTH reached their maximum activity on day 3. From this result, LsRN was selected for the further experiment.

3.5.2 Optimization of LsRN production

To maximize LsRN production, *E. coli* expression hosts and media were compared. *plsRN* was transformed to *E. coli* DH5- α , Top-10 and XL-10 Gold. The media were LB, 3xLB and terrific broth. *E. coli* starters with OD₆₀₀ around 2.0 were inoculated to each medium containing 100 μ g/mL ampicillin without sucrose induction. The cultures were collected every 6 h for 48 h and Ls activity was monitored in extracellular, periplasmic and cytosolic fractions. As shown in Fig. 3.13, the Ls activities were detected in extracellular and periplasmic fractions but undetectable in cytosolic fraction. When expressed by *E. coli* DH-5 α both in LB and terrific broth, around 55% of Ls activity was found in periplasmic fraction. Exceptionally for the expression in 3xLB, only 10% of Ls activities were found in periplasmic fraction. While expressed in *E. coli* Top-10 and XL-10 Gold, more than 60% of Ls activities were found in extracellular fraction. The best host for expression of LsRN was *E. coli* Top-10 cultivated in 3xLB medium for 36 h.

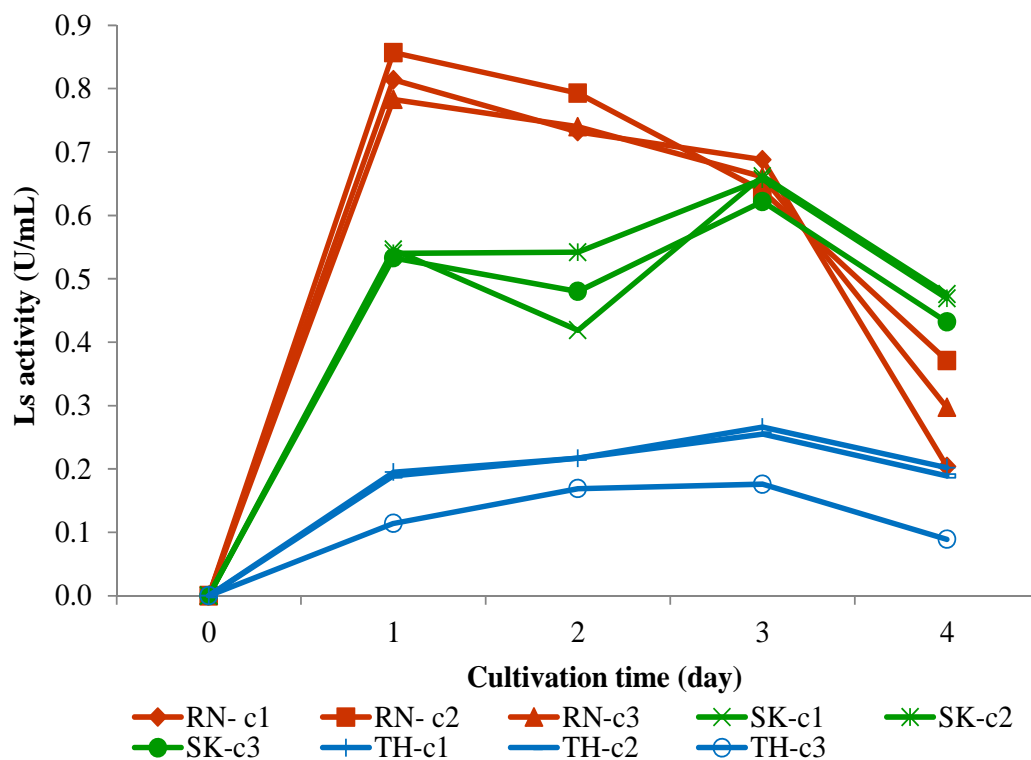


Figure 3.12 Recombinant levansucrase of *B. licheniformis* expressed in *E. coli* Top-10 during 4 day.

Culture supernatants of each cultivation day were collected and directly assayed for Ls activity. The enzymatic reactions were carried out at 50° C in 50 mM citrate buffer, pH 6.0, using 20% (w/v) sucrose as a substrate.

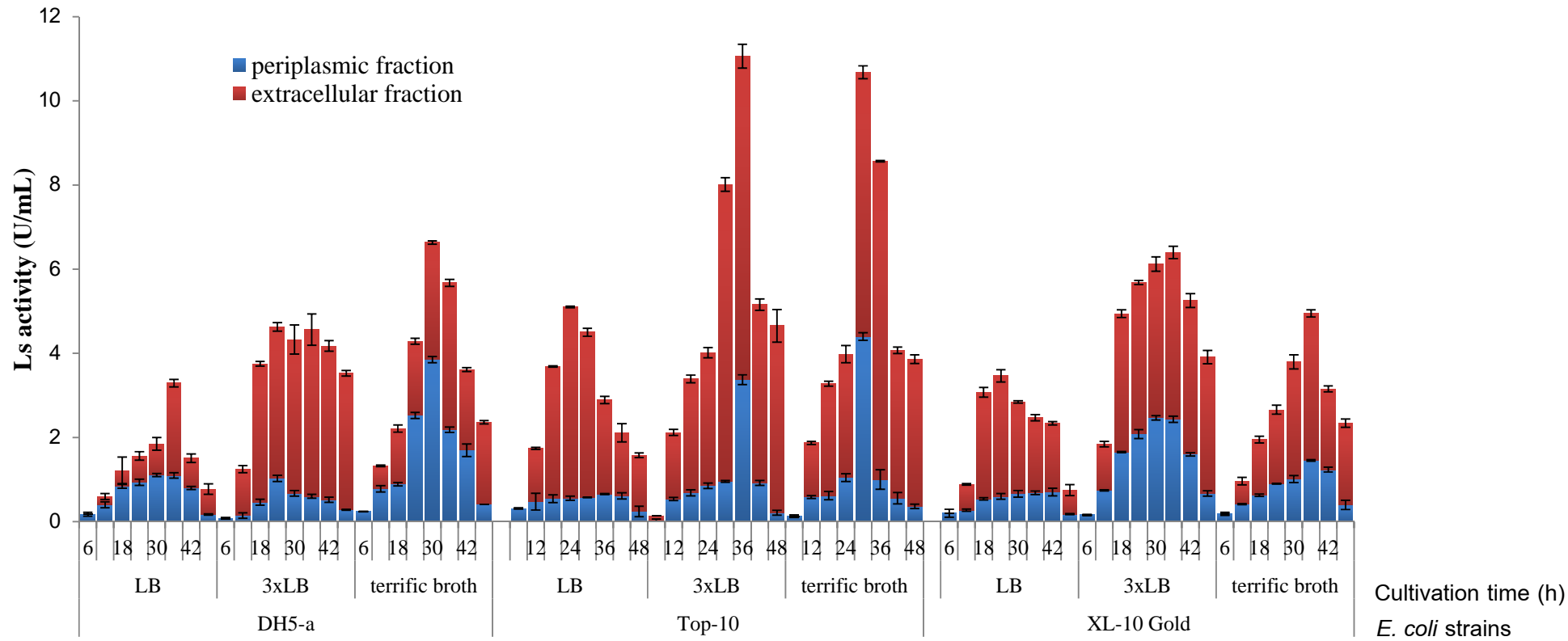


Figure 3.13 Optimization of LsRN production

The samples were collected every 6 hr and prepared according to method. The enzymatic reactions were carried out at 50° C in 50 mM citrate buffer, pH 6.0, using 20% (w/v) sucrose as a substrate.

3.5.3 Expression of *ls* under T7 promoter

3.5.3.1 Amplification and cloning of *ls* to pET19-b

The *ls* was *in vitro* amplified using a primer pair, which was designed according to the *ls* from *lsRN*. The cloning site of the *NcoI* and *BamHI* was incorporated into forward and reverse primers, respectively. An amplified gene product was examined on 0.7% agarose electrophoresis. As shown in Figure 3.14, the correct PCR product with 1.5 kb expected size was recovered and purified from gel. The purified PCR product was restriction digested with *NcoI* and *BamHI* and ligated to the proper sites of the pET19-b to generate an in frame recombinant plasmid designated as pET*lsRN*. The pET*lsRN* was transformed into *E. coli* Top-10 and the transformants were screened on a LB/Ampicillin (100 µg/ml). The positive clone (Fig. 3.15), which contained the appropriate insert was in frame as confirmed by nucleotide sequencing using T7 promoter sequencing primer.

3.5.3.2 Expression of *ls* in *E. coli* BL21 (DE3) and Rosetta (DE3).

The pET*lsRN* was retransformed to expression host, *E. coli* BL-21(DE3) pLysS and *E. coli* Rosetta (DE3) pLysS. The expressions were performed in three media, LB, 3xLB and terrific broth by 1 M IPTG induction. As shown in Fig. 3.16, the Ls activities were detected both in culture media and total cell protein (TCP). The expressed Ls was detected both in extracellular fraction and TCP. When expressed by BL21 (DE3) pLysS, the highest Ls activity of 4.7 U/mL was detected in terrific broth after 16 h induction. While expressed by *E. coli* Rosetta (DE3) pLysS, Ls showed the highest activity was 5.6 U/mL in extracellular fraction after 16 h of induction.

Hence, Ls activities expressed from both expression systems were similar. The expression under putative endogenous promoter was selected by the following reasons:

- 1) Protein was expressed without sucrose or IPTG induction.
- 2) No extra enzyme preparation step was needed.
- 3) Small numbers of protein species found in culture medium made Ls easy to be purified.

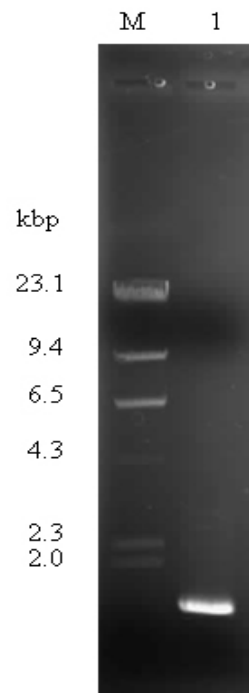


Figure 3.14 *In vitro* amplification of *ls* from *B. licheniformis* RN-01

Lane M: λ HindIII Marker

Lane 1: the PCR product of *ls* of *B. licheniformis* RN-01 (1.4 kb)

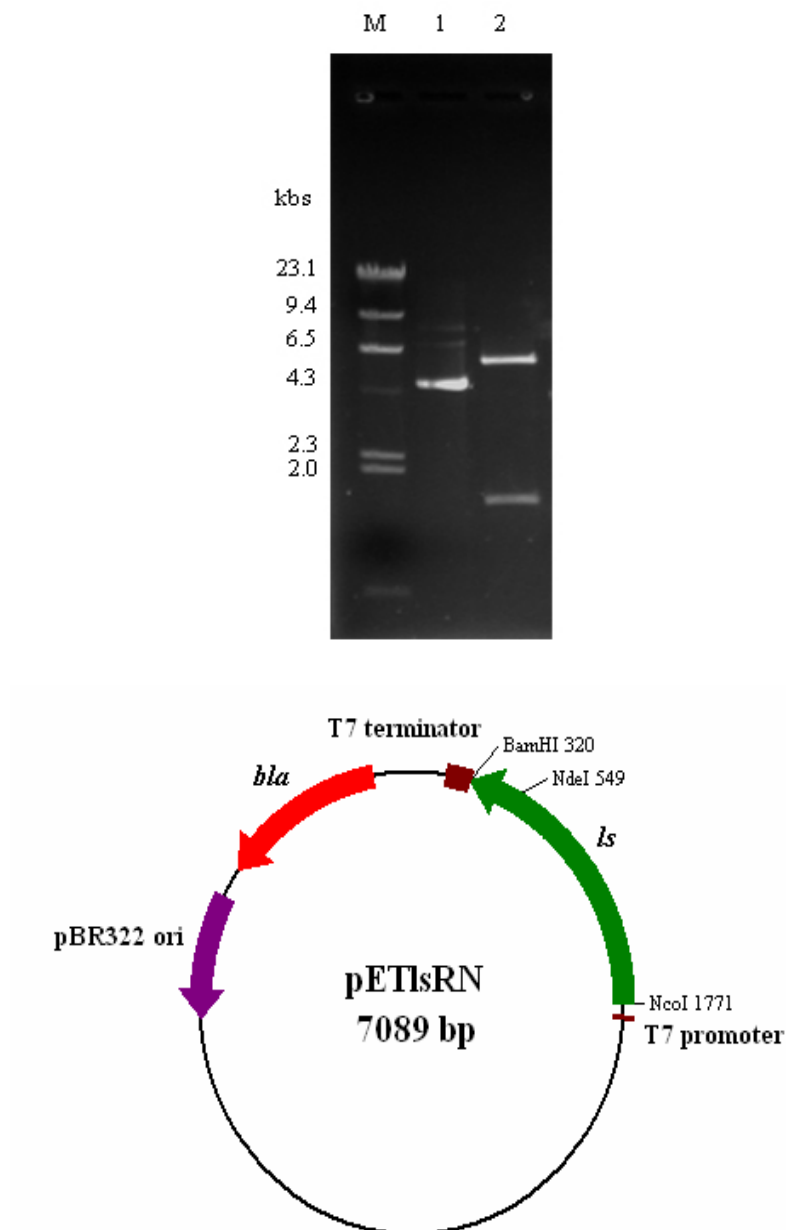


Figure 3.15 Sub-cloning of *ls* from *Bacillus* sp. TN-1 into pET-19b

A) Agarose gel analysis of recombinant plasmids carrying *ls* from *Bacillus* sp.

TN-1

Lane M: λ /HindIII Marker

Lane 1: Undigested pET/*ls*RN

Lane 2: pET/*ls*RN digested by *Nco*I and *Bam*HI

B) Plasmid map of pET/*ls*RN

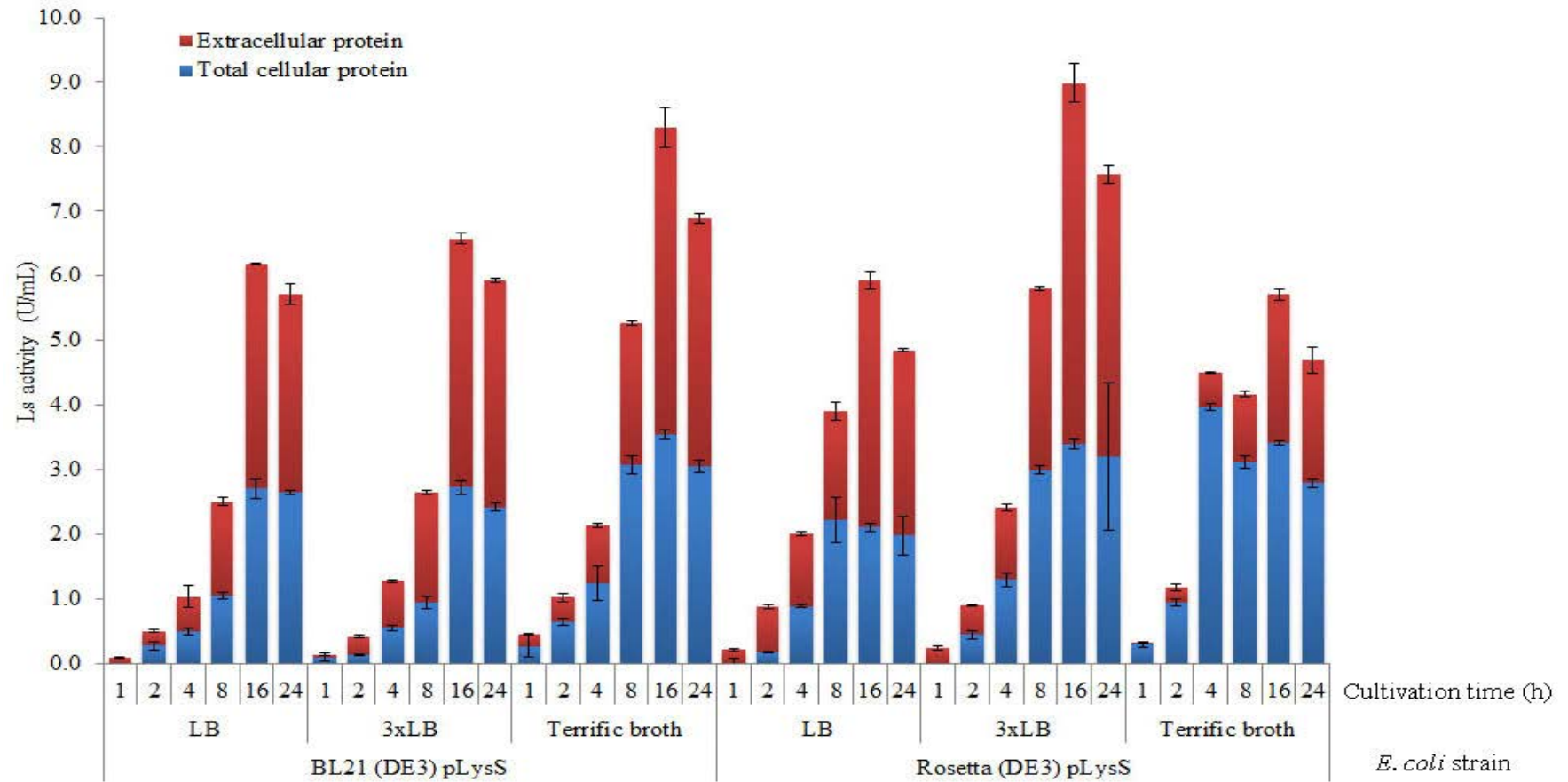


Figure 3.16 Expression of LsRN under T7 promoter

The enzymatic reactions were carried out at 50° C in 50 mM citrate buffer, pH 6.0, using 20% (w/v) sucrose as a substrate.

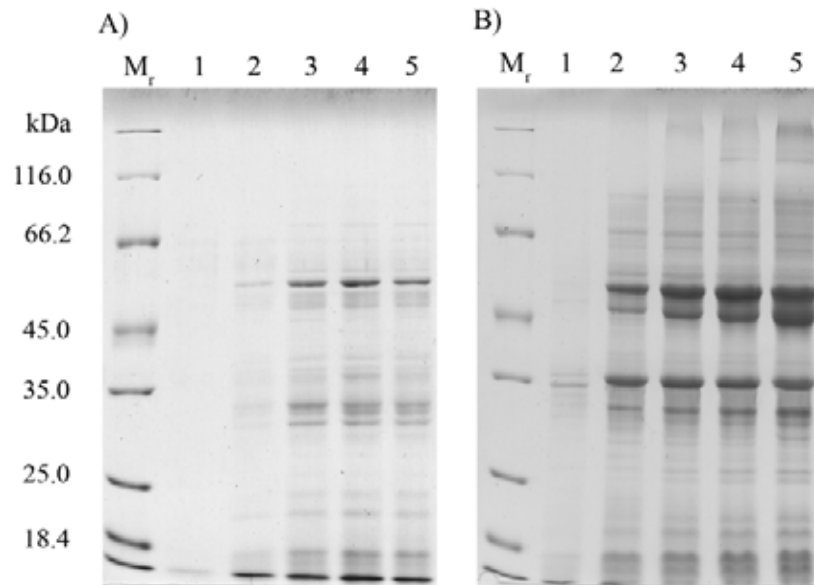


Figure 3.17 Expression of LsRN under T7 promoter

The *E. coli* Rosetta (DE3) pLysS carrying pETLsRN was expressed in 3xLB medium. The expressed LsRN at each time point were analyzed by SDS-PAGE panel A) extracellular protein, panel B) Total cell protein

Lane M_r: Standard protein Mw

Lane 1: *E. coli* Rosetta (DE3)pLysS carrying pET 19b

Lane 2: *E. coli* Rosetta (DE3) pLysS carrying pETLsRN after 2 h of induction

Lane 3: *E. coli* Rosetta (DE3) pLysS carrying pETLsRN after 4 h of induction

Lane 4: *E. coli* Rosetta (DE3) pLysS carrying pETLsRN after 8 h of induction

Lane 5: *E. coli* Rosetta (DE3) pLysS carrying pETLsRN after 16 h of induction

3.6 Purification of levansucrase

3.6.1 Preparation of crude levansucrase

The crude recombinant LsRN was expressed in *E. coli* TOP-10. After 36 h of cultivation in 400 mL of 3xLB, 375 mL of crude enzyme was obtained by centrifugation. The crude enzyme activity was 43.9 U/mL and 24.0 mg protein/mL. The specific activity of the crude enzyme was 1.83 U/mg protein.

3.6.2 DEAE Toyopearl-650M

In order to reduce the salt concentration (in modified 3xLB medium, the NaCl concentration was 0.26 M) of crude enzyme, the culture medium was 4 fold diluted by 10 mM sodium acetate buffer, pH 6.0 and applied onto a DEAE Toyopearl column, then eluted by a linear gradient of 0-1.0 M NaCl in buffer. The chromatogram is shown in Fig 3.18. The active fractions were pooled. Specific activity of LsRN was increased to 61.8 U/mg with 34 purification fold (Table 3.2.). The yield was 88% of the starting crude enzyme due to the surprisingly increase in total activity.

3.6.3 Butyl Toyopearl-650M

An ammonium sulphate crystal was added to DEAE Toyopearl pooled fraction to the final concentration of 1.33 M. The enzyme fraction was subsequently applied onto a Butyl Toyopearl column and eluted by a linear gradient of 1.33-0 M ammonium sulphate in acetate buffer. The specific activity of the active fraction was increased to 417.3 U/mg protein with 258 purification fold and 64% yield (Table 3.2).

3.6.4 Determination of enzyme purity

To determine purity for LsRN, the aliquot samples from each purification step were analyzed by SDS-PAGE. The purified LsRN exhibited a high degree of apparent homogeneity (Fig. 3.20 A)

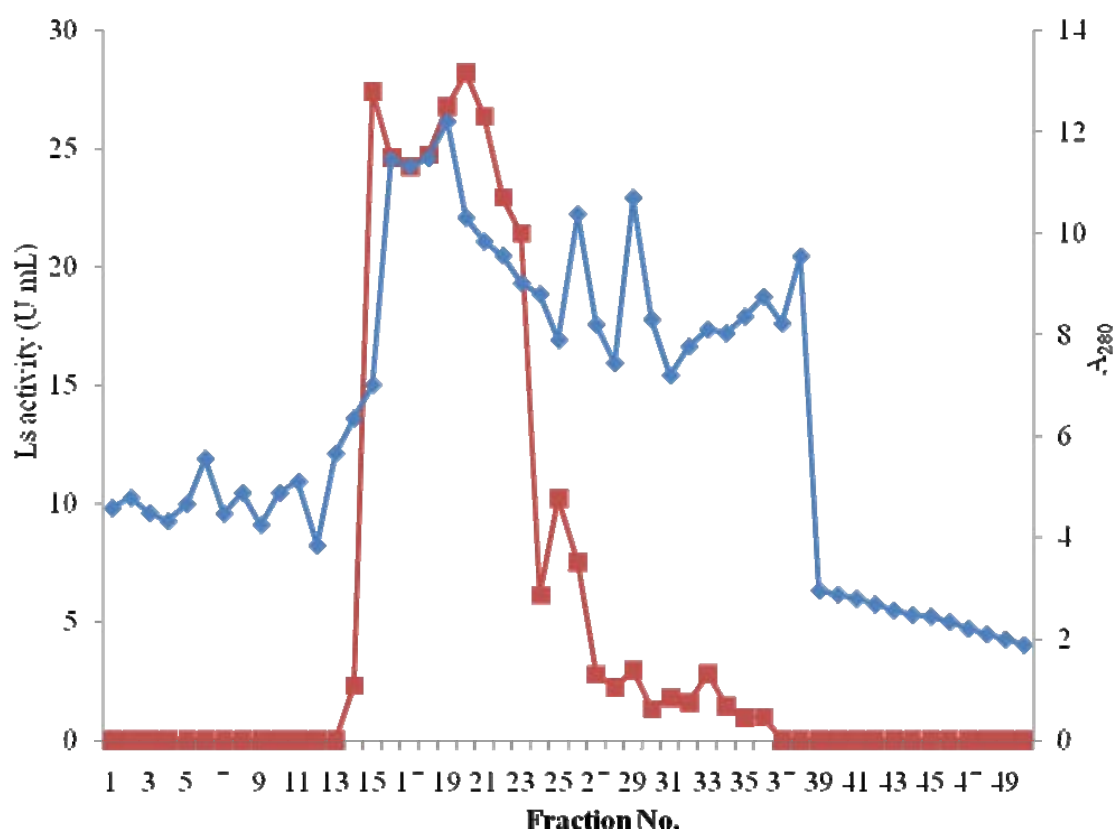


Figure 3.18 DEAE Toyopearl-650M Chromatographic profile of LsRN

The LsRN was applied to DEAE-Toyopearl-650M column equilibrated with 50 mM sodium acetate buffer, pH 6.0. Flow rate was 30 mL/h with 4 mL fraction size. The bound proteins were eluted by a linear gradient of the NaCl concentration (0-1 M). (◆;Ls activity, ■;A₂₈₀)

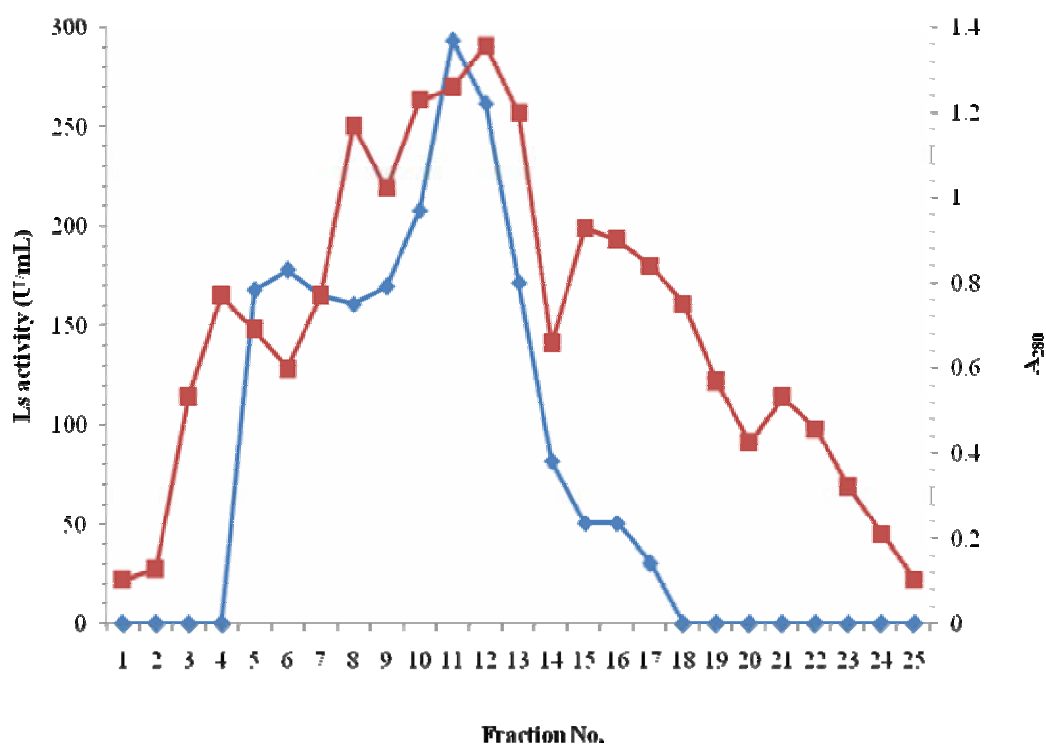


Figure 3.19 Butyl Toyopearl-650M Chromatographic profile of LsRN

The LsRN was applied to Butyl-Toyopearl-650M column equilibrated with 25mM sodium acetate buffer, pH 6.0 containing 1.33 M ammonium sulfate. Flow rate was 25 mL/hr with 4 mL fraction size. The bound proteins were eluted by a decreasing the ammonium sulfate (1.33-0 M). (◆;Ls activity, ■; A₂₈₀)

Table 3.3 Purification of LsRN by two chromatographic steps

Purification step	Volume (mL)	Activity (U/mL)	Protein (mg/mL)	Total Activity ($\times 10^4$ U)	Total Protein (mg)	Specific Activity (U/mg)	Recovery (%)	Fold
Crude	375	43.9	24.0	1.6	9000	1.8	100	1
DEAE Toyopearl 650-M	100	441.1	7.1	4.4	710	62.1	275	35
Butyl Toyopearl 650-M	40	263.2	0.1	1.1	4	2750	69	1528

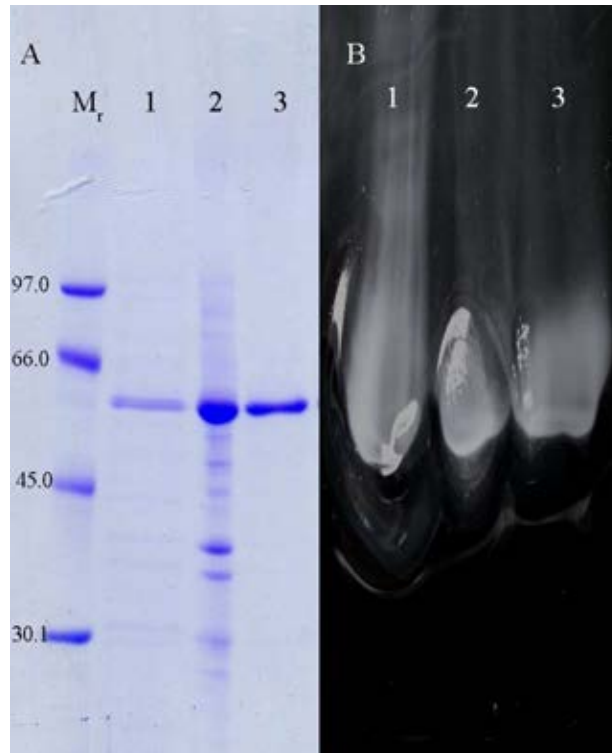


Figure 3.20 SDS-PAGE of the recombinant LsRN

The enzyme expressed by *E. coli* Top-10 cells was purified and each step was analyzed on SDS-PAGE. Panel A: protein staining B: activity staining

Lane M: protein molecular weight marker

Lane 1: crude enzyme

Lane 2: DEAE-Toyopearl pooled fraction

Lane 3: Butyl-Toyopearl pooled fraction.

3.7 Characterization of levansucrase

3.7.1 Determination of Mw of LsRN

The Mw of LsRN was determined by gel filtration and SDS-PAGE combining with a zymogram

3.7.1.1 SDS-PAGE and zymogram

The estimated molecular weight of LsRN was determined by comparing the relative mobility (R_f) of the purified enzyme with the standard molecular weight marker proteins. The purified LsRN showed an estimated size of 52.1 kDa, corresponding to the protein band that produced the mucous-like polymer in the zymogram (Fig 3.20A and B).

3.7.1.2 Sephadex G75 (SF)

The purified enzyme was applied to a Sephadex G75 (SF) column. As shown in Fig 3.21, the enzyme activity was detected in the fraction between bovine serum albumin (Mw: 67 kDa) and egg white ovalbumin (Mw: 43 kDa). The M_w of 54.5 kDa was estimated by comparing with standard proteins.

The size of LsRN determined by SDS-PAGE and Gel filtration chromatography was in the range of 52.1-54.5 kDa, the result revealed that the enzyme was a single polypeptide chain with no subunit structure. The size matched with the calculated Mw from the deduced amino acid sequence obtained (Table 3.3).

Table 3.4 Comparison of Mw of LsRN determined by different techniques

Determination technique	Molecular weight (kDa)
Calculated from deduced amino acid	
Full length protein (482 residues)	53.7
Mature protein (453 residues)	50.9
SDS-PAGE and zymogram	52.1
Gel filtration (Sephadex G75 (SF))	54.5

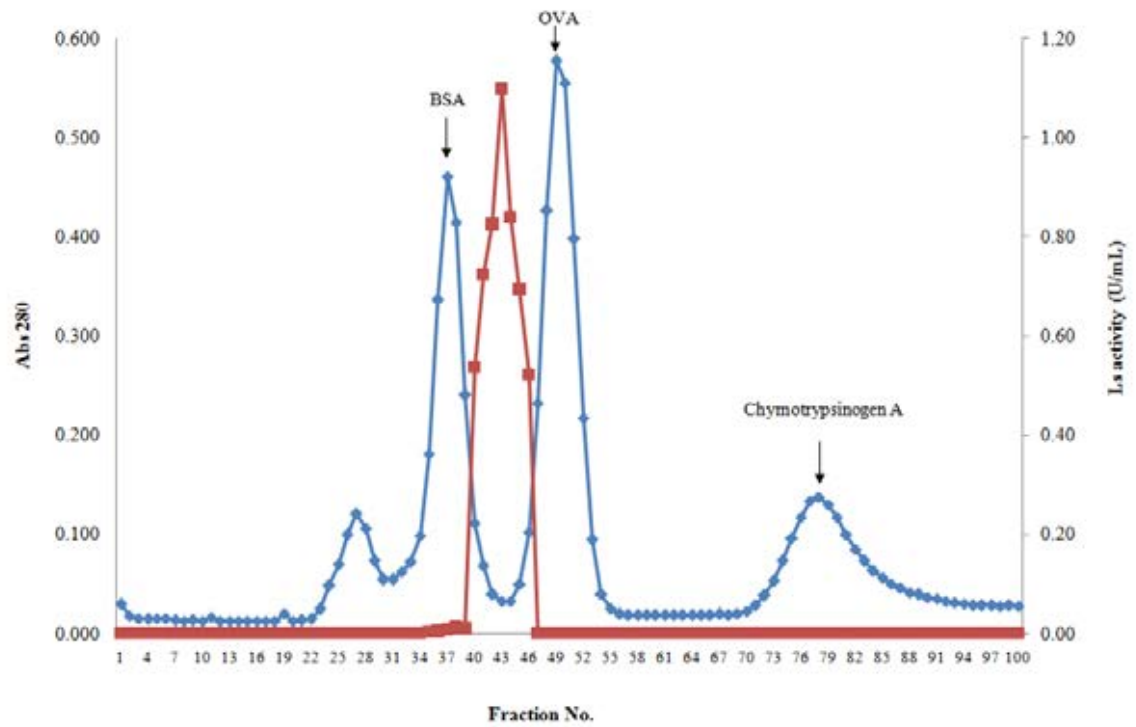


Figure 3.21 Sephadex G75 (SF) Chromatographic profile of LsRN

The LsRN was applied to Sephadex G75 (SF) by using 25 mM sodium acetate buffer, pH 6.0 containing 0.15 M NaCl as a running buffer. Flow rate was 15 mL/h with 2 mL fraction size. (◆: A₂₈₀, ■: Ls activity)

3.7.2 The effect of temperature on LsRN activity and stability.

The effect of temperature on LsRN activity was investigated by incubating the enzyme with 20% (w/v) sucrose in 50 mM acetate buffer pH 6.0 at various temperatures from 20 to 60 °C (Fig 3.22). LsRN showed optimum activity at 50 °C. The activities at 40 and 60°C were approximately 60 and 20% of its maximum activity.

The thermostability of LsRN was investigated by pre-incubating the enzyme for 1 and 6 h at various temperatures ranging from 20 to 60 °C. The remaining enzymatic activities were determined under assayed conditions (Fig 3.23). After 1 h of pre-incubation at the temperature lower than 50 °C, higher than 80% of relative activities still remained. However, a complete loss of activity was obtained at 50 °C. The thermostability after 6 h preincubation revealed the same stability trend as the 1 h preincubation.

3.7.3 The effect of pH on LsRN activity and stability

The effect of pH on LsRN activity was investigated by incubating the enzyme with 20% (w/v) sucrose in buffer pH 3.0-9.0 at 50 °C. A maximal hydrolytic activity of LsRN was observed in 50 mM citrate buffer, pH 6.0. LsRN retained 90 and 80 % of its maximum activity when reacted in buffer pH 5.0 and 7.0, respectively.

The stability of LsRN against various pHs was determined by comparative measuring the retaining activity after pre-incubation in the buffer pH ranging from 3.0 to 9.0. After pre-incubation at 30°C for 1 h, LsRN retained more than 80% of the full activity. When prolonged the incubation period to 6 h, the enzyme still retained more than 70% of the full activity in the pH range 5.0-7.0. When pre-incubated at 50°C, the enzyme retained approximately 50% in the pH 5.0-7.0 but lost almost all activity at the pH below 4.0 and above 8.0.

3.7.4 The effect of metal ions and chelating agent on LsRN activity

The effects of metal ions and chelating agent were determined by measuring the activity in the presence of 1 mM of each metal ion. The results are summarized in Table 3.4. CaCl₂ and MnCl₂ significantly promoted LsRN activity up to 136 and 158% of the control reaction. While NaCl and KCl had no effect on LsRN activity, all other metal ions decreased the enzyme activity, especially ZnCl₂, CuCl₂ and HgCl₂. EDTA also completely inhibited LsRN activity

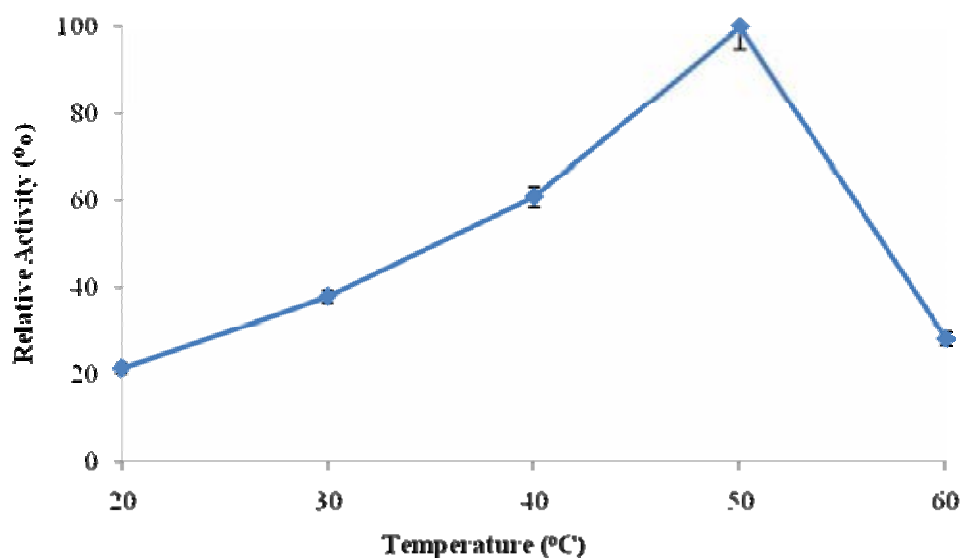


Figure 3.22 Optimum temperature of LsRN

The 0.5 U/mL LsRN was incubated with 20% (W/V) sucrose in 50 mM citrate buffer, pH 6.0 at various temperatures for 15 min. The highest activity at 50 °C was defined as 100% relative activity.

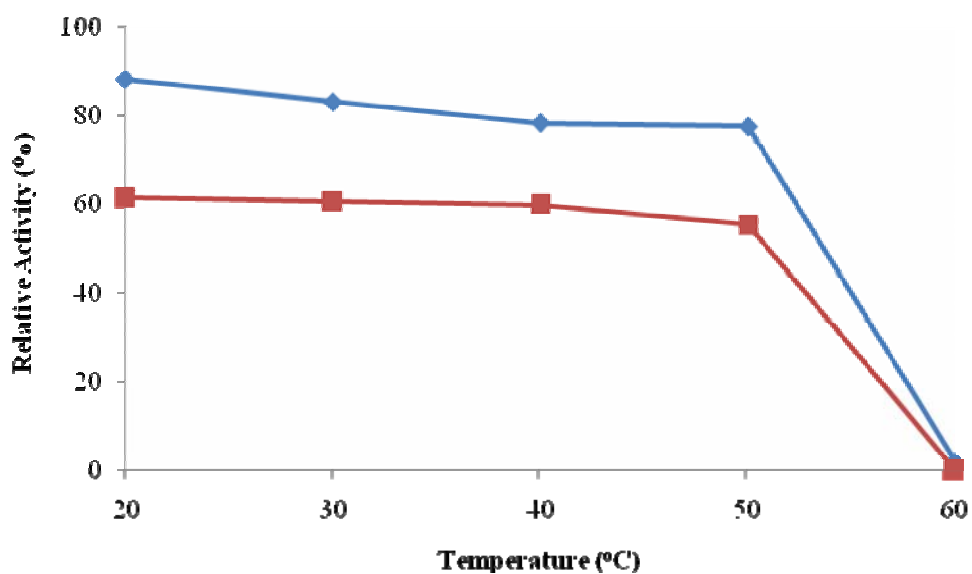


Figure 3.23 Temperature stability of LsRN

The LsRN was incubated in 50 mM citrate buffer, pH 6.0 at various temperatures for 1 hr (◆) and 6 hr (■). The pre-incubated enzymes were diluted to 0.5 U/mL and subsequently incubated with 20% (W/V) sucrose at 50 °C for 15 min. The LsRN activity without pre-incubation was defined as 100% relative activity.

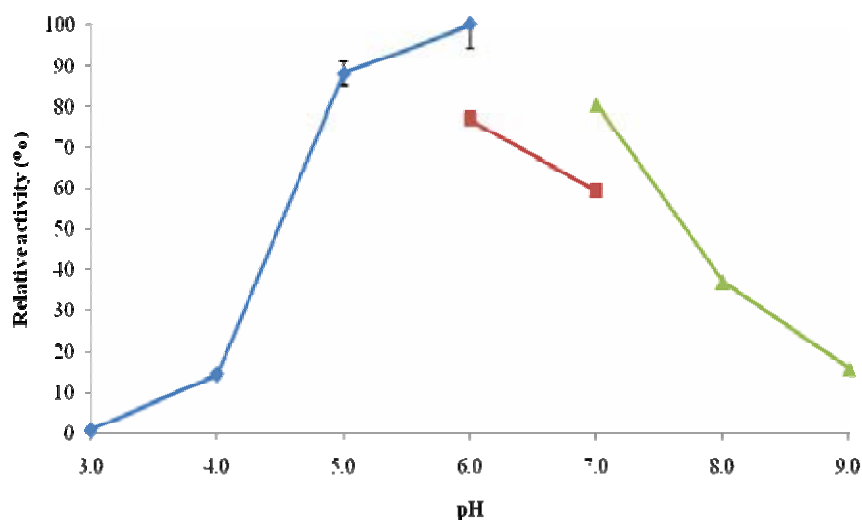


Figure 3.24 Optimum pH of LsRN

The 0.5 U/mL LsRN was incubated with 20% (W/V) sucrose in 50 mM of various buffers for 15 min. The highest activity at pH 6.0 was defined as 100% relative activity. Where the \blacklozenge , \blacksquare , and \blacktriangle represented citrate, phosphate, and tris-HCl buffer, respectively.

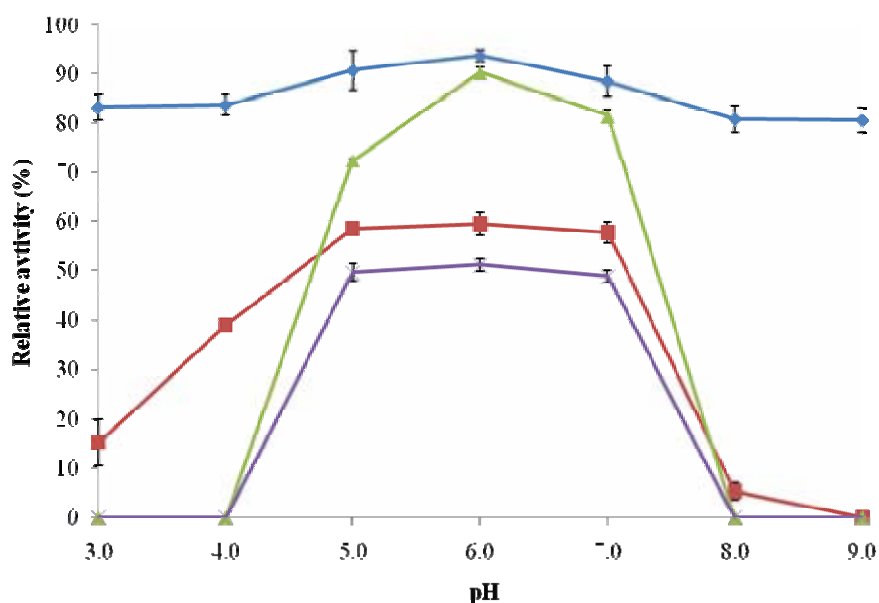


Figure 3.25 pH stability of LsRN

The LsRN was pre-incubated in 50 mM of various pH at two different temperatures, 1 hr at 30°C (\blacklozenge), 1 hr at 50°C (\blacktriangle), 6 hr at 30°C (\blacksquare) and 6 hr at 50°C (\times). The pre-incubated enzymes were diluted to 0.5 U/mL and subsequently reacted with 20% (W/V) sucrose at 50°C for 15 min. The LsRN activity without pre-incubation was defined as 100% relative activity.

Table 3.5 **Effect of metal ions and chelating agent on LsRN activity**

Metal ions	Relative Activity (%)	±SD
None	100	1.8
NaCl	113	4.7
KCl	112	2.6
MgCl ₂	98	7.2
CaCl ₂	136	0.9
FeCl ₂	22	2.6
MnCl ₂	158	4.3
ZnCl ₂	27	1.3
CuCl ₂	2	0.4
CoCl ₂	99	2.3
EDTA	0	0.0
HgCl ₂	0	0.0

3.7.5 The effect of donor substrate concentration on LsRN activity and levan product size distribution

The concentration of sucrose donor was varied from 5-80% (w/v) and the hydrolysis as well as transfructosylation activity of LsRN were measured. The enzyme hydrolysis activity increased as the sucrose concentration increased from 5-50% (w/v), the hydrolysis activity, however, became apparently saturable at the sucrose concentration above 50% (w/v). The transfructosylation activity also increased as the donor substrate increased from 5-20% (w/v) and saturated at the sucrose concentration above 20% (w/v) as shown in Figure 3.26.

To determine levan product pattern synthesized in various sucrose concentration reaction, the LsRN was incubated with 0-80% (w/v) sucrose for overnight and the reactions were analyzed by TLC (Fig 3.27). At 5% (w/v) sucrose, the enzyme completely hydrolyzed sucrose to monosaccharides and synthesized GF₂ and levan. When increased sucrose concentration to 10% (w/v), GF₃ was also detected. At 20% (w/v) sucrose, not only GF₃ was detected but the larger oligosaccharides were also detected.

By combining both results, 20% (w/v) sucrose was the lowest substrate concentration, giving the highest transfructosylation activity. At this sucrose concentration, the LsRN could produce fructan both in the form of oligosaccharides and polysaccharides. The 20% (w/v) sucrose was then used as the substrate concentration throughout this work.

3.7.6 The time course of LsRN reaction

To monitor the enzymatic reaction product, LsRN was incubated with 20% (w/v) sucrose. The reaction mixtures were collected and the products at each time point were analyzed by TLC as shown in Fig. 3.28. At early stage of the reaction, LsRN converted sucrose into monosaccharides, small amount of GF₂ and levan. When prolonged the incubation time, GF₂ and GF₃ amount were increased as well as levan polymer which was obviously more accumulated, relating to the decrease of sucrose concentration in the reaction. However, after 6 h, the amount of GF₂ product was decreased and the disaccharide with the relative migration different from sucrose was found in the reaction mixture. After overnight incubation, the sucrose and GF₂ concentration kept decreasing while the larger oligosaccharides were found besides the levan polymer.

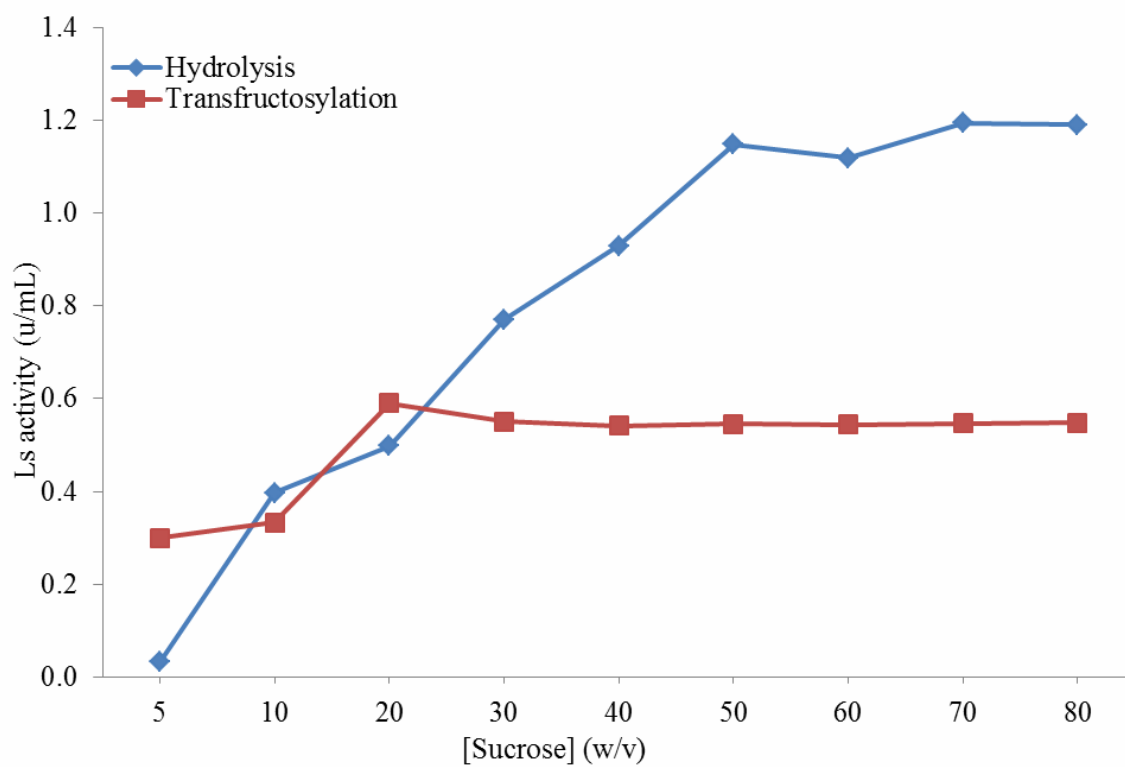


Figure 3.26 Hydrolysis versus transfructosylation of LsRN at various sucrose concentrations

The enzymatic reactions were carried out at 50° C in 50 mM citrate buffer, pH 6.0, using various sucrose concentrations for 10 min.

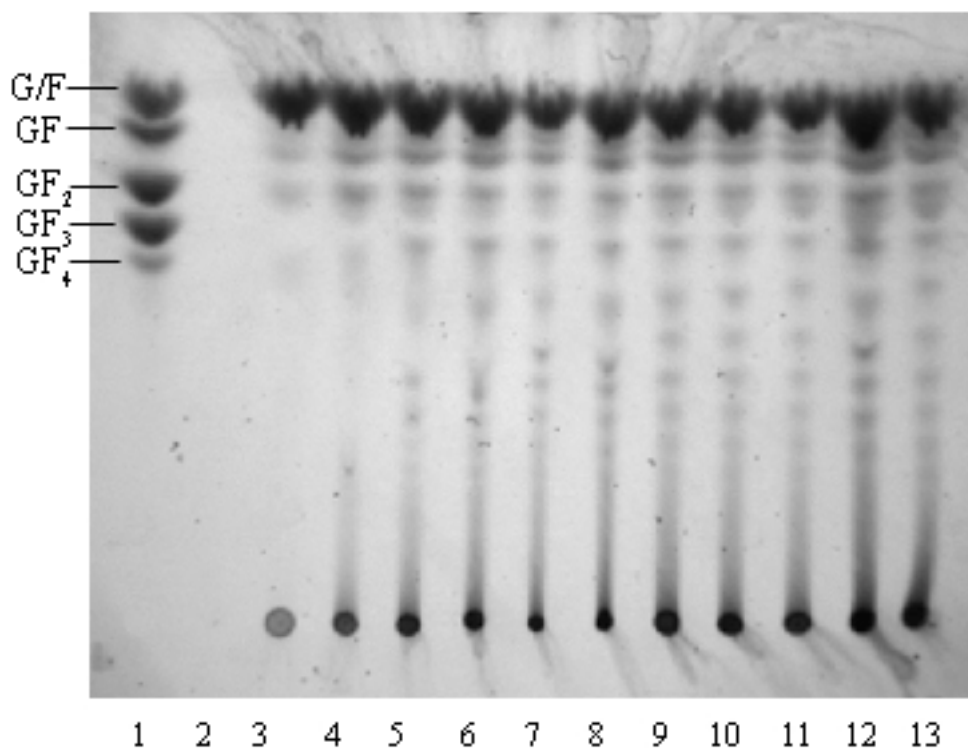


Figure 3.27 TLC analysis of reaction products formed after incubation with various sucrose concentrations

The LsRN was incubated with 0-100% (w/v) sucrose in 50 mM citrate buffer, pH 6.0 at 50° C for overnight. The reaction mixtures were analyzed by TLC

Lane 1: Standard GF-GF4

Lane 2: The reaction mixture with 0% (w/v) sucrose

Lane 3: The reaction mixture with 5% (w/v) sucrose

Lane 4: The reaction mixture with 10% (w/v) sucrose

Lane 5: The reaction mixture with 15% (w/v) sucrose

Lane 6: The reaction mixture with 20% (w/v) sucrose

Lane 7: The reaction mixture with 25% (w/v) sucrose

Lane 8: The reaction mixture with 30% (w/v) sucrose

Lane 9: The reaction mixture with 40% (w/v) sucrose

Lane 10: The reaction mixture with 50% (w/v) sucrose

Lane 11: The reaction mixture with 60% (w/v) sucrose

Lane 12: The reaction mixture with 70% (w/v) sucrose

Lane 13: The reaction mixture with 80% (w/v) sucrose

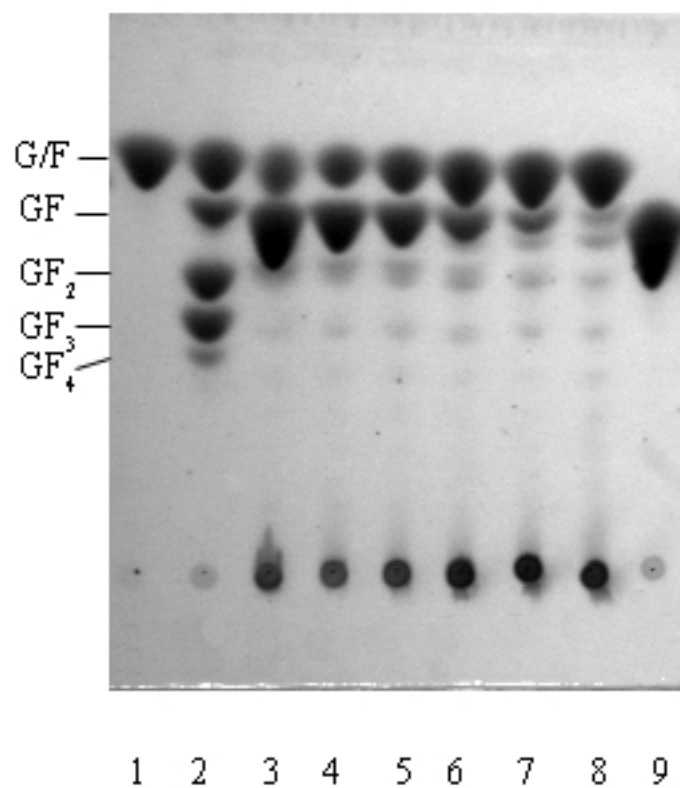


Figure 3.28 TLC analysis of reaction products at different time points

The LsRN was incubated with 20% (w/v) sucrose in 50 mM citrate buffer, pH 6.0 at 50° C. The reaction mixtures were analyzed by TLC

Lane 1: Standard glucose and fructose

Lane 2: Standard GF-GF₄

Lane 3: The reaction mixture after 30 min

Lane 4: The reaction mixture after 1 h

Lane 5: The reaction mixture after 2 h

Lane 6: The reaction mixture after 4 h

Lane 7: The reaction mixture after 6 h

Lane 8: The reaction mixture after 16 h

Lane 9: Standard sucrose

3.7.7 Product pattern of LsRN

LsRN synthesized a broad range of saccharide products; a mixture of oligosaccharides and polysaccharides. To determine the pattern and molecular weight of levan products, HPAEC, MALDI-TOF and HPLC were performed.

The levan oligosaccharide product pattern was analyzed by HPAEC. From the chromatogram (Fig 3.29), glucose which highly accumulated in the reaction was eluted from the column first, following by free fructose molecule and a mixture of disaccharides. The larger oligosaccharides were observed as a group of spitting peaks. The levan oligosaccharides were molecular mass analyzed by MALDI-TOF. The oligosaccharides with molecular mass of 504-4368 corresponded to GF₂-GF₂₅ were detected in the mass/charge range of 500-5000 (Fig 3.30).

The M_w of levan polysaccharide was analyzed by HPLC, using known M_w levan synthesized by levansucrase from *B. subtilis* as a standard (Appendix A). The chromatogram shown in Fig. 3.32 separated levan products into five fractions, the major fraction with 50% of total amount exhibited the highest M_w of 612 kDa. The rest four-fractions were categorized as low M_w levan with the M_w of about 66.3, 28.9, 8.7, and 1.1 kDa, respectively.

3.7.8 The effect of temperature and NaCl on the M_w of levan product pattern

The levan product size synthesized by LsRN at 30 °C and 50 °C were determined by HPLC. As shown in Table 3.5, the wide range of M_w of levan (about 1-600 kDa) was synthesized in a controlled reaction by varying two parameters, temperature and NaCl concentration.

The M_w of levan synthesized at 50 °C was described in 3.7.7, whilst at 30 °C, LsRN synthesized low M_w levan of 11 kDa as a major product, approximately 80% of the total amount. 17% was 1.1 kDa levan and the rest 3 % was the high M_w levan of 542.3 kDa. When increased an ionic strength of the reactions by adding 0.5 M NaCl, the reaction at 50 °C produced a mixture of high and low M_w levan. The major product of 80% of the total amount was a 10.8 kDa. The other low M_w levan; 11.8 and 1.1 kDa in size were also detected, including 3% of high M_w levan of 542.3 kDa. At 30 °C, only low M_w levans were detected, the major product found about 80% of the total amount was 11.8 kDa levan and the smaller; 2.3 kDa (1%) and 1.1 kDa (16%).

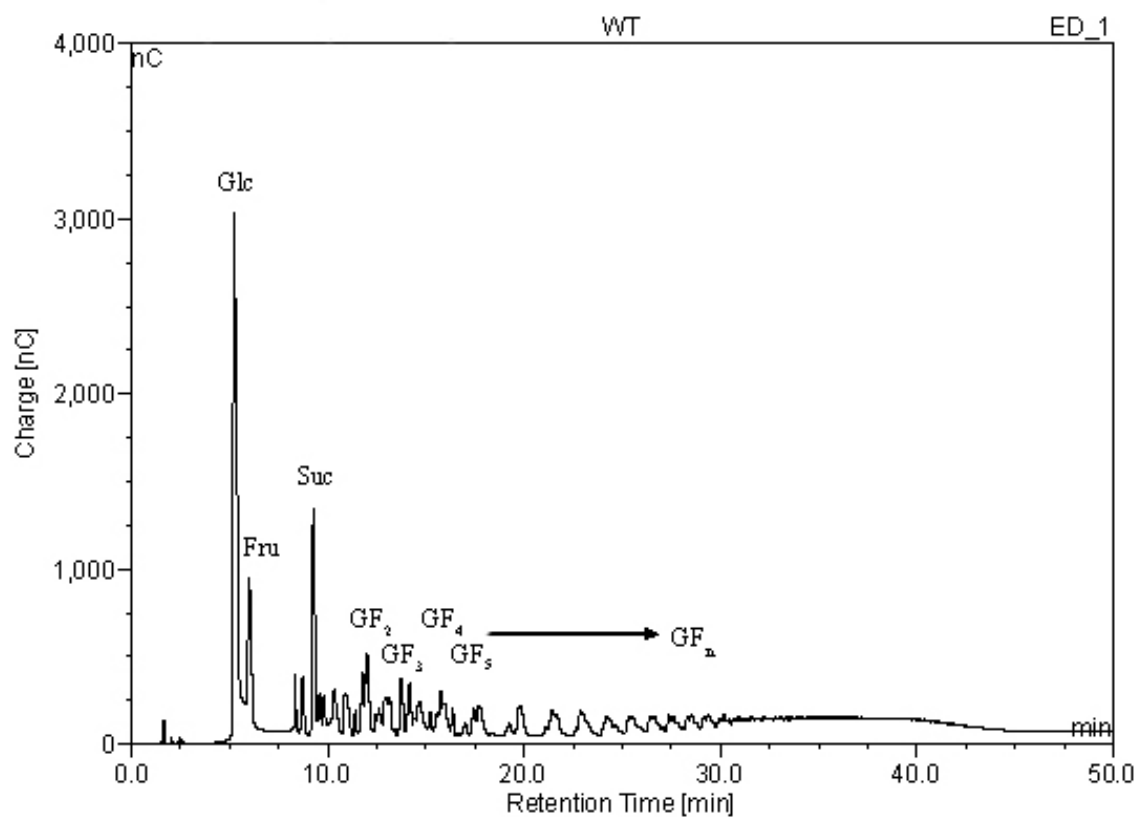


Figure 3.29 Analysis of the product pattern of LsRN by HPAEC

The 0.5 U of LsRN was incubated with 20% (w/v) sucrose at 50 °C for overnight. And the reaction product was partially purified by activated charcoal column and analyzed by HPAEC.

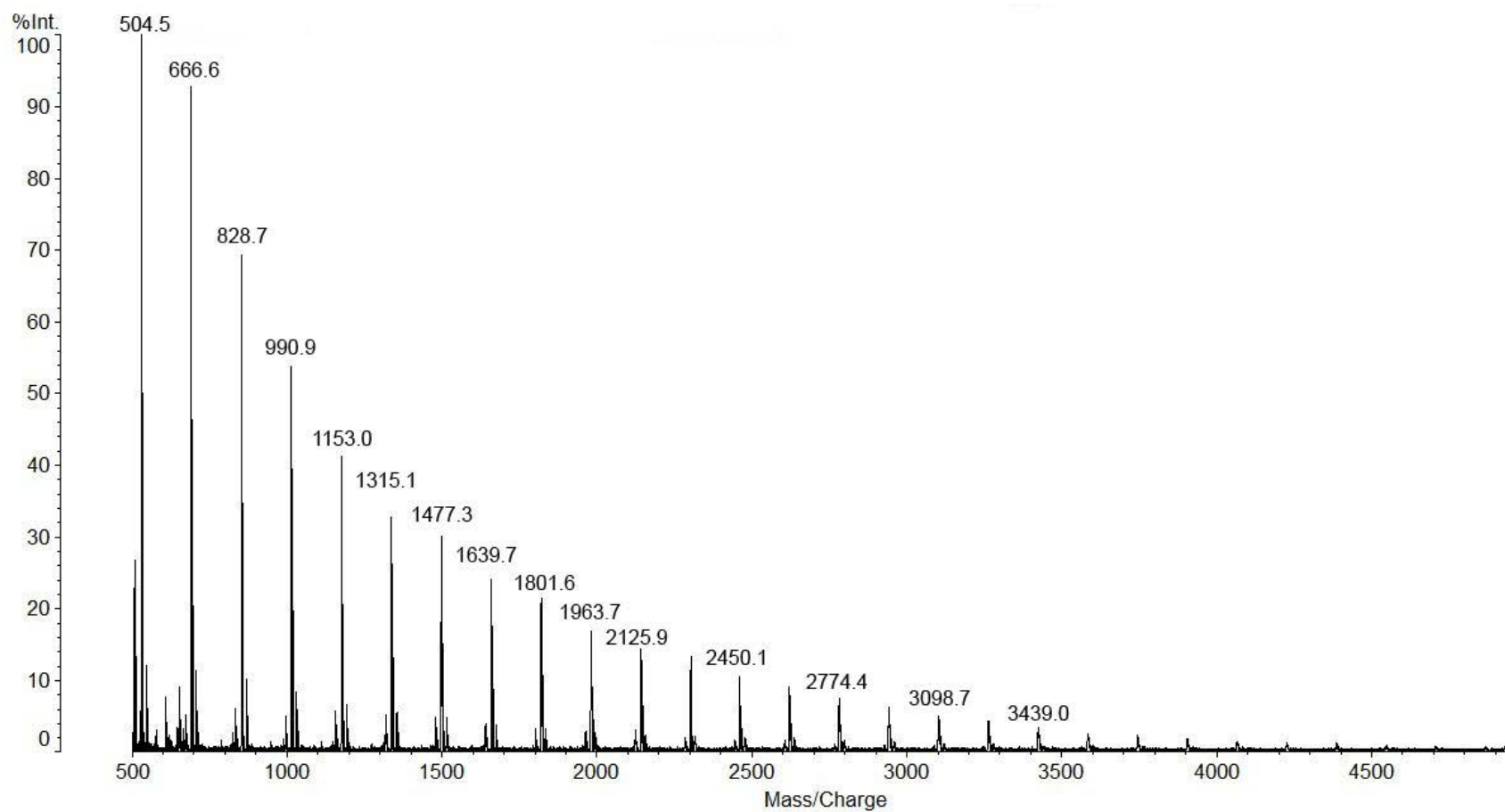


Figure 3.30 MALDI-TOF MS spectrum of LsRN reaction products

The partially purified reaction products were analyzed by MALDI-TOF MS. The molecular mass corresponded to each peak was shown.

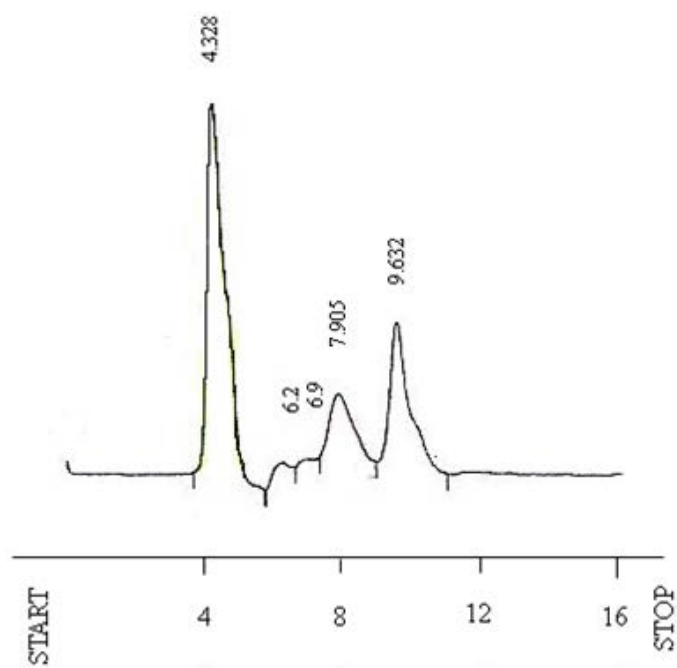


Figure 3.31 Analysis of synthesized levan by HPLC

The reaction products of parameter controlled reaction was purified and M_w estimated by HPLC, using Asahipak column (QF-510HQ).

Table 3.6 Comparison of the M_w of levan synthesized in different reaction conditions.

	Mw of levan synthesized by LsRN (kDa)	
	High M_w	Low M_w
50°C		
without NaCl	612.1 (50)	66.3 (3) 28.9 (4) 8.7 (19) 1.1 (24)
with 0.5 M NaCl	542.3 (3)	10.8 (80) 1.1 (17)
30°C		
without NaCl	542.3 (3)	10.8 (80) 1.1 (17)
with 0.5 M NaCl	Undetectable	11.8 (83) 2.8 (1) 1.1 (16)

The number in parenthesis denotes percentage of each levan product in related to total amount.

3.7.9 Acceptor specificity of LsRN

To examine the acceptor specificity of LsRN, a variety of saccharides were investigated. Sucrose donor in the reaction was constant at 5% (w/v); 0.15 M, while the acceptor concentrations were varied from 0.1-0.5 M. The LsRN transferred the fructose moiety of sucrose to several monosaccharides such as glucose, xylose, galactose and ribose (Fig 3.32). Maltose, cellobiose and lactose could act as disaccharide acceptors. A trisaccharide, raffinose was an effective acceptor, producing larger oligosaccharides than those of other acceptors (Fig 3.33). However, the enzyme was unable to transfer fructosyl moiety to sugar alcohol such as glycerol, sorbitol and xylitol. Moreover, amino acid could not act as acceptor (Fig 3.34).

3.7.10 Kinetic parameters of LsRN

The kinetic parameters of LsRN were determined over the substrate concentration range of 3.13-100 mM under optimal conditions. The results shown in Fig 3.35 A) revealed that LsRN exhibited Michaelis-Menten type kinetics, indicated by the saturation curve of v_0 vs $[s]$. Kinetic parameters were determined from the corresponding Lineweaver-Burk plot shown in Fig 3.35 B). The K_m , k_{cat} , and k_{cat}/K_m values were 9.12 mM, 86.0 s⁻¹, and 9.43 mM⁻¹s⁻¹ for hydrolysis reaction, and 6.94 mM, 32.3 s⁻¹ and 4.65 mM⁻¹s⁻¹ for transfructosylation reaction.

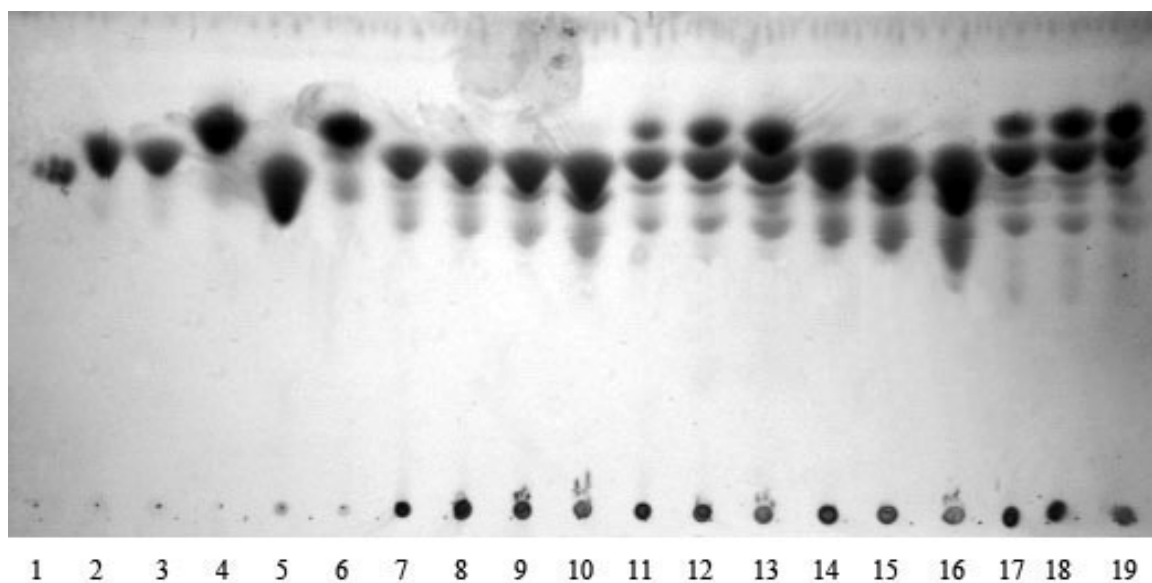


Figure 3.32 Analysis of monosaccharide acceptor specificity of LsRN by TLC

- Lane 1: Sucrose
- Lane 2: Fructose
- Lane 3: Glucose
- Lane 4: Xylose
- Lane 5: Galactose
- Lane 6: Ribose
- Lane 7: LsRN reaction without acceptor
- Lane 8-10: LsRN reaction with 0.15, 0.25 and 0.5 M glucose, respectively
- Lane 11-13: LsRN reaction with 0.15, 0.25 and 0.5 M xylose, respectively
- Lane 14-16: LsRN reaction with 0.15, 0.25 and 0.5 M galactose, respectively
- Lane 17-19: LsRN reaction with 0.15, 0.25 and 0.5 M ribose, respectively

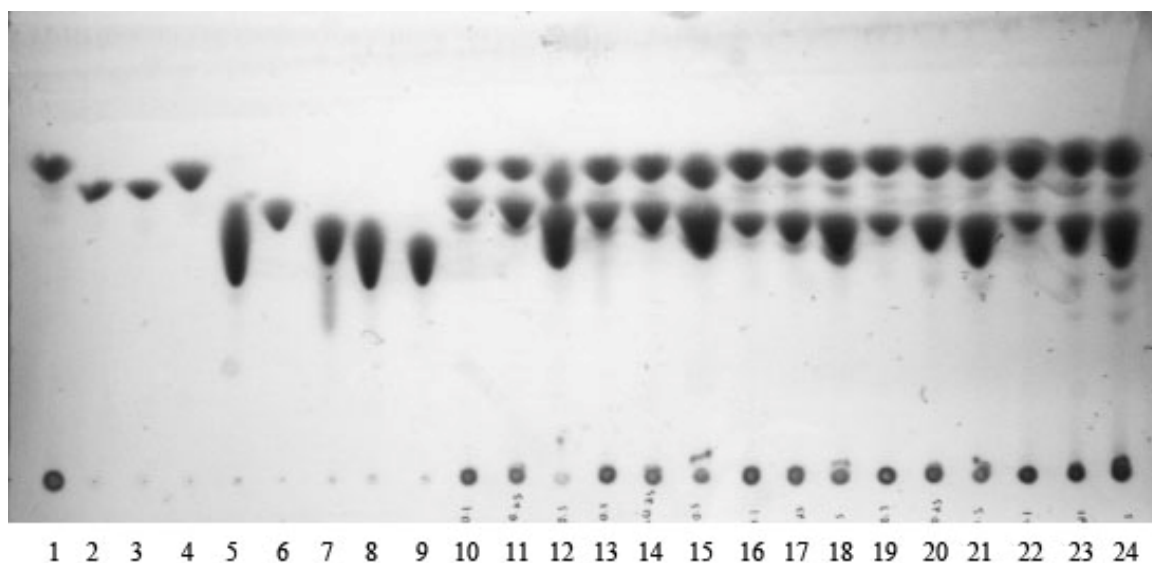


Figure 3.33 Analysis of disaccharide acceptor specificity of LsRN by TLC

- Lane 1: LsRN reaction without acceptor
- Lane 2: Sucrose
- Lane 3: Sucrose
- Lane 4: Glucose
- Lane 5: Maltose
- Lane 6: Cellobiose
- Lane 7: Lactose
- Lane 8: Melibiose
- Lane 9: Raffinose
- Lane 10-12: LsRN reaction with 0.15, 0.25 and 0.5 M maltose, respectively
- Lane 13-15: LsRN reaction with 0.15, 0.25 and 0.5 M cellobiose, respectively
- Lane 16-18: LsRN reaction with 0.15, 0.25 and 0.5 M lactose, respectively
- Lane 19-21: LsRN reaction with 0.15, 0.25 and 0.5 M melibiose, respectively
- Lane 22-24: LsRN reaction with 0.15, 0.25 and 0.5 M raffinose, respectively

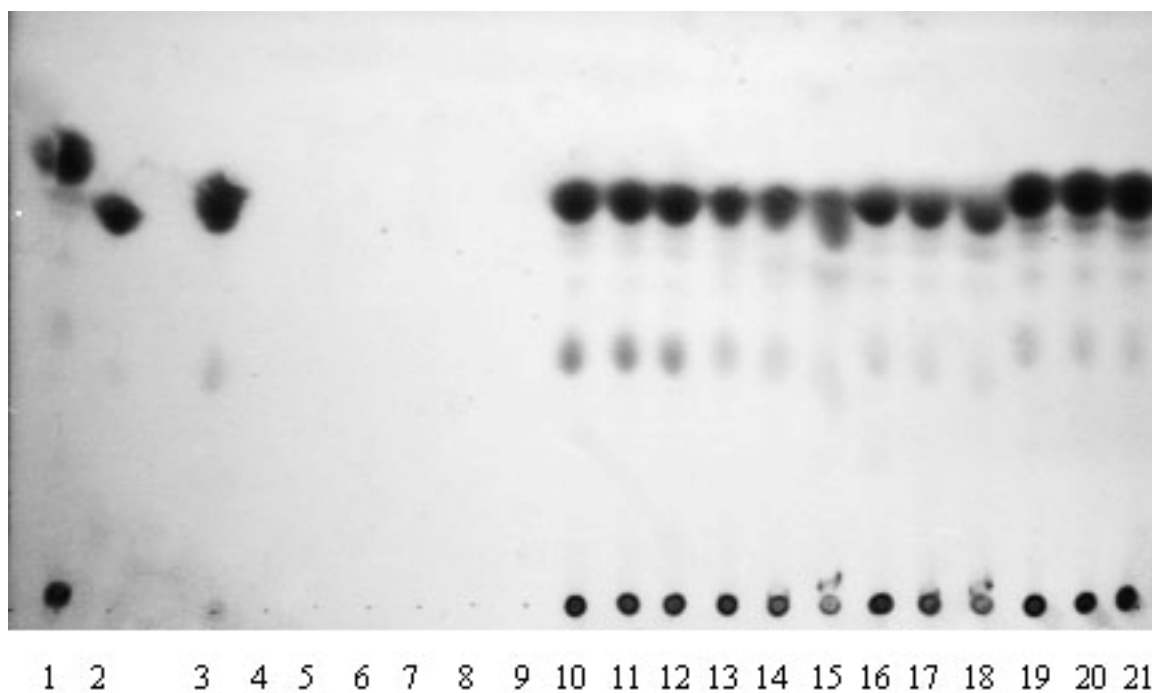


Figure 3.34 Analysis of sugar alcohol and amino acid acceptor specificity of LsRN by TLC

Lane 1:	LsRN reaction without acceptor
Lane 2:	Sucrose
Lane 3:	Glucose
Lane 4:	Glycerol
Lane 5:	Sorbitol
Lane 6:	Xylitol
Lane 7:	Tyrosine
Lane 8:	Threonine
Lane 9:	Serine
Lane 10-12:	LsRN reaction with 0.15, 0.25 and 0.5 M glycerol, respectively
Lane 13-15:	LsRN reaction with 0.15, 0.25 and 0.5 M sorbitol, respectively
Lane 16-18:	LsRN reaction with 0.15, 0.25 and 0.5 M xylitol, respectively
Lane 19:	LsRN reaction with 0.5 M tyrosine
Lane 20:	LsRN reaction with 0.5 M threonine
Lane 21:	LsRN reaction with 0.5 M serine

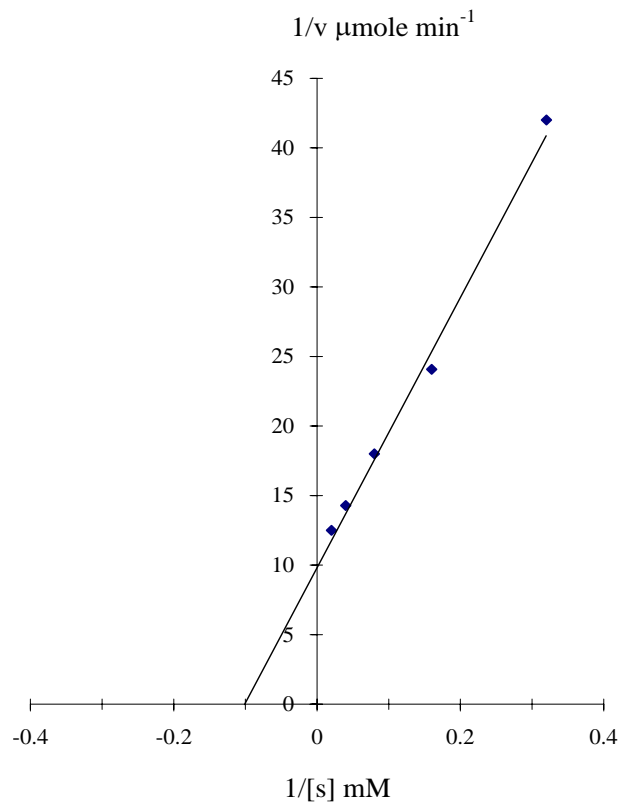
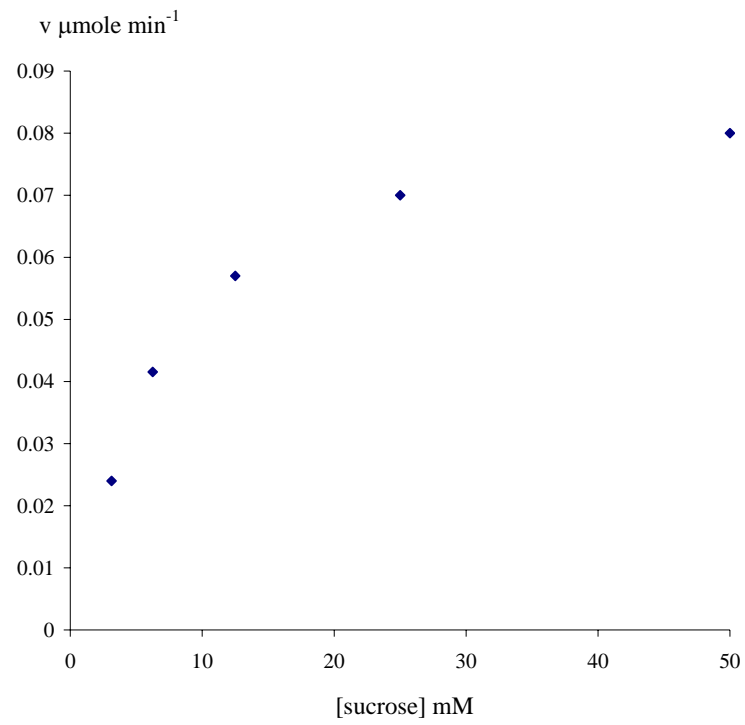


Figure 3.35 Effect of substrate concentration on rate of Ls Hydrolysis

- A) Michaelis-Menten
- B) Lineweaver-Burk

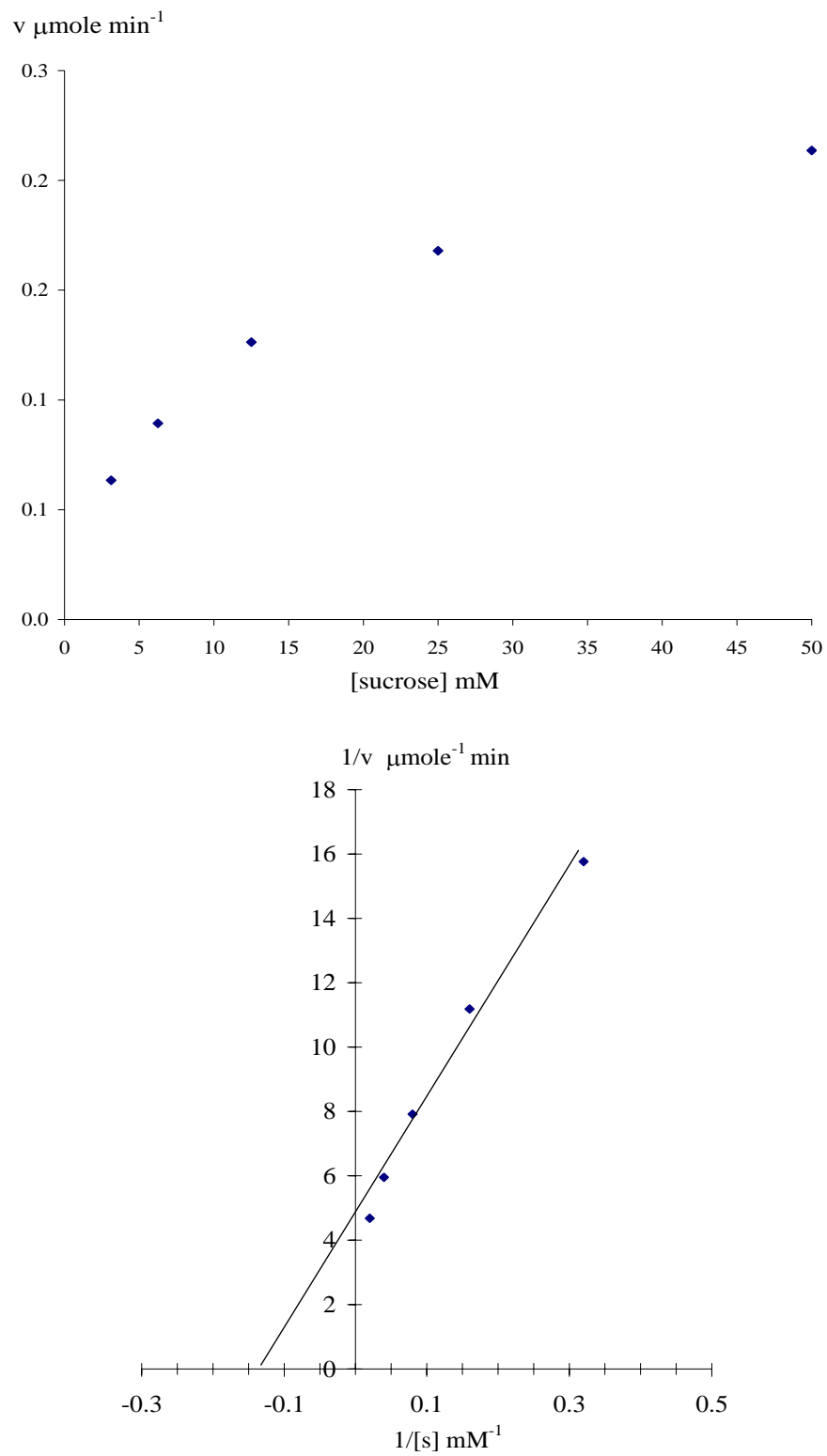


Figure 3.36 Effect of substrate concentration on rate of Ls transfructosylation

- A) Michaelis-Menten
- B) Lineweaver-Burk

3.8 Identification of levan

The polymer synthesized by LsRN was precipitated by ethanol. The polymer was purified by BioGel P-100 (Fig 3.37). Two broad peaks were found. The major high Mw polysaccharide fraction was collected and lyophilized. The polysaccharide was then dissolved in D₂O and chemical structure analyzed by ¹³C-NMR and ¹H-NMR. From the observed resonances in Fig 3.38 A), six main resonances at 106.9, 83.0, 79.3, 78.1, 66.1 and 62.9 ppm were found. The resonances are almost identical to those of *B. subtilis* and *B. polymyxa* shown in Table 3.6. However, the chemical shift of anomeric carbon, 106.9 and 106.4 indicated that the polysaccharide contained two types of linkage. The main linkage was β -(2, 6) while the minor one was β -(2, 1). The ¹H-NMR spectrum (Fig 3.38 B) showed seven protons between 3.5 and 4.2 ppm.

Table 3.7 Comparison of the ¹³C-NMR chemical shift of the levans produced from different Ls sources.

Carbon atom	Chemical Shift (ppm) of the levans formed from:		
	LsRN ^a	<i>B. polymyxa</i> Ls	<i>B. subtilis</i> Ls
C-1	62.9	60.7	60.1
C-2	106.9	104.2	104.4
C-3	79.3	77.0	76.5
C-4	78.1	75.7	75.4
C-5	83.0	80.5	80.5
C-6	66.1	63.6	63.6

^aThis work

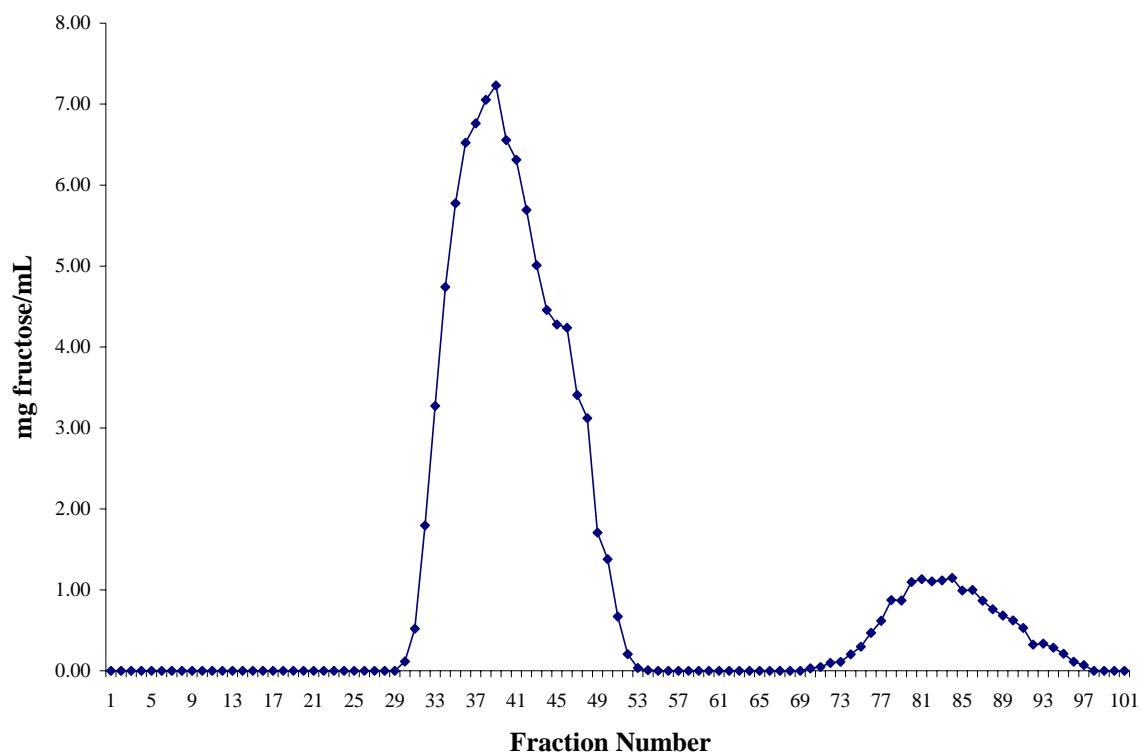


Figure 3.37 Purification of the polymer synthesized from LsRN by Biogel P-100 column

The polymer was load into Biogel P-100 using deionized water as a mobile phase. The 5 mL fractions were collected and monitored for total carbohydrate by phenol-sulfuric acid method.

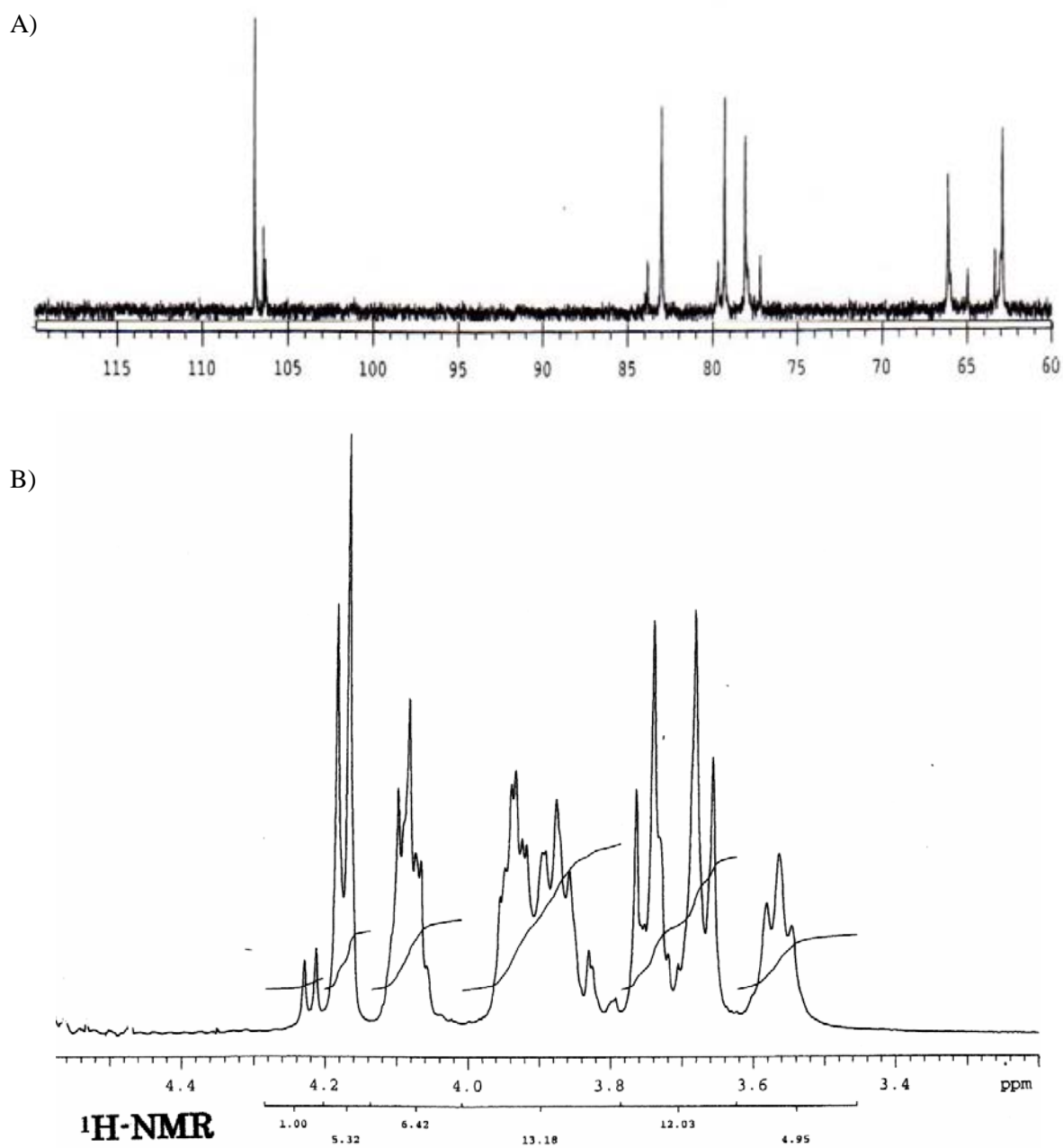


Figure 3.38 Identification of levan polymer synthesized by LsRN

A) $^{13}\text{C-NMR}$ of levan polymer synthesized by LsRN

B) $^1\text{H-NMR}$ of levan polymer synthesized by LsRN

3.9 *In situ* synthesis of levan nanoparticles

To synthesize the levan NPs, 20U of Ls with 20 % (w/v) sucrose in 50 mM citrate buffer was shaken at 50°C. After 16 h, the reaction became highly turbid colloid-like solution without settle at the bottom of the reaction flask (fig 3.39). The colloidal suspension was morphologically analyzed by TEM and AFM.

To analyze by TEM, the suspension was diluted to a million folds in deionized water. The TEM photographs were acquired at 100 kV. The TEM photograph at 10,000 x magnification showed that levan NPs were synthesized concomitantly with the levan polymer to form a dendrimer-like agglomerate. At higher resolution up to 30,000 magnification, the translucent aggregated spheres of NPs were detected. The average particle size estimated by TEM was around 50 nm (Fig 3.40).

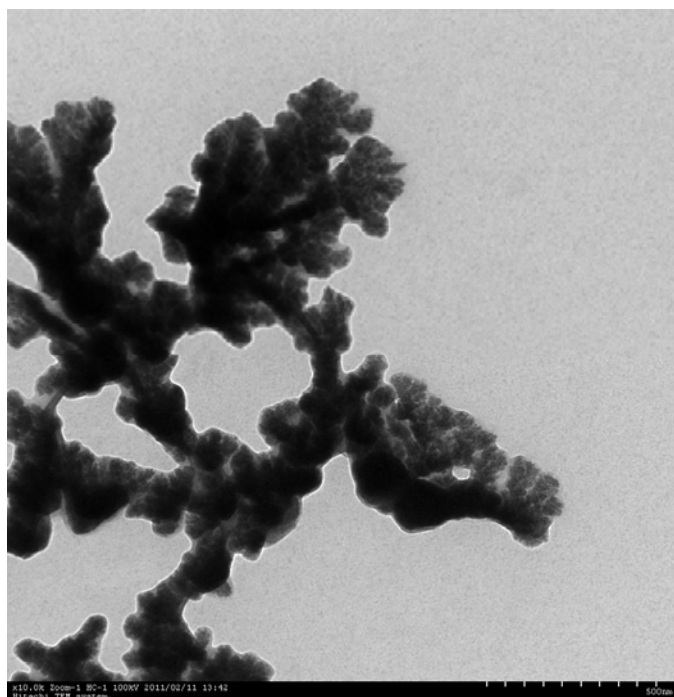
Fig 3.41 showed the AFM images of levan NPs. Height image (fig 3.41 A) and phase image (Fig 3.41 B) were acquired, simultaneously. The height mode of AFM implied the surface properties of particles while the phase mode reflects the stiffness and adhesion of the particles. For height image, it showed agglomerate globular shape with smooth surface. While the flatten image showed almost bright area, indicating the compact packing of NPs in an aggregated form.



Figure 3.39 Suspension of levan nanoparticle

20 U of LsRN was mixed with 20% (w/v) sucrose. The synthesis was performed at 50 °C with 150 rpm shaking. The photo was taken after the reaction proceeds for 16 h.

A)



B)

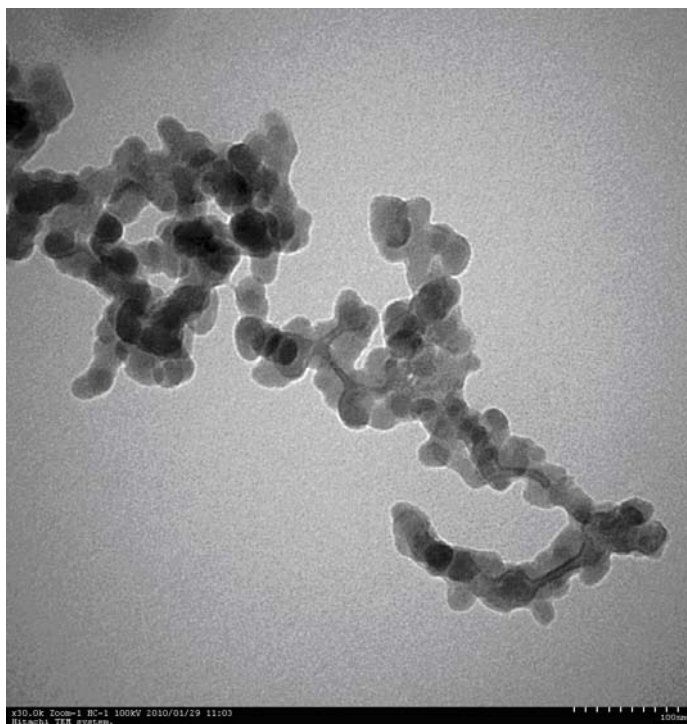


Figure 3.40 TEM-based micrographs of the levan NPs.

Micrographs show TEM of levan NPs at different magnification

- A) an agglomerate of levan NPs (10,000 x magnification)
- B) translucent spheres of levan NPs (30,000 x magnification)

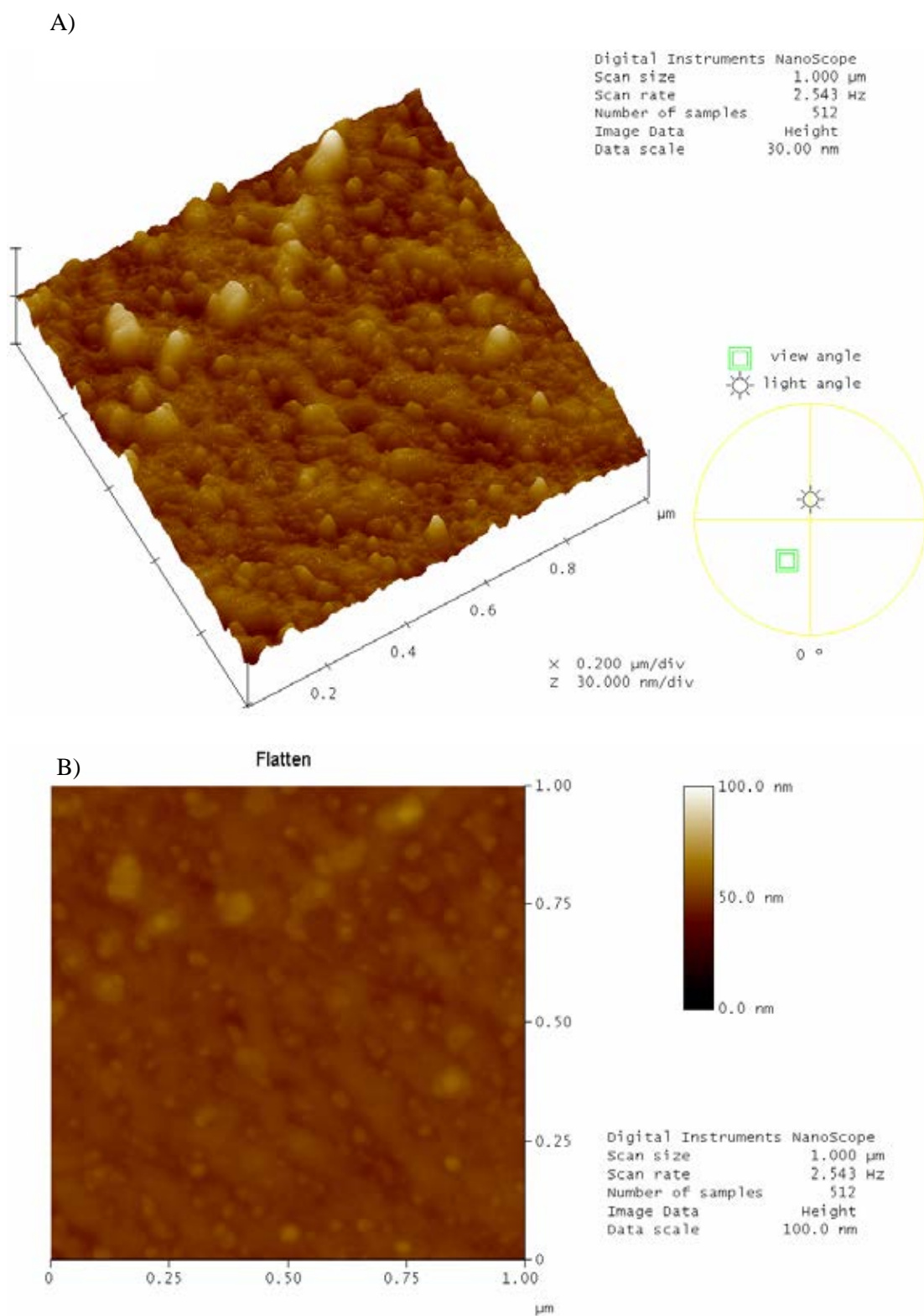


Figure 3.41 AFM photographs

A) Height image

B) Phase image

3.10 Encapsulation of *O*-acetyl- α -tocopherol in levan nanoparticles

To be of use, the levan NPs would need to be able to encapsulate suitable payload compounds. The encapsulation of *O*-acetyl- α -tocopherol into levan NPs was evaluated by the NP self-assembly as the levan was synthesized. The encapsulated NPs revealed a smooth surface and nearly monodisperse with spherical shape (Fig. 3.43), the average particle size (100 nm), as estimated by TEM, was larger than the corresponding unencapsulated levan NPs.

3.11 Analysis of chemical structure of encapsulated levan NPs

Figure 3.44 illustrates FTIR transmittance spectra of levan NPs, *O*-acetyl- α -tocopherol, and *O*-acetyl- α -tocopherol-encapsulated levan NPs. The broadband at around 3255 cm^{-1} found in levan NPs and the tocopherol-encapsulated levan NPs associated to -OH stretching vibration of levan. Bands at 1759 cm^{-1} represented C=O stretching vibration of the acetyl group in *O*-acetyl- α -tocopherol which was also found in tocopherol-encapsulated levan NPs. The band at 1456 cm^{-1} for the phenyl, skeletal and methyl asymmetric bending and 1366 cm^{-1} attributed with methyl symmetric bending was observed in acetyl- α -tocopherol and tocopherol-encapsulated levan NPs. The results thus showed the ability of levan NPs to encapsulate acetyl-tocopherol, a small non-polar compound.

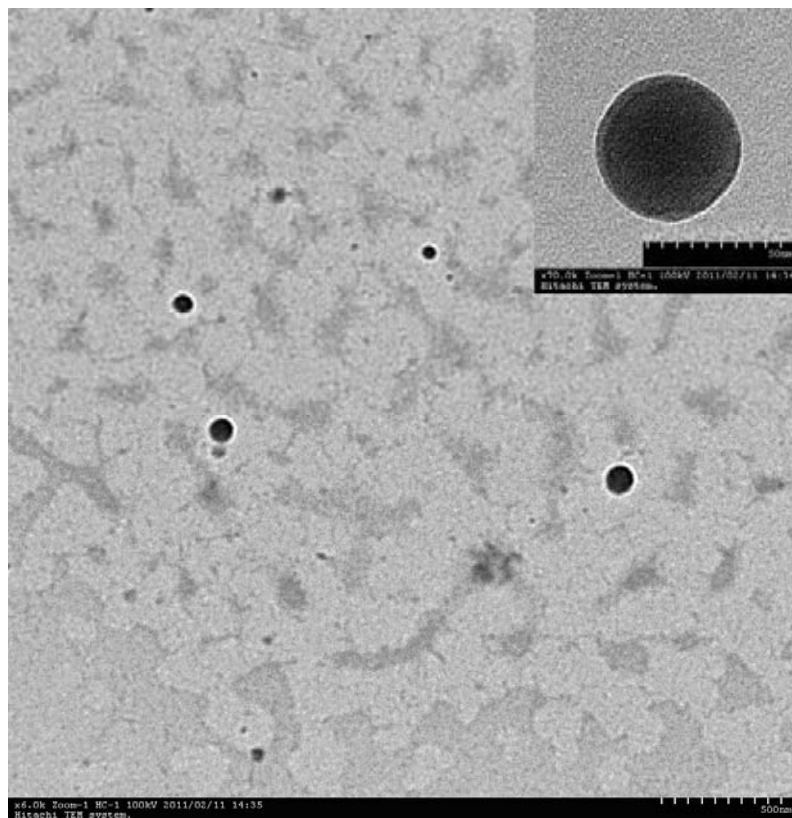


Figure 3.42 TEM-based micrographs of the O-acetyl- α -tocopherol-encapsulated levan NPs

Spheres of encapsulated NPs and the insert at the upper right showed 6,000 and 70,000 magnifications view of an encapsulated NP. TEM was performed at an accelerate voltage of 100 kV.

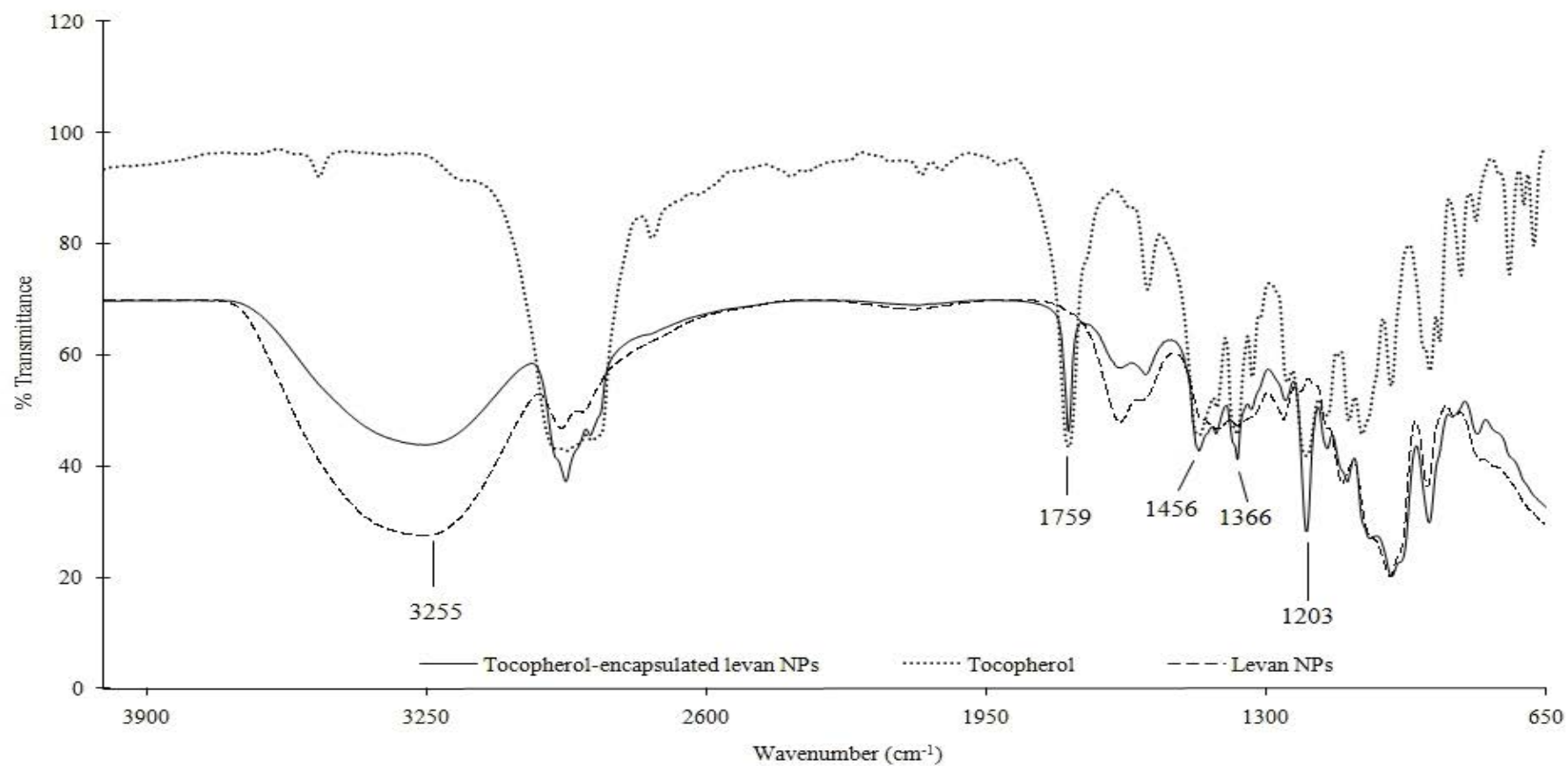


Figure 3.43 Comparison of the FTIR spectra for levan NPs, *O*-acetyl- α -tocopherol and the tocopherol-encapsulated levan NPs

3.12 Identification of amino acid residues involved in product size determination and distribution

To identify amino acid residues that play the role in levan product size determination and distribution, two mutagenesis strategies; rational and random mutagenesis were used in this work.

3.12.1 Homology modeling of LsRN by SWISS-MODEL

Homology modeling of the LsRN was accomplished by SWISS Model, using an X-ray crystallization structure of levansucrase from *B. subtilis* (PDB ID; 1OYG) as a template. The model structure showed a high reliability degree (represented by Z-score) of 0.29 when evaluated by QMEAN4. As shown in Table 3.7, the pseudo-energies of the contributing parameters were given below together with their Z-scores, respecting to scores obtained for high-resolution experimental structures of similar size solved by x-ray crystallography. The predicted model of LsRN showed a high total nativeness degree of 0.78. However, all-atom pairwise energy was higher than the average of the solved structures.

The overall structure of LsRN was almost identical to those from the x-ray structure template. As shown in Fig 3.44, the homology modeling structure (residue 35-482) was folded as five-bladed β -propeller enclosing a funnel-like central cavity. Three acidic residues at the bottom of the funnel-like cavity i.e. D93, D256 and E351 were identified as the catalytic triad. An extra loop of YNKNLID, starting at Y80 was found immediately before the first β -sheet of blade I.

Table 3.8 QMEAN4 global scores

Scoring function term	Raw score	Z-score
C interaction energy	-190.16	0.01
All-atom pairwise energy	-12270.89	-0.54
Solvation energy	-49.94	0.69
Torsion angle energy	-127.94	0.17
QMEAN4 score	0.776	0.29

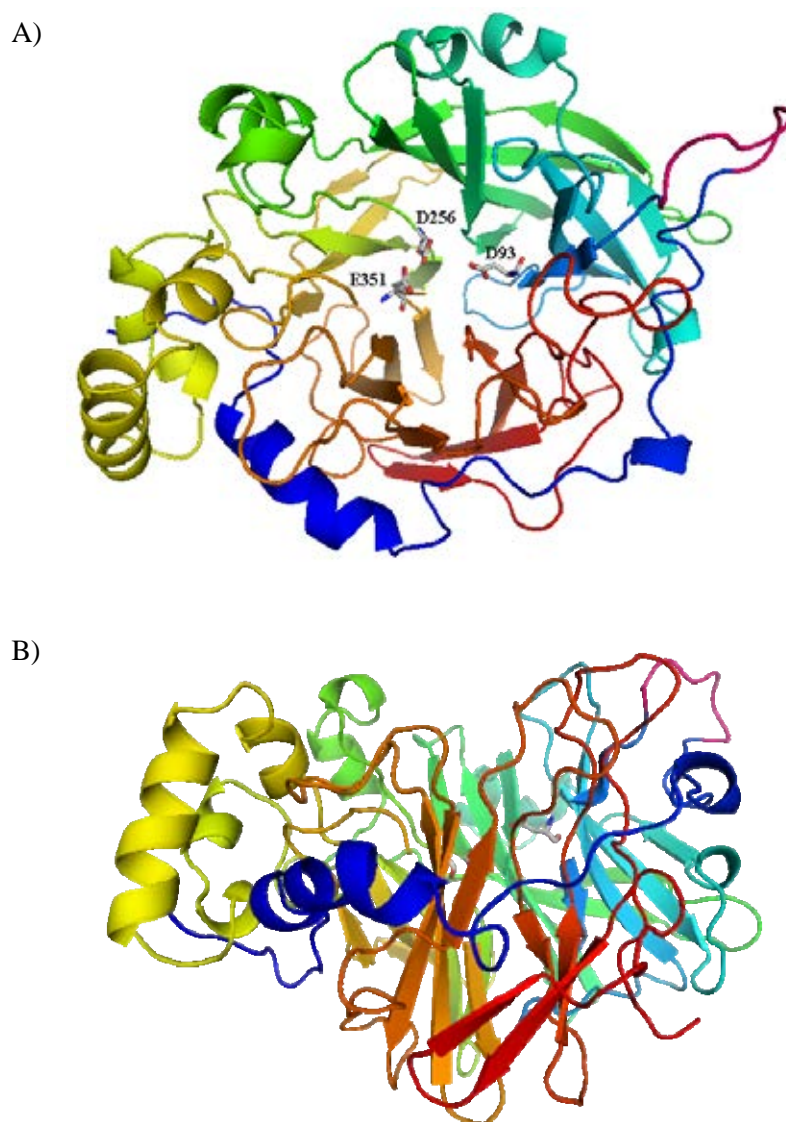


Figure 3.44 Homology modeling structure of LsRN constructed by SWISS-MODEL

Superior (A) and lateral (B) views of the five-bladed β -propeller fold with catalytic residues shown in sticks. The extra loop was shown in pink. The two orientations were shown corresponding to simultaneous 90° rotations about the vertical axis. The protein is colored according to sequence succession (N-terminal in blue and C-terminal in red). Figure was prepared using PyMOL.

3.12.2 Computer-assisted docking of raffinose into LsRN

Owing to lack of availability of a product-bound Ls crystal from any source, an effort to identify the amino acid involved in product size determination was made by carrying out computer-assisted docking of FOS into cavity groove of LsRN. The docking was made by MVD, using raffinose and GF 3D-coordinate-structure series constructed by SWEET2.

3.12.2.1 Selection of the docking protocol

To select the docking protocol of MVD, the re-docking of the known ligand (raffinose) to its structure (apo-levansucrase; 1BYN) was performed. The predicted raffinose-bound structure was superimposed to the solved structure and compared the RMSD of the poses to the x-ray solved structure. By using two search algorithms combined in MVD; MolDock SE and MolDock Optimizer, 40 RMSD values were obtained as shown in Table 3.8. Of these, MolDock SE combined with Ligand Evaluator gave the lowest RMSD values for co-crystallized raffinose (1BYN), that is 0.245 Å deviations between the best poses and the x-ray solved structure.

3.12.2.2 Docking of raffinose to the predicted LsRN structure and X-ray structure of invertase

Raffinose was docked into the homology modeling structure of LsRN by using the combination of search algorithms and scoring functions from 3.12.2.1. The docking structure was superimposed to those of raffinose bound-invertase from *T. maritime* (1W2T). As shown in Fig 3.45, superimposing the two raffinose bound structure by matching the positions of 3 ligand atoms reveals a similar geometry of the ligand, and an almost perfect overlapped of the catalytic triad. D93, D256 and E351 of LsRN were overlap to D19, D190 and E188 of the invertase. However, N251 and R369 of LsRN did not overlap with any amino acid of invertase, implying that N251 and R369 might play a role in transfructosylation.

Table 3.9 RMSD values of re-docked conformations of raffinose in 1BYN

Search Algorithm	Scoring Function	RMSDs Value
MolDock SE	MolDock Score	0.507
	MolDock Score [Grid]	0.374
	Ligand Evaluator	0.245
MolDock Optimizer	MolDock Score	0.618
	MolDock Score [Grid]	0.502
	Ligand Evaluator	0.344

Table shows only the best RMSD values of each docking run.

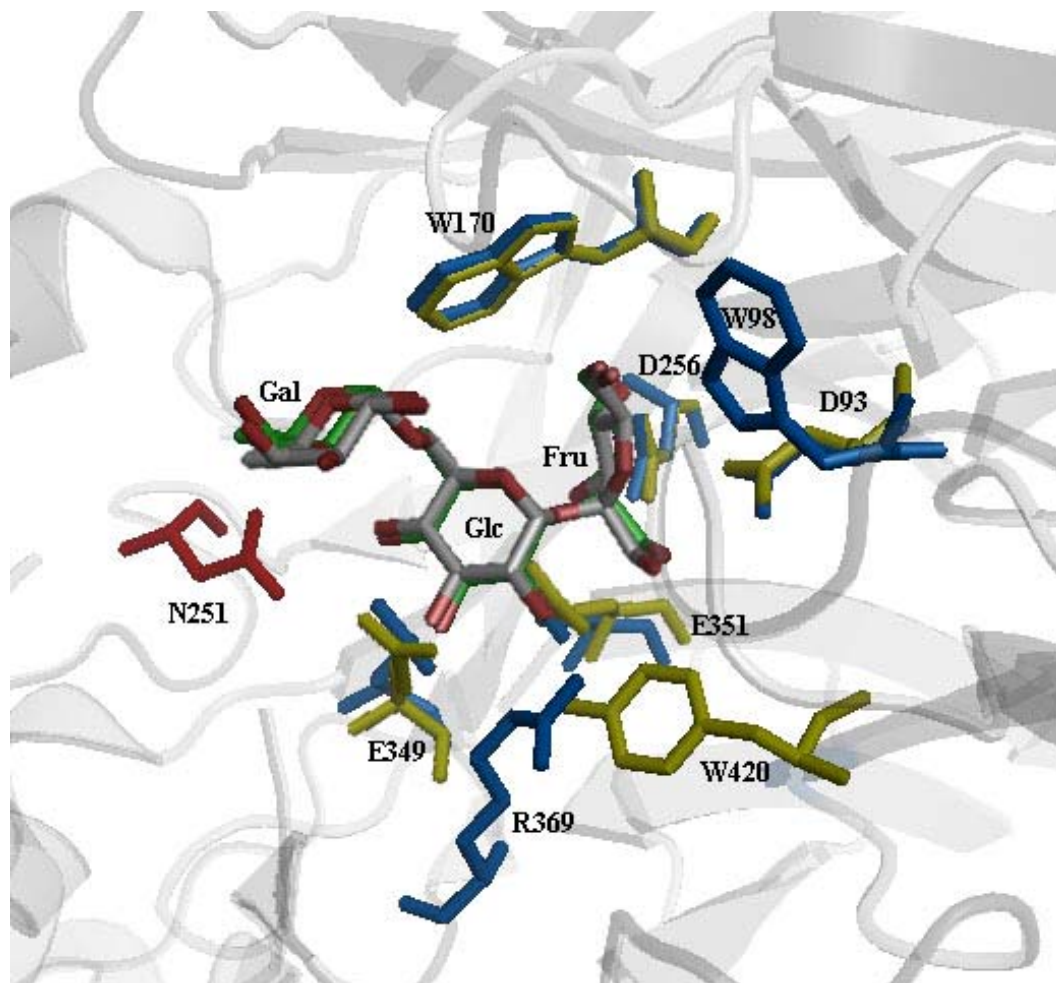


Figure 3.45 Superimposition of raffinose-bound structure of LsRN and invertase from *T. maritima*.

The catalytic triad residues of LsRN (blue) are perfectly overlapped to those of invertase from *T. maritima* (PDB ID; 1W2T shown in yellow). The raffinose-bound structures were superimposed using SuperPose by matching coordinates of the ligand. Carbon backbone of raffinose ligand docked in LsRN and invertase were colored in green and gray, respectively. N251 was painted in red. Figure was prepared using PyMOL.

3.13 Rational mutagenesis of LsRN

From the docking result, N251 was selected for further rational mutagenesis PCR mediated site-directed mutagenesis. The polar uncharged side chain of N251 is eliminated by changing to a small non-polar amino acid alanine, converted to charged side chain by changing to aspartic acid (D), and partially maintained by changing to functionally similar amino acid, lysine (K). Moreover, the amino acid sequence of LsRN was compared to those of Ls from gram negative bacteria, which mainly synthesized FOS. N251 was conserved among gram positive bacteria but substituted by tyrosine (Y) in Ls from gram negative bacteria. From this reason N251 was also changed to Y.

3.13.1 Site-directed mutagenesis of N251

To avoid unequal expression level, PCR primers used for substitution of N251 were designed by using *E. coli* codon preference. The mutated clones were nucleotide sequenced to check the success of substitution. As shown in Fig 3.46, the AAC codon encoded for N in wild type; WT enzyme was substituted with GCG, GAT, AAA and TAT, encoding for A, D, K and Y, respectively.

3.13.2 Purification of N251 mutated enzyme

The mutated plasmids were transformed into *E. coli* Top-10 and cultured using the same condition of WT clone. The levels of protein production by all transformants were similar, but activities of crude N251A was significantly different from other mutated enzymes. The mutated enzymes were purified by the same steps as those of WT Ls. All purified enzymes showed more than three hundred-fold of purification over the crude protein (Table 3.7 and Fig 3.47).

3.13.4 Catalytic properties of N251 mutated enzyme

Substitution of N251 to A completely abolished polysaccharide synthesis, significantly affecting K_m and k_{cat} values for both hydrolysis and transfructosylation reaction (Table 3.8). In all mutations k_m for sucrose of hydrolysis reaction were higher than that of WT enzyme, especially the value for N251Y which was 10-fold higher than that of WT Ls. The catalytic efficiency for both reactions of Ls of all mutated enzymes were decreased, except for transfructosylation of N251K and N251Y.

3.13.5 Levan product pattern of N251 mutated enzyme

The product pattern of mutated enzymes was also analyzed by TLC, HPAEC and MALDI-TOF (Fig 3.48-3.50). N251A and N251Y no longer produced levan polymer, only oligosaccharides up to GF₁₀ and GF₅, respectively, were observed in the reaction. In the other hand, the N251D and N251K retained the product pattern of WT Ls. TLC and HPAEC analyses revealed that the main products of N251D were short chain oligosaccharides while longer oligosaccharides could be synthesized by N251K.

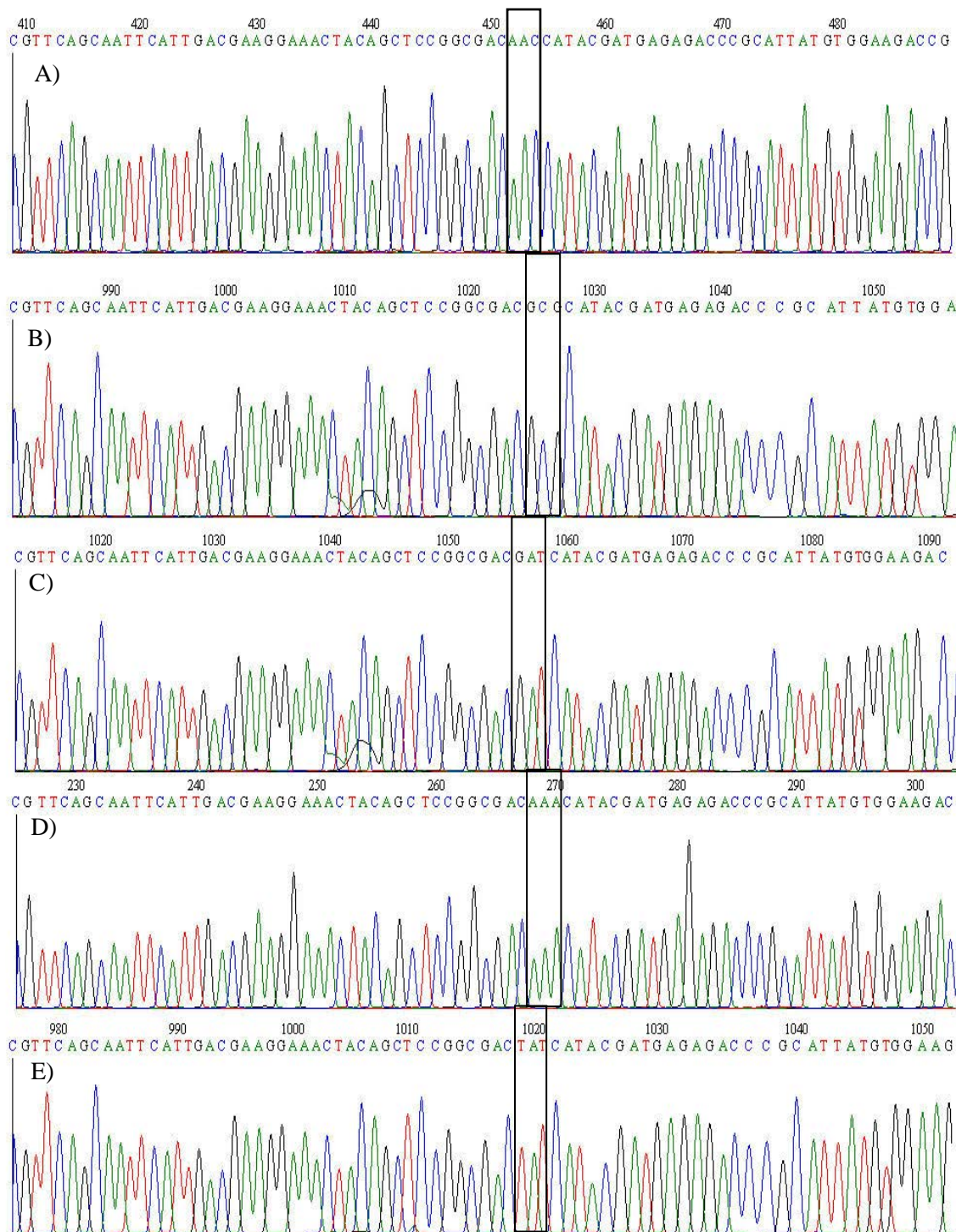


Figure 3.46 Site-directed mutagenesis of asparagine at position 251

The chromatograms of nucleotide sequence N251 mutated gene were compared to those of WT (A)

Panel B); N251A Panel C); N251D
 Panel D); N251K Panel E); N251Y

Table 3.10 Purification of mutated N251

Purification step	Volume (mL)	Activity (U/mL)	Protein (mg/mL)	Total Activity (U)	Total Protein (mg)	Specific Activity (U/mg)	Recovery (%)	Fold
N251A								
Crude	950	0.2	2.1	190	1995	0.1	100	1
DEAE Toyopearl-650M	45	3.4	2.8	153	126	1.2	81	12
Butyl Toyopearl-650M	16	8.5	0.5	136	8	17.0	72	170
N251D								
Crude	950	2.4	2.1	2280	1995	1.1	100	1
DEAE Toyopearl-650M	36	37.6	1.8	1354	65	20.8	59	19
Butyl Toyopearl-650M	23	46.0	0.3	1058	7	151.1	46	137
N251K								
Crude	950	2.2	2.0	2090	1900	1.1	100	1
DEAE Toyopearl-650M	60	18.3	2.1	1098	126	8.7	53	8
Butyl Toyopearl-650M	23	30.9	0.3	711	7	101.6	34	92
N251Y								
Crude	950	2.5	1.9	2375	1805	1.3	100	1
DEAE Toyopearl-650M	53	28.3	3.1	1500	164	9.1	63	7
Butyl Toyopearl-650M	22	41.8	0.2	920	4	230.0	39	177

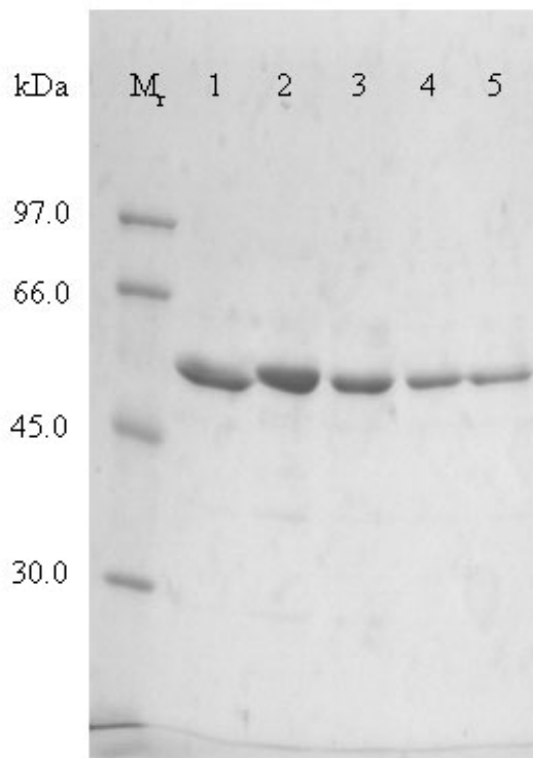


Figure 3.47 SDS-PAGE analysis of purified N251 mutated Ls enzyme

Lane Mr: Standard Mw protein

Lane 1: WT LsRN

Lane 2: N251A Ls

Lane 3: N251D Ls

Lane 4: N251K Ls

Lane 5: N251Y Ls

Table 3.11 Kinetic parameters of N251 Ls

Enzyme	K_m (mM)	k_{cat} (s⁻¹)	k_{cat}/K_m (mM⁻¹s⁻¹)
WT			
Hydrolysis	9.12	86.01	9.43
Transfructosylation	6.94	32.32	4.65
N251A			
Hydrolysis	19.61	27.05	1.38
Transfructosylation	6.67	1.38	0.21
N251D			
Hydrolysis	27.78	28.16	1.01
Transfructosylation	20.83	29.11	1.40
N251K			
Hydrolysis	27.03	57.76	2.14
Transfructosylation	6.06	24.92	4.11
N251Y			
Hydrolysis	100.00	9.82	0.10
Transfructosylation	14.71	101.91	6.93

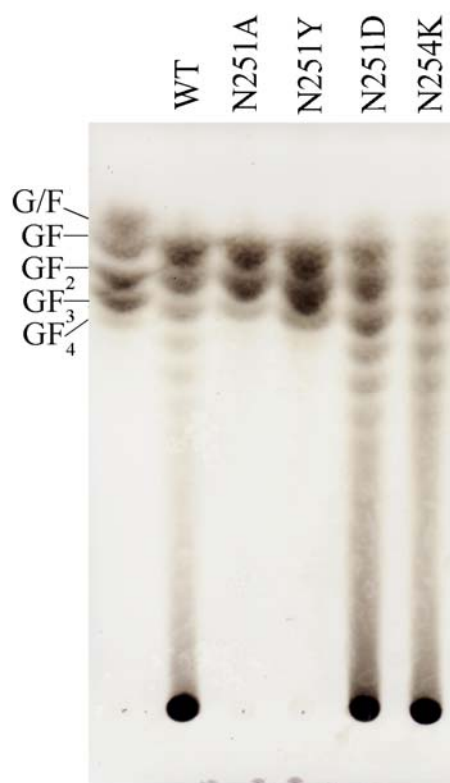


Figure 3.48 TLC analysis of reaction products of mutated N251

The enzymes were incubated with 20% (w/v) sucrose in 50 mM citrate buffer, pH 6.0 at 50° C. The reaction mixtures were analyzed by TLC

Lane 1: Standard GF-GF₄

Lane 2: The reaction mixture of WT

Lane 3: The reaction mixture of N251A

Lane 4: The reaction mixture of N251D

Lane 5: The reaction mixture of N251K

Lane 6: The reaction mixture of N251Y

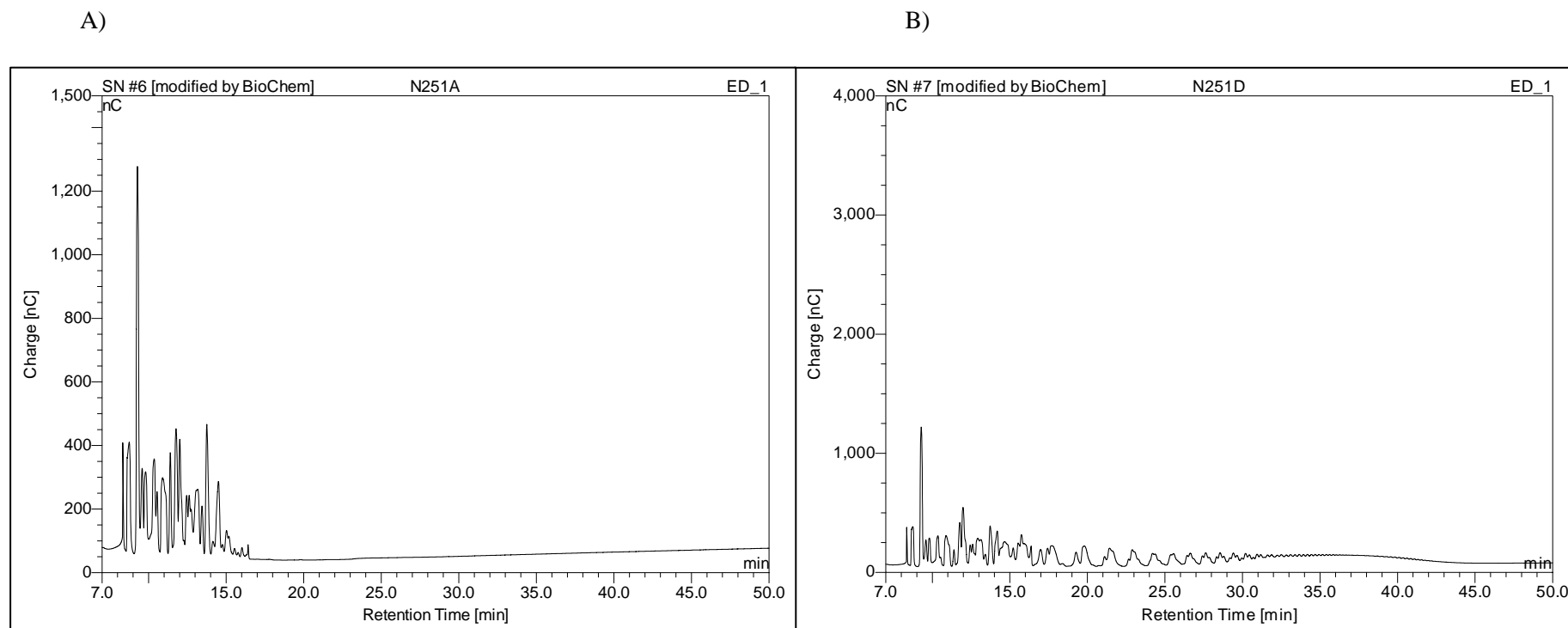


Figure 3.49 Analysis of the product pattern of LsRN by HPAEC

The 0.5 U of the enzymes was incubated with 20% (w/v) sucrose at 50 °C for overnight. The reaction product was partially purified by activated charcoal column and analyzed by HPAEC.

- A) The reaction product of N251A
- B) The reaction product of N251D

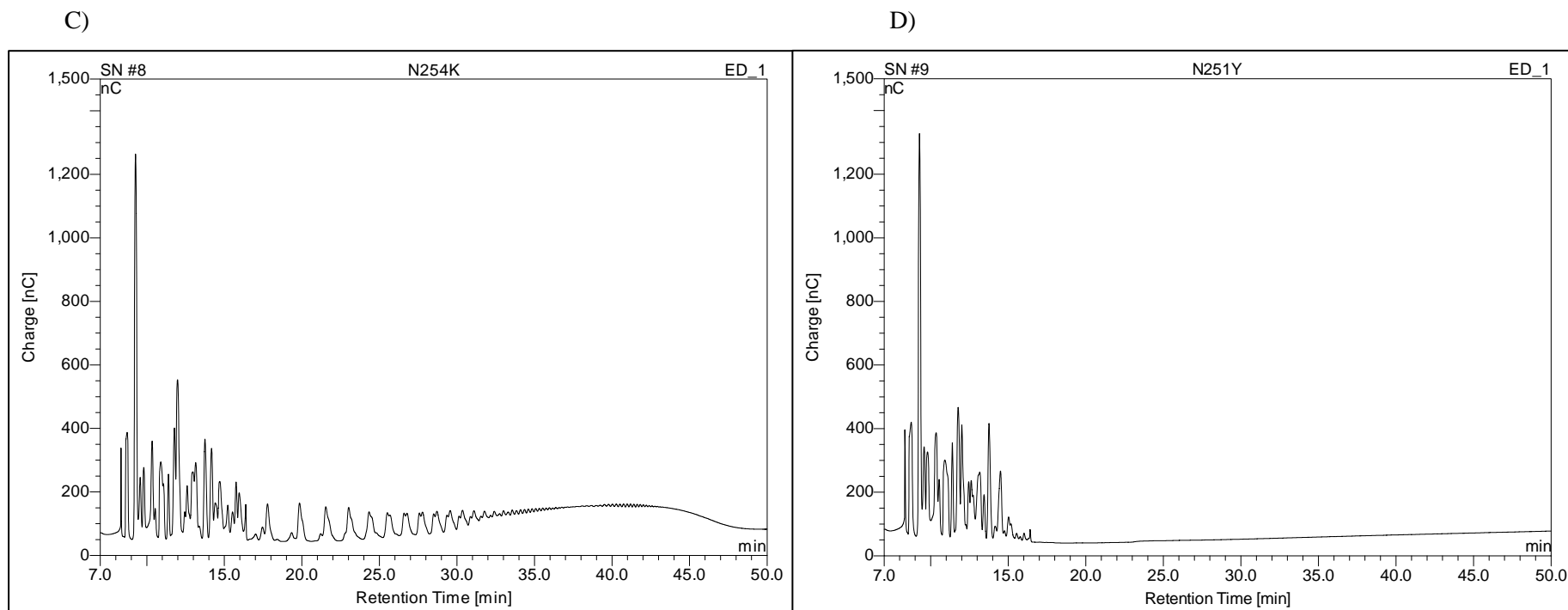


Figure 3.49 (Continue) Analysis of the product pattern of LsRN by HPAEC

The 0.5 U of the enzymes was incubated with 20% (w/v) sucrose at 50 °C for overnight. The reaction product was partially purified by activated charcoal column and analyzed by HPAEC

- C) The reaction product of N251K
- D) The reaction product of N251Y

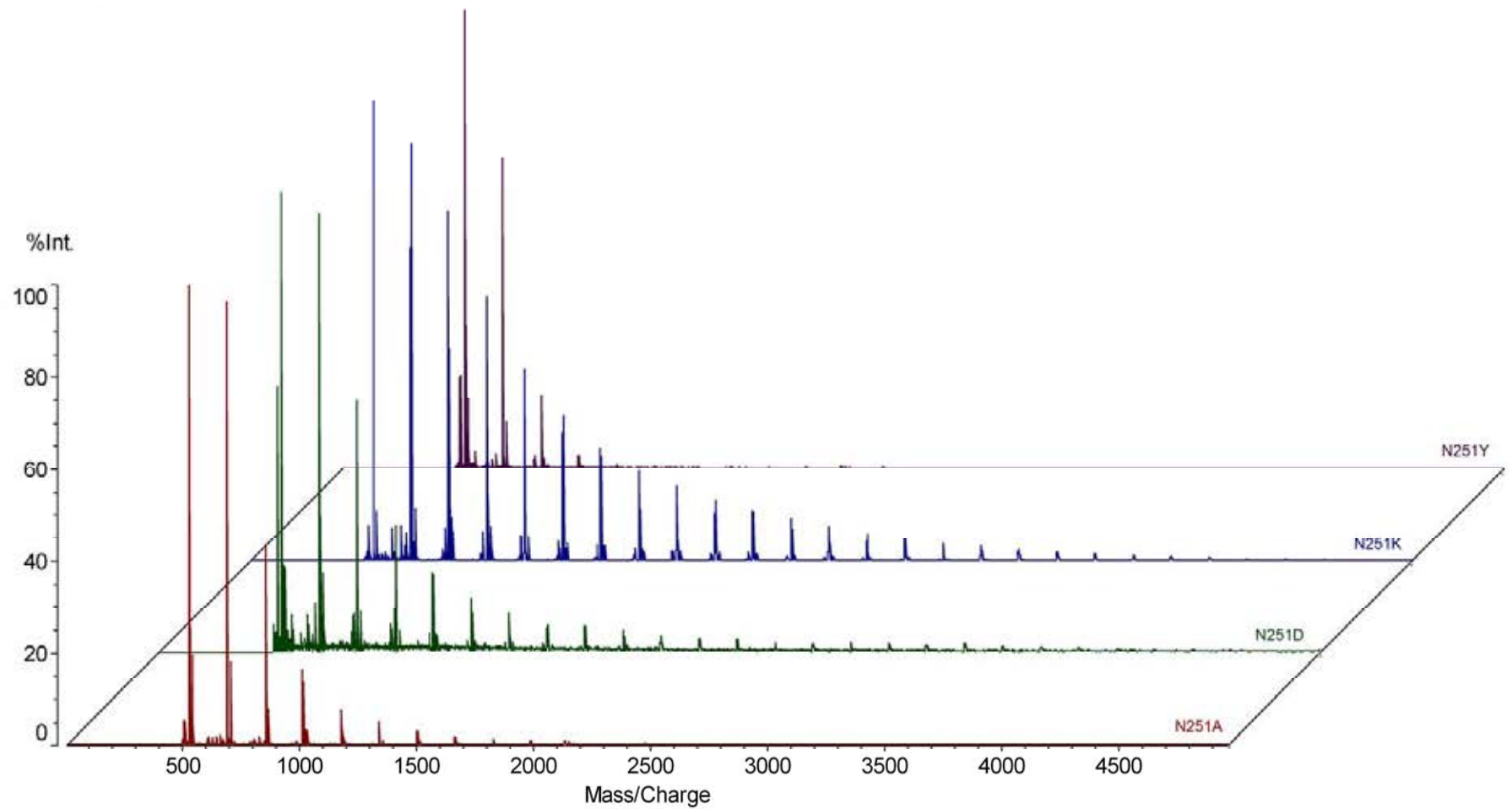


Figure 3.50 MALDI-TOF MS spectrum of mutated enzyme reaction products

3.14 Random mutation

3.14.1 Error prone PCR

The *p/sRN* was used as a DNA template for random mutagenesis by an error-prone PCR. Various concentrations of manganese ion ranging from 50 to 250 μM were doping in the PCR reaction. As shown in Fig 3.51, the Mn^{2+} doping reaction yielded higher amount of PCR product than the control reaction without the addition of MnCl_2 . The PCR products of each Mn^{2+} concentration were purified and subsequently ligated to pBluescripts/SK⁻, resulting in the three mutated libraries.

350 clones from each mutated libraries were cultured in 3xLB medium and crude enzymes were overnight incubated with 20% (w/v) sucrose under optimal conditions. The reaction products were analyzed by TLC and the result was shown in Fig 3.52. The variants that retained hydrolysis activity with differences in product pattern from those of WT were selected. From the primary screening, 6 variants from 50 mM MnCl_2 (variant 10, 29, 52, 77 and 114) and 3 variants from 100 mM MnCl_2 (variant 1, 38 and 148) were selected. After re-culture, some lost their hydrolytic activity, resulting in no transfructosylation product. Only 4 variants, 1, 52, 144 and 148 retained their hydrolytic activity. The nucleotide sequence of all 4 variants revealed mutation type as summarized in Table 3.9. Base substitution both transversion and transition were observed but no deletion and insertion was found in this study. Fig. 3.54 represented the distribution of nucleotide exchange. The mutations were randomly distributed throughout the amplified sequence with a hotspot between nucleotide at position 1234 to 1243.

The amino acid substitutions in LsRN were mapped in its raffinose bound 3D-structure. The change could be categorized into 3 groups. Substitution near catalytic site was W170H. Substitution at the buried residue was A202G. Substitutions at the surface were Q65E, Y246S, Q411L, N414T and N470I.

From Fig 3.54, the structure implied that Y264 is a residue at the opening of the funnel-like cavity and not too far from active site. Based on the direction of raffinose, it could be hypothesized that Y246 is one of the amino acid forming product binding tract for the transfructosylation product. Moreover, there is an accumulation of amino acid Substitution at the molecular surface in the opposite direction of the bound raffinose. For this reason, Y246S/N414T contained both concerning points was selected for further study.

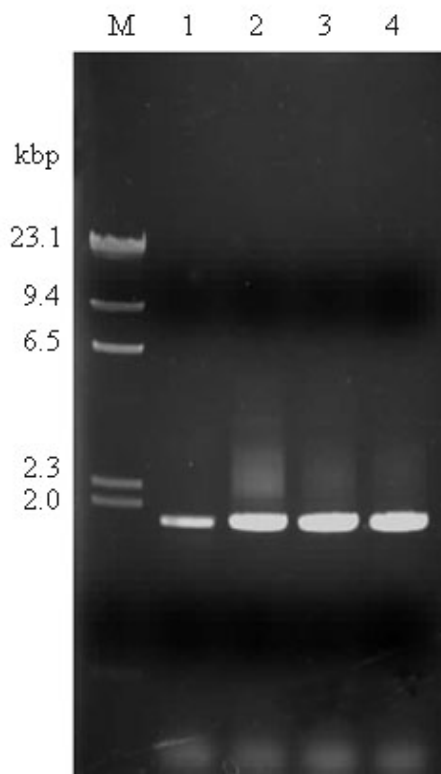


Figure 3.51 Error prone PCR

Various Mn^{2+} concentrations were added into PCR reaction.

Lane M: λ /*Hind*III marker

Lane 2: PCR product without MnCl_2 addition

Lane 3: PCR product with the addition of 250 mM MnCl_2

Lane 4: PCR product with the addition of 100 mM MnCl_2

Lane 5: PCR product with the addition of 50 mM MnCl_2

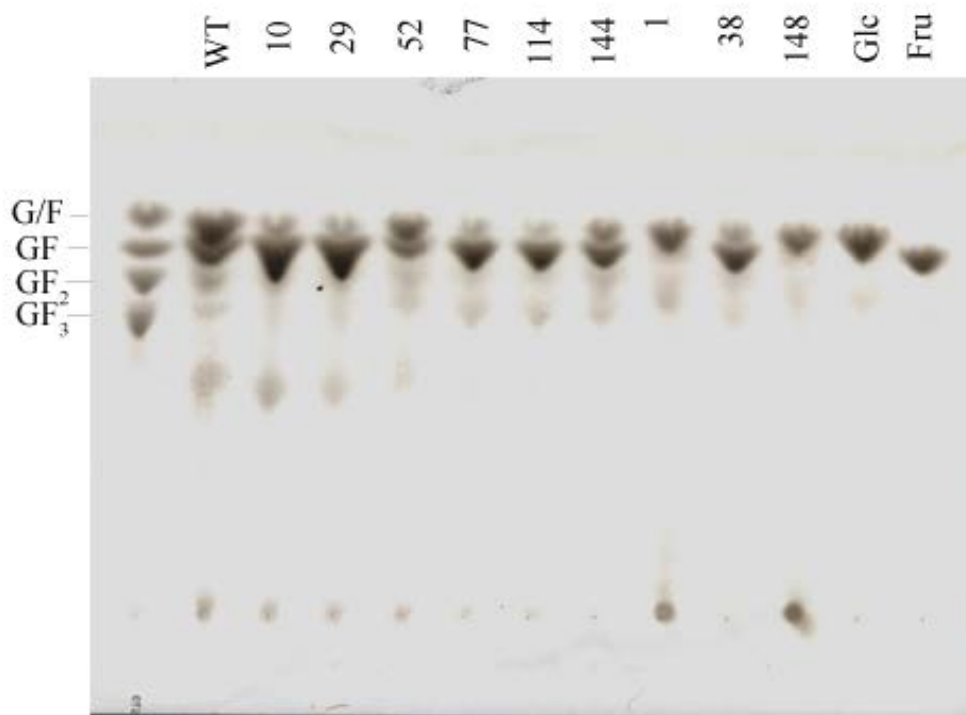


Figure 3.52 TLC analyze of reaction products of the selected mutated clones

- Lane 1: Standard G/F-GF₃
- Lane 2: The reaction product of WT
- Lane 3: The reaction product of variant 10
- Lane 4: The reaction product of variant 29
- Lane 5: The reaction product of variant 52
- Lane 6: The reaction product of variant 77
- Lane 7: The reaction product of variant 114
- Lane 8: The reaction product of variant 144
- Lane 9: The reaction product of variant 1
- Lane 10: The reaction product of variant 38
- Lane 11: The reaction product of variant 148
- Lane 12: Standard glucose
- Lane 13: Standard fructose

Table 3.12 Nucleotide substitutions reflected type of mutations and amino acid substitutions

Clone No.	Nucleotide exchange	Mutation type	Amino acid substitution
Clone 1	T <u>A</u> C → T <u>C</u> C	Transversion	Y246S
	A <u>A</u> T → A <u>C</u> T	Transversion	N414T
Clone 52	C <u>A</u> G → C <u>T</u> G	Transversion	Q411L
	A <u>A</u> C → A <u>T</u> C	Transversion	N470I
Clone144	C <u>A</u> A → G <u>A</u> A	Transversion	Q65E
Clone148	T <u>G</u> G → C <u>A</u> C	Transversion, Transition, Transversion	W170H
	G <u>C</u> T → G <u>G</u> T	Transversion	A202G

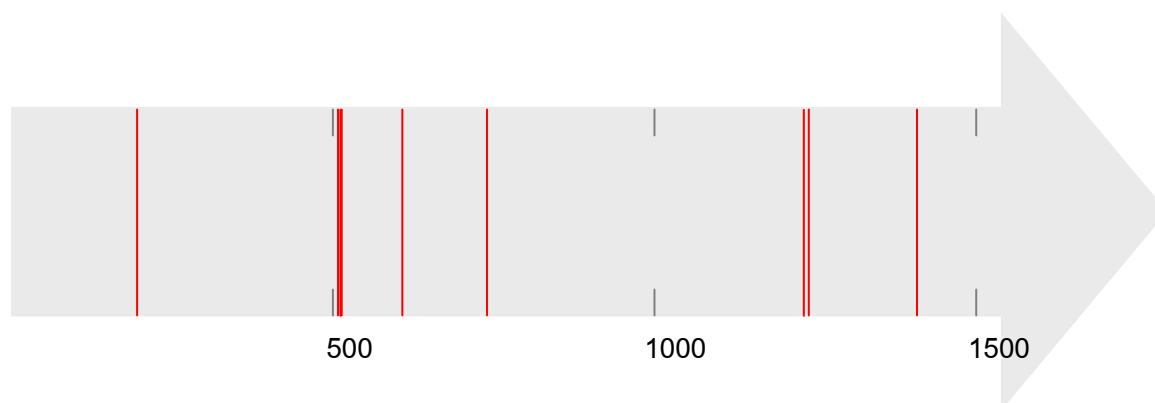


Figure 3.53 Distribution of nucleotide substitutions within *lsRN*

The four clones from 50 and 150 mM MnCl₂ were sequenced. The red lines represented nucleotide substitutions within the gene that was amplified.

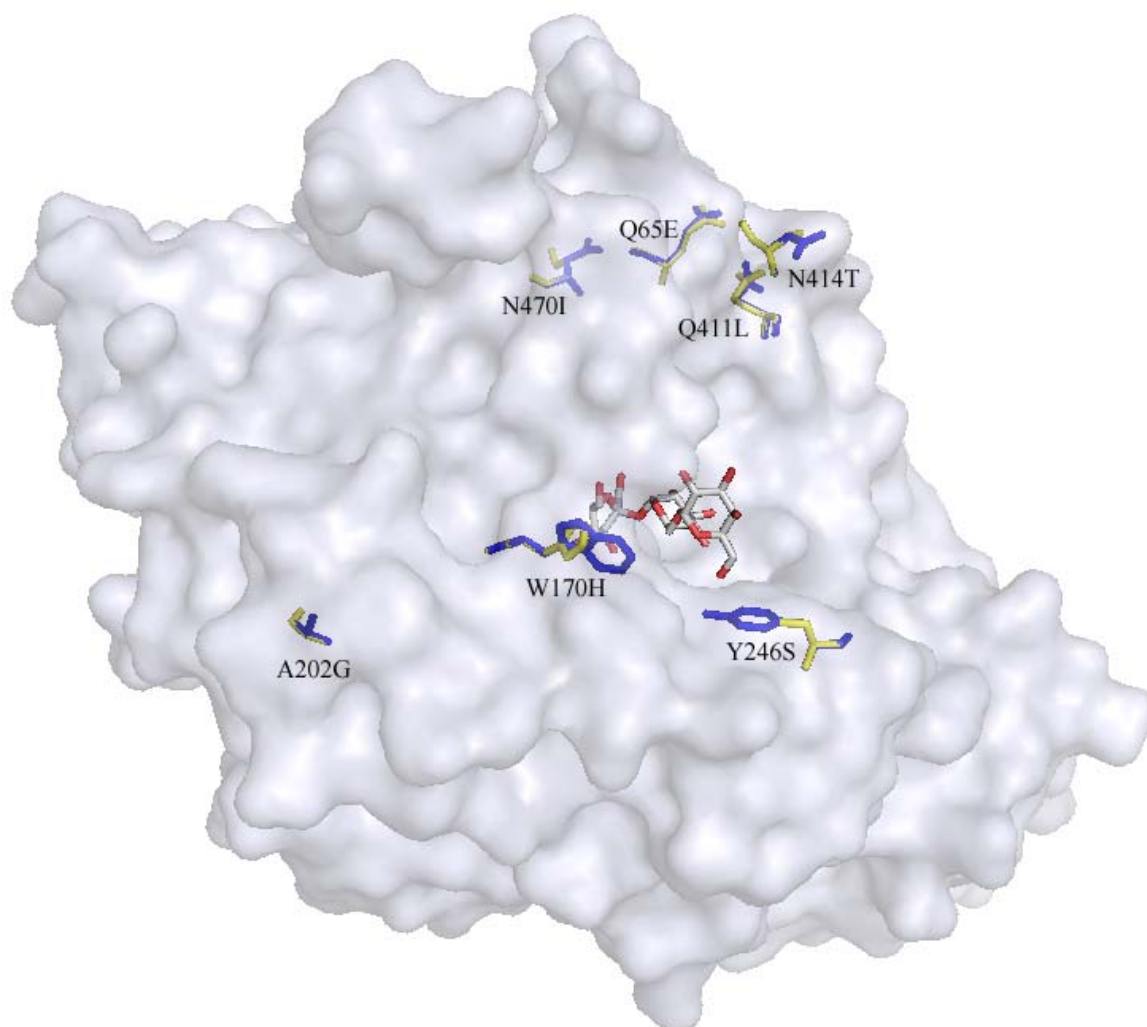


Figure 3.54 Mapping of amino acid exchange on protein structure

The raffinose-bound structure of LsRN and its mutated structure were superimposed using SuperPose. The substitution positions were shown in stick; blue for WT and yellow for mutated enzyme. Carbon backbone of raffinose ligand was shown in white stick with oxygen atoms in red. Figure was prepared using PyMOL.

3.14.2 Site-directed mutagenesis of Y246S and N414T

To check whether the change in product pattern was affected by Y246S or N414T, site-directed mutagenesis was performed. The mutated clones were nucleotide sequenced to verify the change. As shown in Fig 3.55, the TAC codon encoded for Y246 in wild type was exchanged with AGC, encoding for S. The AAT codon encoded for N414 in wild type LsRN was exchanged with ACC, encoding for T.

3.14.3 Purification of Y246S/N414T, Y246S and N414T

The mutated plasmids were transformed into *E. coli* Top-10 and cultured using the same condition of WT clone. The levels of protein production by all transformants were similar, but difference in total Ls activity was observed. The mutated enzymes were purified by the same method as of WT Ls. The purification fold of Y246S was lower than the other two mutated proteins. The purified N414T and Y246S/N414T showed more than a hundred fold of purification over the crude protein (Table 3.10 and Fig 3.56).

3.14.4 Catalytic properties of mutated enzymes

The catalytic properties of the mutated Ls were shown in Table 3.11. In hydrolysis reaction, affinities to sucrose and turnover numbers of all mutated enzymes were higher than those of the WT. While in transfructosylation reaction, the affinity to sucrose of all mutated enzymes was lower than those of WT except for Y246. However, N414T and Y246S/N414T showed higher in k_{cat} values than that of WT in transfructosylation reaction. Interestingly, catalytic efficiency for hydrolysis reaction of Y246S was far higher than those of the others.

3.14.5 Levan product pattern of mutated enzymes

The product pattern of mutated enzymes was also analyzed by TLC, HPAEC and MALDI-TOF (Fig 3.57-3.59). The Y246S/N414T lost its levan production capability, but could synthesize GF₃ to GF₈. The Y246S also lost its ability to synthesize levan but could synthesize GF₃ to GF₁₁. In contrast, the N414T retained the levan synthesizing activity of the WT.

From this result, it implied that amino acid exchange at position 246 could change the product spectrum of the reaction. Thus Y246 was selected for further study.

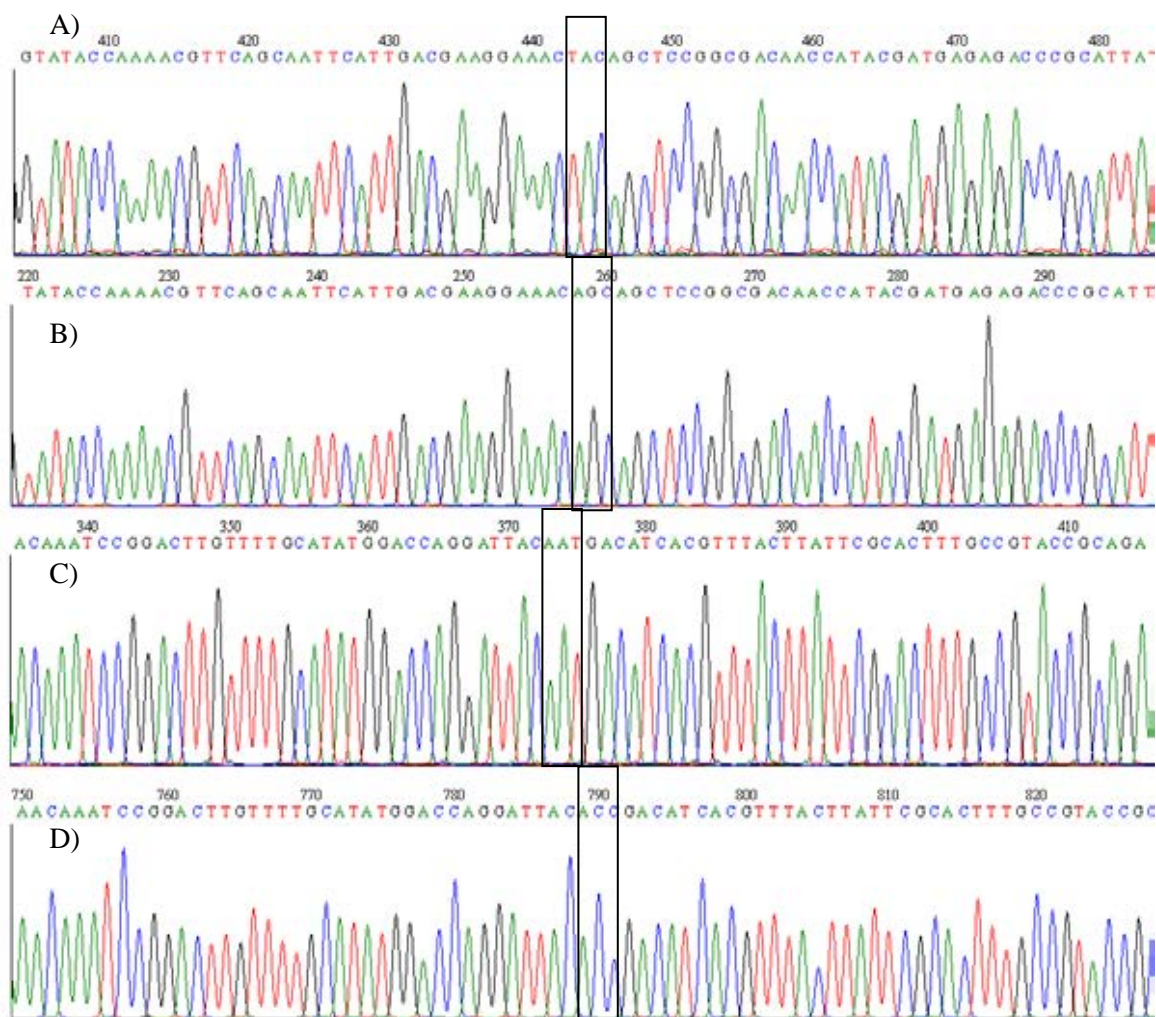


Figure 3.55 Site-directed mutagenesis of Y246S and N414T Ls

The chromatograms of nucleotide sequence of Y246S (B) and N414T (D) mutated gene were compared to those of WT (A and C)

Table 3.13 Purification of Y246S/N414T, Y246S and N414T Ls

Purification step	Volume (mL)	Activity (U/mL)	Protein (mg/mL)	Total Activity (U)	Total Protein (mg)	Specific Activity (U/mg)	Recovery (%)	Fold
Y246S/N414T								
Crude	375	3.8	42.2	1425	15825	0.1	100	1
DEAE Toyopearl-650M	30	37.0	28.4	1110	852	1.3	78	13
Butyl Toyopearl-650M	14	50.0	2.2	700	31	22.6	49	226
Y246S								
Crude	950	9.5	44.0	9025	41800	0.2	100	1
DEAE Toyopearl-650M	70	108.3	24.3	7581	1701	4.5	84	23
Butyl Toyopearl-650M	40	81.9	2.3	3276	92	35.6	36	178
N414T								
Crude	375	5.2	41.6	1950	15600	0.1	100	1
DEAE Toyopearl-650M	30	57.4	23.6	1722	708	2.4	88	24
Butyl Toyopearl-650M	14	50.2	2.2	703	31	22.7	36	227

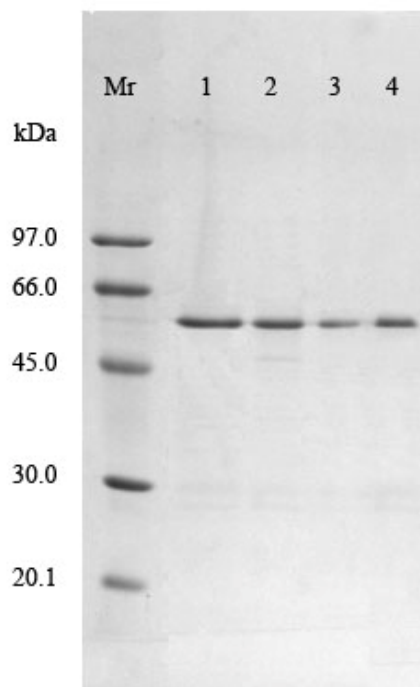


Figure 3.56 SDS-PAGE analysis of purified mutated Ls

Lane Mr: Standard M_r protein

Lane 1: WT LsRN

Lane 2: Y246S Ls

Lane 3: N414T Ls

Lane 4: Y246S/N414T Ls

Table 3.14 Kinetic parameters of mutated enzymes

Ls	K_m (mM)	k_{cat} (s ⁻¹)	k_{cat}/K_m (mM ⁻¹ s ⁻¹)
WT			
Hydrolysis	9.12	86.01	9.43
Transfructosylation	6.94	32.32	4.65
Y246S/N414T			
Hydrolysis	4.20	25.89	6.16
Transfructosylation	55.56	108.41	1.95
Y246S			
Hydrolysis	0.95	33.46	35.22
Transfructosylation	3.57	11.50	3.22
N414T			
Hydrolysis	4.76	7.79	1.64
Transfructosylation	66.67	86.42	1.29



Figure 3.57 TLC analysis of reaction products of mutated Ls

The enzymes were incubated with 20% (w/v) sucrose in 50 mM citrate buffer, pH 6.0 at 50° C. The reaction mixtures were analyzed by TLC

Lane 1: Standard GF-GF₄

Lane 2: The reaction mixture of WT

Lane 3: The reaction mixture of Y246S/N414T

Lane 4: The reaction mixture of Y246S

Lane 5: The reaction mixture of N414T

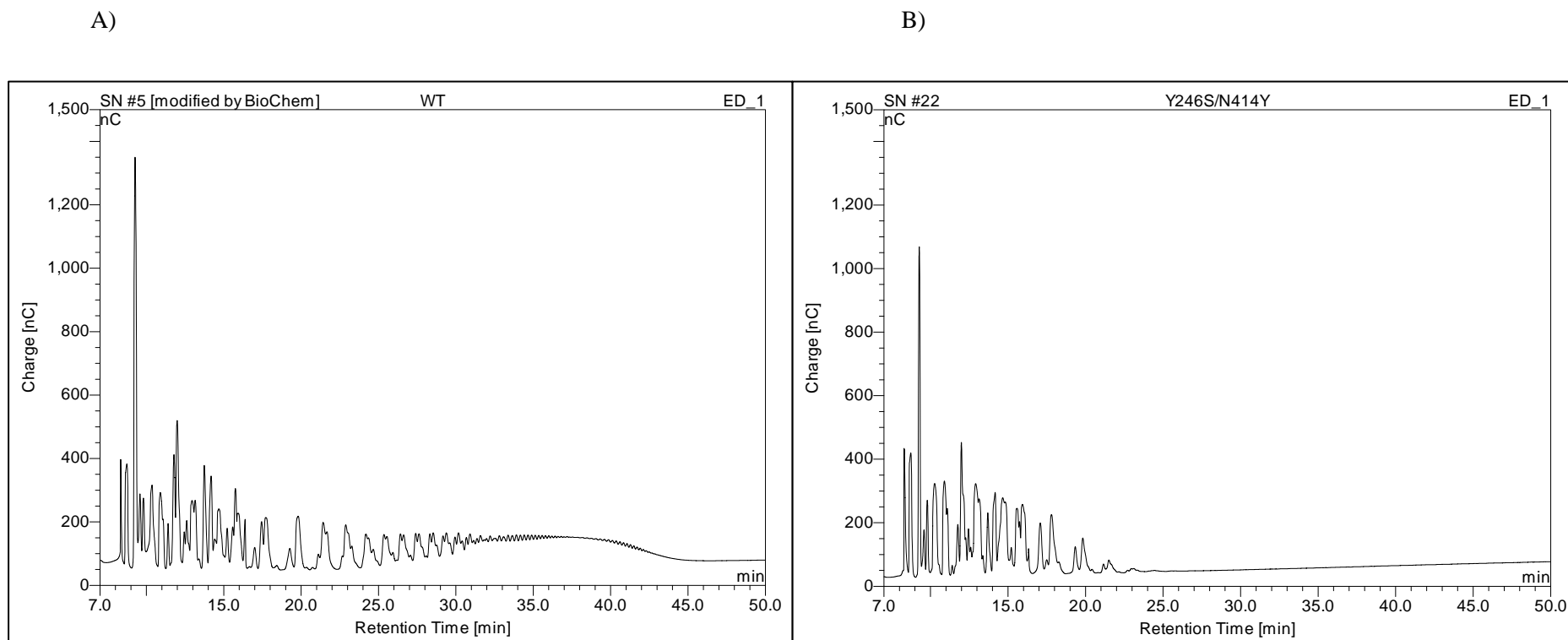


Figure 3.58 Analysis of the product pattern of mutated enzymes by HPAEC

The 0.5 U of the enzymes was incubated with 20% (w/v) sucrose at 50 °C for overnight. The reaction product was partially purified by activated charcoal column and analyzed by HPAEC.

- A) The reaction product of WT LsRN
- B) The reaction product of Y246S/N414T

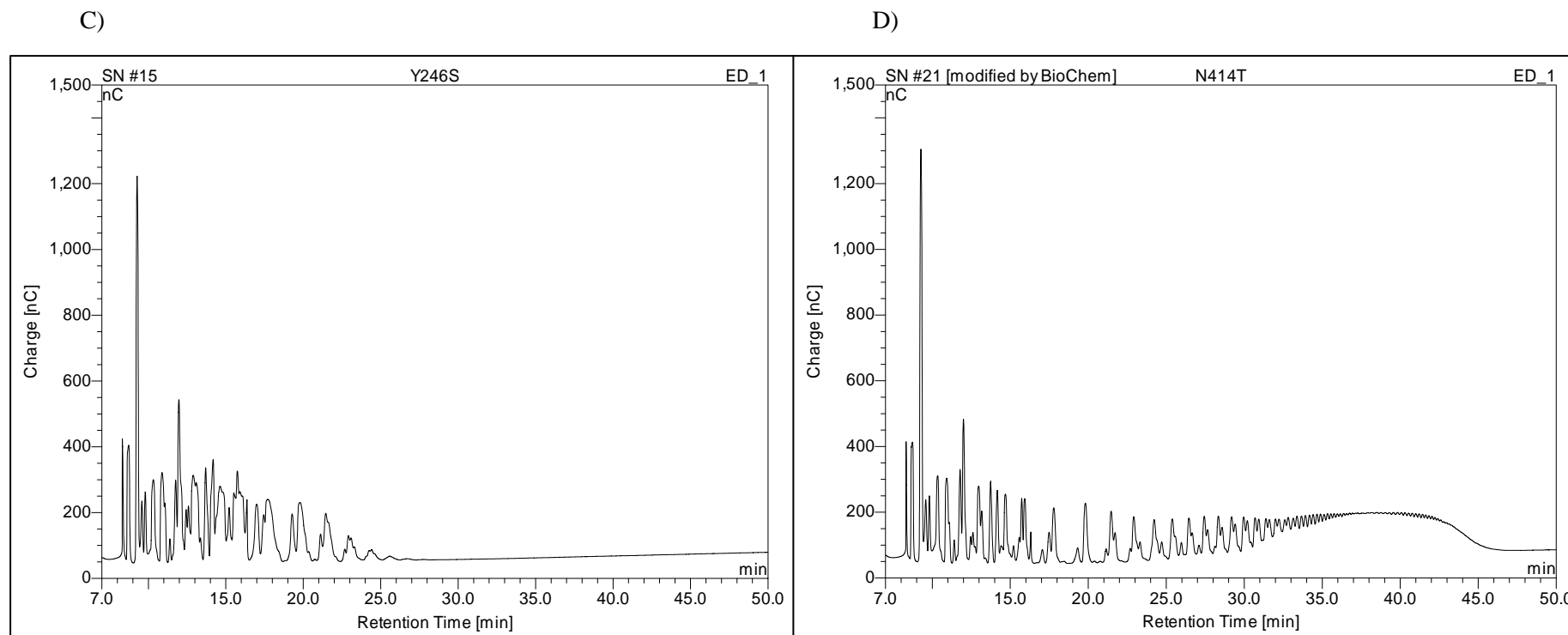


Figure 3.58 Analysis of the product pattern of mutated enzymes by HPAEC

The 0.5 U of the enzymes was incubated with 20% (w/v) sucrose at 50 °C for overnight. The reaction product was partially purified by activated charcoal column and analyzed by HPAEC.

C) The reaction product of Y246S

D) The reaction product of N414T

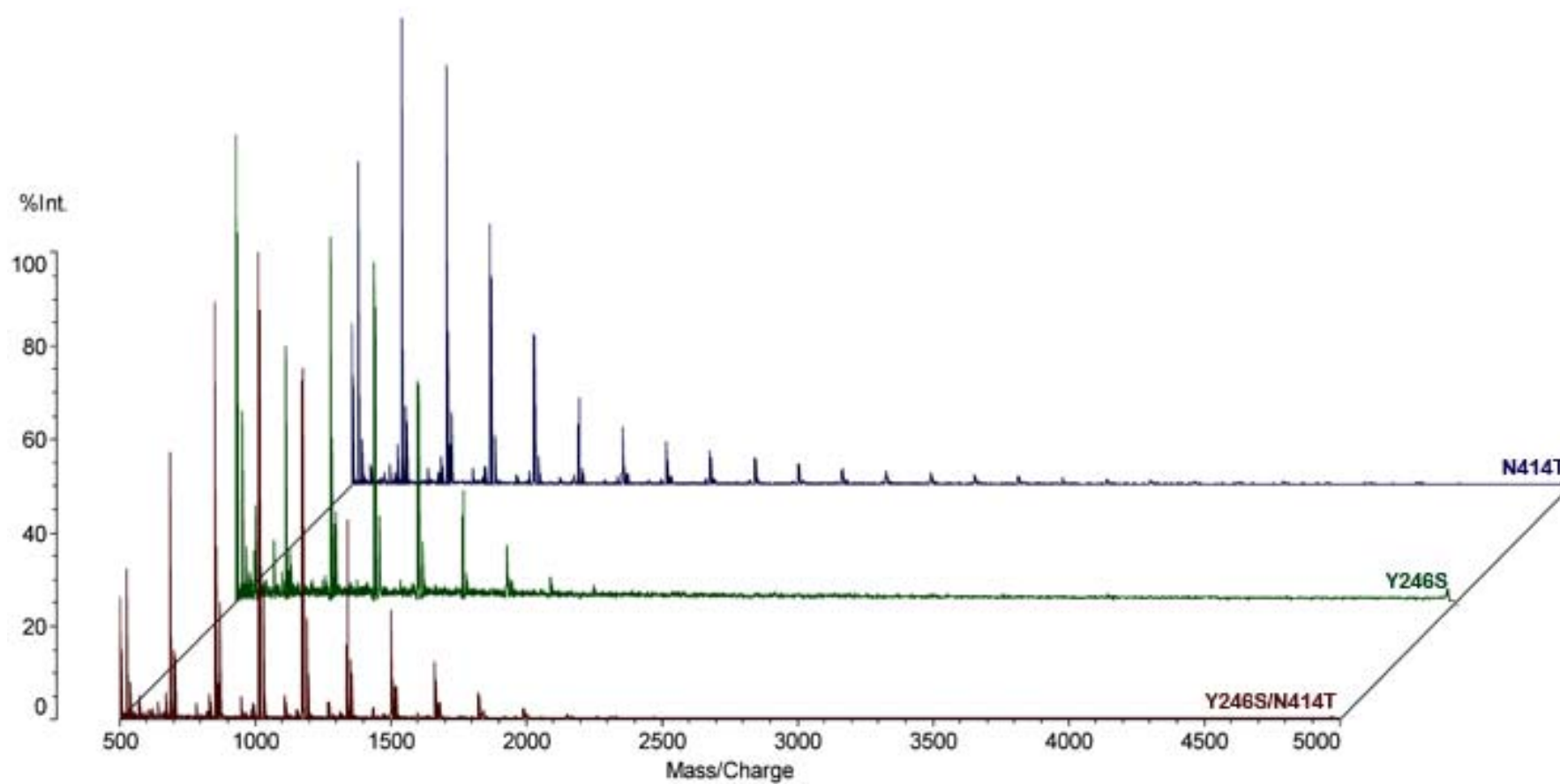


Figure 3.59 MALDI-TOF MS spectrum of the reaction products of Y246S, N414T and Y246S/N414T

3.14.6 Site-directed mutagenesis at Y246

The aromatic side chain of Y246 was eliminated by changing to a small non-polar amino acid alanine, a conversion to other aromatic side chains by changing to W and F. The side chain of Y246 was partially maintained by changing to aliphatic side chains, I and L. Moreover, Y246 was also substituted by polar side chain, D. To verify the substitution, the mutated clones were nucleotide sequenced. As shown in Fig 3.60 all mutated clones were successfully exchanged to desire amino acids.

3.14.7 Purification of Y246 mutated enzymes

All mutated enzymes were purified using the same steps as the WT enzyme. The result was shown in Table 3.12 and Fig 3.61. The purification fold of all mutated enzymes was higher than 100 fold with specific activity varying from 36.4 to 124.7 U mg protein⁻¹.

3.14.8 Catalytic properties of Y246 mutated Ls

The catalytic properties of the mutated Ls were shown in Table 3.13. In hydrolysis reaction, affinity to sucrose of all mutated enzymes was lower than the WT enzyme, except for Y246S. In transfructosylation reaction, Y246A and Y246D showed similar K_m value to WT but K_m of the other mutated enzymes were higher than that of WT enzyme, except for Y246S. When compared the catalytic efficiency, k_{cat}/K_m in transfructosylation of Y246D was 2.4-fold higher than that of WT. Y246S also gave a higher in k_{cat}/K_m value for transfructosylation reaction.

3.14.9 Levan product pattern of Y246 mutated Ls.

The product pattern of mutated enzymes was also analyzed by TLC, HPAEC and MALDI-TOF (Fig 3.63-3.65). No mutated enzyme could retain the capability to synthesize high Mw polymer of the WT enzyme. The mutated enzymes synthesized oligosaccharides with different product pattern. Y246I and Y246L as well as Y246S synthesized the oligosaccharide up to GF₇ and GF₈. The longer oligosaccharide up to GF₁₀ was synthesized by Y246F and Y246W. Y246A and Y246 D could produce oligosaccharide longer than GF₁₀.

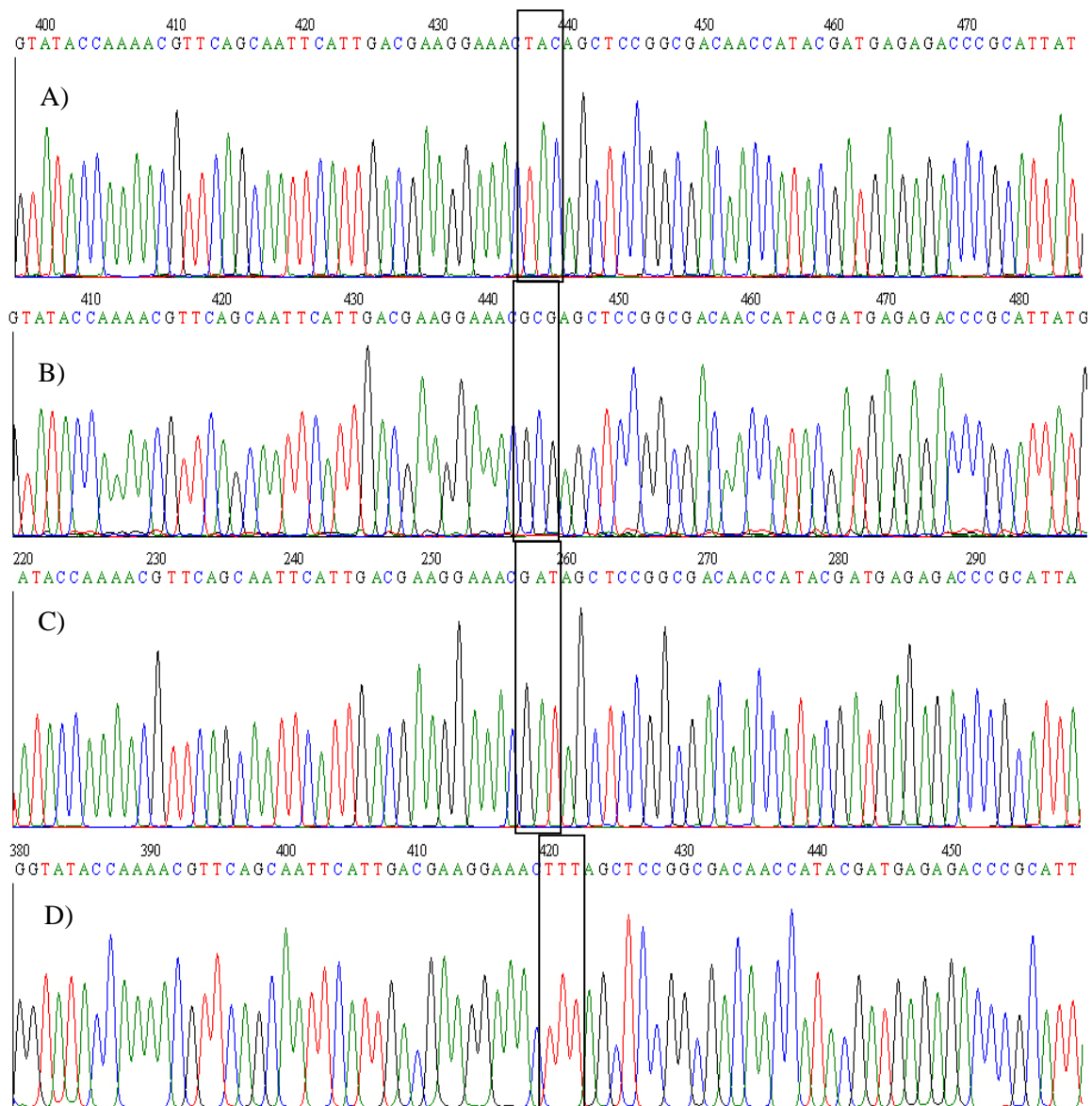


Figure 3.60 Site-directed mutagenesis of Y246

The chromatograms of nucleotide sequence of Y246A (B) Y246D (C) and Y246F (D) mutated gene were compared to those of WT (A)

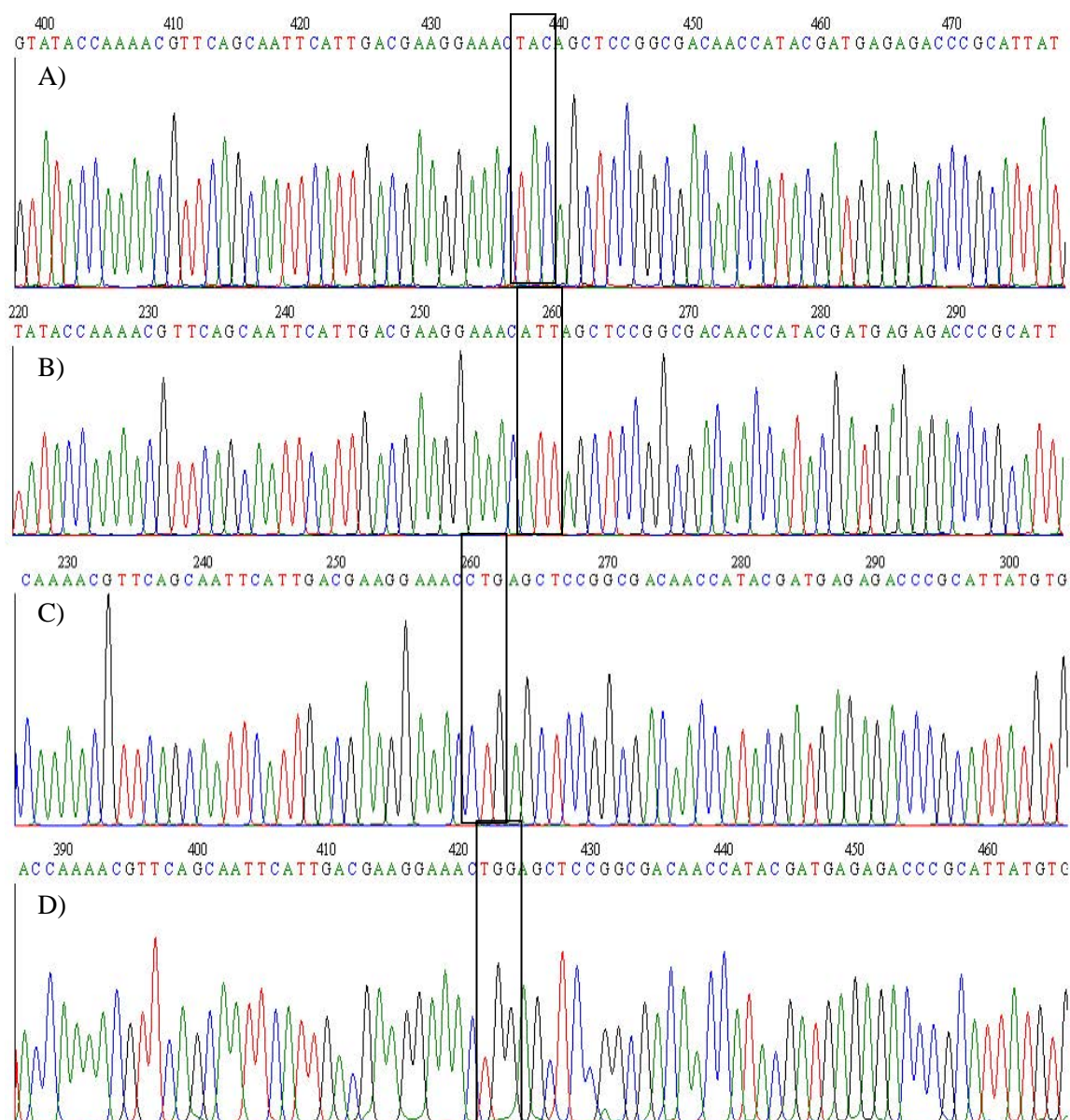


Figure 3.60 Site-directed mutagenesis of Y246

The chromatograms of nucleotide sequence of Y246I (B) Y246L (C) and Y246W (D) mutated gene were compared to those of WT (A)

Table 3.15 Purification of Y246 mutated Ls

Purification steps	Volume (mL)	Activity (U/mL)	Protein (mg/mL)	Total Activity (U)	Total Protein (mg)	Specific Activity (U/mg)	Recovery (%)	Fold
Y246A								
Crude	670	1.4	4.6	938	3082	0.3	100	1
DEAE Toyopearl-650M	50	9.6	2.6	480	130	3.7	51	12
Butyl Toyopearl-650M	28	12.7	0.2	356	6	59.3	38	198
Y246D								
Crude	950	4.6	43.3	4370	41135	0.1	100	1
DEAE Toyopearl-650M	50	83.3	17.0	4165	850	4.9	95	49
Butyl Toyopearl-650M	50	43.8	0.8	2190	40	54.8	50	548
Y246F								
Crude	670	5.9	5.9	3953	3953	1.0	100	1
DEAE Toyopearl-650M	70	33.9	2.9	2373	203	11.7	60	12
Butyl Toyopearl-650M	30	44.9	0.4	1347	12	112.3	34	112
Y246I								
Crude	670	2.8	6.5	1876	4355	0.4	100	1
DEAE Toyopearl-650M	56	19.0	3.3	1064	185	5.8	57	15
Butyl Toyopearl-650M	20	42.9	0.4	858	8	107.3	46	268

Table 3.15 Purification of Y246 mutated Ls

Purification steps	Volume (mL)	Activity (U/mL)	Protein (mg/mL)	Total Activity (U)	Total Protein (mg)	Specific Activity (U/mg)	Recovery (%)	Fold
Y246L								
Crude	670	2.9	8.3	1943	5561	0.3	100	1
DEAE Toyopearl-650M	50	27.5	4.3	1375	215	6.4	71	21
Butyl Toyopearl-650M	28	37.0	0.6	1036	17	60.9	53	203
Y246S								
Crude	950	9.5	44.0	9025	41800	0.2	100	1
DEAE Toyopearl-650M	70	108.3	24.3	7581	1701	4.5	84	23
Butyl Toyopearl-650M	40	81.9	2.3	3276	92	35.6	36	178
Y246W								
Crude	950	4.3	44.0	4085	41800	0.1	100	1
DEAE Toyopearl-650M	83	70.6	21.8	5860	1809	3.2	143	32
Butyl Toyopearl-650M	42	106.2	2.8	4460	118	37.8	109	378

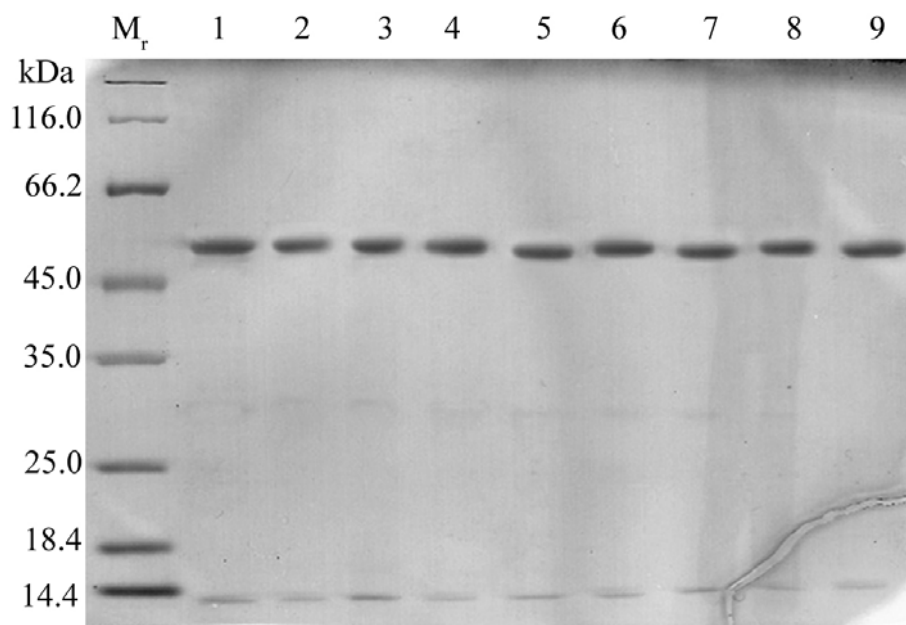


Figure 3.61 Purification of Y246 mutated series of Ls

Lane M_r : Standard molecular weight protein

Lane 1: Wt LsRN

Lane 2: Y246A Ls

Lane 3: Y246D Ls

Lane 4: Y246F Ls

Lane 5: Y246I Ls

Lane 6: Y246L Ls

Lane 7: Y246S Ls

Lane 7: Y246W Ls

Table 3.16 Kinetic parameters of mutated enzymes

Enzyme	K_m (mM)	k_{cat} (s⁻¹)	k_{cat}/K_m (mM⁻¹s⁻¹)
WT			
Hydrolysis	9.12	86.01	9.43
Transfructosylation	6.94	32.32	4.65
Y246A			
Hydrolysis	18.52	50.39	2.72
Transfructosylation	6.67	36.50	5.47
Y246D			
Hydrolysis	26.31	66.67	2.53
Transfructosylation	5.56	62.89	11.31
Y246S			
Hydrolysis	6.67	31.37	4.70
Transfructosylation	3.57	11.50	3.22
Y246I			
Hydrolysis	19.52	47.12	2.41
Transfructosylation	15.77	28.36	1.80
Y246L			
Hydrolysis	18.42	33.23	1.82
Transfructosylation	12.82	22.61	1.76
Y246F			
Hydrolysis	17.24	71.84	4.17
Transfructosylation	10.82	33.53	3.10
Y246W			
Hydrolysis	15.38	53.33	3.47
Transfructosylation	10.00	27.78	2.78

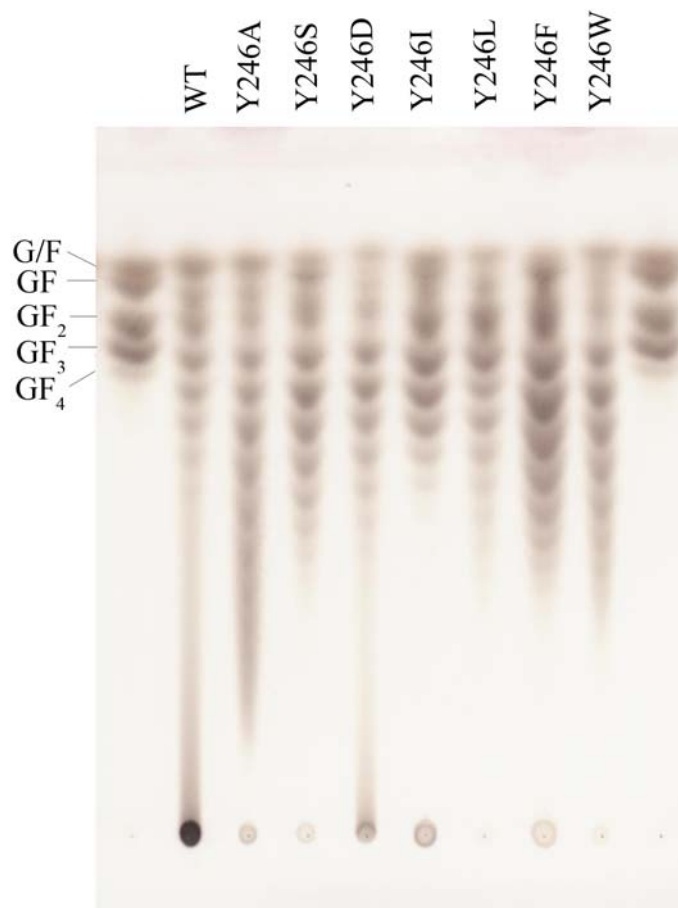


Figure 3.62 TLC analysis of reaction products of mutated enzyme

The enzymes were incubated with 20% (w/v) sucrose in 50 mM citrate buffer, pH 6.0 at 50° C. The reaction mixtures were analyzed by TLC

Lane 1: Standard GF-GF₄

Lane 2: The reaction mixture of WT

Lane 3: The reaction mixture of Y246A

Lane 4: The reaction mixture of Y246S

Lane 5: The reaction mixture of Y246D

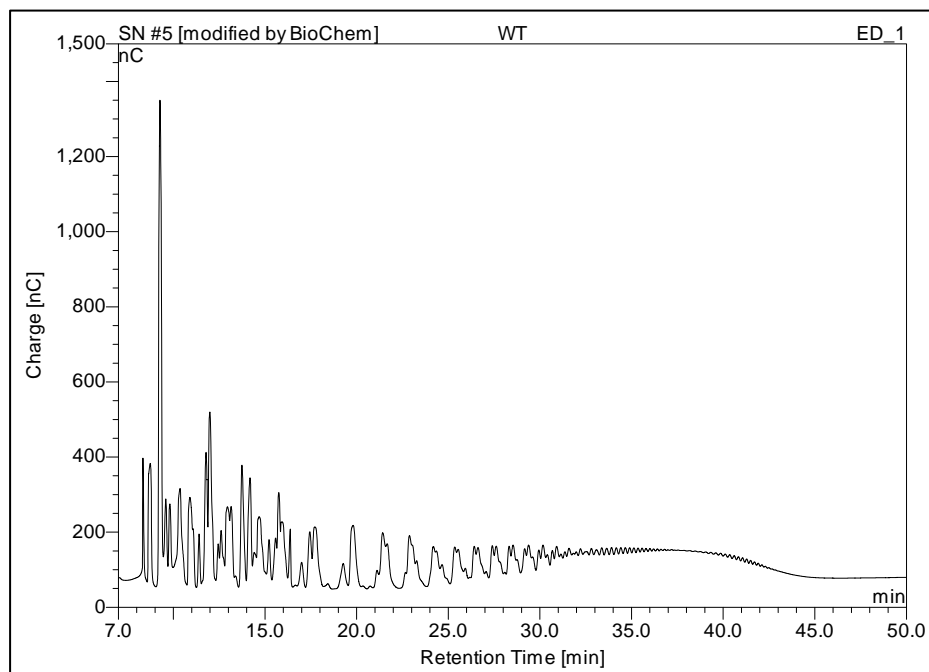
Lane 6: The reaction mixture of Y246I

Lane 7: The reaction mixture of Y246L

Lane 8: The reaction mixture of Y246F

Lane 9: The reaction mixture of Y246W

A)



B)

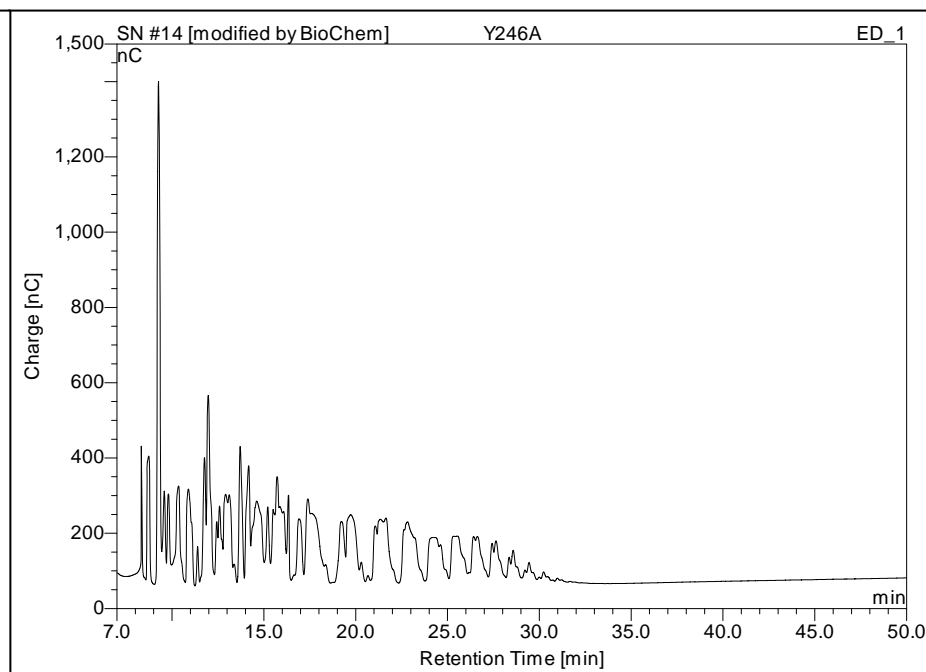
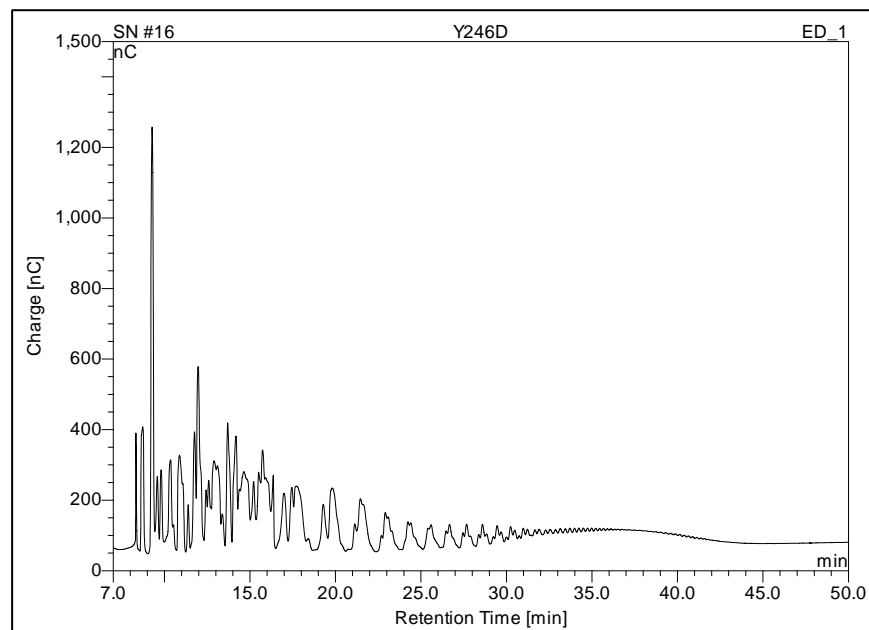


Figure 3.63 Analysis of the product pattern of mutated enzymes by HPAEC

The 0.5 U of the enzymes was incubated with 20% (w/v) sucrose at 50 °C for overnight. The reaction product was partially purified by activated charcoal column and analyzed by HPAEC

- A) The reaction product of WT LsRN
- B) The reaction product of Y246A

C)



D)

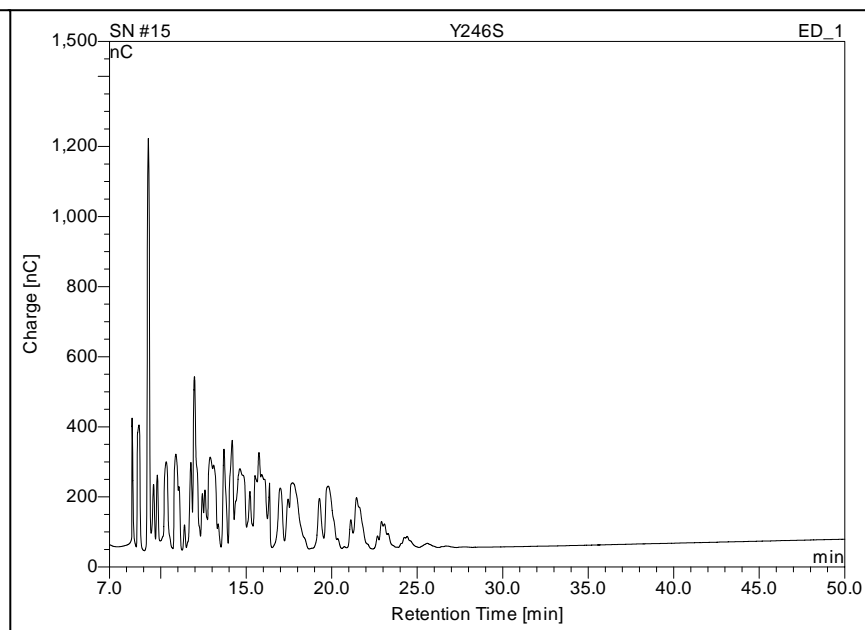


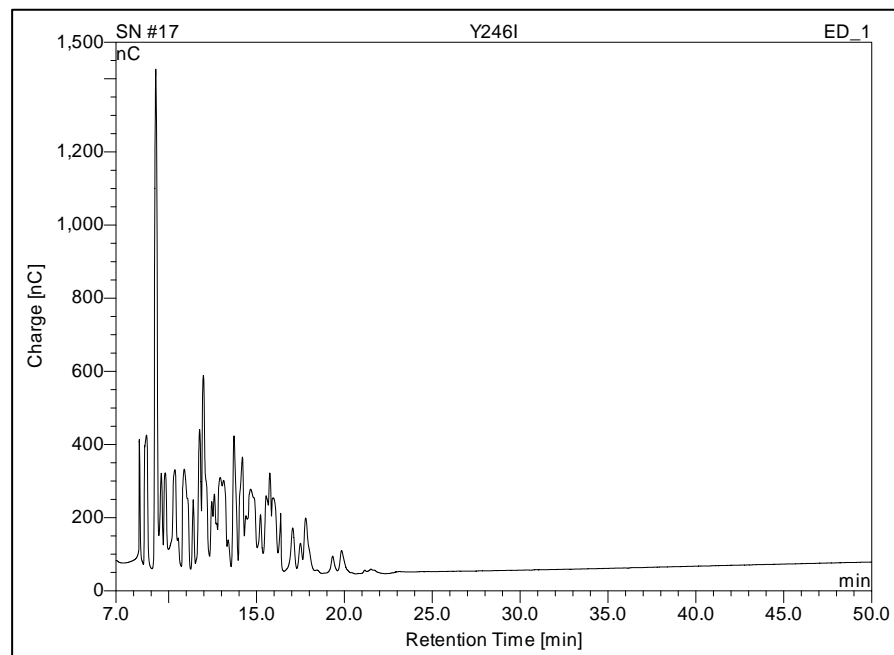
Figure 3.63 Analysis of the product pattern of mutated enzymes by HPAEC

The 0.5 U of the enzymes was incubated with 20% (w/v) sucrose at 50 °C for overnight. The reaction product was partially purified by activated charcoal column and analyzed by HPAEC

C) The reaction product of Y246D

D) The reaction product of Y246S

E)



F)

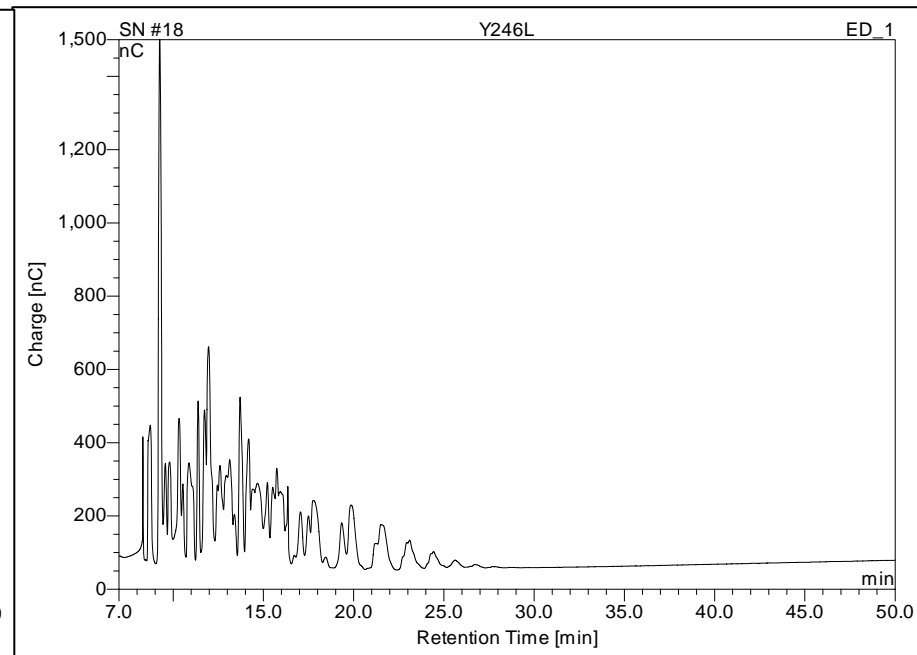


Figure 3.63 Analysis of the product pattern of mutated enzymes by HPAEC

The 0.5 U of the enzymes was incubated with 20% (w/v) sucrose at 50 °C for overnight. The reaction product was partially purified by activated charcoal column and analyzed by HPAEC

E) The reaction product of Y246I

F) The reaction product of Y246L

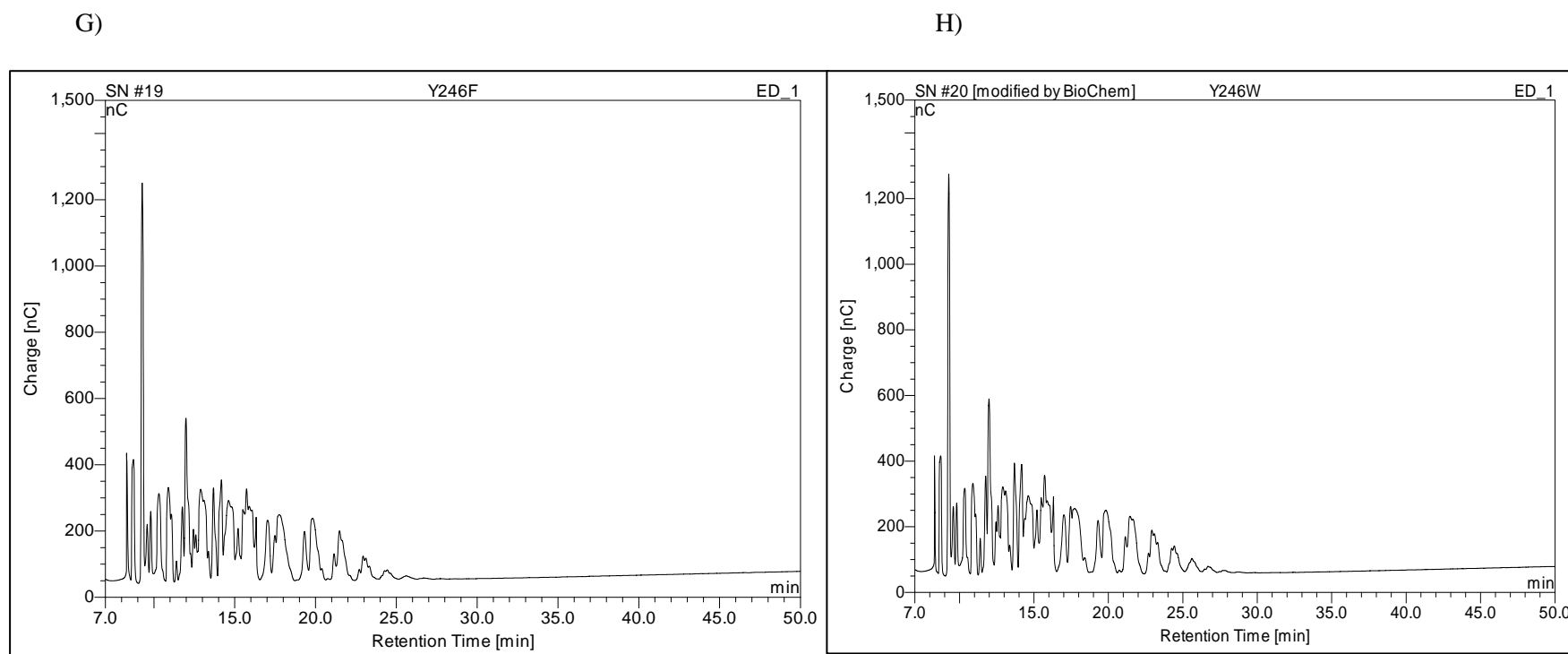


Figure 3.63 Analysis of the product pattern of mutated enzymes by HPAEC

The 0.5 U of the enzymes was incubated with 20% (w/v) sucrose at 50 °C for overnight. The reaction product was partially purified by activated charcoal column and analyzed by HPAEC.

- G) The reaction product of Y246F
- H) The reaction product of Y246W

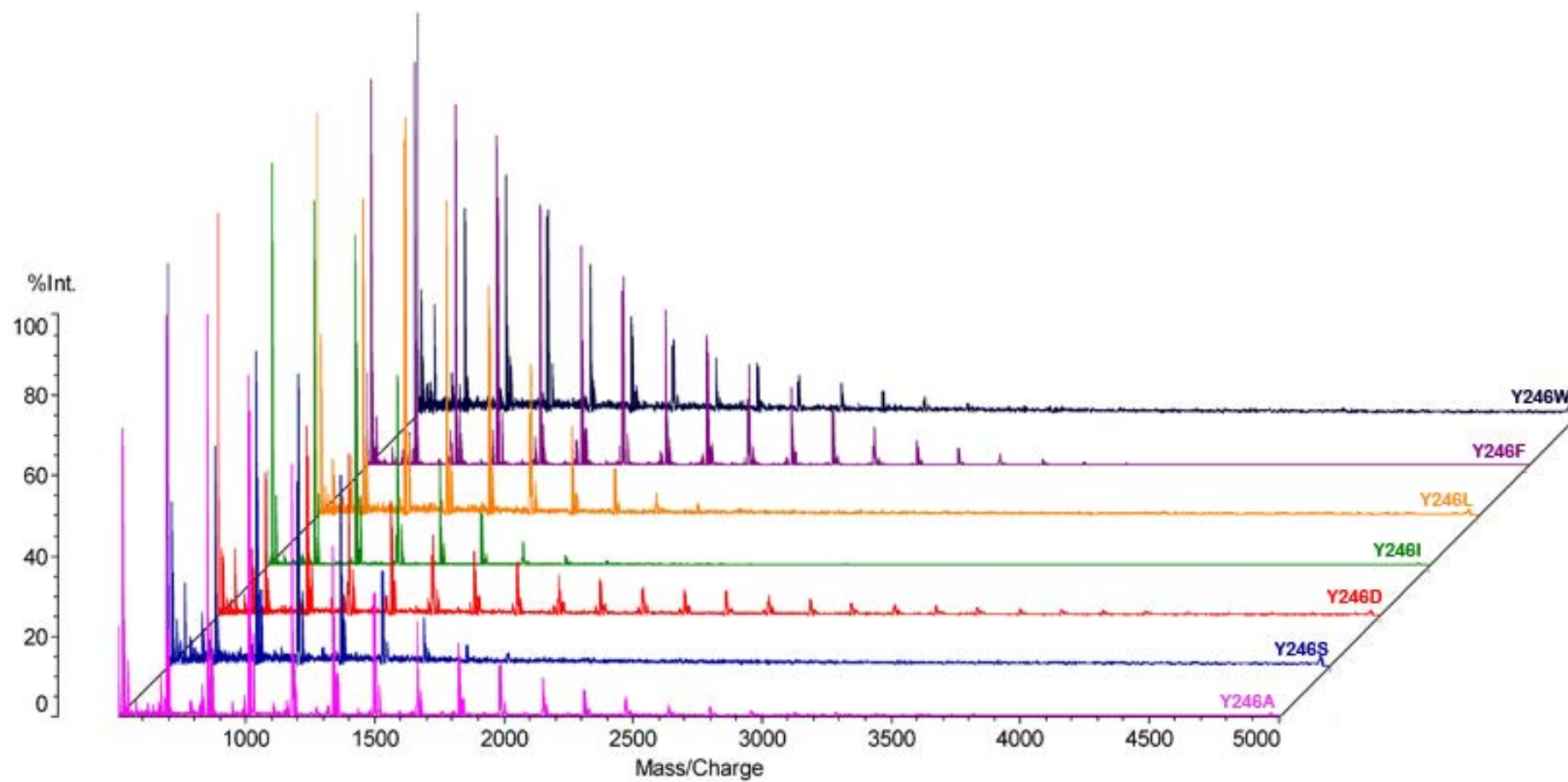


Figure 3.64 MALDI-TOF MS spectrum of the reaction products of Y246 series of Ls

CHAPTER IV

DISCUSSION

4.1 Screening for high activity levansucrase

Due to the versatile applicability of levan and its oligosaccharide, scientists have been tried to identify the new source of levansucrase producing bacterium. Levansucrases from some bacteria are extracellular whereas some are membrane bound or intracellular. In this work *B. circulans*, *B. licheniformis* and *B. subtilis* were tested for Ls activity. The extracellular and membrane-bound proteins were analyzed. No levansucrase activity was observed neither in liquid culture nor membrane-bound fraction of *B. circulans*. This result was contradictory to the work of Oseguea et al., they reported inducible extracellular Ls from *B. circulans*. A 3.0 U/mL of Ls was secreted into the medium containing 3% (w/v) sucrose [89]. In *B. licheniformis* and *B. subtilis*, Ls activities were found both in extracellular and membrane-bound fractions. The major Ls activity was detected as a membrane-bound protein. In contrast to levansucrases from other strains of *B. subtilis*, the enzymes were found in extracellular fraction [108], [109], [110]. Tian et al also reported the occurrence of the Ls from *B. amyloliquefaciens* in both fractions but higher activity was in extracellular fraction [111]. Pabst et al reported membrane-bound Ls of *Actinomyces viscosus* and also a minor Ls activity found in extracellular fraction [112]. Levansucrases from gram negative bacteria were localized either in extracellular or intracellular fractions. Ls of *G. diazotrophicus* SRT4 was found as the extracellular enzyme [37] while Ls from *R. aquatilis* was reported as the intracellular protein [113]. In contrast to those two gram negative Ls, levansucrase from *Z. mobilis* was found both in culture medium and membrane-bound fraction [114], [115].

The overall result showed no levansucrase activity detected in LB culture medium. Sucrose was indispensable for Ls production by *B. licheniformis* and *B. subtilis*. The higher sucrose concentration gave rise to higher level of enzyme production and higher specific activity. The Ls activity of around 5 U/mL was produced by SK-1, RN-01 and TN-1 in 20% (w/v) sucrose containing medium while the maximum Ls activity of 1.2 U/mL was produced by TH4-2 in the same medium. Other microorganisms produced different levels of levansucrase in sucrose containing medium. The Ls from *B. subtilis* NRC 33a was induced at high level with 20% (w/v) sucrose (14.5 U/mL) [108]. *Bacillus cereus* produced inducible extracellular Ls of 37.0 U/mL when grown on 16 % (w/v) sucrose containing medium [116]. *B. circulans* and *B. amyloliquefaciens* were induced to reach their maximum Ls production of 2 and 0.7 U/mL by 3 and 0.7% (w/v) sucrose, respectively [89], [111]. While the industrial

use Ls from *Z. mobilis* was induced by 5% (w/v) raffinose or maltose instead of sucrose to gain 0.63 U/mL of Ls [117]. Moreover, there are two microbial Ls reported as a constitutive enzyme. Ls from *G. diazotrophicus* SRT4 was produced, using glycerol as a sole carbon source [118]. Another was an extracellular Ls from *E. herbicola* NRRL-1678 which was produced in nutrient broth supplemented with corn steep as a nitrogen source [119].

4.2 Identification of the strain TN-1

TN-1 was identified by two classical techniques, biochemical reaction combined with morphological identification and 16S rRNA gene analysis. From biochemical and morphological identification method, TN-1 was identified as *B. lentus*. While the molecular identification revealed the identical to *B. subtilis* with 99 % identity. In fact, these two methods have been generally used to identify microorganisms isolated from natural environments [120], [121]. But both methods fail to distinguish one species from the others if they were isolated from similar environment or share highly similar rRNA genes [122]. To solve this problem, the other genes such as *recA* [123] and *dnaJ* [124] should be further compared.

4.3 Cloning and analysis of *ls*

The PCR technique was used to amplify *ls* from genomic DNA of the selected bacteria. The PCR primers specific to *ls* of *B. licheniformis* were designed base on the genome sequence of *B. licheniformis* ATCC14580. The PCR primers for *ls* of TN-01 were degenerated from Ls gene from *B. amyloliquefaciens*, *B. subtilis* and *B. stearothermophilus*. The PCR product (Fig 3.5 and 3.7) was a single band, indicating the high specificity of the primers to *ls*. The PCR products from *B. licheniformis* and *Bacillus* sp.TN-1 were ligated into pBluescript SK⁻ and pET-17b, respectively. The positive clones were nucleotide sequenced.

The nucleotide sequences of *ls* from *B. licheniformis* RN-01, SK-1 and TH4-2 showed 99% identity to those of *B. licheniformis* ATCC14580. While nucleotide sequence of *ls* from TN-1 was 98% identity to those of *B. subtilis*. The Ls gene comparison result related to the 16S rRNA gene species identification, implying the possibility that TN-1 should be classified in *subtilis* species instead of *lentus* species. The deduced amino acid sequences of *ls* from *B. licheniformis* RN-01, SK-1, TH4-2 and *B. subtilis* TN-1 were compared to the deposited Ls retrieved from GenBank by Blastp. Ls of *B. licheniformis* showed the highest identity to that of *B. atrophaeus* with 79% identity. While Ls from *B. subtilis* TN-1 showed the

highest identity of 97% to Ls from *B.stearothermophilus*. Based on deduced amino acid sequence, levansucrase was divided into four groups. As shown in Fig 4.1, Ls from *B. licheniformis* and *B. subtilis* were categorized in the same group, together with Ls from other *Bacilli* such as *B. atrophaeus*, *B.megaterium*, *B. amyloliquefaciens* and *B.stearothermophilus*. Although they all shared the same common ancestor, but a group of levansucrases from *Bacilli* was diverged before those of *Lactobacillus* and gram negative bacteria. Interestingly, inulosucrase, an enzyme mainly synthesizes β -2, 1 glycosidic linkage was classified in the same group of Ls from *Lactobacillus* and closer to Ls from *Bacilli* than those of Ls from gram negative bacteria. Carlos et al also reported that four subgroups of Ls from bacteria were diverged from their common ancestor before other fructosyltransferases from fungi and plants [125]. Altenbath et al proposed the evolution of levansucrase and other sucrose utilizing enzymes were branched from acid invertase. The enzymes were highly diverged to ubiquitous fructan synthesizing and hydrolyzing enzymes in bacteria, fungi and plants. However, no significant similarities when plant acid invertases were compared to all available sequences of animal proteins [126].

4.4 Expression of *ls*

LsRN was expressed under a putative endogenous promoter and T7 promoter and comparison was made in term of Ls production. The Ls activities were found both in extracellular and periplasmic fraction. The best condition was the expression under its own putative endogenous promoter. *E. coli* Top-10 carrying *plsRN* was grown in 3x LB for 36 h to gain the maximum extracellular Ls activity of 7.7 U/mL. The expression under T7 promoter gave only 5.6 U/mL of extracellular Ls. The expression of levansucrase genes in *E. coli* was frequently accomplished by using T7 promoter [38], [40], [127], [128]. Seo et al. reported the constitutive-like expression of intracellular levansucrase from *R. aquatilis* in *E. coli*. The researchers claimed that the endogenous promoter was functioned, resulting by their close genetic relativity between the two species in *Enterobacteriaceae* family [129].

4.5 Purification of LsRN

The LsRN was purified by two chromatographic steps using DEAE Toyopearl and Butyl-Toyopearl. The purification yielded more than 250 purification fold (around 470 U/mg protein⁻¹) with 60% recovery, obtaining over 90% homogeneity estimated by SDS-PAGE (Fig 3.20). In previous reports, the recombinant levansucrases were usually purified using the fusion His-tag by Ni-NTA [38], [117], [128]. Intracellular recombinant Ls from *L. reuteri* was purified by Ni-NTA and Resource-Q, an anion-exchange column to yield 2.9 purification fold with specific activity of 177 U mg protein⁻¹. But only 7.3 % yield was recovered [128]. Hettwer et al. also reported the purification of *P. syringae* by the two chromatographic steps, TMAE-Fraktogel and Butyl-Fraktogel, to yield 23 purification fold with 44% recovery [7]. Ls of *Streptococcus salivarius* was purified by the same chromatographic steps as those of LsRN and Ls from *P. syringae*. By using Resource-Q and Sephacryl S-300, the purification was achieved, gaining 5 fold of purification with specific activity of 53 U/mg protein⁻¹ [130]. Moreover, the purification of membrane-bound Ls from *Z. mobilis* was simplified by the addition of MnCl₂ before subsequently loaded to Resource-Q column. By this method, 62% of the initial Ls activity was retained with the specific activity of 39.5 U/mg protein⁻¹ [131].

4.6 Characterization of LsRN

The estimated Mw of LsRN from SDS-PAGE and Gel filtration (52 kDa) fell within the same range as those reported for the levansucrase from *B. circulans* (52 kDa) [36], *B.*

megaterium (52 kDa) [89], *B. subtilis* (50 kDa) [111] and *B. amyloliquefaciens* (52 kDa) [132]. The molecular weight of Ls from gram negative bacteria, *Z. mobilis* was 120 kDa by gel filtration and 56 kDa by SDS-PAGE analysis, indicating that Ls of *Z. mobilis* existed as a dimeric protein with two subunits of 56 kDa [133], [134]. The other Ls from gram negative bacteria were also shown to exist in the dimer form i.e. Ls from *R. aquatilis* (120 kDa by gel filtration and 57 kDa by SDS-PAGE) and *L. mesenteroides* (103 kDa by gel filtration and 52 kDa by SDS-PAGE) [113], [38].

The optimum temperature of LsRN was shown to be 50 °C. The optimum temperature within the range of 45-50 °C was reported for the Ls from *B. circulans* [89], *B. subtilis* [135], *B. megaterium* [36], *Z. mobilis* [127] and *L. reuteri* [47]. Whereas the Ls from *P. syringae* and *R. aquatilis* showed the highest activity at 60 °C [7], [113]. The Ls from *G. diazotrophicus* and *L. reuteri* reached their optimum at 30 °C, a lower temperature than that of LsRN [37], [47]. The temperature stability of LsRN was determined by comparative measuring of the total activity after pre-incubation of the purified protein at 20-60 °C for 1 and 6 h. The LsRN was stable at 20-50 °C for an hour but lost 50% of the initial activity after 6 h of pre-incubation at 50 °C. In the previous reports, the thermo-active Ls from *R. aquatilis* lost 50% of initial activity after pre-incubation at 60 °C for 20 min [113]. At the elevated temperatures of 60 °C, levansucrase undergoes an irreversible denaturation, this may be due to the permanent temperature-dependent unfolding [136] and the Ls structure itself. In fact, unlike other β -propeller proteins, Ls was devoid of a molecular velcro, resulting in a loosely folded of protein conformation [40].

Based on the pH profile (Fig 3.25), the pH activity profile of LsRN shared common features of those Ls from *Bacillus* species, which were active within a wide pH range of 5.0 to 7.0 [32]. However, the pH optimum reported for gram negative bacteria were a little more toward the acidic region [128], [137], [138].

The LsRN was significantly activated by calcium and manganese ion. Ca^{2+} was well understood for its binding and subsequently activating of fructosyltransferase [47], [136]. The Mn^{2+} was also reported for 22% activation of Ls from *B. subtilis* [139]. HgCl_2 , CuCl_2 , ZnCl_2 and FeCl_2 significantly inhibited LsRN activity. The Hg^{2+} , Cu^{2+} , Zn^{2+} and Fe^{2+} also inhibited the activity of Ls from *B. subtilis* and *B. circulans* [139], [140].

The effect of sucrose concentration on the reaction rate of the purified LsRN was investigated using a substrate concentration of 5 to 80% (w/v) sucrose under standard reaction conditions. The result, Figure 3.27 showed that the rate of hydrolysis and transfructosylation of LsRN were not significantly inhibited at high substrate concentration (80% sucrose). Indeed, the transfructosylation to hydrolysis ratio of LsRN changed over the investigated

sucrose concentration. At low sucrose concentration, the hydrolytic activity was predominant. When the sucrose concentration fell within the range of 10-20 % the transfructosylation to hydrolysis ratio was around 1, indicating the optimal concentration of sucrose substrate to synchronize both reactions. At the higher sucrose concentration, the rate of transfructosylation reached saturation while hydrolysis underwent a minor inhibition. This may be explained by a competition between two acceptors, a sucrose molecule and a growing levan chain, for the binding at the active site of Ls. To support this explanation, the previous study demonstrated that the addition of levan to the reaction mixture accelerated the transfructosylation reaction with no effect on Mw of synthesized levan [141]. One more reason taken into consideration why the rate of transfructosylation reached saturation could be attributed by the accumulation of free glucose in the reaction. Glucose was reported as an inhibitor of the hydrolysis, transfructosylation and levan-forming activities of Ls from *Z. mobilis*, while fructose did not significantly affect the velocities of these reactions [142].

The kinetic properties of LsRN were also investigated. The results (Fig 3.36 and 3.37) revealed that the kinetics of LsRN followed the Michaelis-Menten model. The *K_m* Michaelis-Menten values (6.9-9.1 mM sucrose) were close for both reactions and other levansucrases, for which *K_m* values ranging from 3 to 40 mM [143], [144], [36]. The *k_{cat}* turnover number for transfructosylation (32.5 s⁻¹) was lower than that of hydrolysis (86.0 s⁻¹), demonstrating that LsRN favored the hydrolysis reaction. Van Hijum et al reported that the Ls from *L. reuteri* had a greater catalytic efficiency for the hydrolysis reaction (10400 M⁻¹s⁻¹) than the transfructosylation reaction (2430 M⁻¹s⁻¹) [128]. The catalytic efficiency (*k_{cat}/K_m*) of LsRN for the hydrolysis (9.43 mM⁻¹s⁻¹) was higher than that for transfructosylation reaction (4.65 mM⁻¹s⁻¹).

4.7 Characterization of levan product

To identify the polymer synthesized by LsRN, the ¹³C- and ¹H-NMR were performed. The NMR spectrum of the polysaccharide produced by LsRN showed six main resonances at 106.9 (C2), 83.0 (C5), 79.3 (C3), 78.1 (C4), 66.1 (C6) and 62.9 (C1) ppm corresponding to the peak position for β-(2-6)-levan. These chemical shifts were almost identical to those obtained from the levan synthesized by *B. subtilis* and *B. polymyxa* [5] [141].

To study the factors affecting the size of synthesized levan, the levan product formed by LsRN at 30 °C and 50 °C were investigated. The wide range of Mw of levan (about 1-600 kDa) was synthesized in a controlled reaction by varying two parameters, temperature and NaCl concentration. At 50 °C, LsRN synthesized high Mw levan (612 kDa) as a major

product. While the rest was a mixture of low Mw levans ranging from 66.3 to 1.1 kDa. At 30 °C, LsRN synthesized low Mw levan (11 kDa) as a major product. When an ionic strength of the reactions was increased by the addition of 0.5 M NaCl, the major product at both temperatures was of the size 11 kDa. This result was corresponded to previous report that the Ls from *Bacillus* sp. TH4-2 synthesized higher molecular weight levan (660 kDa) at a higher temperature than that produced at a lower temperature (8 kDa) [91]. Likewise, Tanaka et al. [141] reported a decrease in the degree of polymerization of levans synthesized by the Ls from *B. subtilis* as the ionic strength of the reaction was increased, with no high Mw levan being obtained in the reaction with 0.8 M phosphate buffer. It was also observed in our study that high Mw levan synthesized was significantly affected by the presence of 0.5 M NaCl. Surprisingly NaCl had no effect on the synthesis of low Mw levan. This may due to the increase in ionic strength disturbed hydrogen bond network of the enzyme to sucrose substrate [44], resulting in the decrease in enzyme processivity and the product was consequently released faster. The turnover rate of hydrolysis reaction was increased while that for transfructosylation was not much affected. Thus the effect of ionic concentration on high Mw levan was more significant than in low Mw levan.

4.8 Enzymatic synthesis of levan nanoparticles

Levan NPs were firstly reported to be formed in the single enzymatic step in this work. The TEM analysis of the levan NPs showed that the average particle size of enzymatic synthesized levan NPs was 50 nm. While the self-assemble of levan NPs by stirring method yielded the average particle size of about 200-537 nm, depending on the levan concentration and stirring speed [49]. Levan tended to form NPs in an aqueous solution, which is probably due to the surfactant-like properties of levan. Levan exhibits both a hydrophilicity nature from the hydroxyl group of the furanose ring and a hydrophobicity nature from the backbone of the sugar ring [31] and so makes possible the arrangement of the molecules in a sugar monolayer which can encapsulate the non-polar molecule inside. In this work, the encapsulation of *O*-acetyl- α -tocopherol into levan NPs was evaluated by the NP self-assembly as the levan was synthesized. Encapsulation was ensured by three washing of the NPs after separation from the oil phase. The average particle size of 100 nm as estimated by TEM, was larger than the corresponding unencapsulated levan NPs. The successful preparation of bovine serum albumin-encapsulated levan NPs had been previously reported and the applicable use as peptide drug nanocarrier was proposed [49].

4.9 Encapsulation of *O*-acetyl- α -tocopherol into levan NPs

The encapsulation of *O*-acetyl- α -tocopherol into levan NPs was evaluated by FTIR. From FTIR transmittance spectra of levan NPs, *O*-acetyl- α -tocopherol, and *O*-acetyl- α -tocopherol-encapsulated levan NPs, the broadband at around 3255 cm⁻¹ found in levan NPs and the tocopherol-encapsulated levan NPs associated to -OH stretching vibration of levan has been previously reported [14]. The band at 1759 cm⁻¹ represented C=O stretching vibration of the acetyl group in *O*-acetyl- α -tocopherol which was also found in tocopherol-encapsulated levan NPs. The band at 1456 cm⁻¹ for the phenyl, skeletal and methyl asymmetric bending and 1366 cm⁻¹ attributed with methyl symmetric bending [145] was observed in acetyl- α -tocopherol and tocopherol-encapsulated levan NPs. The results thus showed the ability of levan NPs to encapsulate acetyl-tocopherol, a small non-polar compound. The potential of levan NPs to be employed as drug nanocarrier is promising.

4.10 Homology modeling of LsRN

The homology modeling of LsRN displayed the similar five-bladed -propeller architecture as its template *B. subtilis* levansucrase. A funnel-like opening provides access to the deep negatively charged pocket. By superposition of LsRN with the Ls from *B. subtilis*, the active site, the catalytic triad was identified at the bottom of the funnel-like cavity. Residues D93, E351 and D256 were proposed to form the catalytic triad of LsRN (Fig 3.45), with E351 acting as the acid-base catalyst, D93 as the nucleophile and D256 as transition state stabilization. Residues involved in the sucrose binding, the -1 (fructosyl residue) and +1 (glucosyl residue) sugar binding subsites (nomenclature according to Davis [146]) were also identified. Residues R255 and W98 hydrogen bonded to fructosyl unit. While residues R369 and E349 were hydrogen bonded to glucosyl units. The cleavage of the sucrose substrate took place between subsites -1 and +1. The enzyme formed a covalent intermediate with the fructose moiety of the cleaved sucrose at subsite -1. The fructose moiety was subsequently coupled to the acceptor molecule. The acceptor molecule in transfructosylation reaction could be composed of fructose moiety and bound to the Ls at the next subsites (-2, -3, -4 and so on), depending on the length of the acceptor molecule [36].

4.11 Mutation at the position N251 influenced transfructosylation reaction and polysaccharide synthesis

The substitution of N251 with alanine or tyrosine totally abolished the polysaccharide production. TLC analysis of the product spectrum showed that catalysis by N251A/Y switched from mainly polysaccharide synthesis to oligosaccharide synthesis and hydrolysis. The N251A/Y formed oligosaccharides of up to three fructosyl units. The biochemical data along with the homology modeling data showed that N251A was located at subsite +2 (Fig 3.46). The kinetic parameters of transfructosylation reaction of N251A were different compared to WT. The K_m value for sucrose was decreased, indicating the higher affinity to sucrose but the catalytic efficiency was significantly decreased (10 fold). While in transfructosylation reaction, the affinity to sucrose of N251A remained in the WT range but the hydrolysis efficiency retained only 60% of the WT enzyme. These data led the conclusion that N251 is directly involved in interaction with the growing fructan chain. The residue stabilized the third fructosyl unit of the growing fructosyl chain and directed it as an acceptor substrate in the optimal position for further transfructosylation steps. Beian et al. also reported similar finding. The asparagine at subsite +2 of levansucrase from *B. megaterium* was substituted by histidine. The substitution affected the coordination of this position with the third sugar residue, resulting in no longer synthesis of levan polymer [45]. On the other hand, this effect was preserved when substitution with structural conserved amino acids, D and K. The substitution with D in Ls of *B. megaterium* retained the polysaccharide synthesis activity [36]. This result was corresponded to our observation where N251D and N251K retained the polymer synthetic activity of the WT LsRN.

Because oligosaccharide products were also used as an acceptor molecule, the binding of oligosaccharide at this subsite instead of fructosyl group of sucrose may involve in the determination of branching degree of levan product. Levan synthesized by WT LsRN had approximately 1 branch point per 15 fructosyl units, while levan synthesized by N251D mutated enzyme had more branch, around 1 branch point per 5 fructosyl units (data not shown). From the result, N251 did not only determine the size of levan product but also the degree of branching.

4.12 Random mutagenesis

The error prone PCR was used to randomly mutate LsRN. The various concentrations of $MnCl_2$ were added into PCR reaction. The Mn^{2+} doping reaction yielded higher amount of

PCR product than those of the control reaction without the addition of MnCl_2 . This may due to Mn^{2+} also acted as a co-factor for *Taq* DNA polymerase, subsequently enhanced the polymerase activity and resulted in higher amount of PCR product. From the obtained nucleotide sequences of all selected variants, the PCR introduced random mutations into the gene at a frequency of around 1 mutation per kb. This mutation frequency corresponded to one amino acid mutation per kb, thus appropriate for in vitro evolution experiments [147]. In addition, the mutation frequency could be controlled by varying the concentration of Mn^{2+} . The higher MnCl_2 concentration added in PCR reaction, the higher frequency of mutation in LsRN gene.

4.13 Y246 controlled the size distribution of levan product

The importance of Y246 to the transfructosylation process of LsRN was determined by site-directed mutagenesis. Substitution of Y246 with A eliminated all of functional groups of Y with small methyl group, resulting in the formation of oligosaccharides up to 20 fructosyl residues. The substitution of Y with W or F to maintain the aromatic ring of Y resulted in the change of the product pattern from mixture of oligosaccharide and polysaccharide in WT LsRN to mainly oligosaccharides up to deca-saccharide. While the substitution with aliphatic non-polar amino acid isoleucine and leucine, the product patterns were shorter than nanosaccharide. These results raised the question whether the substitution at Y246 influenced the conformation of the active site or directly involved in the processivity of the enzyme. Strube et al reported the X-ray structures of mutated Ls from *B. megaterium*, Y247A and Y247W (Y247 in Ls from *B. megaterium* corresponded to Y246 in LsRN). And the results showed that conserved active site architecture of the catalytic triad as well as the functional important amino acids at +1 and -1 subsites were in the intact conformation. Thus the change caused by conformation distort was excluded. They also proposed that this residue together with N251 and K372 (LsRN numbering) formed a platform for a possible stabilization of the acceptor fructan chain [46].

4.13 Three surface motifs play different role in levan synthesis by LsRN

By integration of all mutation results, the three different function surface motifs are proposed in this study. As shown in Figure 4.2, N251 at subsite +2 and the further amino acid, N311, N314 and D348 may form an acceptor binding tract. N251 may bind to fructosyl unit of either sucrose or fructooligosaccharide which is a transfructosylation product of the

enzyme itself. If fructosyl unit of sucrose occupies this site, the enzyme will further elongate the product via β -(2, 6) glycosidic linkage. On the other hand, if the fructosyl unit of fructooligosaccharide binds in this site, the fructosyl moiety from the next sucrose molecule will be transferred to an oligosaccharide acceptor via β -(2, 1) glycosidic linkage. The second motif may compose of Y246, Y194 and so on. This motif may be a product stabilizing tract. The mutation at these positions, especially Y246 makes the product leave from the enzyme easier and gives products of shorter size. The third surface motif may be a donor feeding tract, composed of Q65, Q411, N414 and N470. This tract may be designed to orchestrate the hydrolysis and transfructosylation rate of the bifunctional enzyme levansucrase. Because of high processivity of the LsRN, diffusion of sucrose into an active site without the accumulation of sucrose donor near the opening of the funnel-like catalytic cleft may not be sufficient to synchronize the hydrolysis and transfructosylation rate of LsRN.

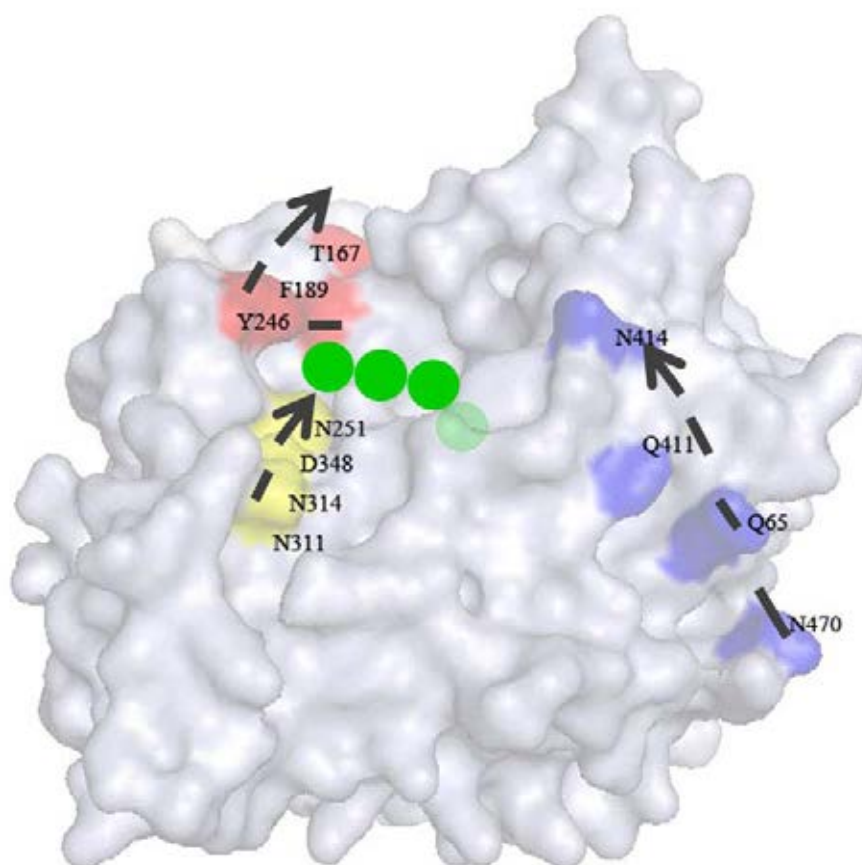


Figure 4.2 Three different function surface motifs of LsRN

The three different function surface motifs of LsRN, acceptor binding site, product stabilizing tract and donor feeding tract are labeled in yellow, red and blue, respectively.

CHAPTER V

CONCLUSION

In order to screen for the high levansucrase-producing bacterium, six strains from three *Bacilli* were cultured in sucrose containing medium. *Bacillus licheniformis* RN-01 produced the highest activity of Ls. The enzyme was mainly found in culture medium and membrane-bound fraction.

When the *ls* from *B. licheniformis* RN-01 was cloned, a sequence of 1,793 bp was obtained from the genomic DNA by PCR amplification. The nucleotide sequence revealed a single open reading frame of 1,445 bp with putative promoter sequence. The deduced amino acid sequence of 482 residues including the signal peptide of 29 amino acids was obtained. The *ls* was expressed in two expression systems, pET-19b and under putative endogenous promoter. When expressed under T7 promoter, the best condition was the expression in *E. coli* Rosetta (DE3) pLysS in terrific broth with addition of 1.0 mM IPTG for 16 h. While expressed under putative endogenous promoter, the best condition was the expression in *E. coli* Top-10 in 3xLB for 36 h.

LsRN was successfully purified by two chromatographic steps, DEAE Toyopearl-650M and Butyl Toyopearl-650M, resulting in more than 250 fold with 60% recovery. The purified enzyme exhibited 95% homogeneity with an apparent M_r of 52 kDa on SDS-PAGE, corresponding to the protein band producing levan polymer on activity-staining gel. The enzyme approaches optimal condition at pH 6.0 and 50 °C. The half-life of LsRN at 50 °C was more than 6 h, while at temperature below 10 °C more than 90% of activity retained after 12 h of incubation. LsRN was significantly activated by CaCl_2 and MnCl_2 but completely inhibited by CuCl_2 , HgCl_2 and EDTA. The LsRN exhibited MM type kinetics. The K_m , k_{cat} , and k_{cat} / K_m values were 9.12 mM, 86.0 s^{-1} , and 9.43 $\text{mM}^{-1}\text{s}^{-1}$ for hydrolysis reaction, and 6.94 mM, 32.3 s^{-1} and 4.65 $\text{mM}^{-1}\text{s}^{-1}$ for transfructosylation reaction.

The structure of the polymer product formed by the LsRN was analyzed by ^{13}C -NMR. Six main resonances at 106.7, 82.8, 77.2, 76.8, 66.0 and 62.8 ppm were found. The chemical shifts corresponded to those of reported levan.

The wide range of Mw of levan (about 1-600 kDa) was synthesized by LsRN in a controlled reaction by varying two parameters, temperature and NaCl concentration. At 50 °C, LsRN synthesized high Mw levan (612 kDa) as a major product. The amount of high Mw levan was about 40% of the total amount, whilst the rest was a mixture of low Mw levans

ranging from 66.3 to 1.1 kDa. At 30 °C, LsRN synthesized low Mw levan (11 kDa) as a major product, approximately 60% of the total amount. When an ionic strength of the reactions was increased by addition of 0.5 M NaCl, the major product at both temperatures was of the size 11 kDa.

The synthesis of levan NPs by a single step enzymatic reaction was performed for the first time. An agglomerated form of levan NPs with the average size of 50 nm was synthesized. The *in situ* encapsulation of *O*-acetyl- α -tocopherol was also performed. The encapsulated NP was verified by FTIR. The signature bands of the vitamin were clearly found in encapsulated levan NPs.

Not only the reaction conditions affected the size of levan product, certain amino acid residues in Ls also involved in product size determination and distribution as investigated by two strategies, rational mutagenesis and random mutagenesis.

From structure comparison of LsRN and invertase from *T. maritima*, N251 at subsite +2 was not superimposed to any residue in invertase, thus implied its role in transfructosylation. Amino acid substitution with A and Y totally abolished the polysaccharide synthetic activity of LsRN. While the substitution with the structural conserved amino acids, D and K, retained the levan synthetic activity of LsRN.

From random mutagenesis by error prone PCR, the mutations were located in three discrete sites of LsRN. They were the buried A202G, and the residues Q65E, Q411L, N414T and N470I at the molecular surface. Y246 located at the surface and not too far from an opening of the funnel-like catalytic cleft was also selected. The substitution of Y246 residue abolished the polysaccharide synthesis of LsRN.

By combining all the mutation results, the three surface motifs were identified in LsRN with the proposed functions. N251 may lie in the acceptor binding motif, Y246 may be the product binding site and the surface residues, Q65, Q411, N414 and N470 may form the sucrose donor feeding tract.

REFERENCES

1. Lee SY, Park SJ, Park JP, Lee Y, Lee SH: Economic Aspects of Biopolymer Production. In: *Biopolymers Online*. Wiley-VCH Verlag GmbH & Co. KGaA; 2005.
2. Rhee SK, Song KB, Kim CH, Park BS, Jang EK, Jang KH: Levan. In: *Biopolymers Online*. Wiley-VCH Verlag GmbH & Co. KGaA; 2005.
3. Kunst F, Rapoport G: Salt stress is an environmental signal affecting degradative enzyme synthesis in *Bacillus subtilis*. *Journal of Bacteriology* 1995, 177(9):2403-2407.
4. Newbrun E, Baker S: Physico-chemical characteristics of the levan produced by *Streptococcus salivarius*. *Carbohydrate Research* 1968, 6(2):165-170.
5. Shih IL, Yu YT, Shieh CJ, Hsieh CY: Selective production and characterization of levan by *Bacillus subtilis* (Natto) Takahashi. *Journal of Agricultural and Food Chemistry* 2005, 53(21):8211-8215.
6. Han YW: Levan production by *Bacillus polymyxa*. *Journal of Industrial Microbiology & Biotechnology* 1989, 4(6):447-451.
7. Hettwer U, Gross M, Rudolph K: Purification and characterization of an extracellular levansucrase from *Pseudomonas syringae* pv. *phaseolicola*. *Journal of Bacteriology* 1995, 177(10):2834-2839.
8. Hettwer U, Jaeckel FR, Boch J, Meyer M, Rudolph K, Ullrich MS: Cloning, nucleotide sequence, and expression in *Escherichia coli* of levansucrase genes from the plant pathogens *Pseudomonas syringae* pv. *glycinea* and *P. syringae* pv. *phaseolicola*. *Applied and Environmental Microbiology* 1998, 64(9):3180-3187.
9. Song KB, Belghith H, Rhee SK: Production of levan, a fructose polymer, using an overexpressed recombinant levansucrase. *Annals of the New York Academy of Sciences* 1996, 799:601-607.
10. Ananthalakshmy VK, Gunasekaran P: Isolation and characterization of mutants from levan-producing *Zymomonas mobilis*. *Journal of Bioscience and Bioengineering* 1999, 87(2):214-217.
11. Van Geel-Schutten GH, Faber EJ, Smit E, Bonting K, Smith MR, Ten Brink B, Kamerling JP, Vliegthart JFG, Dijkhuizen L: Biochemical and Structural Characterization of the Glucan and Fructan Exopolysaccharides Synthesized by the *Lactobacillus reuteri* Wild-Type Strain and by Mutant Strains. *Applied and Environmental Microbiology* 1999, 65(7):3008-3014.

12. Arvidson SA, Rinehart BT, Gadala-Maria F: Concentration regimes of solutions of levan polysaccharide from *Bacillus* sp. *Carbohydrate Polymers* 2006, 65(2):144- 149.
13. Vina I, Karsakevich A, Gonta S, Linde R, Bekers M: Influence of some physicochemical factors on the viscosity of aqueous levan solutions of *Zymomonas mobilis*. *Acta Biotechnologica* 1998, 18(2):167-174.
14. Barone JR, Medynets M: Thermally processed levan polymers. *Carbohydrate Polymers* 2007, 69(3):554-561.
15. Stivala SS, Zweig JE: Physicochemical parameters of partially hydrolyzed *S. salivarius* levan fractions. *Biopolymers* 1981, 20(3):605-619.
16. Semjonovs P, Zikmanis P: An Influence of Levan on the Fermentation of Milk by a Probiotic ABT-Type Starter. *Journal of Food Technology* 2007, 5:123-130.
17. Semjonovs SP, Marauska M, Linde R, Grube M, Zikmanis P, Bekers M: Development of *Bifidobacterium lactis* Bb 12 on β -(2,6)-Linked Fructan-Containing Substrate. *Engineering in Life Sciences* 2004, 4(5):433-437.
18. Marx SP, Winkler S, Hartmeier W: Metabolization of beta-(2,6)-linked fructose-oligosaccharides by different bifidobacteria. *FEMS Microbiology Letters* 2000, 182(1):163-169.
19. Yamamoto Y, Takahashi Y, Kawano M, Iizuka M, Matsumoto T, Saeki S, Yamaguchi H: In vitro digestibility and fermentability of levan and its hypocholesterolemic effects in rats. *Journal of Nutritional Biochemistry* 1999, 10(1):13-18.
20. Kang S. A., Hong K. H., Jang K. H., Kim S. H., Lee K. H., Chang B. I., Kim C. H., Choue R. W.: Anti-obesity and hypolipidemic effects of dietary levan in high fat diet-induced obese rats. *Journal of Microbiology and Biotechnology* 2004, 14(4):796-804.
21. Kang SA, Hong K, Jang KH, Kim YY, Choue R, Lim Y: Altered mRNA expression of hepatic lipogenic enzyme and PPAR α in rats fed dietary levan from *Zymomonas mobilis*. *Journal of Nutritional Biochemistry* 2006, 17(6):419-426.
22. Kim YY, Kang KH, Kang SA, Cho Y, Kim JS, Kim CH, Choue R: Effect of types of levan with or without phytic acid on intestinal environment and mineral absorption in rats *Journal of Foodscience and Biotechnology* 2004, 14(3):450-454.
23. Rairakhwada D, Pal AK, Bhathena ZP, Sahu NP, Jha A, Mukherjee SC: Dietary microbial levan enhances cellular non-specific immunity and survival of common carp (*Cyprinus carpio*) juveniles. *Shell and fish Immunology* 2007, 22(5):477-486.

24. Gupta SK, Pal AK, Sahu NP, Dalvi R, Kumar V, Mukherjee SC: Microbial levan in the diet of *Labeo rohita* Hamilton juveniles: effect on non-specific immunity and histopathological changes after challenge with *Aeromonas hydrophila*. *Journal of Fish Diseases* 2008, 31(9):649-657.
25. Yoo SH, Yoon EJ, Cha J, Lee HG: Antitumor activity of levan polysaccharides from selected microorganisms. *International Journal of Biological Macromolecules* 2004, 34(1-2):37-41.
26. Yoon EJ, Yoo S-H, Cha J, Gyu Lee H: Effect of levan's branching structure on antitumor activity. *International Journal of Biological Macromolecules* 2004, 34(3):191-194.
27. Esawy MA, Ahmed EF, Helmy WA, Mansour NM, El-Senousy WM, El-Safty MM: Production of levansucrase from novel honey *Bacillus subtilis* isolates capable of producing antiviral levans. *Carbohydrate Polymers* 2011, 86(2):823-830.
28. Dahech I, Belghith KS, Hamden K, Feki A, Belghith H, Mejdoub H: Oral administration of levan polysaccharide reduces the alloxan-induced oxidative stress in rats. *International Journal of Biological Macromolecules* 2011, 49(5):942-947.
29. Dahech I, Belghith KS, Hamden K, Feki A, Belghith H, Mejdoub H: Antidiabetic activity of levan polysaccharide in alloxan-induced diabetic rats. *International Journal of Biological Macromolecules* 2011, 49(4):742-746.
30. Monatana polysaccharides corp., your source of levan [<http://www.polysaccharides.us>]
31. Kang SA, Jang KH, Seo JW, Kim KH, Kim YH, Rairakhwada D, Seo MY, Lee JO, Ha SD, Kim CH *et al* (eds.): *Levan: applications and perspectives*: Caister Academic Press; 2009.
32. Rhee SK, Song KB: Levansucrase. In: *Handbook of Food Enzymology*. CRC Press; 2002.
33. Song KB, Seo JW, Kim MG, Rhee SK: Levansucrase of *Rahnella aquatilis* ATCC33071: Gene cloning, expression, and levan formation. *Annals of the New York Academy of Sciences* 1998, 864(1):506-511.
34. Tajima K, Uenishi N, Fujiwara M, Erata T, Munekata M, Takai M: The production of a new water-soluble polysaccharide by *Acetobacter xylinum* NCI 1005 and its structural analysis by NMR spectroscopy. *Carbohydrate Research* 1997, 305(1):117-122.

35. Chambert R, Treboul G, Dedonder R: Kinetic studies of levansucrase of *Bacillus subtilis*. *European Journal of Biochemistry* 1974, 41(2):285-300.
36. Homann A, Biedendieck R, Gotze S, Jahn D, Seibel J: Insights into polymer versus oligosaccharide synthesis: mutagenesis and mechanistic studies of a novel levansucrase from *Bacillus megaterium*. *Biochemical Journal* 2007, 407(2):189- 198.
37. Hernandez L, Arrieta J, Menendez C, Vazquez R, Coego A, Suarez V, Selman G, Petit-Glatron MF, Chambert R: Isolation and enzymic properties of levansucrase secreted by *Acetobacter diazotrophicus* SRT4, a bacterium associated with sugar cane. *Biochemical Journal* 1995, 309 (Pt 1):113-118.
38. Kang HK, Seo MY, Seo ES, Kim D, Chung SY, Kimura A, Day DF, Robyt JF: Cloning and expression of levansucrase from *Leuconostoc mesenteroides* B-512 FMC in *Escherichia coli*. *Biochimica et Biophysica Acta - Gene Structure and Expression* 2005, 1727(1):5-15.
39. Euzenat O, Guibert A, Combes D: Production of fructo-oligosaccharides by levansucrase from *Bacillus subtilis* C4. *Process Biochemistry* 1997, 32(3):237-243.
40. Meng G, Futterer K: Structural framework of fructosyl transfer in *Bacillus subtilis* levansucrase. *Nature Structural & Molecular Biology* 2003, 10(11):935-941.
41. Martinez Fleites C, Ortiz Lombardia M, Pons T, Tarbouriech N, Taylor EJ, Arrieta JG, Hernandez L, Davies GJ: Crystal structure of levansucrase from the Gram-negative bacterium *Gluconacetobacter diazotrophicus*. *Biochemical Journal* 2005, 390(Pt 1):19-27.
42. Alberto F, Jordi E, Henrissat B, Czjzek M: Crystal structure of inactivated *Thermotoga maritima* invertase in complex with the trisaccharide substrate raffinose. *Biochemical Journal* 2006, 395(3):457-462.
43. Seibel J, Moraru R, Gotze S, Buchholz K, Na' amnieh S, Pawlowski A, Hecht HJ: Synthesis of sucrose analogues and the mechanism of action of *Bacillus subtilis* fructosyltransferase (levansucrase). *Carbohydrate Research* 2006, 341(14):2335-2349.
44. Meng G, Futterer K: Donor substrate recognition in the raffinose-bound E342A mutant of fructosyltransferase *Bacillus subtilis* levansucrase. *BMC Structural Biology* 2008, 8:16.
45. Beine R, Moraru R, Nimtz M, Na' amnieh S, Pawlowski A, Buchholz K, Seibel J: Synthesis of novel fructooligosaccharides by substrate and enzyme engineering. *Journal of Biotechnology* 2008, 138(1-2):33-41.

46. Strube CP, Homann A, Gamer M, Jahn D, Seibel J, Heinz DW: Polysaccharide synthesis of the levansucrase SacB from *Bacillus megaterium* is controlled by distinct surface motifs. *Journal of Biological Chemistry* 2011, 286(20):17593-17600.
47. Ozimek LK, Euverink GJ, van der Maarel MJ, Dijkhuizen L: Mutational analysis of the role of calcium ions in the *Lactobacillus reuteri* strain 121 fructosyltransferase (levansucrase and inulosucrase) enzymes. *FEBS letters* 2005, 579(5):1124-1128.
48. Van Hijum SAFT, Kralj S, Ozimek LK, Dijkhuizen L, van Geel-Schutten IGH: Structure-Function Relationships of Glucansucrase and Fructansucrase Enzymes from Lactic Acid Bacteria. *Microbiology and Molecular Biology Reviews* 2006, 70(1):157-176.
49. Sezera AD, Kazakb H, Önerb ET, Akbugaa J: Levan-based nanocarrier system for peptide and protein drug delivery. *Carbohydrate Polymers* 2011, 84:358-363.
50. Kim KH, Chung CB, Kim YH, Kim KS, Han CS, Kim CH: Cosmeceutical properties of levan produced by *Zymomonas mobilis*. *Journal of Cosmetics Science* 2005, 56(6):395-406.
51. Zahoor Ahmad, Rajesh Pandey, Sharma S, Khuller GK: Alginate nanoparticles as antituberculosis drug carriers: formulation development, pharmacokinetics and therapeutic Potential. *The Indian Journal of Chest Diseases & Allied Sciences* 2006, 48(3):171-176.
52. Buyuktimkin B, Wang Q, Kiptoo P, Stewart JM, Berkland C, Siahaan TJ: Vaccine-like controlled-release delivery of an immunomodulating peptide to treat experimental autoimmune encephalomyelitis. *Molecular Pharmaceutics* 2012.
53. Sun F, Ju C, Chen J, Liu S, Liu N, Wang K, Liu C: Nanoparticles based on hydrophobic alginate derivative as nutraceutical delivery vehicle: vitamin D3 loading. *Artificial Cells, Blood Substitutes and Biotechnology* 2012, 40(1-2):113-119.
54. Gao W, Sha B, Zou W, Liang X, Meng X, Xu H, Tang J, Wu D, Xu L, Zhang H: Cationic amylose-encapsulated bovine hemoglobin as a nanosized oxygen carrier. *Biomaterials* 2011, 32(35):9425-9433.
55. Liu M, Gan L, Chen L, Zhu D, Xu Z, Hao Z, Chen L: A novel liposome-encapsulated hemoglobin/silica nanoparticle as an oxygen carrier. *International Journal of Pharmaceutics* In press.
56. Dai W-G, Dong LC, Song Y-Q: Nanosizing of a drug/carrageenan complex to increase solubility and dissolution rate. *International Journal of Pharmaceutics* 2007, 342(1-2):201-207.

57. Sanchez-Garcia MD, Hilliou L, Lagaron JM: Nanobiocomposites of carrageenan, zein, and mica of interest in food packaging and coating applications. *Journal of Agricultural and Food Chemistry* 2010, 58(11):6884-6894.
58. Grenha A, Gomes ME, Rodrigues M, Santo VE, Mano JF, Neves NM, Reis RL: Development of new chitosan/carrageenan nanoparticles for drug delivery applications. *Journal of Biomedical Materials Research Part A* 2010, 92A(4):1265-1272.
59. Sitterberg J, Özçetin A, Ehrhardt C, Bakowsky U: Utilising atomic force microscopy for the characterisation of nanoscale drug delivery systems. *European Journal of Pharmaceutics and Biopharmaceutics* 2010, 74(1):2-13.
60. Nagaraju CVV, Ganesh GNK, Gowthamarajan K, Jawahar N, Kumar R, Senthil V: Design and development of hydrogel nanoparticles for mercaptopurine, vol. 1; 2010.
61. Alishahi A, Mirvaghefi A, Tehrani MR, Farahmand H, Koshio S, Dorkoosh FA, Elsabee Maher Z: Chitosan nanoparticle to carry vitamin C through the gastrointestinal tract and induce the non-specific immunity system of rainbow trout (*Oncorhynchus mykiss*). *Carbohydrate Polymers* 2011, 86(1):142-146.
62. Sharma K, Somavarapu S, Colombani A, Govind N, Taylor KMG: Crosslinked chitosan nanoparticle formulations for delivery from pressurized metered dose inhalers. *European Journal of Pharmaceutics and Biopharmaceutics* In press.
63. Odaci D, Timur S, Telefoncu A: Bacterial sensors based on chitosan matrices. *Sensors and Actuators B: Chemical* 2008, 134(1):89-94.
64. Alex SM, Rekha MR, Sharma CP: Spermine grafted galactosylated chitosan for improved nanoparticle mediated gene delivery. *International Journal of Pharmaceutics* 2011, 410(1-2):125-137.
65. Nakorn PN: Chitin nanowhisker and chitosan nanoparticles in protein immobilization for biosensor applications. *Journal of Metals, Materials and Minerals* 2008, 18 (2):73-77
66. Tang Z-X, Qian J-Q, Shi L-E: Characterizations of immobilized neutral lipase on chitosan nano-particles. *Materials Letters* 2007, 61(1):37-40.
67. Cavalli R, Donalisio M, Civra A, Ferruti P, Ranucci E, Trotta F, Lembo D: Enhanced antiviral activity of Acyclovir loaded into β -cyclodextrin-poly(4-acryloylmorpholine) conjugate nanoparticles. *Journal of Controlled Release* 2009, 137(2):116-122.
68. Yaméogo JBG, Gèze A, Choisnard L, Putaux J-L, Gansané A, Sirima SB, Semdé R, Wouessidjewe D: Self-assembled biotransesterified cyclodextrins as Artemisinin

- nanocarriers – I: Formulation, bioavailability and in vitro antimalarial activity assessment. *European Journal of Pharmaceutics and Biopharmaceutics* In press.
69. Svenson S, Wolfgang M, Hwang J, Ryan J, Eliasof S: Preclinical to clinical development of the novel camptothecin nanopharmaceutical CRLX101. *Journal of Controlled Release* 2011, 153(1):49-55.
 70. Gil ES, Li J, Xiao H, Lowe TL: Quaternary ammonium β -cyclodextrin nanoparticles for enhancing doxorubicin permeability across the in vitro blood–brain barrier. *Biomacromolecules* 2009, 10(3):505-516.
 71. Bilensoy E, Gürkaynak O, Doğan AL, Hıncal AA: Safety and efficacy of amphiphilic β -cyclodextrin nanoparticles for paclitaxel delivery. *International Journal of Pharmaceutics* 2008, 347(1–2):163-170.
 72. Memisoglu-Bilensoy E, Vural I, Bochot A, Renoir JM, Duchene D, Hıncal AA: Tamoxifen citrate loaded amphiphilic β -cyclodextrin nanoparticles: In vitro characterization and cytotoxicity. *Journal of Controlled Release* 2005, 104(3):489-496.
 73. Teijeiro-Osorio D, Remuñán-López C, Alonso MJ: Chitosan/cyclodextrin nanoparticles can efficiently transfect the airway epithelium in vitro. *European Journal of Pharmaceutics and Biopharmaceutics* 2009, 71(2):257-263.
 74. Sortino S, Mazzaglia A, Monsù Scolaro L, Marino Merlo F, Valveri V, Sciortino MT: Nanoparticles of cationic amphiphilic cyclodextrins entangling anionic porphyrins as carrier-sensitizer system in photodynamic cancer therapy. *Biomaterials* 2006, 27(23):4256-4265.
 75. Fan L, Lv Z, Sun M, Luo C, Lu F, Qiu H: Fabrication of magnetic chitosan nanoparticles grafted with β -cyclodextrin as effective adsorbents toward hydroquinol. *Colloids and Surfaces B: Biointerfaces* In press.
 76. Chauvierre C, Manchanda R, Labarre D, Vauthier C, Marden MC, Leclerc L: Artificial oxygen carrier based on polysaccharides–poly(alkylcyanoacrylates) nanoparticle templates. *Biomaterials* 2010, 31(23):6069-6074.
 77. Woitiski CB, Neufeld RJ, Ribeiro AJ, Veiga F: Colloidal carrier integrating biomaterials for oral insulin delivery: Influence of component formulation on physicochemical and biological parameters. *Acta Biomaterialia* 2009, 5(7):2475-2484.
 78. Hui Li Duan, Zhi Qiang Shen, Xin Wei Wang, Fu Huan Chao, Li JW: Preparation of immunomagnetic iron-dextran nanoparticles and application in rapid isolation of

- E.coli* O157:H7 from foods. *World Journal of Gastroenterology* 2005, 11(24):3660-3664.
79. Lu H-D, Zhao H-Q, Wang K, Lv L-L: Novel hyaluronic acid–chitosan nanoparticles as non-viral gene delivery vectors targeting osteoarthritis. *International Journal of Pharmaceutics* 2011, 420(2):358-365.
80. Yoon HY, Koo H, Choi KY, Lee SJ, Kim K, Kwon IC, Leary JF, Park K, Yuk SH, Park JH *et al*: Tumor-targeting hyaluronic acid nanoparticles for photodynamic imaging and therapy. *Biomaterials* In press.
81. Oyarzun-Ampuero FA, Brea J, Loza MI, Torres D, Alonso MJ: Chitosan–hyaluronic acid nanoparticles loaded with heparin for the treatment of asthma. *International Journal of Pharmaceutics* 2009, 381(2):122-129.
82. Sharma R, Ahuja M, Kaur H: Thiolated pectin nanoparticles: Preparation, characterization and *ex vivo* corneal permeation study. *Carbohydrate Polymers* 2012, 87(2):1606-1610.
83. Kim TH, Park YH, Kim KJ, Cho CS: Release of albumin from chitosan-coated pectin beads *in vitro*. *International Journal of Pharmaceutics* 2003, 250(2):371-383.
84. De Souza JRR, de Carvalho JIX, Trevisan MTS, de Paula RCM, Ricardo NMPS, Feitosa JPA: Chitosan-coated pectin beads: Characterization and *in vitro* release of mangiferin. *Food Hydrocolloids* 2009, 23(8):2278-2286.
85. Akiyoshi K, Kobayashi S, Shichibe S, Mix D, Baudys M, Wan Kim S, Sunamoto J: Self-assembled hydrogel nanoparticle of cholesterol-bearing pullulan as a carrier of protein drugs: Complexation and stabilization of insulin. *Journal of Controlled Release* 1998, 54(3):313-320.
86. Seo S, Lee C-S, Jung Y-S, Na K: Thermo-sensitivity and triggered drug release of polysaccharide nanogels derived from pullulan-g-poly(l-lactide) copolymers. *Carbohydrate Polymers* 2012, 87(2):1105-1111.
87. Zhang H-z, Gao F-p, Liu L-r, Li X-m, Zhou Z-m, Yang X-d, Zhang Q-q: Pullulan acetate nanoparticles prepared by solvent diffusion method for epirubicin chemotherapy. *Colloids and Surfaces B: Biointerfaces* 2009, 71(1):19-26.
88. Park K-H, Song H-C, Na K, Bom H-S, Lee KH, Kim S, Kang D, Lee DH: Ionic strength-sensitive pullulan acetate nanoparticles (PAN) for intratumoral administration of radioisotope: Ionic strength-dependent aggregation behavior and ^{99m}Tc retention property. *Colloids and Surfaces B: Biointerfaces* 2007, 59(1):16-23.

89. Oseguera MAP, Guereca L, Lopez-Munguia A: Properties of levansucrase from *Bacillus circulans*. *Applied Microbiology and Biotechnology* 1996, 45(4):465-471.
90. Tabtimthep S: Screening and cloning of crystalline chitin degrading chitinase gene. Master's Thesis. Department of Biochemistry, Faculty of Science: Chulalongkorn University; 2001.
91. Ben Ammar Y, Matsubara T, Ito K, Iizuka M, Limpaseni T, Pongsawasdi P, Minamiura N: Characterization of a thermostable levansucrase from *Bacillus* sp. TH4-2 capable of producing high molecular weight levan at high temperature. *Journal of Biotechnology* 2002, 99(2):111-119.
92. Altschul SF, Gish W, Miller W, Myers EW, Lipman DJ: Basic local alignment search tool. *Journal of Molecular Biology* 1990, 215(3):403-410.
93. Berezin C, Glaser F, Rosenberg J, Paz I, Pupko T, Fariselli P, Casadio R, Ben-Tal N: ConSeq: the identification of functionally and structurally important residues in protein sequences. *Bioinformatics* 2004, 20(8):1322-1324.
94. Larkin MA, Blackshields G, Brown NP, Chenna R, McGettigan PA, McWilliam H, Valentin F, Wallace IM, Wilm A, Lopez R *et al*: Clustal W and Clustal X version 2.0. *Bioinformatics* 2007, 23(21):2947-2948.
95. Gasteiger E, Gattiker A, Hoogland C, Ivanyi I, Appel RD, Bairoch A: ExPASy: the proteomics server for in-depth protein knowledge and analysis. *Nucleic Acids Research* 2003, 31(13):3784-3788.
96. Tamura K, Peterson D, Peterson N, Stecher G, Nei M, Kumar S: MEGA5: Molecular Evolutionary Genetics Analysis Using Maximum Likelihood, Evolutionary Distance, and Maximum Parsimony Methods. *Molecular Biology and Evolution* 2011, 28(10):2731-2739.
97. Benkert P, Biasini M, Schwede T: Toward the estimation of the absolute quality of individual protein structure models. *Bioinformatics* 2010.
98. Thomas Nordahl Petersen, Søren Brunak, Gunnar von Heijne, Nielsen H: SignalP 4.0: discriminating signal peptides from transmembrane regions. *Nature Methods* 2011, 8:785-786.
99. Maiti R, Van Domselaar GH, Zhang H, Wishart DS: SuperPose: a simple server for sophisticated structural superposition. *Nucleic Acids Research* 2004, 32(suppl 2):W590-W594.
100. Bohne A, Lang E, von der Lieth CW: SWEET - WWW-based rapid 3D construction of oligo- and polysaccharides. *Bioinformatics* 1999, 15(9):767-768.

101. Arnold K, Bordoli L, Kopp J, Schwede T: The SWISS-MODEL workspace: a web-based environment for protein structure homology modelling. *Bioinformatics* 2006, 22(2):195-201.
102. Sambrook J, Russell DW: *Molecular Cloning: A Laboratory Manual*, 3 edn. New York: Cold Spring Harbor Laboratory Press, ; 2000.
103. Coligan E. J, Dunn M. B, Speicher W. D, P WT: *Current Protocols In Protein Science*, 1 edn. New Jersey: Wiley & Sons, Inc; 2001.
104. Cirino PC, Mayer KM, Umeno D: Generating Mutant Libraries Using Error-Prone PCR. In: *Directed Evolution Library Creation*. Edited by Arnold FH, Georgiou G, vol. 231. New York: Humana Press; 2003: 3-9.
105. James G: Universal Bacterial Identification by PCR and DNA Sequencing of 16S rRNA Gene PCR for Clinical Microbiology. In. Edited by Schuller M, Sloots TPP, James GSS, Halliday CLL, Carter IWJWJ: Springer Netherlands; 2000: 209-214.
106. Miller GL: Use of dinitrosalicylic acid reagent for determination of reducing sugar. *Analytical Chemistry* 1959, 31(3):426-428.
107. DuBois M, Gilles KA, Hamilton JK, Rebers PA, Smith F: Colorimetric method for determination of sugars and related substances. *Analytical Chemistry* 1956, 28(3):350-356.
108. Abdel-Fattah AF, Mahmoud DA, Esawy MA: Production of levansucrase from *Bacillus subtilis* NRC 33a and enzymic synthesis of levan and Fructo-Oligosaccharides. *Current Microbiology* 2005, 51(6):402-407.
109. Chambert R, Petit-Glatron MF: Hyperproduction of exocellular levansucrase by *Bacillus subtilis*: examination of the phenotype of a sacU^h strain. *Journal of General Microbiology* 1984, 130(12):3143-3152.
110. Euzenat O, Guibert A, Combes D: Production and Purification of *Bacillus subtilis* C4 Levansucrase: Kinetic Characterization of the Enzyme. *Annals of the New York Academy of Sciences* 1998, 864(1):288-294.
111. Tian F, Inthanavong L, Karboune S: Purification and characterization of levansucrases from *Bacillus amyloliquefaciens* in intra- and extracellular forms useful for the synthesis of levan and fructooligosaccharides. *Bioscience, Biotechnology and Biochemistry* 2011, 75(10):1929-1938.
112. Pabst MJ, Cisar JO, Trummel CL: The cell wall-associated levansucrase of *Actinomyces viscosus*. *Biochimica et Biophysica Acta* 1979, 566(2):274-282.

113. Ohtsuka K, Hino S, Fukushima T, Ozawa O, Kanematsu T, Uchida T: Characterization of levansucrase from *Rahnella aquatilis* JCM-1683. *Bioscience, Biotechnology and Biochemistry* 1992, 56(9):1373-1377.
114. Bekers M, Laukevics J, Upite D, Kaminska E, Vigants A, Viesturs U, Pankova L, Danilevics A: Fructooligosaccharide and levan producing activity of *Zymomonas mobilis* extracellular levansucrase. *Process Biochemistry* 2002, 38(5):701-706.
115. Vigants A, Marx SP, Linde R, Ore S, Bekers M, Vina I, Hicke HG: A novel and simple method for the purification of extracellular levansucrase from *Zymomonas mobilis*. *Current Microbiology* 2003, 47(3):198-202.
116. Fawkia M. El-Beih, Azza M. Abdel-Fattah, Doaa A. Hasanein, Mostafa FA, Abdel-Fattah AF: Production and some properties of fructosyltransferase from *Bacillus cereus*. *Journal of Applied Sciences Research* 2009, 5(9):1132-1141.
117. van Hijum SA, Bonting K, van der Maarel MJ, Dijkhuizen L: Purification of a novel fructosyltransferase from *Lactobacillus reuteri* strain 121 and characterization of the levan produced. *FEMS Microbiology Letters* 2001, 205(2):323-328.
118. Hernandez L, Arrieta J, Betancourt L, Falcon V, Madrazo J, Coego A, Menendez C: Levansucrase from *Acetobacter diazotrophicus* SRT4 is secreted via periplasm by a signal-peptide-dependent pathway. *Current Microbiology* 1999, 39(3):146-152.
119. Cote GL: Production of a constitutive, extracellular levansucrase from *Erwinia herbicola* NRRL B-1678. *Biotechnology letters* 1988, 10(12):879-882.
120. Hansen BM, Leser TD, Hendriksen NB: Polymerase chain reaction assay for the detection of *Bacillus cereus* group cells. *FEMS Microbiology Letters* 2001, 202(2):209-213.
121. McIntyre L, Bernard K, Beniac D, Isaac-Renton JL, Naseby DC: Identification of *Bacillus cereus* Group Species Associated with Food Poisoning Outbreaks in British Columbia, Canada. *Applied and Environmental Microbiology* 2008, 74(23):7451-7453.
122. Nakamura LK, Roberts MS, Cohan FM: Relationship of *Bacillus subtilis* clades associated with strains 168 and W23: A proposal for *Bacillus subtilis* subsp. *subtilis* subsp. nov. and *Bacillus subtilis* subsp. *spizizenii* subsp. nov. *International Journal of Systematic Bacteriology* 1999, 49(3):1211-1215.
123. Rodríguez H, de las Rivas B, Muñoz R: Efficacy of recA gene sequence analysis in the identification and discrimination of *Lactobacillus hilgardii* strains isolated from stuck wine fermentations. *International Journal of Food Microbiology* 2007, 115(1):70-78

124. Shah MM, Iihara H, Noda M, Song SX, Nhung PH, Ohkusu K, Kawamura Y, Ezaki T: dnaJ gene sequence-based assay for species identification and phylogenetic grouping in the genus *Staphylococcus*. *International Journal of Systematic and Evolutionary Microbiology* 2007, 57(1):25-30.
125. Alméciga-Díaz CJ, Gutierrez ÁM, Bahamon I, Rodríguez A, Rodríguez MA, Sánchez OF: Computational analysis of the fructosyltransferase enzymes in plants, fungi and bacteria. *Gene* 2011, 484(1–2):26-34.
126. Altenbach D, Ritsema T: Structure-function relations and evolution of fructosyltransferases. In: *Recent Advances in Fructooligosaccharides Research*. Edited by N Shiomi, N Benkeblia, Onodera S. Kerala, India: Research Signpost; 2007: 135–156.
127. Yanase H, Fujimoto J, Maeda M, Okamoto K, Kita K, Tonomura K: Expression of the extracellular levansucrase and invertase genes from *Zymomonas mobilis* in *Escherichia coli* cells. *Bioscience, Biotechnology and Biochemistry* 1998, 62(9):1802-1805.
128. van Hijum SA, Szalowska E, van der Maarel MJ, Dijkhuizen L: Biochemical and molecular characterization of a levansucrase from *Lactobacillus reuteri*. *Microbiology* 2004, 150(Pt 3):621-630.
129. Seo JW, Song KB, Jang KH, Kim CH, Jung BH, Rhee SK: Molecular cloning of a gene encoding the thermoactive levansucrase from *Rahnella aquatilis* and its growth phase-dependent expression in *E. coli*. *Journal of Biotechnology* 2000, 81(1):63-72.
130. Song DD, Jacques NA: Purification and enzymic properties of the fructosyltransferase of *Streptococcus salivarius* ATCC 25975. *Biochemical Journal* 1999, 341 (Pt 2):285-291.
131. Vigants A, Hicke HG, Marx SP: A simple and efficient method for the purification of membrane-bound levansucrase from *Zymomonas mobilis*. *Current Microbiology* 2001, 42(6):415-418.
132. Mäntsälä P, Puntala M: Comparison of levansucrase from *Bacillus subtilis* and from *Bacillus amyloliquefaciens*. *FEMS Microbiology Letters* 1982, 13(4):395-399.
133. Lyness EW, Doelle HW: Levansucrase from *Zymomonas mobilis*. *Biotechnology letters* 1983, 5(5):345-350.
134. Sangiliyandi G, Gunasekaran P: A simple method for purification of thermostable levansucrase of *Zymomonas mobilis* from a recombinant *Escherichia coli*. *Journal of Microbiological Methods* 1998, 33(2):153-156.

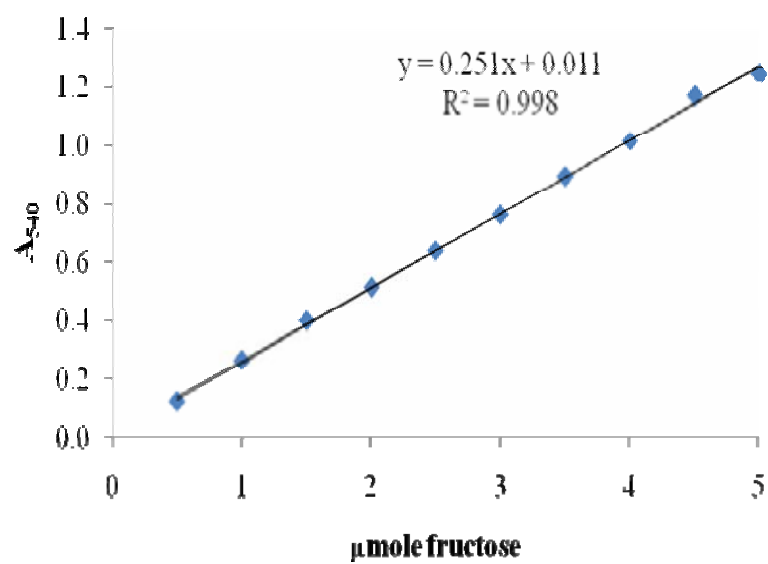
135. Baciú IE, Jördening HJ, Seibel J, Buchholz K: Investigations of the transfructosylation reaction by fructosyltransferase from *B. subtilis* NCIMB 11871 for the synthesis of the sucrose analogue galactosyl-fructoside. *Journal of Biotechnology* 2005, 116(4):347-357.
136. Chambert R, Petit-Glatron MF: Reversible thermal unfolding of *Bacillus subtilis* levansucrase is modulated by Fe^{3+} and Ca^{2+} . *FEBS Lett* 1990, 275(1-2):61-64.
137. Tieking M, Ehrmann MA, Vogel RF, Ganzle MG: Molecular and functional characterization of a levansucrase from the sourdough isolate *Lactobacillus sanfranciscensis* TMW 1.392. *Applied Microbiology and Biotechnology* 2005, 66(6):655-663.
138. Waldherr FW, Meissner D, Vogel RF: Genetic and functional characterization of *Lactobacillus panis* levansucrase. *Archives of Microbiology* 2008, 190(4):497-505.
139. Esawy MA, Mahmoud DAR, Fattah AFA: Immobilisation of *Bacillus subtilis* NRC33a levansucrase and some studies on its properties. *Brazilian Journal of Chemical Engineering* 2008, 25:237-246.
140. Heba A. El-Refai, Fattah AFA-, Mostafa FA: Immobilization and properties of *Bacillus circulans* levansucrase. *Acta Pharmaceutica Scientia* 2009, 51:149-156.
141. Tanaka T, Oi S, Yamamoto T: Synthesis of levan by levansucrase: Some factors affecting the rate of synthesis and degree of polymerization of levan. *The Journal of Biochemistry* 1979, 85(1):287-293.
142. Crittenden RG, Doelle HW: Identification and characterization of the extracellular sucrases of *Zymomonas mobilis* UQM 2716 (ATCC 39676). *Applied Microbiology and Biotechnology* 1994, 41(3):302-308.
143. Batista FR, Hernandez L, Fernandez JR, Arrieta J, Menendez C, Gomez R, Tambara Y, Pons T: Substitution of Asp-309 by Asn in the Arg-Asp-Pro (RDP) motif of *Acetobacter diazotrophicus* levansucrase affects sucrose hydrolysis, but not enzyme specificity. *Biochem J* 1999, 337 (Pt 3):503-506.
144. Ortiz-Soto ME, Rivera M, Rudino-Pinera E, Olvera C, Lopez-Munguia A: Selected mutations in *Bacillus subtilis* levansucrase semi-conserved regions affecting its biochemical properties. *Protein Engineering, Design and Selection* 2008, 21(10):589-595.
145. Naghibzadeh M, Amani A, Amini M, Esmailzadeh E, Mottaghi Dastjerdi N, Faramarzi MA: An insight into the interactions between α -tocopherol and chitosan in ultrasound-prepared nanoparticles. *Journal of Nanomaterials* 2010, 2010:7.

146. Davies GJ, Wilson KS, Henrissat B: Nomenclature for sugar-binding subsites in glycosyl hydrolases. *Biochemical Journal* 1997, 321 (Pt 2):557-559.
147. Fujii R, Kitaoka M, Hayashi K: One-step random mutagenesis by error-prone rolling circle amplification. *Nucleic Acids Research* 2004, 32(19):e145.

APPENDICES

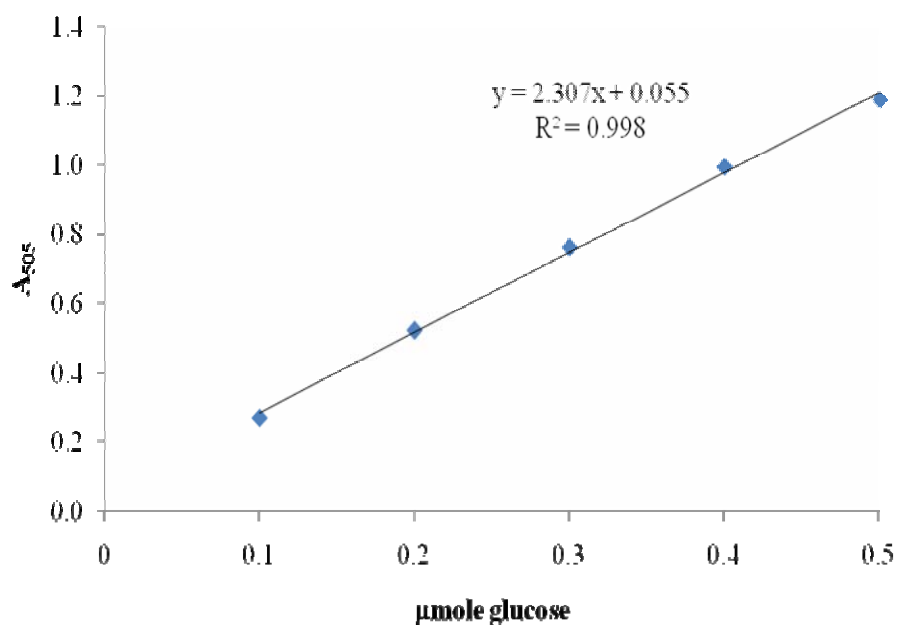
APPENDIX A

Standard curve of fructose determined by DNS method



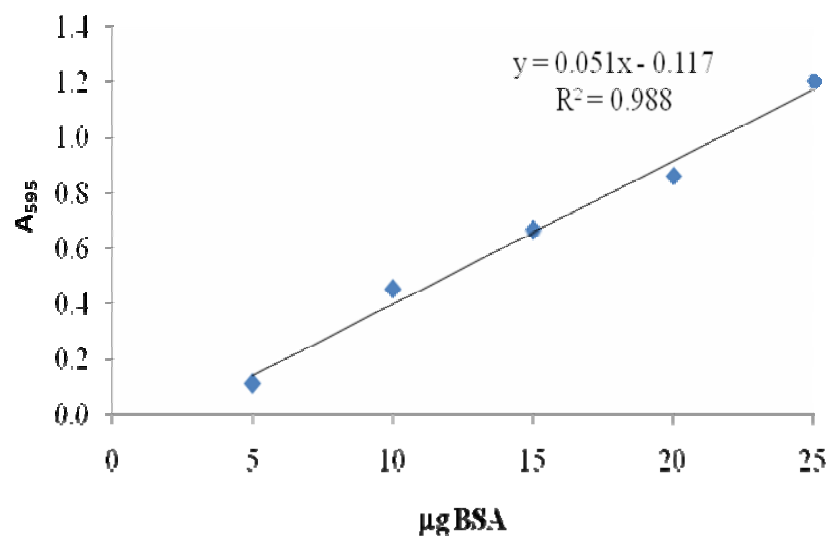
APPENDIX B

Standard curve of glucose determined by glucose oxidase kit



APPENDIX C

Standard curve of BSA by Bradford method



BIOGRAPHY

Miss. Santhana Nakapong finished her B.Sc. in Biochemistry from Kasetsart University in 2001 and Master Degree in Biochemistry from Faculty of Science, Chulalongkorn University in 2004. In 2007, she applied for the Ph.D. candidate at department of Biochemistry, Chulalongkorn University.